Czech Technical University in Prague
Faculty of Electrical Engineering
Department of Telecommunication Engineering

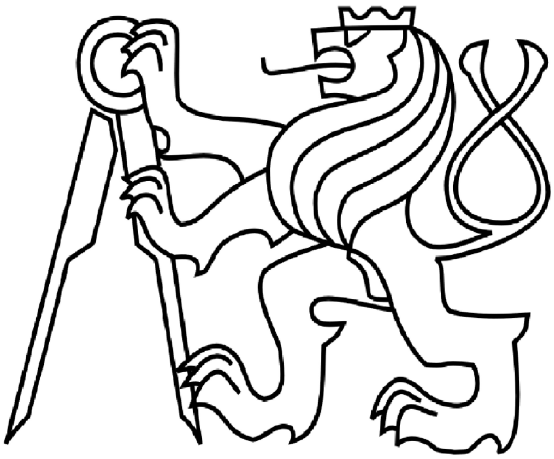

# Advanced Allocation of Resources for Device-to-Device Communication in Future Mobile Networks

**Doctoral Thesis**

**Mehyar Najla**

Prague, August 2020

Ph.D. programme: P2612 Electrical Engineering and Information Technology
Branch of study: 2601V013 Telecommunication Engineering

**Supervisor: Ing. Pavel Mach, Ph.D.**
**Supervisor-Specialist: Doc. Ing. Zdeněk Bečvář, Ph.D.**

# Declaration

I declare that the work presnted in this dissertation thesis is my work, and the achieved results are the findings of my research monitored and directed by my supervisors in parallel with the contributions of other co-authors in the corresponding published papers.

In Prague, August 2020 .....

Mehyar Najla

# Abstract

Device-to-Device (D2D) communication is a promising technique to increase the capacity and the spectral efficiency of the future mobile networks. In D2D communication, two devices (denoted as a D2D pair) communicate directly with each other without passing through the base station (BS). This direct communication offloads the data traffic from the BS. The data between the devices in D2D communication is exchanged using either the conventional band of the mobile network (in-band) or another band that is not used by the underlying devices in the mobile network (out-band). The in-band D2D communication includes two modes: shared and dedicated. In the shared mode, the D2D pairs reuse the resources allocated to the conventional cellular users while, in the dedicated mode, the D2D pairs use their own dedicated resources that are not used by the conventional cellular users. In both modes, the D2D pairs can mutually reuse the channels of each other to increase the spectral efficiency of D2D communication.

In this dissertation thesis, a novel principle of allocating shared as well as dedicated resources to every D2D pair, simultaneously, is proposed. Further, the resource allocation in both modes is separately optimized. To this end, a game theoretic approach for the channel allocation in the dedicated mode and a heuristic channel allocation algorithm for the shared mode are proposed. Both schemes for the dedicated and shared modes aim to maximize the sum capacity of the D2D pairs maintaining the minimal capacity requirements of the D2D pairs and the conventional cellular users in the dedicated and shared modes, respectively. Moreover, we propose a combination between the conventional in-band D2D communication that uses radio frequency (RF) and the out-band visible light communication (VLC) D2D to maximize the sum capacity of D2D pairs. For this proposed RF-VLC D2D, two schemes selecting between RF and VLC bands for the individual D2D pairs are designed. While the first scheme for RF/VLC band selection is an iterative interference-based heuristic approach, the second one is a quick machine learning-based band selection that relies only on a limited amount of information related to the channels among the D2D users in RF and VLC.

The band selection, resource allocation, and other radio resource management algorithms in D2D communication require the knowledge of the quality of the D2D channels among the D2D users. The estimation of the D2D channels with the conventional reference signals consumes extra radio resources. Therefore, this dissertation thesis proposes a machine learning-based framework for the prediction of D2D channel gains by relying only on the commonly-known

cellular channel gains between the users and the surrounding BSs. This idea takes advantage of the dependency of both D2D and cellular channels on the network's topology and environment. The predicted D2D channel gains can be used to perform any radio resource management algorithm related to D2D. Finally, this dissertation thesis shows that the users' cellular gains can also be used to predict, directly, the D2D transmission power setting or the association of users in networks with flying base stations. The results of the performed simulations confirm the efficiency of all proposed solutions for the different targeted problems in D2D communication. Consequently, this dissertation thesis, including the different proposed algorithms and the prediction schemes, paves the way towards the deployment of D2D communication for a massive numbers of D2D pairs.

**Keywords:** Device-to-Device communication, resource allocation, radio frequency, visible light communication, channel prediction, mahcine learning, game theory

# Abstrakt

Přímá komunikace mezi zařízeními (D2D) je slibnou technikou pro zvýšení kapacity a spektrální účinnosti budoucích mobilních sítí. D2D komunikace umožňuje přenos dat mezi dvěma zařízeními (označované jako D2D pár) přímo mezi sebou bez nutnosti přeposílat data prostřednictvím základové stanice. Data mezi zařízeními využívající D2D komunikaci jsou vyměňovány buď pomocí pásma určeného pro mobilní sítě (tzv. in-band D2D komunikace), nebo v pásmu, které nepoužívají žádná zařízení v mobilní síti (tzv. out-band D2D komunikace). In-band D2D komunikace zahrnuje dva alokační módy: sdílený a vyhrazený. Ve sdíleném módu, D2D páry využívají stejné zdroje, které jsou přiděleny konvenčním uživatelům buňkové mobilní sítě. Na druhou stranu, ve vyhrazeném módu D2D používají dedikované zdroje, které běžní uživatelé buňkové mobilní sítě nepoužívají. V obou přenosových módech D2D páry vzájemně sdílejí přenosové kanály, aby se zvýšila spektrální účinnost přenosu prostřednictvím D2D komunikace.

V této disertační práci je navržen nový princip přidělování sdílených i vyhrazených prostředků v případě kdy jsou tyto využívány více D2D páry současně. Dále je cílem práce optimalizovat alokaci zdrojů v obou módech. Za tímto účelem je navržen přístup založený na teorii her pro přidělování kanálů ve vyhrazeném režimu a heuristický algoritmus pro přidělování kanálů pro sdílený režim. Cílem obou schémat je maximalizovat celkovou kapacitu D2D párů při zachování jejich požadavků na minimálních kapacitu , a to jak v případě vyhrazeného módu tak i v případě sdíleného módu. Dále je navržena metoda pro maximalizaci kapacity D2D párů založená na kombinaci konvenční in-band D2D komunikace, která používá rádiové frekvence (RF), a out-band D2D komunikace, využívající viditelné světlo (VLC). K tomu jsou navržené dvě schémata výběru mezi RF a VLC pásmy pro každý D2D pár. Zatímco první schéma je založené na iterativní metodě potřebující znalosti interference mezi jednotlivými D2D páry, druhé schéma je založeno na strojovém učení využívající pouze minimální množství informací o kanálech mezi D2D uživateli v RF a VLC režimech.

Výběr pásma, alokace zdrojů a další algoritmy správy rádiových zdrojů pro D2D komunikaci vyžadují znalost kvality D2D kanálů (tj. kanálů mezi D2D uživateli). Odhad kanálů mezi D2D uživateli referenčními signály použitými v klasické mobilní síti by vyžadovalo velké množství rádiových prostředků. Tato disertační práce proto navrhuje metodu pro predikci kvality D2D kanálů založenou na strojovém učení využívající pouze informací běžně dostupných v mobilní síti. Konkrétně se jedná o využití znalosti rádiových kanálu mezi

uživateli a okolními základnovými stanicemi, ze kterých jsou následně predikovány kvality kanálů mezi D2D uživateli. Takto predikované D2D kanály lze poté s výhodou použít k provádění jakéhokoli algoritmu správy rádiových zdrojů, který vyžaduje znalost kvality D2D kanálů. Tato disertační práce také ukazuje, že znalost kanálů získaných predikcí lze využít nejen ke správě rádiových prostředků pro D2D komunikaci (např. pro nastavení vysílacího výkonu D2D uživatelů), ale také pro asociaci uživatelů v mobilních sítích s létajícími základnovými stanicemi. Výsledky provedených simulací potvrzují efektivnost všech navrhovaných řešení pro různé cílené problémy v D2D komunikaci. Tato dizertační práce, včetně různých navrhovaných algoritmů a predikčních schémat, tedy otevírá cestu pro nasazení D2D komunikace pro mobilní sítě příštích generací, a to především pro velké množství uživatelů v síti.

**Klíčová slova:** Příma kommunikace mezi zařízeními, přidělování zdrojů, rádiové frekvence, komunikace ve viditelném světle, predikce kanálu, strojové učení, teorie her

# Acknowledgements

I would like to thank my supervisors, Dr. Pavel Mach and Prof. Zdenek Becvar, for their guidance and their unlimited support. For four years, they were an infinite source of information as well as motivation until this work has been accomplished.

I would like also to thank Prof. David Gesbert from Eurecom-France who was supervising my internship at Eurecom.

To my family in Syria, no thanking words are enough! My mum, dad, sister, and aunt Liena are the main reason that has been pushing me to work more and more. They have given me love and support. They have believed in me and made me believe in myself. To them I can only say: I am lucky to have you as my family!

My family in Prague, Dunja, has been always by my side in my dark before bright moments. She has been a loving, supportive, and understanding partner. To her I say: Hvala srce moje! mnogo te volim!

Finally, I would like to thank my uncle, Nabil Salameh, whose favour changed my life. Without the help of this great person, my Ph.D. would have stayed a dream. To him I give my highest respect and appreciation.

# Contents

# Chapter 1

# Introduction

In future mobile networks, data traffic and network load are expected to increase dramatically with the increasing number of users and their requirements. To cope with this increase, a part of the data traffic can be offloaded from the conventional base stations (BSs) via a Device-to-Device communication (i.e., D2D) [1]. The D2D communication is a direct communication between two user equipment (UEs) composing a D2D pair. Within the D2D pair, the data is sent directly from one UE (a transmitter) to another UE (a receiver), without relaying the data through the BS, as in the conventional cellular communication [2].

The D2D communication can exploit the spectrum allocated to the cellular operators used for the conventional cellular communications forming an in-band D2D communication [3]. In the in-band D2D communication, two main modes are available for the D2D pairs, a shared and a dedicated [4]. In the shared mode (also known as underlay mode), the D2D pairs communicate over the same channels used by the conventional cellular users (CUEs) to increase the spectral efficiency at the cost of interference among the D2D pairs and the CUEs [2]. In contrast, within the D2D dedicated mode also known as overlay mode, the D2D pairs exploit their own dedicated frequencies which are not used by the CUEs [3]. Although the dedicated mode usually reaches a lower spectral efficiency compared to the shared mode, the dedicated mode is preferred in scenarios with a very high density of users, as the interference among the D2D pairs and the CUEs is hard to manage in such scenario [5]. In both dedicated and shared modes, an efficient resource allocation is required to enhance the communication quality in terms of the achievable sum capacity of D2D pairs and/or the spectral efficiency. Designing an optimal resource allocation scheme is, however, a challenge due to the very high complexity of unconstrained resource allocation problems in D2D communication [4].

In addition to the in-band D2D communication, there exists an out-band D2D communication, where the D2D exploits a spectrum that is different from the one used by the conventional cellular communications [2]. One of the promising out-band technologies is Visible light communication (VLC). The VLC systems operate at wavelengths of 380-750 nm (i.e., frequency bands of 400-790 THz) and can achieve high data rates [66]. Taking into account the

very wide bandwidth and reachable high data rates of VLC, a combination of VLC and conventional Radio Frequency (RF) bands together for D2D communication is a promising way to suppress interference in the network, as there is no interference between the two bands [7]. Nevertheless, in a scenario with multiple D2D pairs, it is critical to design an efficient algorithm to determine if a D2D pair should operate in RF or in VLC.

Another essential challenge related to the D2D communication is the requirement on the knowledge of the quality of D2D channels between the D2D UEs (DUEs) for resource allocation, RF/VLC band selection, or other radio resource management procedures. Such knowledge can be obtained via conventional approaches based on the transmission of reference signals to estimate the channel quality [8]. However, such solutions imply a very high amount of signaling. This high signaling cost motivates to predict the D2D channels from other information commonly available in the network.

This dissertation thesis aims to optimize the resource allocation in both D2D dedicated and shared modes and study the RF-VLC combination for the D2D communication. Moreover, to facilitate D2D communication for a massive amount of devices, the problem of the D2D channels' prediction is addressed. Based on this, the contributions of this dissertation thesis are, shortly, summarized as follows:

- A novel concept of combining shared and dedicated D2D modes is introduced. Then, two new resource allocation schemes in D2D dedicated and shared modes are proposed, enabling the reuse of multiple channels by multiple D2D pairs.

- A new combination between VLC out-band D2D with the in-band RF D2D (denoted as RF-VLC D2D) is introduced. Moreover, two algorithms for RF/VLC band selection in RF-VLC D2D within a scenario with multiple D2D pairs are designed.

- A D2D channel prediction framework which relies on the knowledge of the cellular channel gains between the UEs and the surrounding BSs is proposed. Then, two additional applications of the prediction scheme, power control in D2D communication and UEs' association in networks with flying BSs (FlyBSs), are presented such that obtaining the knowledge of the D2D channel gains as an intermediate step is not needed.

The thesis is organized as follows. First, the current state-of-the art is summarized in Chapter 2. Then, the dissertation objectives are illustrated in Chapter 3. Chapter 4 presents the results of the dissertation thesis. Finally, Chapter 5 concludes the thesis, summarizes its contributions with respect to the state-of-the art, and clarifies the possible future research directions.

# Chapter 2

# Literature Review

D2D communication, illustrated in Figure 1, is an emerging paradigm enhancing spectral and energy efficiencies of the mobile networks [9]. Hence, D2D has grabbed the attention of many researchers to solve the variety of problems and challenges related to D2D. This Chapter summarizes the current state-of-the-art related to D2D communication and aspects of the mobile networks within the scope of this dissertation thesis. Moreover, the gaps in the state-of-the-art are outlined to provide a motivation towards the problems addressed dissertation thesis. The structure of the this chapter is as follows. First, the work related to the D2D communication modes and the mode selection in D2D communication is detailed. Then, the existing resource allocation schemes in D2D communication, including both the shared and dedicated modes, are described. Moreover, the current work on the combination between RF and VLC bands in the mobile networks is presented. Finally, the existing work on the determination of the channel quality in the mobile networks is summarized.

## 2.1 D2D Communication Modes

The D2D communication can be classified according to the spectrum utilization into the in-band D2D (operating over the same spectrum used for conventional

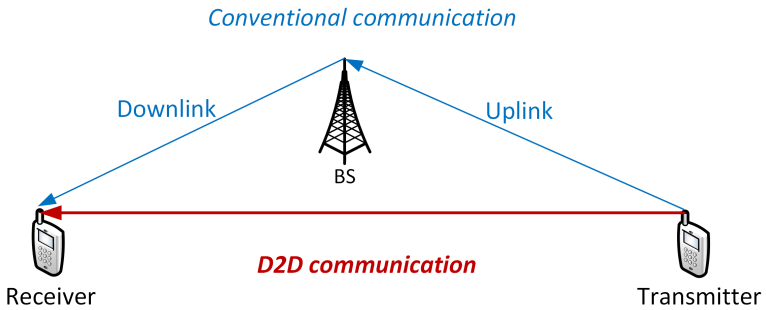


Figure 1. Principle of Device-to-Device (D2D) communication with respect to conventional communication in mobile networks where the data is relayed through the BS.

cellular communications) or the out-band D2D (exploiting another spectrum that is different from the one dedicated for conventional cellular communications) [1]-[3].

The D2D pairs operating via the in-band D2D can exploit either the *dedicated* mode (i.e., overlay) or the *shared* mode (i.e., underlay) [10]. The dedicated mode is distinguished by the fact that the D2D pairs access dedicated resources with respect to the CUEs communicating conventionally through the BS [11]. Consequently, the interference between the D2D pairs and the CUEs is efficiently avoided, but the system can experience a low spectral efficiency. In case of the shared mode, the D2D pairs reuse the same resources as the CUEs [12]. Although this mode enables a higher frequency reuse when compared to the dedicated mode, the mutual interference between the CUEs and the D2D pairs is a challenge. This interference can be too strong and can vary frequently and significantly, especially in the case with a dense presence of UEs. Thus, although, the shared mode offers a higher spectral efficiency than the dedicated one, the higher efficiency is usually at the cost of highly complex solutions for the resource allocation and management [13], [14]. The shared and dedicated modes of the in-band D2D communication are illustrated in Figure 2

In the scenarios with a high density of users, where the interference between the CUEs and the D2D pairs is strong and hard to manage, the reliability of the communication cannot be easily guaranteed and the overall quality of services (QoS) can be impaired [5], [14]. Thus, the D2D pairs with strict requirements on QoS should prefer the dedicated mode, which is suitable for the services

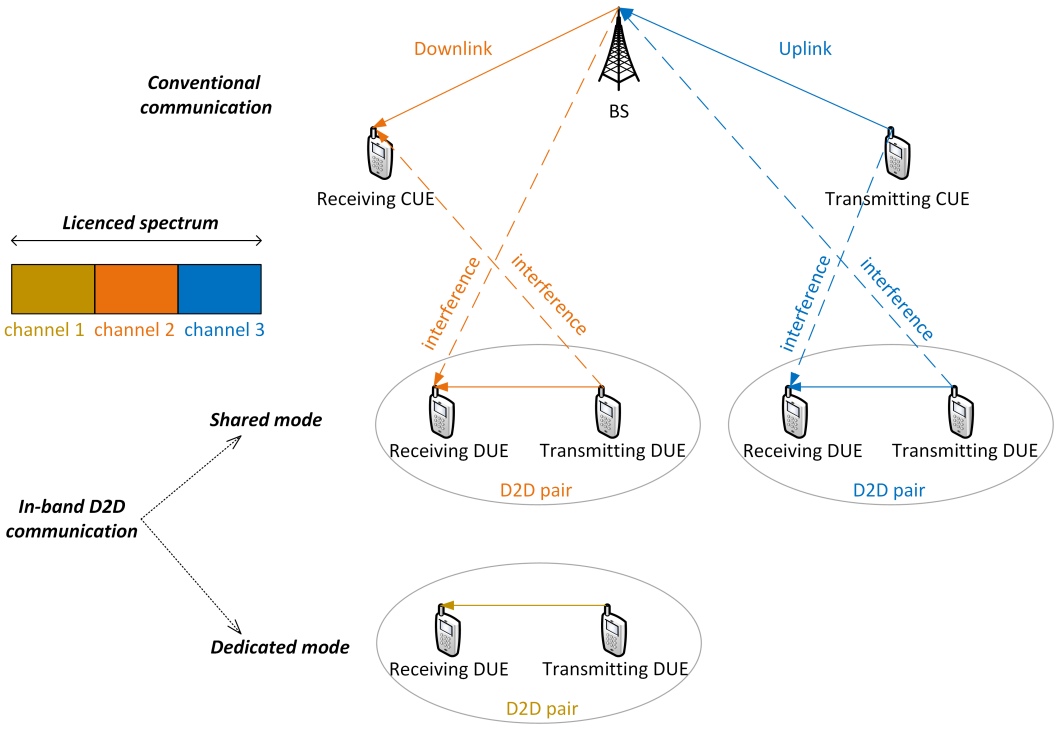


Figure 2. Communication modes in in-band D2D communication where the conventional and the D2D communications, both, access the listened spectrum.

that require a highly reliable communication with a low risk of an unexpected interference from the CUEs.

Concrete and up-and-coming examples of the use cases for the dedicated mode are the direct communication of vehicles or public safety communications [15]. In such use cases, an ultra-reliable communication with a guaranteed minimum communication capacity should be ensured. In the shared mode, however, interference might lead to the situations when such guarantee is simply not possible and the unreliability of the communication can have grievous consequences [16]. Hence, the dedicated resources are commonly considered for the vehicular or public safety communications.

In recent years, a significant effort has been invested to address the problem of the selection of a suitable mode for the D2D pairs. The research works related to mode selection can be classified into papers selecting: 1) between the cellular conventional mode (where the users communicate through the BS and not directly) and the shared or dedicated mode [17]-[22], 2) between the dedicated and shared modes [23], [24], and 3) among the cellular, dedicated, and shared modes [25]-[27]. Most of the existing works focusing on mode selection for D2D pairs expect that each D2D pair uses just one communication mode (cellular, dedicated, or shared). Only in [21], the authors propose to allow the DUEs to access radio resources in the cellular and shared modes at the same time. The paper addresses the routing problem deciding whether data should be routed through the BS (cellular mode) or transmitted directly between the DUEs in the shared mode.

However, none of the existing papers studies the possibility of combining the shared and dedicated modes, by allowing the DUEs to communicate directly accessing resources in both, shared and dedicated modes, simultaneously. This gap in the existing state of the art limits the achievable sum capacity of D2D pairs.

## 2.2 Resource Allocation in D2D Communication

In each of the shared and dedicated modes in the in-band D2D, the resources should be allocated efficiently in order to improve the sum capacity and the spectral efficiency of the network [28]. To this end, the D2D pairs reuse the channels of each others to increase the spectral efficiency of the D2D communication. However, the channel reuse among a set of D2D pairs leads to an interference among these pairs. Hence, the channel reuse is highly dependent on the mutual interference between the D2D pairs in order to decide which D2D pairs should reuse the same channel(s) [29]. Moreover, the D2D pairs reusing the same channel(s) can exploit power control to mitigate the resulting interference [30].

In the current state-of-the-art, most of the papers simplify the channel allocation problem by: i) restricting the number of D2D pairs that are allowed to reuse a single channel ([25], [31]-[36] ), and/or ii) restricting the number of

channels that can be allocated to each D2D pair ([17], [24], [26], [27], [37]-[45]). These restrictions decrease the achievable sum capacity and, thus, a question arises about whether enabling the reuse of multiple channels by multiple D2D pairs would significantly enhance the sum capacity of D2D pairs.

The next two subsections summarize, with details, the state-of-the-art related to resource allocation in D2D dedicated and shared modes, respectively.

### 2.2.1 Channel Allocation in D2D Dedicated Mode

In the dedicated mode, one of the key challenges is the allocation of the available bandwidth to the D2D pairs. The authors in [25] and [31] present channel allocation schemes that divide the dedicated bandwidth to multiple channels with different bandwidths so that each D2D pair gets exactly one channel. In both [25] and [31], the optimal allocation is achieved for the case when the interference from other neighboring cells is nonexistent. However, in real networks, the interference from other cells always exists and we can expect that the level of interference will even increase in the future due to the densification of mobile networks. Such inter-cell interference impacts the optimal channel allocation for the D2D pairs in the dedicated mode. Moreover, neither [25] and [31] assume the reuse of each channel by more than one D2D pair resulting in a lower spectral efficiency.

A simplified channel reuse in the dedicated mode is presented in [24], [26], and [37]. Although all these studies consider that either two D2D pairs ([26]) or multiple D2D pairs ([24], [37]) can access the same channel, each D2D pair is allowed to occupy just one channel at any time. The papers [46]-[48] exploit the reuse of multiple channels by multiple D2D pairs to guarantee a minimal SINR for every D2D pair while using the minimal possible number of channels. In these works, however, the D2D pairs do not benefit fully from the reuse, as only a limited number of channels is used and the sum capacity is not maximized. In [49], the authors maximize the sum capacity of D2D pairs in the dedicated mode considering that the D2D pairs reuse all available channels. Nevertheless, the authors do not consider the constraint on the minimal capacity $C_{min}$ that should be guaranteed to the individual D2D pairs. Thus, the solution proposed in [49] can lead to the situation when some D2D pairs end up with zero data rate as these are forbidden to transmit at any channel due to the interference caused to other D2D pairs. Note that the ideas presented in [24]-[49] cannot be easily extended to maximize the sum capacity and, at the same time, to guarantee $C_{min}$, since the capacity maximization under the constraint on $C_{min}$ for every D2D pair requires completely different solutions.

In summary, the existing resource allocation methods for the dedicated mode either restrict the number of D2D pairs reusing a single channel (e.g., [25] and [31]) or limit the number of channels that can be occupied by a single D2D pair (e.g., [24], [26], and [37]). As an exception, the papers [46]-[49] allow the reuse of multiple channels by multiple D2D pairs in the dedicated mode. These papers target either the sum capacity maximization ([49]) or the minimization of the amount of consumed resources in order to guarantee the

minimal required individual capacity ($C_{min}$) for all D2D pairs ([46]-[48]). However, none of these papers maximizes the sum capacity while guaranteeing $C_{min}$ to every D2D pair.

### 2.2.2 Channel Allocation in D2D Shared Mode

In the shared mode, most of the existing channel allocation algorithms assume a restriction on either the number of D2D pairs that can reuse a single channel ([32]-[36]) or the number of channels that can be occupied by each D2D pair ([17], [24], [26], [27], [38]-[45]). An exception to these restrictions is represented by [50], where a non-cooperative selfish game for the channel reuse is proposed. The solution allows the reuse of multiple channels by multiple D2D pairs in the shared mode. Nevertheless, the designed game does not converge in realistic scenarios with the presence of strong mutual interference among D2D pairs. Hence, the solution is applicable only to scenarios with a very low number of D2D pairs separated by large distances from each other. Except [50], the reuse of multiple channels by multiple D2D pairs is not allowed by any state-of-the-art papers in the shared mode. At the same time, extending the existing schemes to allow the reuse of multiple channels by multiple pairs is not straightforward if not impossible.

## 2.3 RF-VLC Combination in Mobile Networks

In addition to the in-band D2D, there is also an option of the out-band D2D, where the direct communication exploits a different spectrum with respect to the one used by the conventional cellular communication and, usually, the out-band D2D adopts other wireless technologies [2]. One of the promising out-band technologies is Visible light communication (VLC), which exploits visible light for data transmission. Hence, VLC systems operate in higher frequency bands and have a much wider spectrum at their disposal when compared to the conventional radio systems (400-790 THz) [66],[51]. As a consequence, VLC is able to provide data rates in the order of Gbps [52],[53]. For example, 4.5 Gbps throughput is achieved by the VLC systems employing carrier-less amplitude & phase modulations and a recursive least square-based adaptive equalizer as described in [52] and [53], respectively. In [54], the authors show that a combination of 16–quadrature amplitude modulation and orthogonal frequency division multiplexing (OFDM) or wavelength multiplex (RGB) allow to reach 3.4 Gbps throughput.

These above-mentioned advantages of VLC have motivated the researchers towards studying the possibility of exploiting VLC in parallel with the conventional in-band radio frequencies to improve mobile networks' performance [55]. Such RF-VLC combination benefits from the fact that there is no interference between RF and VLC bands [56]. To this end, the combination between the conventional RF and VLC bands for data transmission is investigated, e.g., in [57]-[61]. In these studies, the authors focus on indoor downlink exploitation of the VLC band through VLC access points deployed at the room's ceiling.

For the out-band D2D communication, the use of VLC is considered only in [62] and [63], where the mobile devices are equipped with a Light Emitting Diode (LED) for the transmission of the light and a photodetector for the light reception (see Figure 3). In [62], the authors propose a game theory-based mechanism choosing the optimal mode of VLC communication from three candidate modes in order to enhance the channel capacity. The first mode is a direct VLC communication (VLC D2D), the second mode is an indirect VLC communication through the access point and the third mode represents a mix of the first two modes. In other words, the paper investigates the behavior of the conventional D2D deployed in VLC bands. In [63], an optical repeater-assisted VLC D2D system is presented. The VLC repeater enables VLC for longer distances and allows to enhance the range of VLC when the direct link between the users is not available. This is an analogy to D2D relaying [64] as addressed frequently in the conventional D2D in RF bands. However, even [63] is focused purely on VLC bands and does not consider any combination of RF and VLC for the D2D communication.

However, the concept combining the in-band RF and out-band VLC for the D2D communication is not addressed in the literature. Such combination is expected to enhance the performance of the D2D communication taking an advantage of the following facts. First, there is no mutual interference between RF and VLC bands (see [7] and [56]). Second, the VLC signal is strongly attenuated with distance and with directional differences [65], thus, interference to other D2D pairs operating in VLC is naturally suppressed. At the same time, RF band still enables to preserve the benefits of the common D2D communication for larger distances at which VLC cannot operate. Of course, the combination of RF and VLC for D2D communication introduces new challenges related to the volatility of both sides of the communication chain and the proximity of users [66]. In detail, the RF-VLC D2D may suffer from a low scalability of VLC for longer distances in addition to its susceptibility to the changes of the users' orientations. In fact, even small turns in the users'

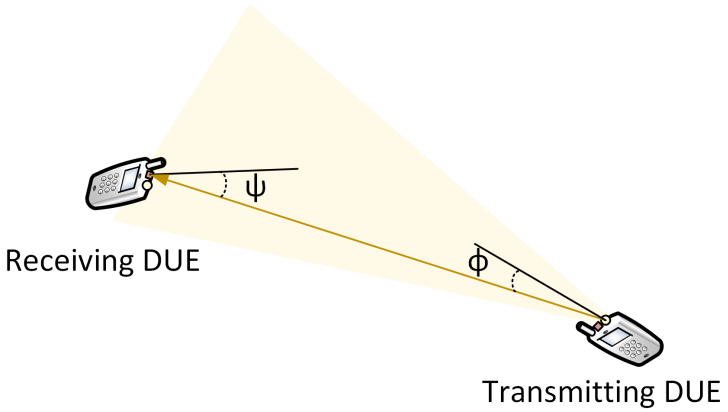


Figure 3. Principle of VLC D2D where a LED (shown in yellow) and a photodetector (shown in red) are used for data transmission and reception, respectively. Note that $\phi$ is the irradiance angle and $\psi$ is the incidence angle.

orientations in terms of irradiance and incidence angles [66], may result in a sudden decrease in the channel quality. The irradiance and incidence angles, which are based on UEs' orientations, are illustrated in Figure 3.

## 2.4 Determination of Channel Quality in Mobile Networks

In mobile networks, the knowledge of channel state information (CSI), which is related to the quality of the communication channels between the connected devices, is a key aspect, as the channels' quality knowledge is required to perform many essential radio resource management algorithms [67]. Conventionally, the UEs (or the BS) use dedicated resources to periodically transmit "reference signals" for the estimation of the communication channel quality [68]. However, these reference signals consume a lot of resources and the increases the number of resources consumed by the transmitted reference signals leads to a very high amount of signaling overhead [68].

To reduce the signaling overhead, several channel prediction schemes are proposed. These schemes predict the quality of the communication channel from other channels of known quality and are focused on the prediction of the channel quality between a single UE and an antenna at the BS at a specific frequency based on either: i) knowing the channel between this UE and the BS antenna at another frequency [69]-[78], or ii) knowing the channel between this BS antenna and another UE that is close to the original UE [79], or iii) knowing

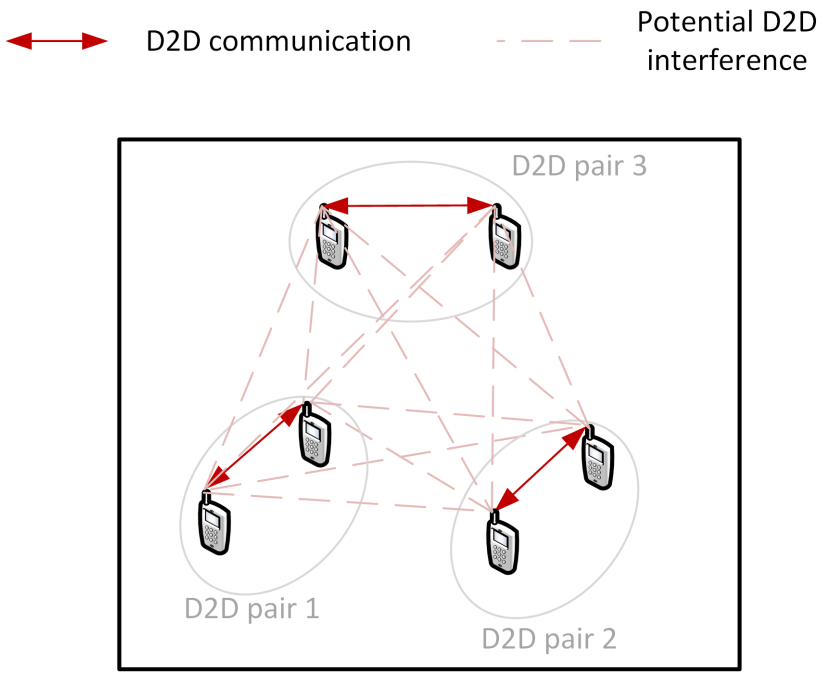


Figure 4. An example with three D2D pairs (six DUEs) showing the D2D channels that need to be estimated to get a full CSI knowledge.

the channel between this UE and another close-by antenna at the same BS [80].

In D2D communication, the CSI knowledge is essential for radio resource management (e.g., mode selection, channel allocation, power control,...etc). A major part of the existing radio resource management algorithms assume apriori measurement of the D2D channel gains, i.e., channel gains among all UEs involved in the D2D communication (e.g., [81]). Considering the D2D communication within a cell with X users in it, there are X(X-1) direct and interference D2D channels to be measured (see Figure 4). Such a high number of channels to be measured implies a very high signaling overhead. In some cases, the full CSI knowledge can be relaxed to a partial knowledge, where only a subset of the distributed D2D channel gains is required (e.g., in [82]). Nevertheless, even the partial knowledge of the D2D channel gains implies a substantial cost in terms of an additional signaling overhead on top of the one generated in classical cellular communications. Thus, predicting the D2D channels from other information available at the network (without the measurements and the additional signaling overhead resulted from the additional D2D reference signals) is a key challenge, in order to enable D2D communication for a massive amount of D2D devices. Although solving the D2D channel prediction problem is crucial and can be even a game-changer in D2D communication, no solution for this D2D channel prediction problem yet exists in the literature.

# Chapter 3

# Dissertation Objectives

The general objective of this dissertation thesis is to optimize the resource allocation in D2D communication and to study the RF-VLC D2D combination in addition to solving the CSI knowledge problem. In detail, the thesis aims:

- **Objective 1:** To study the combination of shared and dedicated communication modes for D2D communication.

- **Objective 2:** To propose channel allocation schemes in, both, dedicated and shared modes enabling the reuse of multiple channels by multiple D2D pairs in order to maximize the sum capacity under the constraints related to the minimal requirements of the D2D pairs in the dedicated mode and the cellular users in the shared mode.

- **Objective 3:** To study the combination of VLC and RF for D2D communication and, then, propose RF/VLC band selection scheme to efficiently determine the most suitable band (RF or VLC) for every D2D pair in a multi-user scenario.

- **Objective 4:** To propose a solution enabling radio resource management for a high number of UEs in D2D communication by predicting the D2D channel gains from other information already available in the network in order to reduce the signaling overhead making D2D communication feasible.

# Chapter 4

# Dissertation Results

In this chapter, the principle of combining shared and dedicated modes together for every D2D pair is presented. Then, two resource allocation schemes for the D2D dedicated and shared modes are, respectively, proposed. Both schemes for dedicated and shared modes enable the reuse of multiple channels by multiple D2D pairs maximizing the D2D pairs' sum capacity while maintaining the minimal individual capacity requirements of the D2D pairs in the case of dedicated mode and the minimal allowed reduction in the capacity of the conventional cellular users in the shared mode. Moreover, the concept of utilizing VLC together with RF for D2D communication is studied. Then, two algorithms for RF/VLC band selection in multi-user scenario are presented. While the first band selection algorithm is an iterative heuristic interference-based algorithm, the second algorithm is machine learning-based and requires less channel information with respect to the first one. In the last section of this chapter, the CSI knowledge problem in D2D communication is solved by proposing the D2D channel quality prediction scheme that relies on the knowledge of the cellular gains between the users and the surrounding base stations. Then, the same principle is used to show that the cellular gains between the users and the surrounding base stations can also be used to predict the D2D radio resource management decisions (e.g., power control decisions) directly with no knowledge of the D2D channels. Finally, the application of the proposed D2D channel prediction on an example of the UEs' association in networks with flying base stations (FlyBSs) is illustrated.

## 4.1 Combined Shared and Dedicated D2D Communication

In this section, we introduce the principle of combining the shared and dedicated modes by allowing every D2D pair to access dedicated (not used by the CUEs) and shared (used by the CUEs) resources at the same time. The aim of this combination is to improve the sum capacity of D2D pairs. Note that the channel reuse among the D2D pairs in this section is limited as optimizing the channel reuse is not the main scope of this section. Nevertheless, later in Section 4.2,

the channel reuse among the D2D pairs is, further, improved in the dedicated and shared modes, respectively. This section includes the conference paper [4C].

# Combined Shared and Dedicated Resource Allocation for D2D Communication

Pavel Mach, Zdenek Becvar, Mehyar Najla
Dpt. of Telecommunication Eng., Faculty of Electrical Engineering, Czech Technical University in Prague, Czech Republic
machp2@fel.cvut.cz, zdenek.becvar@fel.cvut.cz, najlameh@fel.cvut.cz

***Abstract*—Device-to-device (D2D) communication is an effective technology enhancing spectral efficiency and network throughput of contemporary cellular networks. Typically, the users exploiting D2D reuse the same radio resources as common cellular users (CUEs) that communicate through a base station. This mode is known as shared mode. Another option is to dedicate specific amount of resources exclusively for the D2D users in so-called a dedicated mode. In this paper, we propose novel combined share/dedicated resource allocation scheme enabling the D2D users to utilize the radio resources in both modes simultaneously. To that end, we propose a graph theory-based framework for efficient resource allocation. Within this framework, neighborhood relations between the cellular users and the D2D users and between the individual D2D users are derived to form graphs. Then, the graphs are decomposed into subgraphs to identify resources, which can be reused by other users so that capacity of the D2D users is maximized. The results show that the sum D2D capacity is increased from 1.67 and 2.5 times (depending on a density of D2D users) when compared to schemes selecting only between shared or dedicated modes.**

***Keywords—device-to-device communcation, mode selection, resource allocation, shared allocation, dedicated allocation.***

## I. Introduction

Device-to-device (D2D) communication is an emerging paradigm enhancing spectrum and energy efficiency of mobile communications systems [1]. The D2D enables direct communication of two devices in proximity without involvement of a base station, which is typically denoted as eNB in mobile networks. The direct communication allows saving radio resources by avoiding two-hop transmission of the data (to eNB and to the user). The D2D can be classified according to spectrum utilization into an in-band D2D (using license radio resources allocated to conventional cellular users) or an out-band D2D (exploiting unlicensed frequency bands, such as WiFi direct, ZigBee or Bluetooth) [2].

The D2D users (DUEs) accessing license band (i.e., in-band D2D) can use three communications modes: 1) $cellular$ mode, 2) $dedicated$ mode, also known as overlay, and 3) $shared$ mode, also known as underlay. In case of the cellular mode, the DUEs communicate through the eNB as in a conventional cellular network. The dedicated mode is distinguished by the fact that the DUEs access dedicated resources with respect to the cellular users (CUEs). Consequently, interference between the DUEs and the CUEs is efficiently avoided, but the system may experience a low spectral efficiency or an insufficient amount of resources for both types of users. In case of the shared mode, the DUEs reuse the same resources as the CUEs. Although this mode enables the highest frequency reuse when compared to other two modes, interference between the CUEs and the DUEs is the most challenging aspect here.

In recent years, significant effort has been invested to address the problem of mode selection, that is, the selection of the most profitable mode for the DUEs and efficient resources allocation. The research works related to the mode selection can be classified into papers selecting: 1) between the cellular mode and the shared or dedicated mode [3]-[8], 2) between the dedicated and shared modes [9][10], and 3) among the cellular, dedicated, and shared modes [11]-[13]. Most of the existing works focusing on the mode selection and resource allocation for DUEs expect that each DUE uses just one communication mode (cellular, dedicated, or shared). However, in [7], the authors propose to allow the DUEs to access the radio resources in the cellular and shared modes at the same time. The paper addresses routing problem deciding whether data should be routed through eNB (cellular mode) or transmitted directly between DUEs using shared mode.

In this paper, we propose a Combined Shared/Dedicated resource allocation scheme labeled as CSD. The key difference between [7] and CSD is that instead of routing problem we address resource allocation problem when the DUEs always communicate directly accessing resources in both shared and dedicated mode simultaneously. To that end, the main objective of the proposed CSD is to maximize the capacity of DUEs, while the performance of the CUEs is not impaired due to power restriction of the DUEs in the shared mode. To increase the resource utilization by the DUEs, several DUEs can access the same resources if they are not neighbors, that is, if interference among them is below a predefined threshold ($\tau_N$). In this regard, we propose a novel graph theory-based framework for determination of two neighborhood relations: i) between the CUEs and the DUEs, and ii) among the DUEs. The neighborhood relations are then exploited for the allocation of resources to the D2D pairs.

The rest of the paper is organized as follows. The next section describes the system model. The graph theory based framework for the proposed resource allocation is introduced in Section III. The Section IV explains the proposed resource allocation. Section V is dedicated for description of the simulation scenario and a discussion of the simulation results. The last section gives our conclusion and future works.

## II. System model

This section describes system model. We assume a single cell scenario with one eNB. Within coverage area of the eNB, $C$ CUEs and $D$ D2D pairs exploiting uplink cellular network resources are deployed. Each D2D pair is composed of one DUE transmitter (DUE-T) sending data to the DUE receiver (DUE-R). The DUEs of the same D2D pair always communicate directly, i.e., the cellular is not applied for the DUEs. The allocation of resources to the DUEs is fully controlled by the eNB as considered, e.g., in [11][13].

978-1-5386-6355-4/18/$31.00 ©2018 IEEE

We assume general multiple access technology, such as OFDMA or SC-FDMA, where the available bandwidth is divided into $n$ channels, represented in our case by resource blocks (RBs). The whole bandwidth is split into shared and dedicated regions. The shared region contains $n_s$ RBs that are accessible by both the CUEs and DUEs. Consequently, interference between the CUEs and the DUEs has to be taken into consideration in this region. In contrast, the dedicated region is composed of $n_d$ RBs, which are accessible only by the DUEs and, thus, there is no mutual interference between the DUEs and the CUEs.

The SINR observed by the eNB at the $r$-th RB is calculated as:

$$\gamma_e^r = \frac{g_{Ce}^r P_C^r}{NI^r + \sum_{i=1}^{D^r} g_{T_i e}^r P_i^{s,r}} \tag{1}$$

where $g_{Ce}^r$ is the channel gain between the CUE and eNB at the $r$-th RB, $P_C^r$ represents the transmission power of the CUE at the $r$-th RB, $NI^r$ stands for the thermal noise plus interference observed by the eNB from adjacent cells at the $r$-th RB, $g_{T_i e}^r$ is the channel gain between the $i$-th DUE-T and the eNB at the $r$-th RB, $P_i^{s,r}$ corresponds to the transmission power of the $i$-th DUE-T in the shared region at the $r$-th RB, and $D^r$ is the number of DUE-Ts transmitting at the $r$-th RB, because the proposed scheme allows to reuse the same RB by more than one D2D pair if interference between the D2D pairs is below a predefined threshold as explained later.

In the shared region, the transmitting power of the DUE-T is restricted in order to limit interference caused to the CUEs. The restriction of the transmission power for each DUE-T in the shared region is defined by the eNB so that the signal received by the eNB from the i-th DUE-T ($RSS_{di}$) is:

$$RSS_{di} = \frac{NI_e}{\tau_{DUE}} \tag{2}$$

where $\tau_{DUE}$ is the D2D threshold defining the amount of interference caused by the DUE-T with respect to the noise plus interference from the adjacent eNBs measured at the given eNB ($NI_e$). Since we assume $\tau_{DUE} = 10$, the level of interfering signal from the DUE-T received at the eNB is 10 times smaller than the level of interference from other sources. Hence, the performance of the CUEs can be considered as unimpaired at all by the proposed algorithm. Then, SINR observed by the DUE-R of the $j$-th D2D pair at the $r$-th RB in the shared region can be expressed as:

$$\gamma_j^{s,r} = \frac{g_{T_j R_j}^r P_j^{s,r}}{NI^r + \sum_{\substack{i=1 \\ i \neq j}}^{D^r} g_{T_i R_j}^r P_i^{s,r} + g_{CR_j}^r P_C^r} \tag{3}$$

where $g_{T_j R_j}^r$ is the channel gain between the DUE-T and the DUE-R of the same $j$-th D2D pair at the $r$-th RB, $g_{T_i R_j}^r$ stands for the channel gain between the $i$-th DUE-T and the $j$-th DUE-R at the $r$-th RB, $g_{CR_j}^r$ represents the channel gain between the CUE and the $j$-th DUE-R at the $r$-th RB, $P_j^{s,r}$ and $P_i^{s,r}$ are the transmission powers of the $j$-th and $i$-th DUE-T at the $r$-th RB, respectively. From (3), we can observe that interference to the D2D pairs in the shared region originates from other D2D pairs reusing the same resources (similarly as in (1)) and by the CUEs, which occupy the reused resources.

The SINR observed by the $j$-th DUE-R at the $r$-th RB in the dedicated region is defined as:

$$\gamma_j^{d,r} = \frac{g_{T_j R_j}^r P_j^{d,r}}{NI^r + \sum_{\substack{i=1 \\ i \neq j}}^{D^r} g_{T_i R_j}^r P_i^{d,r}} \tag{4}$$

where $P_j^{d,r}$ is the transmission power of the $j$-th DUE-T in the dedicated region and $P_i^{d,r}$ is the transmission power of the $i$-th DUE-T, which causes interference to the $j$-th D2D pair. The transmission power of the DUE-Ts in the dedicated region is not restricted as in the shared region, because the dedicated resources are not shared with the CUEs. Note that in the simulation, we consider several $P_i^{d,r}$ values and we analyze its impact on the performance.

## III. Graph theory-based framework for proposed CSD

To allocate resources to the D2D pairs properly by the proposed CSD and to avoid harmful interference, the eNB has to be aware of: 1) the list of D2D pairs that can reuse RBs already assigned to the CUEs, and 2) the list of RBs that can be reused by more than one D2D pair. Both above-mentioned aspects are determined by the eNB through the knowledge of two types of the neighborhood relations: 1) between the CUEs and the DUEs, and 1) among the DUEs. The following subsections describe a determination of the CUEs and the DUEs neighbors and explain exploitation of the neighborhood relations for the resource allocation to the D2D pairs.

### A. Determination of CUE and DUE neighbors

The DUEs may reuse RBs allocated to the CUEs that are not their neighbors. In the proposed scheme, the CUE is considered to be a neighbor of the $j$-th D2D pair if:

$$\gamma_j^{s,r} < \gamma_{min} \tag{5}$$

where $\gamma_{min}$ is minimal SINR guaranteeing reliable communication. Notice that the classification whether the CUE is neighbor or not does not solely depends on signal received from the CUE at the DUE-R. Even distant CUE can be considered as the neighbor just because the received signal quality is low. This situation can happen, for example, if the D2D-T and the D2D-R are far away from each other or if the D2D-T is in vicinity of the eNB and its transmission power is restricted according to (2) to avoid interference to the eNB. Moreover, the CUE is considered to be a neighbor even if DUE-R is strongly interfered from the CUEs belonging to other cells since the D2D pair is not able to reuse these resources due to interference.

The $\gamma_j^{s,r}$ is obtained by the eNB from channel quality report, e.g., by means of CSI reports as defined in LTE [14], sent by individual DUE-R. In this regard, the eNB dedicates specific intervals when the D2D-R should listen to the CUEs' transmissions and determine which RBs can be reused in the shared region. During these intervals, the D2D-T cannot use the RBs in the shared region for data transmission. Nevertheless, the effect on throughput is negligible as these intervals can be scheduled only sparingly (e.g., one interval with duration of 1 ms is dedicated for this purpose per one or several seconds depending on speed of the CUEs).

Besides the CUEs' neighbors, each D2D pairs may have several DUE neighbors. The D2D pairs may reuse the same RBs if they are not mutual neighbors, that is, if interference among them is below the predefined threshold. In this paper,

the $i$-th D2D pair is considered to be the neighbor of the $j$-th D2D pair if the received signal strength from the $i$-th DUE-T at the side of the $j$-th DUE-R is:

$$RSS_{ij} > \frac{NI_{R_j}}{\tau_N} \tag{6}$$

where $NI_{R_j}$ is the thermal noise plus interference observe at the $j$-th DUE-R and $\tau_N$ is the threshold distinguishing neighbors both in the shared and dedicated regions. The threshold $\tau_N$ allows to adjust the level of interference among the D2D pairs and the amount of D2D pairs, which are able to reuse the same RBs. If $\tau_N < 1$, the $i$-th D2D pair is the neighbor of the $j$-th pair despite the fact that it generates higher interference than $NI_j$ resulting in a higher reuse of the RBs. If $\tau_N > 1$, interference among the D2D pairs is lower than $NI_j$, but the reuse factor is decreased as well. The proper selection of $\tau_N$ could be seen as an optimization problem. Hence, if we define $C^s$ and $C^d$ as capacities in the shared and dedicated regions, the objective is to find $\tau_{N,opt}$ so that:

$$[\tau_{opt}] = \underset{\tau_N}{\operatorname{argmax}}(C^s + C^d), \tau_N \in \{\tau_{N,min}, \tau_{N,max}\} \tag{7}$$

Due to the limited space, we leave a derivation of $\tau_{N,opt}$ analytically for future research and we just investigate its impact on the performance by simulations.

The D2D pairs can find their neighbors by means of discovery procedure proposed in [15], where the DUE-R measures experienced SINR of the received discovery messages send by other DUE-Ts. Then, the D2D-R sends SINR report to the eNB. Notice that the DUE-R may send reports from measurement of the CUE and the DUE neighbors at the same time.

### *B. Forming graphs, graph decomposition into subgraphs, and determination of maximal cliques*

Based on the channel quality reported by the DUE-Rs for determination of the neighborhood relations, as explained in previous subsections, two graphs are created: one for shared region, one for the dedicated region. The graph for shared region is denoted as $G^s = (V_x^s, E_x^s)$, where $V_x^s$ represents individual D2D pairs that are able to reuse the RBs in the shared region (vertices of graph), and $E_x^s$ represents interference between the D2D pairs in the shared region. Analogously, the graph for dedicated region is denoted as $G^d = (V_x^d, E_x^d)$, where $V_x^d$ represents the D2D pairs using the RBs in the dedicated region and $E_x^d$ shows neighborhood relations (by means of interference) between the D2D pairs in the dedicated region.

To allow the eNB allocate the RBs to the D2D pairs in both regions, the eNB further decomposes $G^s$ and $G^d$ into a set of subgraphs so that each subgraph contains only D2D pairs that can potentially reuse the same RBs. In case of $G^s$, the individual subgraphs $(G^{s,1}, G^{s,2}, ..., G^{s,C})$ are composed of the D2D pairs that are able to reuse the RBs assigned to the same CUE. Consequently, the number of subgraphs in shared region is exactly the same as the number of the CUEs. Moreover, the number of RBs available for each subgraph corresponds to the number of RBs assigned to individual CUEs. In case of $G^d$, the individual subgraphs $(G^{d,1}, G^{d,2}, ..., G^{d,D})$ are composed of the D2D pairs that can reuse the RBs assigned to other D2D pairs in the dedicated region (i.e., one subgraph is created for each D2D pair). Notice that in the dedicated region, the D2D pairs receives always some RBs allocated to them by default and the RBs that can be reused from other D2D pairs.

To properly allocate the RBs to the D2D pairs within each subgraph, the maximal cliques in all subgraphs are found by the eNB. In general, the clique in $G$ is defined as a subset of vertices (in our case subset of D2D pairs), $C \subseteq V$, such that resulting subgraph is a complete graph. Then, the clique is called a maximal clique in $G$ if there is no clique $C'$ such that $C' \supset C$. In other words, the maximal clique is not a subset of any other cliques in $G$. As a consequence, the D2D pairs in the same maximal clique cannot reuse the same RBs. The eNB finds all maximal cliques in $G^s$ and $G^d$ subgraphs by means of Bron-Kerbosch algorithm [16]. The complexity of the algorithm is in the worst case $O(3n/3)$, where n is the number of D2D pairs. Despite the fact that Bron-Kerbosch algorithm is NP-hard, it can be used even in large networks as demonstrated in [17].

The creation of the graphs $G^s$ and $G^d$ and their further decomposition into subgraphs and determination of the maximal cliques is illustrated in Fig. 1. In Fig. 1a, $G^s$ is composed of the D2D pair 1, 2 and 4 as these can utilize the RBs in the shared region according to (5). Then, three subgraphs are created (each for single CUE): $G^{s,1}$ indicating that the D2D pair 1 and 4 can reuse the RBs allocated to the CUE 1, $G^{s,2}$ saying that resources used by the CUE 2 can be exploited by the D2D pair 4, and $G^{s,3}$ showing that the D2D pair 1 and 2 can reuse the RBs allocated to the CUE 3. In Fig. 1a, $G^d$ is decomposed into four subgraphs (each for one D2D pair): $G^{d,1}$ indicating that the RBs assigned to the D2D pair 1 can be fully reused by the D2D pair 4, $G^{d,2}$ showing the RBs for the D2D pair 2 can be reused by the D2D pair 3 and 4, etc. Finally, the eNB finds all maximal cliques within each subgraph ($N_{mc}$). For example, there are two maximal cliques $\{1\}$ and $\{4\}$ in $G^{s,1}$ ($N_{mc}^{s,1} = 2$), one maximal clique $\{4\}$ for $G^{s,2}$ ($N_{mc}^{s,2} = 1$), and one maximal clique $\{1, 2\}$ for $G^{s,3}$

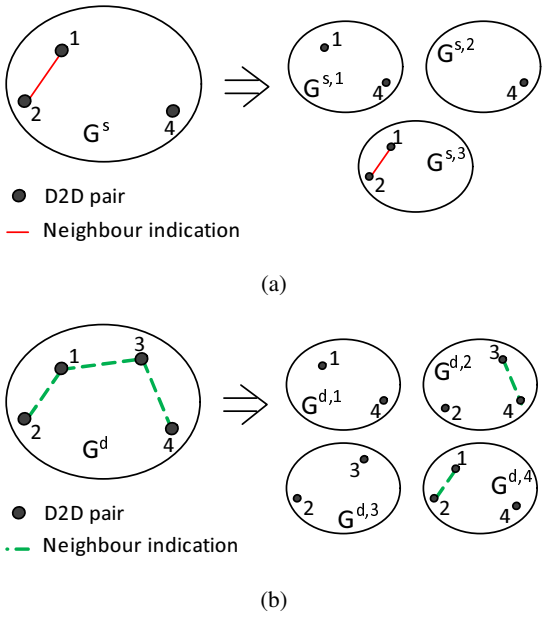


Fig. 1: Example of $G^s$ and $G^d$ determination and their decomposition into subgraphs and maximal cliques.

($N_{mc}^{s,3} = 1$). Analogously, there are two maximal cliques $\{1\}$ and $\{4\}$ in $G^{d,1}$ ($N_{mc}^{d,1} = 2$), two maximal cliques $\{2\}$ and $\{3,4\}$) exists in $G^{d,2}$ ($N_{mc}^{d,2} = 2$), etc.

### C. Formulation of objectives for the proposed CSD scheme

The objective of the proposed CSD resource allocation scheme is to maximize sum D2D capacity ($C$). The $C$ is a sum of the capacities in the shared region ($C^s$) and in the dedicated region ($C^d$). As the $C^s$ and $C^d$ are independent, we can maximize these two capacities separately. Hence, the first objective is to maximize $C^s$ as:

$$C^s = \max \left( \sum_{z=1}^{C} \left( \sum_{k=1}^{N_{mc}^{s,z}} \left( \sum_{r=1}^{n_{mc}^{s,z}} \Gamma_k^{s,z,r} \right) \right) \right) \quad \text{s.t.} \quad n_{mc}^{s,z} \leq n_c^z, \ \forall z, \quad P_j^{s,r} \text{ restricted acc. (2)} \tag{8}$$

where $n_{mc}^{s,z}$ is the number of RBs in individual maximal clique, $N_{mc}^{s,z}$ represents the number of maximal cliques found in the individual subgraphs, $\Gamma_k^{s,z,r}$ is the transmission efficiency representing the number of bits transmitted in the $r$-th RB of the $k$-th maximal clique of the D2D pairs reusing resources assigned to the $i$-th CUE, and $n_c^z$ is the amount of RBs allocated to the $z$-th CUE. Note that $\Gamma_k^{s,z,r}$ is derived from $\gamma_j^{s,r}$ in the shared region. The capacity in shared region is restricted by the number of RBs available in each maximal clique ($n_{mc}^{s,z}$) and by the power constrains according to (2).

The second objective is to maximize $C^d$ as:

$$C^d = \max \left( \sum_{z=1}^{D} \left( \sum_{k=1}^{N_{mc}^{d,z}} \left( \sum_{r=1}^{n_{mc}^{d,z}} \Gamma_k^{d,z,r} \right) \right) \right) \quad \text{s.t.} \quad n_{mc}^{d,z} \leq n_d^z \ \ \forall z \tag{9}$$

where $N_{mc}^{d,z}$ is the number of maximal cliques found in individual subgraphs, $\Gamma_k^{d,z,r}$ stands for the transmission efficiency in the dedicated region, and $n_d^z$ is the amount of RBs allocated by default to the $z$-th D2D pair. The capacity in the dedicated region is restricted by the amount of RBs available in each maximal clique ($n_{mc}^{d,z}$) analogously to the shared region.

## IV. Algorithm for proposed CSD scheme

The allocation of resources according to CSD scheme is composed of: 1) allocation of RBs to the CUEs as this directly impacts the amount of RBs in both shared and dedicated regions, 2) allocation of RBs to the DUEs in the shared region, and 3) allocation of the RBs available for the DUEs in the dedicated region. To this end, we propose the algorithm for allocation of resources that can be divided into seven subsequent steps:

1) Allocation of $n_s$ RBs to the CUEs in the shared region, i.e., the region where RBs are accessible by both the CUEs and the DUEs. The amount of RBs in the shared region depends on two factors: 1) current requirements of the CUEs and 2) the amount of RBs that can be used by the DUEs in the shared and dedicated regions. The second factor takes into account the fact that not all D2D pairs may be able to reuse the RBs in the shared region due to the power restriction according to (2). For example, if the eNB would allocate all the RBs to the CUEs, some D2D pairs may not be able to communicate at all. In this paper we consider the same amount of RBs available in both shared and dedicated regions. A dynamic allocation of the amount of RBs in individual regions considering two above-mentioned factors is left for future research.
2) Determination if individual D2D pairs can reuse the RBs allocated to the CUE(s) in the shared region if (5) is fulfilled (as explained in Section 3).
3) Determination if multiple D2D pairs can reuse the same RBs assigned to the same CUE. This is done by finding all maximal cliques in individual subgraphs $G^{s,z}$, where $1 \leq z \leq C$ (see Fig. 1a).
4) Allocation of the resources to individual D2D pairs in the shared region maximizing $C^s$. This is done by allocation of the RBs to the D2D pairs with the highest transmission efficiency according to (8).
5) Allocation of the default amount of RBs ($n_d^i$) in the dedicated region to each D2D pair, where the default number of the RBs allocated to the $i$-th D2D pair $n_d^i$ is calculated as:

$$n_d^i = n_d \frac{N_{mc}^{d,i}}{\sum_{z=1}^{D} N_{mc}^{d,z}} \tag{10}$$

The $n_d^i$ is proportional to the amount of maximal cliques as this determines how many times the RBs allocated by default to the D2D pair can be reused in the dedicated region by the other D2D pairs.
6) Determination of the RBs, which can be potentially reused and by whom these can be reused depending on the allocation of RBs in the previous step and the knowledge of neighborhood relations among D2D pairs obtained from subgraphs $G^{d,z}$, where $1 \leq z \leq D$ (see Fig. 1b).
7) Allocation of resources to individual D2D pairs in the dedicated region maximizing $C^d$. This is done by the allocation of the RBs to the D2D pairs with the highest transmission efficiency according to (9).

The example of allocation process according to the proposed algorithm is shown in Fig. 2, where $n_s$ = $n_d$ = 8 RBs and neighborhood relations are taken from Fig. 1. The allocation process is as follows:

1) The eNB allocates RBs to the CUEs in the shared region.
2) The eNB identifies that the D2D pair 1 and 2 can reuse RBs allocated to the CUE 1 and CUE 3, while the D2D pair 4 reuses RBs assigned to the CUE 2. The D2D pair 3 is not able to reuse any RBs in the shared region.
3) The eNB determines that the D2D pair 1 and 2 are mutual neighbors (i.e., orthogonal RBs have to be allocated to them in the shared region), while the D2D pair 4 has no neighbors that are able to reuse the RBs of the CUE 2.
4) According to (8), the eNB allocates all RBs assigned to the CUE 1 to the D2D pair 1 since the D2D pair 1 has higher transmission efficiency at these RBs than the D2D pair 2. Contrary, the D2D pair 2 reuses all RBs allocated to the CUE 3 as it experiences higher transmission efficiency at these RBs than the D2D pair 1. Finally, the D2D pair 4 reuses all RBs allocated to the CUE 2.
5) The eNB allocates $n_d^i$ RBs to individual D2D pairs taken into account (10). According to Fig. 1b, all subgraphs contain two maximal cliques. Hence, each D2D pair obtains $n_d^i$ = 2 RBs by default.
6) The eNB determines that the D2D pair 1 can reuse RBs allocated to the D2D pair 4, the D2D pair 2 can reuse the

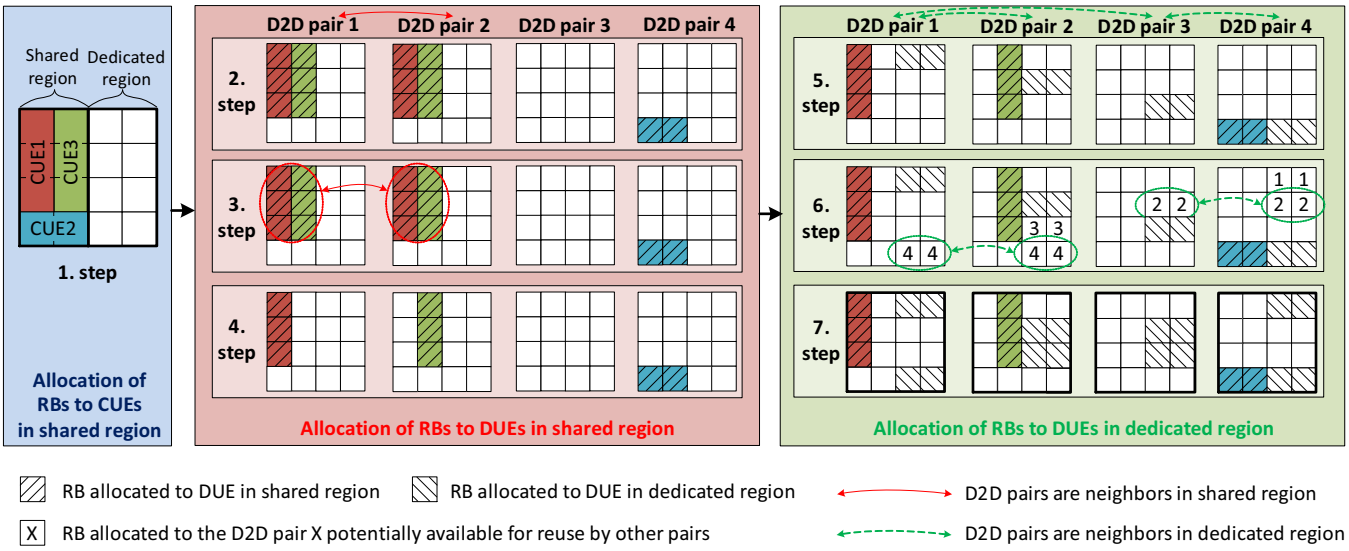


Fig. 2: Example of allocation process according to proposed allocation algorithm.

RBs assigned to the D2D pair 3 and 4, the D2D pair 3 can reuse the RBs allocated to the D2D pair 2, and the D2D pair 4 can reuse the RBs assigned to the D2D pair 1 and 2.

7) To meet (9), the eNB decides that the RBs allocated by default to the D2D pair 1 can be fully reused by the D2D pair 4 since the D2D pair 1 experiences higher transmission efficiency than the D2D pair 2 at these RBs. Similarly, the RBs allocated to the D2D pair 2 should be reused solely by the D2D pair 3 since it has higher transmission efficiency at these RBs than the D2D pair 4. Then, the RBs allocated by default to the D2D pair 3 are available for reuse by the D2D pair 2, and the RBs of the D2D pair 4 are reused by the D2D pair 1.

## V. Simulations

This section describes simulation scenario and models used for evaluation and, then, simulation results are presented and discussed.

### A. Simulation scenario

The performance of the proposed scheme is evaluated in MATLAB simulator. We assume square simulation area with size of 500 m. The simulation area contains one eNB deployed in the middle of the area, 20 CUEs and up to 75 D2D pairs. Both the positions of the CUEs and the D2D pairs are generated randomly with uniform distribution. The maximum distance of the UEs creating D2D pair is set to 200 m. We assume that D2D pairs always communicate directly as communication through the eNB (i.e., cellular mode) introduces no benefits. Further, we assume a physical layer data frame with duration of 10 ms and channel bandwidth of 20 MHz like in LTE. Each frame is composed of 2 000 RBs used either for data transmission (75 % of RBs) or for signaling (25 % of RBs). We consider that the amount of RBs in the shared and dedicated regions available for the data transmission is split equally, that is, 750 RBs are intended for shared region accessible by the CUEs and the D2D pairs and the other 750 RBs in dedicated region is accessed only by the D2D pairs.

TABLE I: Parameters and settings for simulations

| Parameter | Value |
|---|---|
| Simulation area | 500x500 |
| Number of CUEs | 20 |
| Number of D2D pairs | 5–75 |
| Max. distance between DUE-T and DUE-R | 200 m |
| Carrier frequency | 2 GHz |
| Channel bandwidth | 20 MHz |
| Signaling overhead | 25 % |
| Number of RBs in shared/dedicated regions | 750/750 |
| Transmission power of CUE and DUEs in dedicated region | 10, 15, 20 dBm |
| $\tau_N$ | -30–0 |
| $\gamma_{min}$ | -9.478 dB |
| $\tau_{DUE}$ | 10 dBm |
| Number of simulation drops | 200 |

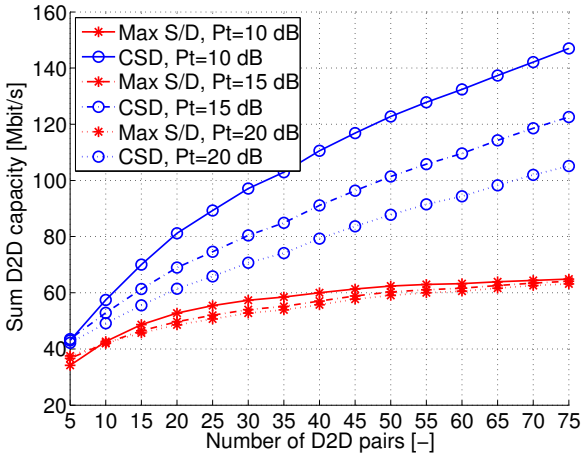


Fig. 3: Sum capacity depending on number of D2D pairs.

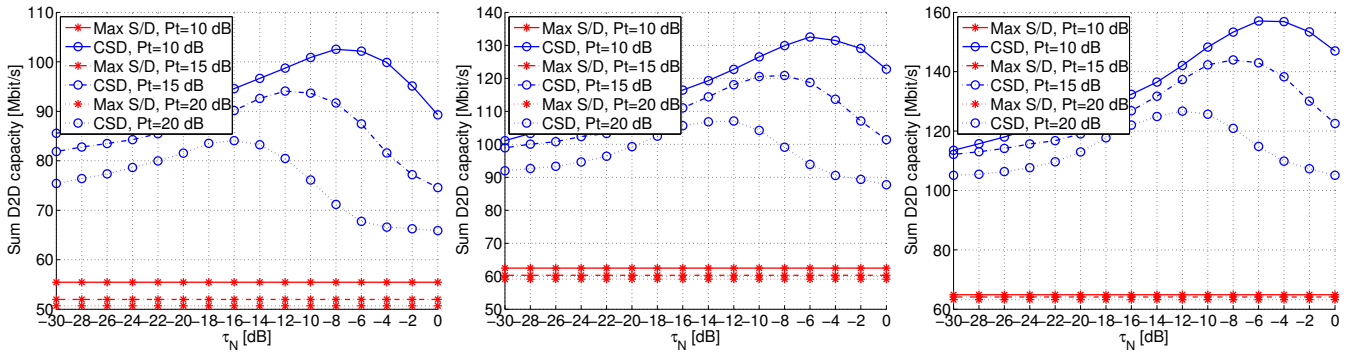


(a) 25 D2D pairs (b) 50 D2D pairs (c) 75 D2D pairs

Fig. 4: Sum D2D capacity depending on $\tau_N$.

The calculation of path loss for CUE-eNB, DUE-eNB, CUE-DUE, and DUE-DUE is done according to the models defined by 3GPP for evaluation of the D2D proximity services [18].

The simulation results are averaged out over 200 simulation drops. During each drop, new positions of the CUEs and the D2D pairs are generated. All simulation parameters are summarized in Table I.

### B. Simulation results

The simulations results compare the proposed CSD with schemes based on [9][10], which are the only most recent schemes considering the D2D pairs use solely either dedicated or shared resources so that the capacity is maximized (labeled Max S/D).

Fig. 3 shows the sum D2D capacity depending on the number of deployed D2D pairs. Notice that we do not analyze the capacity of the CUEs as our objective is to enhance performance of the DUEs while the CUEs are not affected by power restrictions in shared region). The proposed CSD allocation significantly outperforms the existing Max S/D scheme selecting either shared or dedicated resources. If transmission power of the CUEs and the D2D pairs in the dedicated region is set to lower values (e.g., 10 dB in our figure), the CSD brings approximately 2.3 times higher capacity for 75 D2D pairs deployed in the system when compare to Max S/D scheme. Even though the gain of the CSD over Max S/D is lowered if Pt is set to 15 dB (roughly 2 times higher capacity) and 20 dB (roughly 1.67 times higher capacity), the proposed CSD scheme is superior to Max S/D. The main reason why the capacity of the CSD is increasing with a decreasing Pt is that the D2D pairs are more interfered in the shared region by the CUEs and also interference among D2D pairs in the dedicated region is increased as well.

The performance of the CSD is influenced by a setting of the neighborhood threshold $\tau_N$ as already discussed in Section III. While in Fig. 3 $\tau_N$ = 0 dB is considered, Fig. 4 shows the impact of $\tau_N$ on the sum D2D capacity. We consider $\tau_N$ varying between -30 dB and 0 dB. Notice that for better clarity, we express in the simulations $\tau_N$ in dB while in (6) $\tau_N$ is without unit . It is seen that the optimal value of $\tau_N$ is depends on the transmission power $Pt$ and also on the amount of D2D pairs in the system (see Fig. 4). In general, if the transmission power $Pt$ is increased, $\tau_N$ should be set to lower values to achieve the maximal capacity. For example, if there are 25 D2D pairs in the system, the optimal value for $\tau_N$ is -8 dB, -12 dB, and -16 dB for Pt = 10, 15, and 20 dBm, respectively (see Fig. 4a). If the number of D2D pairs is increased to 50 or event to 75, the optimal values of $\tau_N$ are slightly higher (by 2-4 dB) when compared to the case with only 25 D2D pairs in the system. The reason why, $\tau_N$ should be set to lower values for higher $Pt$ is that the D2D pairs are able to reuse resources in shared region more efficiently for lower $\tau_N$ than for higher $\tau_N$. Moreover, $\tau_N$ should be set to higher values for the higher numbers of D2D pairs because an increased ratio of the resource that can be reused by the D2D pairs (achieved by lower $\tau_N$) is not able to outweigh significant interference among D2D pairs themselves. As in previous figure, the sum D2D capacity is degraded for higher Pt since the D2D pairs are interfered by the CUEs in shared region more significantly.

The optimal setting of neighborhood threshold $\tau_N$ also leads to a higher gain achieved by the proposed CSD over the Max S/D scheme. The sum capacity with the optimum threshold $\tau_N$ is increased by 2.5, 2.3, and 2 times for $Pt$ = 10, 15, and 20 dBm, respectively, for 75 D2D pairs. Note that appropriate setting of $\tau_N$ in real network can be considered as future work.

## VI. Conclusions

This paper has proposed the combined shared/dedicated resource allocation scheme for D2D communications. The proposed CSD scheme allows the D2D pairs to utilize resources in both shared and dedicated regions simultaneously. In addition, the same resources can be exploited by several D2D pairs in order to enhance spectral efficiency of the system and to increase overall sum D2D throughput. In this regard, we have introduced graph theory based framework for the purpose of efficient resource allocation. Within this framework, the eNB creates graph showing neighborhood relations between the CUE and D2D pairs and between individual D2D pairs. After decomposition of the graphs into subgraphs and determination of the maximal cliques, the eNB is able to allocate resources maximizing sum D2D throughput. The results indicate that the D2D capacity can be significantly improved (more than twice) when compared to the scheme selecting only the shared or the dedicated region.

As a future work, we intend to perform in-depth theoretical analysis for deriving of optimal D2D neighborhood threshold.

## ACKNOWLEDGMENT

This work has been supported by Grant No. GA17-17538S funded by Czech Science Foundation.

## REFERENCES

[1] P. Mach and Z. Becvar, "In-Band Device-to-Device Communication in OFDMA Cellular Networks: A Survey and Challenges," *IEEE Comunnications Surveys & Tutorials*, 17(4), pp. 1885-1922, 2015.

[2] A. Asadi, Q. Wang, and V. Mancuso, "A Survey on Device-to-Device Communication in Cellular Networks," *IEEE Comunnications Surveys & Tutorials*, 16(4), pp. 1801-1819, 2014.

[3] R. Wang, J. Zhang, S.H. Song, and K. B. Letaief, "QoS-Aware Joint Mode Selection and Channel Assignment for D2D Communications," IEEE ICC, 2016.

[4] M. Klugel and W. Kellerer, "Leveraging The D2D-Gain: Resource Efficiency Based Mode Selection for Device-to-Device Communication," IEEE Globecom, 2016.

[5] Y. Liu, "Optimal Mode Selection in D2D-Enabled Multibase Station Systems," *IEEE Communication Letters*, 20(3), 470-473, 2016.

[6] M. Azam, et al., "Joint Admission Control, Mode Selection, and Power Allocation in D2D Communication Systems," *IEEE Transactions on Vehicular Technology*, 65(9), 7322-7333, 2016.

[7] E. Naghipour and M. Rasti, "A Distributed Joint Power Control and Mode Selection Scheme for D2D Communication Underlaying LTE-A Networks," IEEE WCNC, 2016.

[8] H.-J. Chou and R. Y. Chang, "Joint Mode Selection and Interference Management in Device-to-Device Communications Underlaid MIMO Cellular Networks," *IEEE Transactions on Wireless Communications*, 16(2), 1120-1134, 2017.

[9] F. Jiang, "Mode Selection and Resource Allocation for Device-to-Device Communications in 5G Cellular Networks," *China Communications*, 13(6), 32-47, 2016.

[10] D. Ma, N. Wang, and X. Mu, "Resource Allocation for Hybrid Mode Device-to-Device Communication Networks," IEEE WCSP, 2016.

[11] Y. Huang, et al., "Mode Selection, Resource Allocation, and Power Control for D2D-Enabled Two-Tier Cellular Network," *IEEE Transactions on Communications*, 64(8), 3534-3547, 2016.

[12] Y. Li, M. C. Gursoy, and S. Velipasalar, "Joint Mode Selection and Resource Allocation for D2D Communications under Queueing Constraints," IEEE Infocom Workshop, 2016.

[13] J. Kim, S. Kim, J. Bang, and D. Hong, "Adaptive Mode Selection in D2D Communications Considering the Bursty Traffic Model," I*EEE Communications Letters*, 20(4), 712-715, 2016.

[14] H. A. M. Ramli and M. A. Sukor, "Performance Analysis on Automated and Average Channel Quality Information (CQI) Reporting Algorithm in LTE-A," IEEE ICCCE, 2016.

[15] M. Naslcheraghi, L. Marandi, and S. A. Ghorashi, "A Novel Device-to-Device Discovery Scheme for Underlay Cellular Networks," ICEE, 2017.

[16] C. Bron, J. Kerbosch, "Algorithm 457: Finding All Cliques on an Undirected Graph," *ACM Communication Magazine*, 16(9), 1973, pp. 575-577.

[17] J. Cheng, Y. Ke, A. W.-Ch Fu, J. X. Yu, L. Zhu, "Finding Maximal Cliques in Massive Networks," *ACM Transaction on Database Systems*, 36(4), 2011.

[18] 3GPP TR 36.843 "Study on LTE device to device proximity services," (Release 12), V12.0.1, 2014.

## 4.2 Resource allocation in In-band D2D Communication

This section deals with the optimization of resource allocation in dedicated and shared modes, respectively.

### 4.2.1 Enabling the reuse of Multiple Channels by Multiple Pairs in D2D Dedicated Mode

In this subsection, the reuse of multiple channels by multiple D2D pairs is enabled in the D2D dedicated mode to maximize the sum capacity of D2D pairs under the constraint of guaranteeing a minimal required capacity for every D2D pair. This subsection includes the journal paper [1J], which is an extension of the conference paper [2C].

# Reuse of Multiple Channels by Multiple D2D Pairs in Dedicated Mode: Game Theoretic Approach

Mehyar Najla, *Student Member, IEEE,* Zdenek Becvar, *Senior Member, IEEE,* and Pavel Mach, *Member, IEEE,*

***Abstract*—Device-to-device communication (D2D) is expected to accommodate high data rates and to increase the spectral efficiency of mobile networks. The D2D pairs can opportunistically exploit channels that are not allocated to conventional users in a dedicated mode. To increase the sum capacity of D2D pairs in the dedicated mode, we propose a novel solution that allows the reuse of multiple channels by multiple D2D pairs. In the first step, the bandwidth is split among D2D pairs so that each pair communicates at a single channel that guarantees a minimal capacity for each pair. Then, the channel reuse is facilitated via a grouping of the D2D pairs into coalitions. The D2D pairs within one coalition mutually reuse the channels of each other. We propose two approaches for the creation of the coalitions. The first approach reaches an upper-bound capacity by optimal coalitions determined by the dynamic programming. However, such approach is of a high complexity. Thus, we also introduce a low-complexity algorithm, based on the sequential bargaining, reaching a close-to-optimal capacity. Moreover, we also determine the optimal power allocated to each reused channel. Simulations show that the proposed solution triples the sum capacity of the state-of-the-art algorithm with the highest performance.**

***Keywords*—Device-to-device; Dedicated mode; Game theory, Resource allocation, Channel reuse**

## I. Introduction

High data rates and low latencies are required to enable new services and to increase the number of connected devices in the future mobile networks. To accommodate these demands, a direct communication between two user equipments (UEs) in proximity of each other, known as Device-to-Device (D2D) communication, is considered as a promising technology [1], [2]. Two D2D UEs (DUEs), a transmitter ($\text{DUE}_T$) and a receiver ($\text{DUE}_R$), create a single D2D pair, within which the data is transmitted directly, i.e., without being relayed through a base station (in this paper, denoted as gNB in line with 3GPP terminology for 5G mobile networks) [3].

The D2D communication enables two possible modes: 1) a *shared mode* in which the D2D pairs reuse the resources allocated to common cellular UEs (CUEs) communicating via the gNB and 2) a *dedicated mode* in which the D2D pairs use dedicated resources that are not assigned to the CUEs [4],[5]. Although, the shared mode offers a higher spectral efficiency than the dedicated one, the higher efficiency is usually at the cost of highly complex solutions for the resource allocation and management. Moreover, the shared mode leads to a mutual interference among the CUEs and the DUEs. This interference can be too high and can vary frequently and significantly, especially in the case with a dense presence of the UEs. Consequently, the reliability of the communication cannot be easily guaranteed and overall quality of services (QoS) can be impaired due to the interference in the shared mode [6]. Thus, the DUEs with strict requirements on QoS should prefer the dedicated mode, which is suitable for the services that require highly reliable communication with a minimum risk of an unexpected interference from the CUEs. Concrete and up-and-coming examples of the use cases for the dedicated mode are the direct communication of vehicles or public safety communication. In such use cases, an ultra-reliable communication with a guaranteed minimum communication capacity should be ensured. In the shared mode, however, interference might lead to the situations when such guarantee is simply not possible and the unreliability in the communication can have grievous consequences. Hence, the dedicated resources are commonly considered for the vehicular or public safety communications. Thus, in this paper, we focus on the dedicated mode for D2D communication.

One of the key challenges in the dedicated mode is the allocation of the available bandwidth to the D2D pairs. The authors in [7] and [8] present channel allocation schemes that divide the dedicated bandwidth to channels with different bandwidths so that each D2D pair gets exactly one channel. In both [7] and [8], the optimal allocation is achieved for the case when the interference from other neighboring cells is nonexistent. However, in real networks, the interference from other cells always exists and we can expect the level of interference will even increase in the future due to the densification of mobile networks. Such inter-cell interference impacts the optimal channel allocation for the D2D pairs in the dedicated mode. Moreover, neither [7] nor [8] assume the reuse of each channel by more than one D2D pair resulting in a lower spectral efficiency.

A simplified channel reuse in the dedicated mode is presented in [9][10][11]. Although all these studies consider that either two D2D pairs [9] or multiple D2D pairs [10][11] can access the same channel, each D2D pair is allowed to occupy just one channel at any time. The papers [12]–[14] exploit the reuse of multiple channels by multiple D2D pairs to guarantee a minimal SINR for every D2D pair while using the minimal possible number of channels. In these works, however, the D2D pairs do not benefit fully from the reuse, as only a limited number of channels is used and the sum capacity is not maximized. In [15], the authors maximize the sum capacity of D2D pairs in the dedicated mode considering that the D2D

This work has been supported by grant No. GA17-17538S funded by Czech Science Foundation and by the grant of Czech Technical University in Prague No. SGS17/184/OHK3/3T/13.

M. Najla, Z. Becvar and P. Mach are with the Faculty of Electrical Engineering, Czech Technical University in Prague, Czech republic Technicka 2, 166 27 Prague e-mails: {najlameh, zdenek.becvar, machp2}@fel.cvut.cz

pairs reuse all available channels. Nevertheless, the authors do not consider the constraint on the minimal capacity $C_{min}$ that should be guaranteed to the individual D2D pairs. Thus, the solution proposed in [15] can lead to the situation when some D2D pairs end up with zero capacity as these are forbidden to transmit at any channel due to the interference caused to other D2D pairs. Note that the ideas presented in [12]–[15] cannot be easily extended to maximize the sum capacity and, at the same time, to guarantee $C_{min}$, since the capacity maximization under the constraint on $C_{min}$ for every D2D pair requires completely different solutions.

In summary, the existing resource allocation methods for the dedicated mode either restrict the number of D2D pairs reusing a single channel (e.g., [7][8]) or limit the number of channels that can be occupied by a single D2D pair (e.g., [9][10][11]). As an exception, the papers [12]–[15] allow the reuse of multiple channels by multiple D2D pairs in the dedicated mode. These papers target either the sum capacity maximization ([15]) or the individual minimal capacity ($C_{min}$) satisfaction ([12]–[14]). However, none of these papers maximizes the sum capacity while guaranteeing $C_{min}$ to every D2D pair.

Despite our focus on the dedicated mode in this paper, we survey also research targeting the shared mode and we also summarize related works on the channel reuse not considering D2D communication at all in order to justify the novelty of our solution from a broader perspective. Most of the existing channel allocation algorithms in the shared mode assume a restriction on either the number of D2D pairs that can reuse a single channel [16]–[20] or the number of channels that can be occupied by each D2D pair [21]–[29]. An exception to these restrictions is represented by [30] and [31]. These papers allow the reuse of multiple channels by multiple D2D pairs in the shared mode. Nevertheless, the channel allocation approaches from [30] and [31] depend on the presence of the CUEs. In other words, the optimized utility function in [30] is convex only if the interference caused to the CUEs by the D2D pairs is taken into account. The utility function becomes non-convex if the dedicated mode is considered and the presented solution becomes infeasible. Similarly, in [31], the presented solution adds the D2D pairs sequentially to the channels, which are already occupied by the CUEs. Hence, the decision of the D2D pairs whether to communicate over the given channel or not is based on the interference from/to the CUEs. Moreover, when the D2D pair reuses the channel according to [31], the D2D pair sets its transmission power at this channel based on the allowed interference imposed by this D2D pair to the corresponding CUE. Considering this, the channel and power allocations in [31] essentially depend on the existence of the CUEs that are completely absent in the dedicated mode and can be absent even in the shared mode with (very realistic) situation when the CUEs do not occupy all channels.

Besides the work addressing the reuse of channels for D2D communication, ongoing research is focused also on multiple links communicating over multiple channels for other scenarios and concepts. For example, in [32], many-to-many matching game is exploited to allocate multiple channels to multiple cellular links (i.e., links from multiple UEs to the gNB) in non-orthogonal multiple access-based networks. Since the matching games generally fall into the category of non-cooperative games, every link aims to selfishly maximize its own capacity. Consequently, the matching approach does not guarantee any $C_{min}$ to individual links. Although the cooperative "coalitions' formation games" are also used widely for the channel reuse problem, e.g., in cognitive femtocell networks [33] or in cloud radio access networks [34], these approaches allow the users in the coalition to reuse a single channel only. Moreover, both [33] and [34] cannot be simply extended to the case where the UEs can access multiple channels, because [33] considers the coalitions' creation problem in the partition form (different problem compared to channel reuse problem in D2D communication) and [34] solves the coalitions' formation problem with a predefined final number of coalitions, but this number is usually not known in advance as it should be an output of the optimization.

In our paper, we focus on the resource allocation in D2D dedicated mode and we propose a solution that allows the reuse of multiple channels by multiple D2D pairs to maximize the sum capacity while guaranteeing $C_{min}$ to individual D2D pairs. The major contributions of the paper are summarized as follows:

- We present and solve the problem of reusing multiple channels by multiple pairs as a coalition structure generation problem in order to put the D2D pairs into disjoint coalitions in a way that all D2D pairs in the same coalition can reuse the channels of each other. We derive the optimal coalitions by means of the dynamic programming reaching a theoretical maximum sum capacity while each D2D pair is still guaranteed to receive at least $C_{min}$.
- Since the dynamic programming is of a high complexity, we also propose a sequential bargaining game to determine the coalitions of the D2D pairs mutually reusing multiple channels. The heuristic sequential bargaining-based approach is of a low complexity and reaches a close-to-optimal performance.
- In order to facilitate the channel reuse in an efficient way, we analytically derive the optimal initial channel bandwidth allocation for the D2D pairs in the dedicated mode if interference from other cells is considered.
- Furthermore, we analytically determine the optimal allocation of the DUEs' transmission power over the reused channels within the coalitions. Since the defined optimization problem for power allocation is not convex, we approximate the problem to the convex one and we discuss the assumptions under which this approximation is realistic.
- We demonstrate that the proposed solution combining the optimal allocation of the bandwidth available to the D2D pairs, the novel reuse of multiple channels by multiple D2D pairs exploiting sequential bargaining game, and the optimal power allocation significantly outperforms state-of-the-art solutions and reaches close-to-optimal sum capacity of the D2D pairs. Moreover, we show that our proposed algorithm is of a low complexity and exhibits very short convergence time. This allows its implementation in real networks.

Note that a basic idea of the sequential bargaining solution for the coalitions' creation in its simplified version without

any optimization and also without the optimal bandwidth and power allocations is presented in our prior conference paper [35].

The rest of the paper is organized as follows. In Section II, the system model is described and the targeted problem is formulated. In Section III, the proposed resource allocation scheme for D2D communication in the dedicated mode is presented. The simulations results are discussed in Section IV. Last, Section V concludes the paper and outlines possible future research directions.

## II. System model and problem formulation

In this section, we first describe the system model and, then, we formulate the problem, which is solved later in the next sections of this paper.

### A. System model

In our model, $N$ D2D pairs are uniformly deployed within an area. Each D2D pair is composed of one DUE$_T$ and one DUE$_R$. The DUE$_T$ and the DUE$_R$ in a single D2D pair are fixed for a specific time interval (such as, e.g., a communication session during which the transmitter sends data to the receiver). This assumption is in line with the common purpose of the D2D communication when a high amount of data is transmitted from one device to another, as assumed in, e.g., [36]. The distance $d$ between the DUE$_T$ and the DUE$_R$ creating the D2D pair is at most equal to a maximal distance $d_{max}$ (i.e., $d \leq d_{max}$) guaranteeing a reliable D2D communication similarly as considered, e.g., in [38]–[40]. Thus, the scenario where the DUE$_T$ and the DUE$_R$ are not able to communicate directly and data is sent in a conventional way via the gNB (i.e., if $d > d_{max}$) is out of the scope of this paper.

The whole bandwidth $B$ dedicated for D2D communication is split into $K = N$ channels (as in [7] and [8]) to serve all $N$ D2D pairs. The capacity of the $n$-th D2D pair at the $k$-th channel ($C_{n,k}$) is defined as:

$$C_{n,k} = B_k log_2\left(1+\gamma_{n,k}\right) = B_k log_2\left(1+\frac{p_{n,k}\, g_{n,n}}{\sigma_o B_k + \sum_{\substack{t\in N_k \\ t\neq n}} p_{t,k} g_{t,n} + I_d}\right) \quad (1)$$

where $B_k$ is the bandwidth of the $k$-th channel, $\gamma_{n,k}$ is the signal to interference plus noise ratio (SINR) of the $n$-th D2D pair at the $k$-th channel, $p_{n,k}$ is the transmission power of the $n$-th DUE$_T$ at the $k$-th channel, $g_{n,n}$ is the channel gain between the $n$-th DUE$_T$ and the $n$-th DUE$_R$, $p_{t,k}$ is the transmission power of the $t$-th DUE$_T$ at the $k$-th channel, $g_{t,n}$ is the channel gain between the $t$-th DUE$_T$ and the $n$-th DUE$_R$, $N_k$ represents the set of D2D pairs communicating at the $k$-th channel, $\sigma_o$ is the white noise power spectral density [41], and $I_d$ stands for the background interference received from adjacent cells. The background interference is measured by the receiver of each D2D pair and reported to the gNB. As this interference represents the sum interference from all sources (namely the interference from neighboring gNBs and UEs in other cells), it can be derived from RSRP/RSRQ reported even in a conventional network according to 3GPP. Note that we focus on the dedicated mode, where the D2D pairs experience no interference from the CUEs in the same cell. Consequently, we leave the CUEs out of the model.

We assume, without loss of generality, that the same minimal communication capacity $C_{min}$ is guaranteed to all D2D pairs. Based on [7] and [8], $C_{min}$ is defined as the minimal capacity that can be guaranteed to the D2D pair with the worst SINR if the total bandwidth (spectrum) is split among the $N$ D2D pairs proportionally to $g_{n,n}$ (i.e., $B_n = \frac{g_{n,n}}{\sum_{n=1}^{n=N} g_{n,n}}$). Then, $C_{min}$ is defined as:

$$C_{min} = \frac{g_{n,n}^{min}}{\sum_{n=1}^{n=N} g_{n,n}} B\ log_2\left(1+\frac{P_{max}\, g_{n,n}^{min}}{\sigma_o \frac{g_{n,n}^{min}}{\sum_{n=1}^{n=N} g_{n,n}} B + I_d}\right) \quad (2)$$

where $g_{n,n}^{min}$ is the minimal channel gain among all D2D pairs, i.e., $g_{n,n}^{min} = min\{g_{i,i}\}$, $\forall i = 1,\ldots,N$, and $P_{max}$ is the maximal transmission power that can be used by the D2D pair over all channels. Note that $P_{max}$ in (2) is considered in order to achieve the highest possible $C_{min}$ that can be guaranteed to each D2D pair.

As in many recent papers (e.g., [16],[17],[42]), we also assume full knowledge of channel state information (CSI) in our system. Although this assumption can be seen too demanding due to the high signaling overhead and the impracticality in real networks, there are already works that relax this problem and allow to obtain all channel gains among D2D pairs at a very low cost. For example in [43], deep neural networks are exploited to predict the D2D channel gains with a very high accuracy in both line-of-sight and even non-line-of-sight scenarios with no additional overhead. Moreover, we consider a fully controlled D2D communication, thus the gNB is aware of the devices under its coverage in order to manage them [2].

### B. Problem formulation

The objective of this paper is to maximize the sum communication capacity of the D2D pairs in the dedicated mode while the minimum capacity is guaranteed to each D2D pair. The sum capacity is maximized by an efficient allocation of the communication channels and their reuse in such a way that multiple channels can be reused by multiple D2D pairs. We denote the set of $L$ coalitions of the D2D pairs as $\mathbf{CS} = \{cs_1, cs_2, ...cs_L\}$. Each coalition $cs_l$ includes all D2D pairs that mutually reuse all channels allocated to all D2D pairs in $cs_l$. The coalitions are formed so that the sum capacity of the D2D pairs is maximized while the minimal capacity $C_{min}$ of each D2D pair is still guaranteed. To improve the sum capacity, we also determine a vector $\mathbf{B}$ of the communication channels bandwidths for all $N$ D2D pairs, i.e., $\mathbf{B} = \{B_1, B_2, \ldots., B_N\}$. To exploit the overall bandwidth allocated to each D2D pair (including reused channels) efficiently, we further find a set of vectors $\mathbf{P} = \{P_1, P_2, ..., P_N\}$, where every vector $P_n$ contains the transmission powers of the $n$-th D2D pair at all channels allocated to this pair. Note that every vector $P_n$ is of $|K_n|$ length, where $K_n$ is the subset of channels allocated to the $n$-th D2D pair. Hence, $K_n$ contains all channels of all D2D pairs, which are in the same coalition with the $n$-th pair. The

optimization problem over **B**, **CS**, and **P** is then formulated as:

$$\mathbf{B}^*, \mathbf{CS}^*, \mathbf{P}^* = \underset{\mathbf{B},\mathbf{CS},\mathbf{P}}{\operatorname{argmax}} \sum_{n=1}^{n=N} \sum_{k \in K_n} B_k log_2\left(1+\gamma_{n,k}\right) \quad (3)$$

$$\text{s.t.} \sum_{k \in K_n} B_k log_2(1+\gamma_{n,k}) \geq C_{min}\ \forall n \in \{1,2,...N\} \quad (a)$$

$$0 < B_n \leq B\ \forall n \in \{1,2,...N\} \quad (b)$$

$$\sum_{n=1}^{n=N} B_n = B \quad (c)$$

$$\sum_{k \in K_n} p_{n,k} = P_{max}\ \forall n \in \{1,2,...N\} \quad (d)$$

where $\mathbf{B}^*$, $\mathbf{CS}^*$, and $\mathbf{P}^*$ are the optimal **B**, **CS**, and **P**, respectively. The constraint (a) ensures that the sum capacity of any D2D pair over all the channels allocated to this pair (including the reused channels within the coalition) is not below $C_{min}$, (b) limits the size of each channel with respect to the maximum available bandwidth $B$, (c) guarantees that the sum of all channel bandwidths is equal to $B$ (i.e., that the dedicated spectrum is fully utilized to maximize the capacity), and (d) limits the sum transmission power of each D2D pair over all channels to the maximal allowed transmission power $P_{max}$.

The problem defined in (3) is a non-convex mixed integer non-linear programming (MINLP). The problem is MINLP due to following reasons. First, the objective function and constraint (a) are both non-linear. Second, the optimization is done over mixed integer and non-integer variables. More precisely, the coalitions' formation can be seen as an integer programming problem [46] optimizing integer variables (representing the creation of the coalitions) while the bandwidth allocation together with the power allocation represent continuous non-integer variables. The MINLP problems are known to be NP-hard and, thus, solving all three sub-problems jointly in an optimal way is very difficult. Thus, in the next section, we solve the optimization problem from (3) by determining the bandwidth allocation, the coalitions' formation and the power allocation.

## III. The proposed resource allocation scheme

To solve the optimization problem from (3), we separate it into three sub-problems. First, we analytically derive the optimal channel bandwidth allocated to each D2D pair in the initial phase (i.e., determination of **B**). Second, we solve the coalitions' creation problem allowing the reuse of multiple channels by multiple D2D pairs (i.e., determination of **CS**). The channel reuse problem is solved by the dynamic programming, which composes the optimal coalition structure and demonstrates an upper bound performance. However, the dynamic programming is of a high complexity, which makes it impractical for real networks. Thus, we propose also a low-complexity algorithm based on the sequential bargaining to handle the reuse. Third, we determine the optimal power allocation for the D2D pairs at each channel (i.e., determination of **P**). Note that, in the following subsections, the solutions solving the sub-problems of bandwidth allocation, coalitions' formation, and power allocation are denoted as $\mathbf{B}^{**}$, $\mathbf{CS}^{**}$, and $\mathbf{P}^{**}$, respectively.

### A. Initial allocation of channel bandwidth for individual D2D pairs

Before the channel reuse by D2D pairs takes place, each D2D pair is allocated with a dedicated channel of a certain bandwidth to guarantee the required channel capacity $C_{min}$ for all D2D pairs. This channel can be then reused by other pairs in the main phase of the proposed approach (described in the next subsections). The sub-problem of optimizing **B** from the problem defined in (3) is reformulated as:

$$\mathbf{B}^{**} = \underset{\mathbf{B}}{\operatorname{argmax}} \sum_{n=1}^{n=N} B_n log_2\left(1+\gamma_{n,n}\right) \quad (4)$$

$$\text{s.t.}\ \ C_{n,n}^{nr} = B_n log_2\left(1+\gamma_{n,n}\right) \geq C_{min}\ \forall n \in \{1,2,...N\} \quad (a)$$

$$(b), (c) \text{ taken from } (3)$$

where $\gamma_{n,n} = \frac{p_{n,n}\, g_{n,n}}{\sigma_o B_n + I_d}$ is the SINR of the $n$-th D2D pair at the $n$-th dedicated channel with no-reuse and the constraint (a) ensures that the capacity of every $n$-th D2D pair at the $n$-th dedicated channel with no-reuse ($C_{n,n}^{nr}$) is, at least, equal to the minimal required capacity $C_{min}$. It is worth to mention that each D2D pair can transmit with $P_{max}$ (i.e., $p_{n,n} = P_{max}$) at its allocated channel in this initial phase, because only one channel without reuse is exploited by each D2D pair and the interference among the D2D pairs is absent in this phase.

The solution of (4) for the case with no interference from the adjacent cells (i.e., with $I_d = 0$) is derived in [7] and [8]. However, in a realistic case with a dense deployment of cells and a high density of communicating UEs, the interference $I_d$ is significant with respect to the noise and cannot be neglected. In such case, the solution proposed in [7] and [8] is not optimal. Thus, we determine the optimal allocation of the bandwidth for the channel assigned to each D2D pair initially (without channel reuse) in the following proposition.

**Proposition 1.** *Considering the background interference from the adjacent cells $I_d$, the optimal allocation of the bandwidth $B_n$ to the n-th channel assigned to the n-th D2D pair guaranteeing the fulfillment of $C_{min}$ for all D2D pairs is:*

$$B_n = \frac{C_{min}}{log_2\left(1 + \frac{P_{max} g_{n,n}}{\sigma_o \frac{g_{n,n}^{min}}{\sum_{n=1}^{n=N} g_{n,n}} B + I_d}\right)} \quad (5)$$

*Proof.* The proof of Proposition 1 is in Appendix A. ∎

If $\sum_{n=1}^{n=N} B_n < B$ after the channel allocation, the rest of the bandwidth is added to the channel of the D2D pair with the highest $g_{n,n}$ in order to maximize the sum capacity of the D2D pairs as defined in (4). Consequently, the highest capacity in the initial allocation phase is achieved by the D2D pair with the best channel quality similarly like in [7] and [8]. Then, with a high probability, this particular D2D pair

forms a coalition with other pairs during the generation of the coalition structure (as described in the next subsection). Thus, the above-mentioned assignment of the rest of the bandwidth is beneficial for other D2D pairs as their capacity can be significantly enhanced as well by joining the coalition, which contains the D2D pair with the highest $g_{n,n}$.

The initial resource allocation is centrally managed by the gNB based on the knowledge of the channel quality of all D2D pairs in a similar way as assumed, e.g., in [16], [17], or [42].

### *B. Optimal coalition structure generation for channel reuse*

After the initial channel bandwidth allocation to the D2D pairs, the reuse of channels is implemented. To determine which D2D pairs should mutually reuse their channels, we formulate the problem of coalitions' formation. The problem is understood as a coalition structure generation problem in game theory [44]–[46]. For any set of players, the coalition structure is a set of coalitions **CS**= $\{cs_1, cs_2, \ldots, cs_L\}$ such that each element $cs_l \in$ **CS** is the set of players composing one coalition. Note that each player can belong only to a single coalition. For our channel reuse case, the problem is to find the coalition structure over $N$ D2D pairs in such a way that the D2D pairs in each coalition mutually reuse the channels of each other. Based on this, our goal is to find the coalition structure that maximizes the sum capacity of D2D pairs while guaranteeing the minimal capacity required by each pair. Consequently, the sub-problem of optimizing **CS**, from the problem defined in (3), is written as:

$$\mathbf{CS}^{**} = \underset{\mathbf{CS}}{\operatorname{argmax}} \sum_{n=1}^{n=N} \sum_{k \in K_n} B_k log_2 \left(1 + \gamma_{n,k}\right) \qquad (6)$$

$$\text{s.t. } (a) - (d) \text{ taken from } (3)$$

Fig. 1 illustrates the channel reuse problem presented as a coalition structure generation with an example of three D2D pairs (i.e., three players' coalition structure game). The example represents all possible coalitions created for the problem of three D2D pairs. Note that the D2D pairs within the same coalition transmit at the same time over all channels of all D2D pairs in the same coalition. For example, if three D2D pairs create one coalition (as in Fig. 1e), all these D2D pairs transmit over all three channels simultaneously and mutually interfere with each other. The D2D pairs in different coalitions are supposed to transmit at the same time, but at different channel(s), thus no interference occurs among the different coalitions.

To find the optimal solution for the problem defined in (6) and to determine the optimal structure of the coalitions, the dynamic programming [46][47] is a suitable solution. In the dynamic programming, the values of a gain function $V$ for each possible coalition $cs_x$ composed of $X$ D2D pairs (where $X \in \{1, 2, \ldots, N\}$) should be calculated. However, the problem defined in (6) is different from the general coalition structure generation problems due to the constraint (a). Therefore, in order to solve (6), the gain function should take the constraint (a) into account to guarantee $C_{min}$ for each D2D pair even

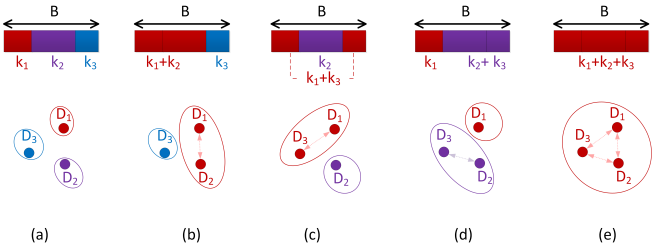


Fig. 1: The possible coalitions' creation for three D2D pairs. Note that the dashed arrows represent the interference introduced by the channel reuse.

after the channel reuse. Thus, we build up the gain function $V(cs_x)$ of the coalition $cs_x$, which is composed of $X$ D2D pairs, as follows:

$$V(cs_x) = \begin{cases} C_{cs_x} & \text{if } C_{D_y} > C_{min},\ \forall D_y \in cs_x \\ 0 & \text{otherwise} \end{cases} \qquad (7)$$

where $C_{cs_x}$ is the sum capacity of all D2D pairs in the coalition $cs_x$ mutually reusing the channels of all D2D pairs in $cs_x$, and $C_{D_y}$ is the sum capacity of the D2D pair $D_y$ over the communication channels, including the reused channels, in $cs_x$ (note that $D_y$ represents the $y$-th D2D pair from the coalition $cs_x$). Note that to calculate (7), the transmission powers of the D2D pairs over the reused channels are optimized based on subsection III-D presented later in this paper.

The dynamic programming-based solution is of a high complexity as the general complexity of dynamic programming is $O(3^N)$, where $N$ is the number of D2D pairs. Thus, such solution is not practical for the real networks and we propose a low-complexity algorithm in the next subsection to solve the coalitions' creation problem.

### *C. Low-complexity channel reuse based on sequential bargaining*

In this subsection, we describe the proposed low-complexity algorithm for the channel reuse to solve (6). The proposed solution is based on the sequential bargaining allowing multiple D2D pairs to reuse multiple channels simultaneously. This reuse is enabled by the fact that all D2D pairs in the same coalition always use all channels allocated to them previously during the initial allocation phase (as shown in Fig. 1e). Moreover, all channels in the coalition are used simultaneously by all D2D pairs in that particular coalition.

Before the proposed sequential bargaining process is initiated, we calculate the utilities for all possible coalitions of any two D2D pairs ($D_i$ and $D_j$) in the system. The utility function is defined as:

$$U_{i,j} = \begin{cases} -\infty & \text{if } C_{i,i} + C_{i,j} < C_{min} \\ -\infty & \text{if } C_{j,i} + C_{j,j} < C_{min} \\ G_{i,j} & \text{otherwise} \end{cases} \qquad (8)$$

where $C_{i,i}$ ($C_{j,i}$) and $C_{i,j}$ ($C_{j,j}$) are the capacities of the $i$-th ($j$-th) D2D pair at the $i$-th and $j$-th channels, respectively. If the reuse would lead to a decrease in the capacity below $C_{min}$

for any of the D2D pairs, the coalition is not allowed and the utility function $U_{i,j}$ is set to $-\infty$, see (8). In contrast, if both D2D pairs keep the capacity at least at $C_{min}$, a gain $G_{i,j}$ introduced by the new coalition of the pairs $D_i$ and $D_j$, even if it is negative, is calculated as:

$$G_{i,j} = (C_{i,i} + C_{i,j} + C_{j,i} + Cj,j) - (C^{nr}_{i,i} + C^{nr}_{j,j}) \quad (9)$$

where $C^{nr}_{i,i}$ and $C^{nr}_{j,j}$ correspond to the capacities of the $i$-th and $j$-th D2D pairs without channel reuse (see Section III-A). Note that from the structure of the utility function $U_{i,j}$ and from (9), we observe that $U_{i,j} = U_{j,i}$.

*Remark 1:* If the D2D pairs $D_i$ and $D_j$ form togther one coalition, the communication channel $k_i$ is reused by the pair $D_j$ while the pair $D_i$ reuses the channel $k_j$. In other words, both $D_i$ and $D_j$ communicate over both channels $k_i$ and $k_j$ at the same time.

*Remark 2:* Since the utility $U_{i,j}$ in (8) is calculated for any two D2D pairs $D_i$ and $D_j$ creating one coalition and accessing the two shared channels $k_i$ and $k_j$ assigned originally to each of them, the transmission powers $p_{i,i}$, $p_{i,j}$, $p_{j,i}$, and $p_{j,j}$ that are required to derive $U_{i,j}$ are calculated as $p_{x,y} = \frac{B_y}{B_x+B_y} p_{max}$, where $x$ and $y$ stand for either $i$ or $j$ to represent all four powers $p_{i,i}$, $p_{i,j}$, $p_{j,i}$, and $p_{j,j}$. For more details on the power allocation, please refer to the optimal power allocation derived later in Section III-D).

After obtaining the individual utilities $U_{i,j}$, these are inserted into a bilateral utility matrix $\boldsymbol{U}$:

$$\boldsymbol{U} = \begin{bmatrix} -\infty & \dots & U_{1,N} \\ \vdots & \ddots & \vdots \\ U_{N,1} & \dots & -\infty \end{bmatrix} \quad (10)$$

where the diagonal elements are set to $-\infty$ (i.e., $U_{i,i} = -\infty$). The reason for setting $U_{i,i} = -\infty$ is that the diagonal elements contain the utilities of the $i$-th D2D pair making a coalition with itself. Such coalition is automatically disregarded as, in principal, a D2D pair cannot make any new coalition with itself. The reason why we do not set the diagonal values simply to "0" is that in some special cases even the coalitions with slightly negative utilities can be initially created as long as $C_{min}$ is guaranteed. In contrast, the elements $U_{i,j}$ equal to $-\infty$ (i.e., the elements for which $C_{min}$ is not guaranteed as well as all diagonal elements) are omitted in the reminder of the process, because these should not lead to the creation of any coalition. This way, the complexity of the whole bargaining process is significantly decreased, as the search space (i.e., the number of the possible coalition structures among the D2D pairs) is reduced.

After all the entries in $\boldsymbol{U}$ equal to $-\infty$ are removed, the rest of the elements are sorted in a descending order taking into account that every couple of symmetric elements is considered as one element ($U_{i,j} = U_{j,i}$). The sorting serves further to indicate the priorities for coalitions' creation so that the coalitions yielding the highest capacity gains are created preferentially. This ordering is motivated by the fact that a higher bilateral utility represents, in our case, a lower interference among two D2D pairs. Thus, these D2D pairs are expected to end up in the same coalition also in the case of optimal coalitions created by the dynamic programming. Hence, it is likely that the proposed low-complexity solution leads to a close-to-optimal performance.

The sorted elements $U_{i,j}$ from $\boldsymbol{U}$ represent a vector of sub-games (denoted as $\boldsymbol{U^*}$) that are played sequentially over time in the way that one sub-game is played in every time step. Consequently, when the sub-game $s$ is played, the coalition structure $\mathbf{CS_s}$ is created resulting in the sum capacity $C_{\mathbf{CS_s}}$. At the beginning of the algorithm, the sub-game is played only between two D2D pairs (e.g., $D_i$ and $D_j$) over their respective channels ($k_i$ and $k_j$) allocated in the initial phase. In this case, the coalition is simply created if both $D_i$ and $D_j$ agree to reuse their dedicated channels among each other. However, when some coalitions already exist, the sub-game is extended to all members of all related coalitions. Thus, if the pair $D_i$ wants to join the coalition $cs_x$ composed of two or more other D2D pairs, the sub-game $s$ is played between the pair $D_i$ and all the D2D pairs already included in the coalition $cs_x$. The pair $D_i$ joins the coalition $cs_x$ if and only if the pair $D_i$ as well as all pairs in $cs_x$ agree. Each D2D pair $D_j$ agrees to accept the pair $D_i$ into $cs_x$ if the capacity of the pair $D_j$ is not lower than $C_{min}$ and if the sum capacity of the D2D pairs composing $\mathbf{CS_s}$ is higher than the sum capacity of the D2D pairs composing $\mathbf{CS_{s-1}}$ (i.e., if $C_{\mathbf{CS_s}} > C_{\mathbf{CS_{s-1}}}$); where $\mathbf{CS_{s-1}}$ is the coalition structure created in the previous sub-game $s-1$ with the sum capacity of $C_{\mathbf{CS_{s-1}}}$.

Furthermore, to get closer to the creation of the optimal coalitions, we enhance the proposed sequential bargaining process by testing to create larger coalitions even if the coalitions of two pairs are not beneficial (i.e., $C_{\mathbf{CS_s}} < C_{\mathbf{CS_{s-1}}}$). Thus, we try the coalitions of three pairs even if the previous coalitions with two pairs can lead to a decreased performance. In other words, if the creation of the coalitions with any two pairs leads to a negative gain (all bilateral utilities are negative), the two D2D pairs playing the first sub-game in the sorted utilities are forced to test the reuse of their channels even if the sum capacity is decreased. Then, the rest of the sub-games are played out normally as described before and the D2D pair is added only if the sum capacity of D2D pairs is increased. This way, we keep the possibility of making coalitions with more than two D2D pairs and we prevent the possibility that the algorithm gets stuck in local optima.

In the last step, the formed coalition structure $\mathbf{CS_s}$ is compared with two other coalition structures: i) $\mathbf{CS_{all}} = cs_1$ where all D2D pairs create one coalition $cs_1$ and reuse all the channels; ii) $\mathbf{CS_0} = \{cs_1, ..., cs_N\}$ where each D2D pair represents a stand-alone coalition and no channel reuse is exploited (i.e., the initial allocation from Section III-A). Among the three coalition structures $\mathbf{CS_s}$, $\mathbf{CS_{all}}$, and $\mathbf{CS_0}$, the one that reaches the highest sum capacity of D2D pairs is chosen. Note that the sum capacity of $\mathbf{CS_{all}}$ is set to zero if $\mathbf{CS_{all}}$ does not guarantee $C_{min}$ for all D2D pairs. There are two reasons for the inclusion of this last step. The first reason is a potential consequence of the special case (described in previous paragraph) when all elements of (10) are negative and the sum capacity decrement is acceptable in the first sub-game. This sum capacity decrement makes it necessary to compare the sum capacity in the final formed coalition

structure $\mathbf{CS_s}$ with the sum capacity achieved by the initial allocation (i.e., $C_{\mathbf{CS_0}}$), in order to guarantee that $C_{\mathbf{CS_s}} > C_{\mathbf{CS_0}}$. The second reason is, generally, the very low probability of reaching the coalition structure where all D2D pairs reuse all of the available channels (i.e., $\mathbf{CS_{all}}$) through the played sub-games. Nevertheless, with a very low density of D2D pairs, the probability that the D2D pairs can reuse all the channels and compose one coalition is higher. Thus, selecting the best-performing coalition structure among $\mathbf{CS_s}$ and $\mathbf{CS_{all}}$ can further improve the performance.

The above-described algorithm for the sequential bargaining-based channel reuse is summarized in Algorithm 1. The algorithm is supposed to run centrally at the gNB (as explained in Section II.A). Thus, no special synchronization between the D2D links is needed with respect to the common D2D communication fully controlled by the network [2], because all the D2D pairs within the coalition use all the channels of each other at the same time. Note that within every step from the previously described coalitions' formation solution, the capacities are calculated (line 8 from Algorithm 1) with the optimized transmission power allocation derived in the following subsection III-D.

### D. Power allocation to channels

In this subsection, we aim to optimize the power allocation and set the transmission power of every D2D pair at every channel allocated to this pair based on the created coalition structure. We take into account the maximum power budget for each D2D pair to fulfill the constraint (d) in (3) and (6). The problem of power allocation is non-convex. Thus, an iterative method is required to solve such problem. However, any iterative method would increase the time complexity of the overall resource allocation scheme. Thus, we transform the problem to a convex one by maximizing the capacity of each D2D pair separately. In other words, the transmission power of each D2D pair at each individual channel allocated to this pair is set in a selfish way so that the sum capacity of every single D2D pair is maximized.

**Algorithm 1** Sequential bargaining algorithm to solve channel reuse problem for $N$ D2D pairs

1: Estimate utility matrix $\boldsymbol{U}$ with size $N \times N$
2: Eliminate utilities equal to $-\infty$ from the matrix $\boldsymbol{U}$
3: Sort remaining utilities in descending order into vector $\boldsymbol{U^*}$
4: Initialize $\mathbf{CS_0} = \{cs_1, \ldots, cs_N\}$; $cs_i = \{D_i\}$, $\forall i \in \{1, \ldots, N\}$
5: **for** $s = 1 :$ length($\boldsymbol{U^*}$) **do**
6: Sub-game is played between pairs $D_i \in cs_x$ and $D_j \in cs_y$ where $U_{i,j} \equiv \boldsymbol{U^*}(s)$
7: Update $\mathbf{CS_s}$ (i.e., merge $cs_x$ and $cs_y$ into one coalition $cs_z$)
8: Estimate all $\sum_{k \in K_n} B_k log_2(1+\gamma_{n,k})$ $\forall n \in \{1, \ldots N\}$ and corresponding $C_{\mathbf{CS_s}}$
9: **if** $\exists n \in \{1, \ldots N\} : \sum_{k \in K_n} B_k log_2(1+\gamma_{n,k}) < C_{min}$ **or** $C_{\mathbf{CS_s}} < C_{\mathbf{CS_{s-1}}}$ **then**
10: **if** $\exists s \; : \; \boldsymbol{U^*(s)} > 0$ **or** $s \neq 1$ **then**
11: $\mathbf{CS_s} = \mathbf{CS_{s-1}}$
12: **end if**
13: **end if**
14: **end for**
15: **if** in $\mathbf{CS_{all}}$ $\exists n \in \{1, \ldots N\} : \sum_{k \in K_n} B_k log_2(1+\gamma_{n,k}) < C_{min}$ **then** $C_{\mathbf{CS_{all}}} = 0$ **end if**
16: $\mathbf{CS_s} = \{\mathbf{CS_s} \in \{\mathbf{CS_s}, \mathbf{CS_{all}}, \mathbf{CS_0}\} : C_{\mathbf{CS_s}} = max(C_{\mathbf{CS_s}}, C_{\mathbf{CS_0}}, C_{\mathbf{CS_{all}}})\}$

The problem of maximizing the sum capacity of the D2D pair $D_n$ over all $|K_n|$ channels reused by this pair $D_n$ is formulated as:

$$\max(C_n) = \max \left( \sum_{k \in K_n} B_k log_2 \left( 1 + \frac{p_{n,k} g_{n,k}}{\sigma_o B_k + \sum_{\substack{t \in N_k \\ t \neq n}} p_{t,k} \, g_{t,k} + I_d} \right) \right) \tag{11}$$

$$\text{s.t.} \sum_{k \in K_n} p_{n,k} = p_{max} \quad (a)$$

The optimization problem (11) is, still, not convex and, thus, it cannot be solved analytically in a simple way. However, if the channel between the $DUE_T$ and the $DUE_R$ is of a high quality, we can assume that $\gamma_{n,k} = \frac{p_{n,k} g_{n,n}}{\sigma_o B_k + \sum_{\substack{t \in N_k \\ t \neq n}} p_{t,k} \, g_{t,k} + I_d} >> 1$ in (11), similarly as in [7]. Note that this assumption can be justified in most of the cases since: i) the $\text{DUE}_T$ and the $\text{DUE}_R$ are typically close to each other due to the requirements on the efficiency of the D2D communication (see Section II-A.), ii) the transmission power of the $\text{DUE}_T$ is set to $P_{max}$, and iii) the coalitions are formed to maximize the sum capacity of D2D pairs leading to a relatively low interference among D2D pairs in the same coalition (i.e., $\sum_{\substack{t \in N_k \\ t \neq n}} p_{t,k} \, g_{t,k}$ is low). Then, we can adopt the simplification $log_2(1 + \gamma_{n,k}) \approx log_2(\gamma_{n,k})$. In the cases with a low SINR, this approximation might not hold. Nevertheless, if the D2D pairs are interfering with each other significantly, these are not encouraged to be in the same coalition as the bilateral utilities of these (in (8)) have a high probability to be negative. Thus, the problem of maximizing $C_n$ is simplified to:

$$\max(C_n) = \max \left( \sum_{k \in K_n} B_k log_2 \left( \frac{p_{n,k} g_{n,k}}{\sigma_o B_k + \sum_{\substack{t \in N_k \\ t \neq n}} p_{t,k} \, g_{t,k} + I_d} \right) \right) \tag{12}$$

$$\text{s.t.} \sum_{k \in K_n} p_{n,k} = p_{max}$$

The maximization problem in (12) is convex, thus, the optimum is determined as:

$$\frac{\delta \, C_n}{\delta \, p_{n,k}} = 0; \tag{13}$$

After solving (13), we get the power allocation to the individual reused channels as:

$$p_{n,k} = \frac{B_k}{\sum_{k \in K_n} B_k} p_{max} \tag{14}$$

By deriving the transmission powers of all D2D pairs over all the corresponding channels based on (14), a sub-optimal power allocation ($\mathbf{P^{**}}$) is reached. The transmission power $p_{n,k}$

defined in (14) is inserted to (9) for the determination of the gains $G_{i,j}$ and to derive the bilateral utilities $U_{i,j}$ in (8) (see *Remark 2* in Section III-C).

## IV. Performance evaluation

The simulations are carried out in Matlab to evaluate the performance of the proposed resource allocation scheme and to compare it with the competitive algorithms. To this end, the simulation scenario and parameters are presented in the next subsection. Then, the competitive algorithms and performance metrics are defined. Last, the simulation results are presented and discussed.

### A. Simulation scenarios

We consider an area of 500×500 $m^2$. The simulation results are averaged out over 1000 simulation drops. For each drop, $N$ $\text{DUE}_T$ are uniformly distributed within the area. The position of the $\text{DUE}_R$ for each D2D pair is generated with respect to the position of the $\text{DUE}_T$ to guarantee that the distance between the transmitter and the receiver is not higher than $d_{max}$. The distance between the transmitter and the receiver is randomly generated with the uniform distribution between 0 and $d_{max}$. The angle of the receiver with respect to the transmitter is also uniformly generated between 0° and 360°. The number of D2D pairs remains the same for all 1000 drops, but we run different 1000 drops for every tested value of $N$ from 5 to 50. Note that the CUEs are not considered as these operate in a different band in case of the dedicated mode as explained in Section II-A.

For the modeling of radio channel, we follow 3GPP recommendation for D2D communication defined in [48]. Hence, the path loss model is defined as $PL = 89.5 + 16log_2(d)$, where $d$ is the distance between the transmitter and the receiver. The maximal transmission power for every D2D pair is set to $P_{max}$ = 20 dBm. The background interference from neighboring cells $I_d$ is modeled randomly for each drop following a normal distribution with a mean value of −80 dBm and a standard deviation of 15 dB. This level of interference from neighboring base stations represents a high interference scenario, which can be expected in future mobile networks with dense small cells deployment [37]. The detailed parameters of the simulations are summarized in Table I.

TABLE I: Simulation parameters.

| Parameter | | Value |
|---|---|---|
| Carrier frequency | $f_c$ | 2 GHz |
| Bandwidth | $B$ | 20 MHz |
| Noise power spectral density | $\sigma_o$ | −174 dBm/Hz |
| Interference level from neighboring cells | $I_d$ | $\mathcal{N}(-80, 15)$ dBm |
| Number of D2D pairs | $N$ | 5 − 100 |
| Maximal transmission power of D2D pair | $P_{max}$ | 20 dBm |
| Default maximal distance between $DUE_T$ and $DUE_R$ | $d_{max}$ | 50 $m$ ([38]–[40]) |

### B. Competitive algorithms and performance metrics

To the best of our knowledge, there is no solution targeting the reuse of multiple channels by multiple D2D pairs in the dedicated mode with the goal of maximizing the sum capacity of D2D pairs and guaranteeing the minimal capacity for each individual D2D pair. Nevertheless, we compare our proposed algorithm with the schemes that target similar objectives or address similar problem. Thus, the proposed resource allocation algorithm, encompassing the optimal channel bandwidth allocation (derived in Section III-A), the channel reuse algorithm (Section III-B and III-C), and the optimal power allocation (Section III-D), is compared with the following state-of-the-art schemes:

1) *No reuse* [7],[8]: This scheme, designed for the dedicated mode, distributes whole available bandwidth $B$ among the D2D pairs in the way that communication capacity is maximized while $C_{min}$ is guaranteed to each D2D pair. However, the channels cannot be reused by the D2D pairs and each channel is occupied by just one pair. Note that the channel allocation in [7] and [8] is not optimal if there is the background interference $I_d$ as considered in our case.
2) *Single reuse* [9]: In this algorithm, the total bandwidth is divided into several channels with equal bandwidths (we consider six channels as in [9]). Every channel is allocated to a single D2D pair, i.e., six D2D pairs are served. The Hungarian algorithm is implemented to solve a matching problem between the six channels and the unserved D2D pairs to enable the D2D channel reuse. As defined in [9], up to two D2D pairs can reuse each channel. Thus, the solution allows twelve (2×number of channels) D2D pairs to be served, while the rest of the D2D pairs are provided with no resources. Even if this leads to an unfairness among the D2D pairs, it also yields a high capacity for the served D2D pairs as only those having a high channel quality between $\text{DUE}_T$ and $\text{DUE}_R$ access the available channels.
3) *Empty channel protocol (ECP)* [10]: For this case, the total bandwidth is also divided into several channels with equal bandwidth (in our case six channels as in [10]). First, every channel is allocated to a single D2D pair (i.e., six D2D pairs are served). Then, empty channel protocol adds the unserved D2D pairs to the channels so that all unserved D2D pairs reuse the channels already assigned to other D2D pairs. Note that the D2D pairs are not allowed to exploit multiple channels simultaneously and only one channel can be used by every D2D pair. Still, each channel can be reused by multiple D2D pairs at the same time.

The performance of the proposed and competitive algorithms is assessed by means of the sum capacity of D2D pairs defined as $C = \sum_{n=1}^{n=N} \sum_{k \in K_n} C_{n,k}$ . We also investigate the percentage of satisfied D2D pairs, that is, the D2D pairs for which the minimal capacity is granted (i.e., the percentage of the D2D pairs with $C \geq C_{min}$).

### C. Simulation results

In this section, we first compare the performance of the proposed resource allocation scheme with the competitive

state-of-the-art algorithms. Then, we analyze thoroughly the proposed scheme and we show the added value of the individual sub-parts of the proposal.

*1) Comparison of the proposed scheme with competitive algorithms:* In this subsection, we compare the performance of the full proposed resource allocation scheme, containing optimal bandwidth allocation, channel reuse based on sequential bargaining (SB), and optimal power allocation (denoted as "Proposal with SB (Alg. 1)"), with all above-mentioned competitive algorithms. Also, we show the performance of the optimal solution, where the optimal bandwidths are allocated to the channels, the optimal channels are allocated to the D2D pairs via the dynamic programming (i.e., the optimal coalitions are created) (Section III-B), and finally, the optimal powers are allocated to the D2D pairs (denoted as "Proposal - optimum"). Although the optimal solution is not practical due to the high complexity of the dynamic programming, it is used as a benchmark for our scheme as it achieves the maximal possible sum capacity. In addition, we also test the performance of the sub-optimal greedy algorithm for the creation of the coalitions with a complexity equal to $O(N^3)$. The greedy algorithm outlined for a general coalitions' creation in [49] is modified to guarantee $C_{min}$ and we combine it with the optimal initial channel allocation and the optimal power allocation of our proposed scheme. Hence, we denote the algorithm as "Proposal with m-greedy").

Fig. 2 illustrates the impact of the number of D2D pairs on the sum capacity of all D2D pairs. The capacity is increasing for the proposed as well as competitive algorithms with more D2D pairs in the system despite the fact that the interference among D2D pairs increases. The reason for this phenomenon is twofold. First, with the increasing number of D2D pairs, more options of the D2D pairs' coalitions are available to provide a higher benefit from the reuse. Second, with the increasing number of D2D pairs, these pairs use generally narrower channel(s) while the total transmission power over these channels remains the same (the overall transmitting power across all channels is not changed). Consequently, SINR at these channels increases with a decrease in the channel bandwidth, because the noise level decreases proportionally to the channel bandwidth (see (1)). This trend, i.e., increasing SINR with a narrower channels goes against the trend of a potential higher interference among the D2D pairs in the same coalition. In case the interference would be too strong (even potentially leading to a decrease in the sum capacity), there would be no benefit to create such coalition and the coalition is not created. Hence, the positive impact of noise reduction with a higher number of D2D pairs always overweights the interference and the sum capacity does not start decreasing even with a large $N$.

We see that the sum capacity of all three competitive schemes saturates quickly and reaches approximately 223 Mbps (ECP), 297 Mbps (Single reuse), and 294 Mbps (No reuse) for 50 D2D pairs. The proposal with sequential bargaining leads to a significant gain with respect to all competitive algorithms. The gain ranges from 20% to 200%, from 55% to 297%, from 55% to 295%, when compared to the No reuse, Single reuse, ECP algorithms, respectively. The gain of the proposal with respect to the existing solutions increases with the number of D2D pairs, since a higher number of D2D pairs leads to more opportunities for the multiple reuse in case of our proposed scheme. Note that the proposal with m-greedy, also, outperforms the existing solutions, but its sum capacity is from 2% to 13% below the sequential bargaining approach. Besides, Fig. 2 also shows the performance of the proposal with the optimal coalitions' creation by the dynamic programming. Due to the very high complexity, we cannot show results for more than ten D2D pairs as the results cannot be obtained in a realistic time frame. The difference between the optimal coalition structure derived by dynamic programming and the low-complexity sequential bargaining approach is negligible (1.2% for 10 D2D pairs) and the low-complexity solution reaches almost optimal performance. Note that such a good performance of the proposed sequential bargaining with respect to the optimum is thanks to the sorting of the bilateral utilities in descending order and, also, allowing the creation of the coalitions with negative utilities if no bilateral utility is positive, see Section III.C.

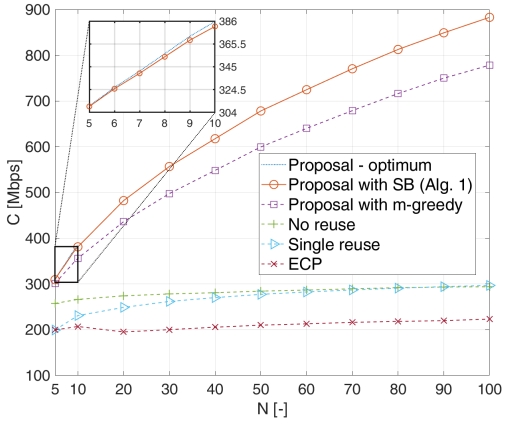


Fig. 2: Sum capacity of D2D pairs over number of D2D pairs for $d_{max}$ = 50 m.

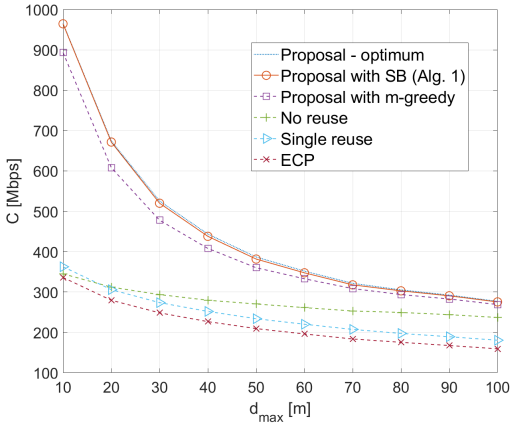


Fig. 3: Sum capacity of D2D pairs over maximum distance between $DUE_T$ and $DUE_R$ of the same D2D pair ($N$ = 10).

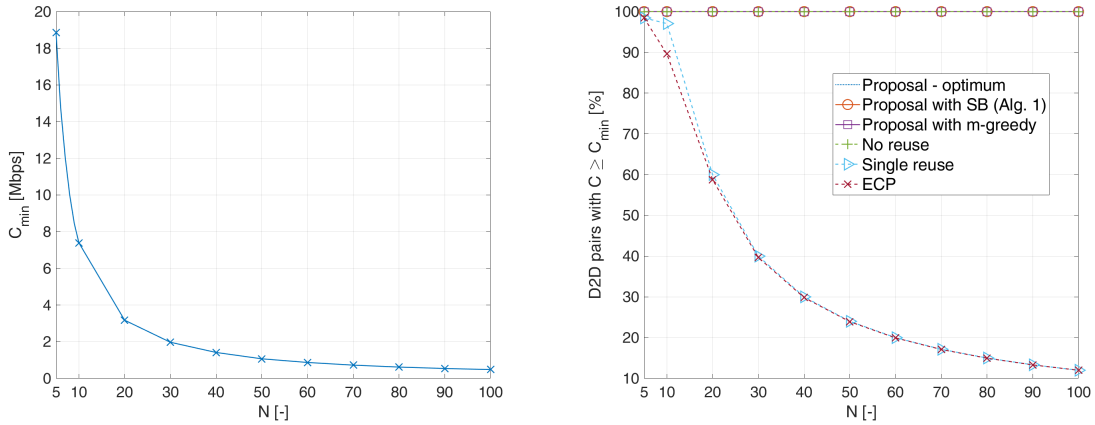


(a) (b)

Fig. 4: Minimum capacity $C_{min}$ that can be guaranteed to all D2D pairs according to (2) (a), and percentage of D2D pairs for which $C_{min}$ is guaranteed (b).

Furthermore, we investigate the impact of the maximum distance between the $\text{DUE}_T$ and $\text{DUE}_R$ (i.e., $d_{max}$) on the sum capacity in Fig. 3 for $N = 10$. It is obvious that the longer $d_{max}$ is, the lower sum capacity is observed. The reason for such behavior is that the signal between the $\text{DUE}_T$ and the $\text{DUE}_R$ is more attenuated for a larger $d_{max}$ and the D2D communication becomes less efficient. Figure 3 also shows that the proposal with sequential bargaining outperforms all competitive algorithms significantly and also overcomes the proposal with m-greedy. The gain introduced by the proposed algorithm with sequential bargaining ranges from 16.4% to 180%, from 53% to 166%, from 73% to 187% in comparison to the No reuse, Single reuse, and ECP algorithms, respectively. The proposal with m-greedy reaches from 2% to 10% lower sum capacity with respect to the sequential bargaining. The gain is less significant for a larger $d_{max}$ as the interference among D2D pair is more significant with respect to the useful signal and the possibility of sharing communication channels decreases. From Fig. 3, we further see that the proposed low-complexity algorithm with sequential bargaining reaches almost the optimal capacity obtained by the dynamic programming disregarding $d_{max}$.

The proposed algorithm is designed to guarantee the minimal capacity $C_{min}$ to all D2D pairs (see (3)). The minimal capacity $C_{min}$ is derived as the capacity that is guaranteed to all D2D pairs in the case of no reuse (according to [7] and [8] as explained in (2) in Section II-A). The minimal capacity $C_{min}$ decreases with the number of D2D pairs $N$, since the bandwidth $B$ is divided among a higher number of D2D pairs (see Fig. 4a). In Fig. 4b, we verify the fulfillment of the constraint on $C_{min}$. The proposals with optimal coalitions, sequential bargaining as well as with m-greedy guarantee $C_{min}$ for every D2D pair over all investigated numbers of D2D pairs in all simulation drops. Thus, although every D2D pair is exposed to interference from other D2D pairs in the same coalition, there is no D2D pair that experiences a capacity below $C_{min}$. Note that there is no difference between the percentage of the satisfied D2D pairs for the proposed algorithm with optimal coalitions' creation and sequential bargaining-based coalitions' creation. Also No reuse algorithm (proposed in [7] and [8]) satisfies $C_{min}$ for all D2D pairs. In contrast, the Single reuse algorithm and the EPC do not guarantee $C_{min}$ to all D2D pairs due to the equal channel bandwidth allocation and limited channel reuse.

*2) Analysis of the proposed resource allocation scheme:* In this subsection, we analyze the impact of individual sub-parts of the proposed scheme on the sum capacity of D2D pairs and the contribution of individual sub-parts to the gains achieved with respect to the competitive algorithms. To that end, we show the impact of the following individual sub-parts of the proposed algorithm:

1) *Proposal - opt. BW*: Illustrates the gain of stand-alone optimal channel bandwidth allocation for scenario with the background interference (Section III-A) while no channel reuse is considered. This way we show the impact of interference on the bandwidth allocation with respect to [7] and [8], where the authors neglect this interference.
2) *Proposal - reuse only*: Performance of the stand-alone proposed channel reuse (Section III-C) is demonstrated on the top of the channel bandwidth allocation according to [7], [8], i.e., if the $n$-th D2D pair has the bandwidth $B_n = \frac{g_{n,n}}{\sum_{n=1}^{n=N} g_{n,n}} B$ while the transmitting power among all channels is distributed equally.
3) *Proposal - reuse with opt. BW*: One can expect that the consideration of interference for the bandwidth allocation can influence also the efficiency of the reuse phase. Thus, we present this scheme in order to demonstrate the contribution of the derived optimal bandwidth allocation (i.e., combined Section III-A and Section III-C). As this algorithm also assumes the equal power allocation over all channels, the gain of the optimal power allocation over channels is illustrated by the difference between this algorithm and the proposal with sequential bargaining.

For the sake of Fig. 5 clarity, we do not show the per-

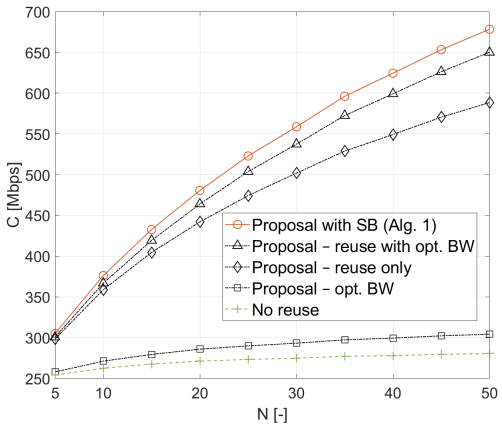


Fig. 5: Impact of individual subparts of proposed algorithm (bandwidth allocation, channel reuse, power allocation) on sum capacity of D2D pairs ($d_{max} = 50\,m$).

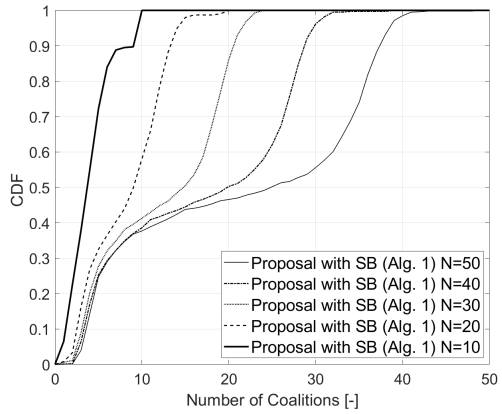


Fig. 6: Cumulative Distribution Function (CDF) of number of coalitions created by the sequential bargaining for different numbers of D2D pairs.

formance of the optimal coalitions' creation and we depict only the No reuse algorithm [7], [8], which serves as a basis for the bandwidth allocation performance. We see that a high gain ranging from 19.5% to 106% with respect to No reuse algorithm is introduced by the reuse of multiple channels by multiple D2D pairs (as proposed in Section III-C, in Fig. 5 labeled as "Proposal - reuse only"). The gain is a result of the proposed reuse of channels by the D2D pairs whenever it is beneficial. In addition, Fig. 5 also shows that the gain introduced by the optimal bandwidth allocation considering the background interference (in Fig. 5 depicted as "Proposal - opt. BW" and derived in Section III-A) with respect to the same approach disregarding the interference (i.e., No reuse according to [7] and [8]) introduces only a gain of up to 8.1% for $N = 50$. However, if the optimal bandwidth allocation considering interference is applied together with the proposed reuse ("Proposal - reuse with opt. BW" in Fig. 5), the synergy effect of both leads to an additional gain of up to 22.5% added on the top of the reuse gain. The reason for such gain of the proposed optimal bandwidth allocation applied together with the reuse is that the bandwidths of the individual channels are derived with respect to the background interference. If the interference from the adjacent cells is neglected for the bandwidth allocation, the reuse phase is impaired by the non-optimal bandwidth allocation and, consequently, some well-performing coalitions are not established.

The impact of the optimal power allocation (determined in Section III-D) is represented by the difference between two top lines in Fig. 5 ("Proposal with SB (Alg. 1)" and "Proposal - reuse with opt. BW"). The additional gain with respect to No reuse (up to 8.6%) is a result of the power allocation over the channels assigned to each D2D pair taking into account the inequality among the bandwidths of these channels.

In addition to the analysis of the impact of individual subparts of the proposed algorithm, we also give more insight into the size of the resulting coalitions. Cumulative distribution function of the number of coalitions resulting from the proposed sequential bargaining game (see Section III-C) is depicted in Fig. 6. In roughly 40% of the cases, less than ten coalitions are created disregarding the number of pairs. This relatively low number of coalitions indicates that there is a high probability that multiple D2D pairs reuse the channels of other D2D pairs. The figure shows that at least one coalition is composed of more than one D2D pair (i.e., the channel(s) are reused) in 90%, 99%, and 100% of the cases for $N = 10$, $N = 20$, and $N > 20$, respectively. In other words, almost always, the number of created coalitions is lower than the number of D2D pairs $N$, thus, multiple D2D pairs reuse multiple channels. Note that each D2D pair represents one coalition if this D2D pair communicates only at its dedicated channel without reuse.

*3) Feasibility of the proposed scheme:* The worst case time complexity of Algorithm 1 is $O(N^2 log N)$, since the bilateral utility matrix $\boldsymbol{U}$ in (10) is of $N \times N$ size and its entries are sorted in descending order (sorting of $n$ elements results in the complexity $O(nlog(n))$. Nevertheless, the proposed algorithm is based on the bargaining sub-games that are played sequentially over time. Thus, we investigate also the feasibility of the proposed scheme for real networks by analyzing the convergence of the proposed algorithm. The number of time steps of the proposed algorithm over the number of D2D pairs $N$ to reach 95% and 90% of the maximum capacities is illustrated in Fig. 7a and Fig. 7b, respectively. The figures confirm that reaching 95% and 90% of the maximum capacity is quick even for a high number of D2D pairs. For realistic scenarios with, for example, 20 D2D pairs, only 14 and 10 steps (bargaining sub-games) are performed in average to reach 95% and 90% of the maximum sum D2D capacity, respectively. Even for 50 D2D pairs (which is rather an extreme case for an area of $500 \times 500$ m), only 35 and 24 time steps in average are carried out to reach 95% and 90% of the maximum capacity. Note that the complexity of dynamic programming is $3^N$, thus, the complexity of the sequential bargaining-based solution is negligible.

We also show a step-by-step increase in the sum capacity of D2D pairs after each sub-game is played out for selected

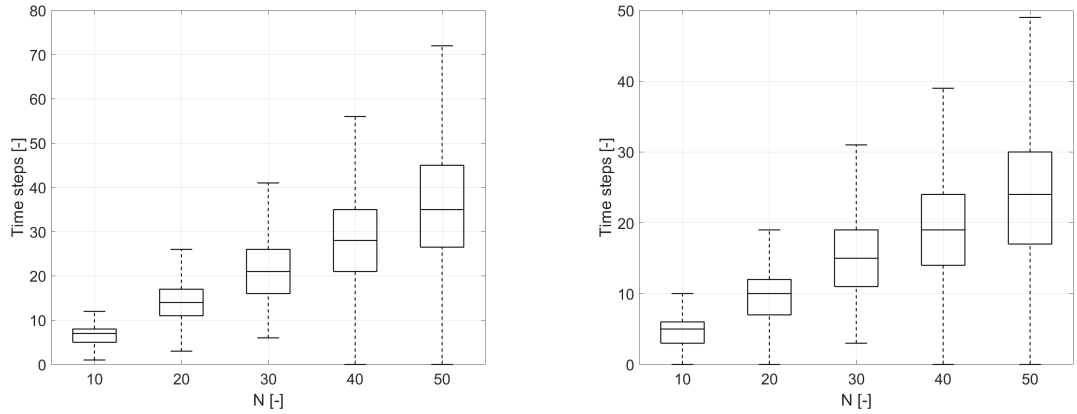


(a) (b)

Fig. 7: Number of time steps corresponding to number of bargaining sub-games required to reach 95% (a) and 90% (b) of the sum capacity of D2D pairs.

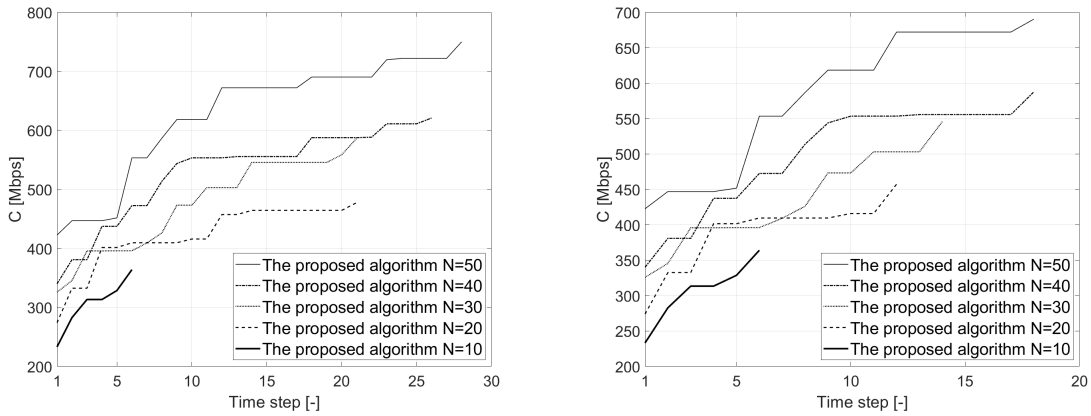


(a) (b)

Fig. 8: Example of evolution of sum capacity over time steps in one drop for different number of D2D pairs $N$. The endpoint for each line illustrates the step when 95% (a) and 90% (b) of sum D2D capacity is reached.

samples of results in Fig. 8. The capacity is increasing steeply during the first steps and promptly converges close to the maximum. Even after very first steps, the gain with respect to the best performing competitive solution is significant (up to 281.5 Mbps in average for No reuse [7],[8] as shown in Fig. 2). The low number of time steps and the steep growth of the sum capacity over the time steps, demonstrated in Fig. 7 and Fig. 8, confirm the feasibility of the proposed solution for the real-world mobile networks.

## V. Conclusion

In this paper we have proposed a new resource allocation scheme allowing multiple pairs to reuse multiple channels for the D2D communication in the dedicated mode. The proposed resource allocation scheme encompasses an initial bandwidth allocation, channel reuse, and power allocation over the reused channels. The channel reuse is presented as a coalition structure generation problem, where the D2D pairs composing one coalition reuse the channels dedicated to each other. The coalition structure generation problem is optimally solved by the algorithm based on dynamic programming. As the dynamic programming is of a high complexity, we also develop a low-complexity sequential bargaining algorithm solving the reuse problem while reaching close-to-optimal sum capacity of D2D pairs. The performance analysis shows that the sum capacity of D2D pairs is significantly increased by the proposed resource allocation scheme compared to the existing algorithms. In addition, although the interference is imposed among D2D pairs reusing the same channel, the minimal required capacity for each D2D pair is still guaranteed after the channel reuse.

A potential future direction should aim at a power control among D2D pairs in every coalition in order to further increase the spectral efficiency. Another topic for further study is the allocation of resources when the multiple channels are used by multiple D2D pairs without the requirement on forcing the D2D pairs to reuse their channels only mutually while still guaranteeing the minimal capacity to each D2D pair.

## APPENDIX A

To solve the problem of channel bandwidth presented in (4), we adopt the approximation $log_2(1+\gamma_{n,n}) \approx log_2(\gamma_{n,n})$ like in Section III-D and under the same assumptions. By applying this approximation into sub-problem (4) and after several simple mathematical operations, the objective function from (4) is rewritten as:

$$\sum_{n=1}^{n=N} B_n log_2\left(1+\frac{p_{n,n}\, g_{n,n}}{\sigma_o B_n + I_d}\right) = \sum_{n=1}^{n=N} log_2\left(\frac{p_{n,n}\, g_{n,n}}{\sigma_o B_n + I_d}\right)^{B_n} = log_2 \prod_{n=1}^{n=N}\left(\frac{p_{n,n}\, g_{n,n}}{\sigma_o B_n + I_d}\right)^{B_n} \quad (15)$$

To accommodate realistic scenarios, adjacent cells with a high data traffic are considered. Thus, the resulting interference is high; allowing the assumption: $\sigma_n + I_d \approx I_d$. Hence, the objective function of (4) presented in (15) is simplified to:

$$log_2 \prod_{n=1}^{n=N}\left(\frac{p_{n,n}\, g_{n,n}}{I_d}\right)^{B_n} \quad (16)$$

By the integration of (16) into (4) and by substituting $p_{n,n}$ by $P_{max}$ in the objective function according to the constraint (d) in (4), the sub-problem (4) is presented as:

$$\mathbf{B}^{**} = argmax\ log_2 \prod_{n=1}^{n=N}\left(\frac{P_{max}\, g_{n,n}}{I_d}\right)^{B_n} \quad (17)$$

$$\text{s.t. } B_n log_2\left(\frac{P_{max}\, g_{n,n}}{I_d}\right) \geq C_{min}\ \forall n \in \{1,2,...N\} \quad (a)$$

$$0 < B_n \leq B\ \forall n \in \{1,2,...N\} \quad (b)$$

$$\sum_{n=1}^{n=N} B_n = B \quad (c)$$

The constraint (a) ensures that the approximated capacity of every $n$-th D2D pair on the $n$-th dedicated channel with no-reuse is higher than the minimal capacity $C_{min}$. The constraints (b) and (c) are the same constraints as described in (4).

The maximization of any function $f = log_2(f')$ can be solved by maximizing $f'$. The problem (17) is in a form of argmax$[(a_1)^{B_1}(a_2)^{B_2}\ldots(a_N)^{B_N}]$, where $a_1, a_2, \ldots, a_N$ are constants. Thus, taking into account the constraints (b) and (c), maximizing (17) is achieved by assigning the maximum possible part of the bandwidth to the D2D pair with the maximal $a_n$. In other words, the D2D pair with the highest $g_{n,n}$ is granted with the maximal allowed part of the dedicated bandwidth. However, the constraint (a) should be also satisfied. We are able to guarantee $C_{min}$ if any $n$-th D2D pair is allocated with a channel of a bandwidth equal to $B_n = \frac{C_{min}}{log_2\left(1+\frac{P_{max}\, g_{n,n}}{\sigma_{max}+I_d}\right)}$, where $\sigma_{max}$ is the highest possible expected noise at the channel with the bandwidth $B_n$. The noise $\sigma_{max}$ is, then, estimated as follows. The D2D pair with the lowest channel quality (i.e., the pair with $g^{min}_{n,n}$) is allocated with a channel of a bandwidth $\frac{g^{min}_{n,n}}{\sum_{n=1}^{n=N} g_{n,n}} B$ to guarantee $C_{min}$. Thus, any other $n$-th D2D pair requires less bandwidth to guarantee $C_{min}$, since the channel gain of the $n$-th D2D pair is always higher than $g^{min}_{n,n}$. Thus, the noise at the channel of the $n$-th D2D pair with the bandwidth $B_n$ is at most equal to the noise at the channel dedicated to the D2D pair with the lowest channel quality (i.e., $\sigma_n = \sigma_n B_n \leq \sigma_o \frac{g^{min}_{n,n}}{\sum_{n=1}^{n=N} g_{n,n}} B = \sigma_{max}$). Hence, the bandwidth of the channel dedicated for any $n$-th D2D pair always guaranteeing $C_{min}$ is:

$$B_n = \frac{C_{min}}{log_2\left(1+\frac{p_{max}\, g_{n,n}}{\sigma_o \frac{g^{min}_{n,n}}{\sum_{n=1}^{n=N} g_{n,n}} B + I_d}\right)} \quad (18)$$

This concludes the proof.

## REFERENCES


[1] M. N. Tehrani, et al., "Device-to-Device Communication in 5G Cellular Networks: Challenges, Solutions, and Future Directions," *IEEE Communications Magazine*, 52(5), pp. 86–92, 2014.

[2] P. Mach, et al., "In-Band Device-to-Device Communication in OFDMA Cellular Networks: A Survey and Challenges," *IEEE Communications Surveys & Tutorials*, vol. 17, no. 4, pp. 1885–1922, 2015.

[3] X. Huang, S. Tang, Q. Zheng,and Q. Chen, "Dynamic Femtocell gNB On/Off Strategies and Seamless Dual Connectivity in 5G Heterogeneous Cellular Networks," *IEEE Access*, vol. 6, pp. 21359–21368, 2018.

[4] D. Zhai, et al., "Energy-Saving Resource Management for D2D and Cellular Coexisting Networks Enhanced by Hybrid Multiple Access Technologies," *IEEE Transactions on Wireless Communications*, 16(4), pp. 2678–2692, 2017.

[5] P. Mach, et al., "Combined Shared and Dedicated Resource Allocation for D2D Communication," *IEEE VTC-Spring*, pp. 1–7, 2018.

[6] J. Dai, et al., "Analytical Modeling of Resource Allocation in D2D Overlaying Multihop Multichannel Uplink Cellular Networks," *IEEE Transactions on Vehicular Technology*, 66(8), pp. 6633–6644, 2017.

[7] Y. Huang, et al., "Mode Selection, Resource Allocation, and Power Control for D2D-Enabled Two-Tier Cellular Network," *IEEE Transactions on Communications*, 64(8), pp. 3534–3547, 2016.

[8] C. H. Yu, et al., "Resource Sharing Optimization for Device-to-Device Communication Underlaying Cellular Networks," *IEEE Transactions on Wireless Communications*, 10(8), pp. 2752–2763, 2011.

[9] Y. Li, et al.,"Joint Mode Selection and Resource Allocation for D2D Communications Under Queueing Constraints," *IEEE Conference on Computer Communications Workshops (INFOCOM WKSHPS)*, pp. 490-495, 2016.

[10] D. Ma, et al.,"Resource Allocation for Hybrid Mode Device-to-Device Communication Networks," *WCSP*, pp. 1-5, 2016.

[11] Y. Zhang, et al., "Incentive compatible overlay D2D system: A group-based framework without CQI feedback," *IEEE Transactions on Mobile Computing*, 17(9), pp. 2069–2086, 2018.

[12] D. H. Lee, et al.,"Resource allocation scheme for device-to-device communication for maximizing spatial reuse," *IEEE Wireless Communications and Networking Conference (WCNC)*, pp. 112–117, 2013.

[13] W. Zhibo, et al.," Clustering and power control for reliability improvement in Device-to-Device networks," *IEEE Globecom Workshops (GC Wkshps)*, pp. 573–578, 2013.

[14] Z. Y. Yang, et al.," Efficient resource allocation algorithm for overlay D2D communication," *Computer Networks*, 124, pp. 61–71, 2017.

[15] A. Abrardo, et al.," Distributed power allocation for D2D communications underlaying/overlaying OFDMA cellular networks," *IEEE Transactions on Wireless Communications*, 16(3), pp. 1466–1479, 2016.

[16] R. AliHemmati, et al., "Power Allocation for Underlay Device-to-Device Communication over Multiple Channels," *IEEE Transactions on Signal and Information Processing over Networks*, 4(3), pp. 467–480, 2017.

[17] R. AliHemmati, et al., "Multi-Channel Resource Allocation Toward Ergodic Rate Maximization for Underlay Device-to-Device Communications," *IEEE Transactions on Wireless Communications*, 17(2), pp. 1011–1025, 2017.

[18] Y. Qian, T. Zhang, and D. He, "Resource Allocation for Multichannel Device-to-Device Communications Underlaying QoS-Protected Cellular Networks," *IET Communications*, 11(4), pp. 558–565, 2017.

[19] Y. Xiao, et al., "A Bayesian overlapping coalition formation game for device-to-device spectrum sharing in cellular networks," *IEEE Transactions on Wireless Communications*, 14(7), pp. 4034–4051, 2015.

[20] M. Hasan, et al., "Distributed Resource Allocation for Relay-Aided Device-to-Device Communication Under Channel Uncertainties: A Stable Matching Approach," *IEEE Transactions on Communications*, 63(10), pp. 3882–3897, 2015.

[21] A. Asheralieva, et al., "Bayesian Reinforcement Learning-Based Coalition Formation for Distributed Resource Sharing by Device-to-Device Users in Heterogeneous Cellular Networks," *IEEE Transactions on Wireless Communications*, 16(8), pp. 5016–5032, 2017.

[22] S. Maghsudi, et al., "Channel Selection for Network-Assisted D2D Communication via No-Regret Bandit Learning With Calibrated Forecasting," *IEEE Transactions on Wireless Communications*, 14(3), pp. 1309–1322, 2015.

[23] Y. Li, et al., "Coalitional Games for Resource Allocation in the Device-to-Device Uplink Underlaying Cellular Networks," *IEEE Transactions on Wireless Communications*, 13(7), pp. 3965–3977, 2014.

[24] A. Asheralieva, et al., "An Asymmetric Evolutionary Bayesian Coalition Formation Game for Distributed Resource Sharing in a Multi-Cell Device-to-Device Enabled Cellular Network," *IEEE Transactions on Wireless Communications*, 17(6), pp. 3752–3767, 2018.

[25] J. Kim, et al., "Adaptive Mode Selection in D2D Communications Considering the Bursty Traffic Model," *IEEE Communications Letters*, 20(4), pp. 712–715, 2016.

[26] T. Liu, et al., "Resource Allocation for Device-to-Device Communications as an Underlay Using Nash Bargaining Game Theory," *ICTC*, pp. 366–371, 2015.

[27] S. A. Kazmi, at al., "Mode Selection and Resource Allocation in Device-to-Device Communications: A Matching Game Approach," *IEEE Transactions on Mobile Computing*, 16(11), pp. 3126-3141, 2017.

[28] W. Zhao, and S. Wang, "Resource Sharing Scheme for Device-to-Device Communication Underlaying Cellular Networks," *IEEE Transactions on Communications*, 63(12), pp. 4838–4848, 2015.

[29] R. Wang, et al. "Qos-Aware Joint Mode Selection and Channel Assignment for D2D Communications," *IEEE International Conference on Communications (ICC)*, pp. 1–6, 2016.

[30] R. Yin, et al., "Joint Spectrum and Power Allocation for D2D Communications Underlaying Cellular Networks," *IEEE Transactions on Vehicular Technology*, 65(4), pp. 2182–2195, 2015.

[31] P. Mach, et al., "Resource Allocation for D2D Communication with Multiple D2D Pairs Reusing Multiple Channels," *IEEE Wireless Communications Letters*, 2019.

[32] B. Di, et al.," Sub-channel assignment, power allocation, and user scheduling for non-orthogonal multiple access networks," *IEEE Transactions on Wireless Communications*, 15(11), pp. 7686–7698, 2016.

[33] T. LeAnh, et al.," Distributed power and channel allocation for cognitive femtocell network using a coalitional game in partition-form approach," *IEEE Transactions on Vehicular Technology*, 66(4), pp. 3475–3490, 2016.

[34] B. Zhang, et al.," Resource allocation for 5G heterogeneous cloud radio access networks with D2D communication: a matching and coalition approach," *IEEE Transactions on Vehicular Technology*, 67(7), pp. 5883–5894, 2018.

[35] M. Najla, Z. Becvar, and P. Mach , 'Sequential Bargaining Game for Reuse of Radio Resources in D2D Communication in Dedicated Mode," *IEEE VTC-spring*, 2020.

[36] J. Huang, et al.," Big data routing in D2D communications with cognitive radio capability," *IEEE Wireless Communications*, 23(4), pp. 45–51, 2016.

[37] J. G. Andrews, et al., "What Will 5G Be?," *IEEE Journal on selected areas in comm.*, 32(6), pp. 1065–1082, 2014.

[38] M. Pischella, et al., "A Joint Multiplexing and Resource Allocation Algorithm for Asynchronous Underlay D2D Communications," *IEEE VTC Spring*, pp. 1–5, 2018.

[39] L. Melki, et al., "Interference Management Scheme for Network-Assisted Multi-Hop D2D Communications," *IEEE 27th Annual International Symposium on Personal, Indoor, and Mobile Radio Communications (PIMRC)*, pp. 1–5, 2016.

[40] T. D. Hoang, et al., "Energy-Efficient Resource Allocation for D2D Communications in Cellular Networks," *IEEE Transactions on Vehicular Technology*, 65(9), pp. 6972–6986, 2016.

[41] 3GPP TS 36.214, "Evolved Universal Terrestrial Radio Access (E-UTRA); Physical layer; Measurements," v10.1.0, Rel.10, 2011.

[42] W. Lee, et al., "Transmit Power Control Using Deep Neural Network for Underlay Device-to-Device Communication," *IEEE Wireless Communications Letters*, 8(1), pp. 141–144, 2019.

[43] M. Najla, et al.," Predicting Device-to-Device Channels from Cellular Channel Measurements: A Learning Approach ," *arXiv:1911.07191*, 2019.

[44] T. Rahwan, et al.,"An Improved Dynamic Programming Algorithm for Coalition Structure Generation," *Proceedings of the 7th international joint conference on Autonomous agents and multiagent systems*, vol. 3, pp. 1417–1420, 2008.

[45] T. Rahwan et al.,"An Anytime Algorithm for Optimal Coalition Structure Generation," *Journal of artificial intelligence research*, vol. 34, pp. 527–567, 2009.

[46] T. Rahwan et al.,"A Coalition Structure Generation: A Survey," *Artificial Intelligence*, vol. 229, pp. 139–174, 2015.

[47] F. Cruz et al.,"Coalition Structure Generation Problems: Optimization and Parallelization of the IDP Algorithm in Multicore Systems," *Concurrency and Computation: Practice and Experience*, 29(5), p.e3969, 2017.

[48] 3GPP TR 36.843, "Study on LTE Device to Device Proximity Services; Radio Aspects," v12.0.1, Rel. 12, 2014.

[49] A. Farinelli, et al.,"A hierarchical clustering approach to large-scale near-optimal coalition formation with quality guarantees," *Engineering Applications of Artificial Intelligence 59*, pp. 170–185, 2017.

### 4.2.2 Enabling the reuse of Multiple Channels by Multiple Pairs in D2D Shared Mode

In this subsection, the reuse of multiple channels by multiple D2D pairs is enabled in the D2D shared mode in order to maximize the sum capacity of D2D pairs under the constraint of guaranteeing that the decrease in the capacity of the cellular users is below a pre-defined relative threshold. This subsection includes the journal paper [5J].

# Resource Allocation for D2D Communication With Multiple D2D Pairs Reusing Multiple Channels

Pavel Mach, *Member, IEEE*, Zdenek Becvar, *Senior Member, IEEE*, and Mehyar Najla, *Student Member, IEEE*

***Abstract*—In this letter, the goal is to maximize sum capacity of device-to-device (D2D) communication through a reuse of each radio channel by multiple D2D pairs while each D2D pair can access multiple channels. Since existing approaches cannot be easily extended to enable reuse of multiple channels by multiple D2D pairs in scenario with a high interference among the D2D pairs, we propose a novel resource allocation consisting of two phases. In an initial phase, all available channels are assigned by the Hungarian algorithm so that each channel is occupied by just one D2D pair. In a reuse phase, multiple D2D pairs are sequentially added to the individual channels according to their priority expressed by channel quality and received interference from already added D2D pairs. The proposal significantly outperforms existing solutions and reaches close to theoretical upper bound capacity despite a very low complexity of the proposed algorithm.**

***Index Terms*—Device-to-device, channel allocation, capacity, multiple channels reuse.**

## I. Introduction

DEVICE-TO-DEVICE (D2D) communication is a concept enabling a direct communication of user equipments (UEs) without a need to transmit data through a base station (BS) [1]. To fully benefit from the D2D concept, multiple D2D pairs should reuse each available channel and all D2D pairs should access multiple channels to maximize the spectrum usage.

The reuse of a single channel by more than one D2D pair underlying cellular communication is considered, e.g., [2]–[7]. These papers target to maximize the capacity of the D2D pairs while guaranteeing quality of service to the cellular UEs (CUEs). However, all these papers assume that each D2D pair can access at most one channel at a time. Although this assumption notably simplifies the channel allocation problem, a capacity gain introduced by the channel reuse is fairly limited. The use of more channels by single D2D pair is assumed in [8] and [9]. Still, in these papers, sharing of one channel by multiple D2D pairs is not possible due to the complexity of the resulting solution. The reuse of each channel by multiple D2D pairs while multiple channels can be exploited by each D2D pair is assumed in [10]. The authors propose a non-cooperative selfish game for the channel reuse. However, the game does not converge in realistic scenarios with the presence of mutual interference among D2D pairs. Hence, the solution is applicable only to scenarios with a very low number of the D2D pairs separated by large distances from each other.

As the papers [2]–[10] cannot be easily adapted to allow the D2D pairs communicating over multiple channels while reusing each channel by multiple D2D pairs in scenarios with interference among the D2D pairs, we introduce a novel two-phase channel allocation scheme. In an initial phase, each channel is allocated to one D2D pair by a common Hungarian algorithm. The core part of the proposed channel allocation scheme is a reuse phase that maximizes a sum D2D capacity through the reuse of multiple channels by multiple D2D pairs. The allocation of multiple D2D pairs to each channel is managed by a novel low complexity priority-based sequential algorithm. The algorithm adds the D2D pairs sequentially to the channels according to channel quality and interference from D2D pairs already occupying the channel. We also derive an optimal power allocation for the D2D pairs to show upper bound performance.

## II. System Model

Let's consider a cellular network consisting of one BS, $\mathcal{N} = \{n_1, n_2, \ldots, n_N\}$ CUEs, and $\mathcal{M} = \{m_1, m_2, \ldots, m_M\}$ D2D pairs. Without loss of generality the uplink bandwidth is split into *N* orthogonal channels of an equal width ($b_n$) so that each channel is occupied by just one CUE (i.e., the CUE *n* accesses the channel *n*). The D2D pairs access the channels in an underlay mode [1] as all available channels are assumed to be occupied by the CUEs (i.e., heavy loaded BS is assumed). The channel occupancy by the D2D pair is defined by a binary parameter $\varrho_m^n$, where $\varrho_m^n = 1$ ($\varrho_m^n = 0$) means that the D2D pair *m* occupies (does not occupy) the channel *n*.

The signal to interference plus noise ratio (SINR) at the BS and the channel *n* is defined as:

$$\gamma_n^n = \frac{p_n^n g_{n,b}^n}{\sigma^2 + I_b^n + \sum_{m \in \mathcal{M}} \varrho_m^n p_m^n g_{m,b}^n}, \tag{1}$$

where $p_n^n$ and $p_m^n$ are the transmission powers of the CUE *n* and of the D2D transmitter (D2D-Tx) *m*, respectively; $g_{n,b}^n$ is the channel gain between the CUE *n* and the BS at the channel *n*; $g_{m,b}^n$ is the channel gain between the D2D-Tx *m* and the BS at the channel *n*; $\sigma^2$ is the noise; and $I_b^n$ represents the inter-cell interference at the BS from the CUEs and the D2D pairs in adjacent cells using channel *n*. Note that we model the system with a single BS, but we still consider inter-cell interference from the neighboring cells as in the real networks. The SINR observed by the *m*-th D2D receiver (D2D-Rx) is:

$$\gamma_m^n = \frac{p_m^n g_{m,m}^n}{\sigma^2 + I_m^n + p_n^n g_{n,m}^n + \sum_{k \neq m} \varrho_k^n p_k^n g_{k,m}^n}, \tag{2}$$

Manuscript received February 11, 2019; accepted March 4, 2019. Date of publication March 7, 2019; date of current version August 21, 2019. This work was supported in part by the Czech Science Foundation under Grant GA17-17538S, and in part by the Grant Agency of Czech Technical University in Prague under Project SGS17/184/OHK3/3T/13. The associate editor coordinating the review of this paper and approving it for publication was G. Yu. *(Corresponding author: Pavel Mach.)*

The authors are with the Department of Telecommunication Engineering, Faculty of Electrical Engineering, Czech Technical University in Prague, 166 27 Prague, Czech Republic (e-mail: machp2@fel.cvut.cz; zdenek.becvar@fel.cvut.cz; najlameh@fel.cvut.cz).

Digital Object Identifier 10.1109/LWC.2019.2903798

where $g^n_{m,m}$ is the channel gain between the D2D-Tx *m* and the D2D-Rx *m* at the channel *n*; $g^n_{n,m}$ represents the channel gain between the CUE *n* and the D2D-Rx *m* at the channel *n*; $g^n_{k,m}$ stands for the channel gain between the D2D-Tx *k* and the D2D-Rx *m* at the channel *n*, and $I^n_m$ is the inter-cell interference caused to the D2D-Rx *m* at the channel *n*.

## III. Problem Formulation

Our goal is to maximize a sum D2D capacity (defined as a sum of capacities of all D2D pairs at all channels) while a certain capacity $c^c_{min}$ is still guaranteed to the CUEs. Thus, the objective is formulated as:

$$\begin{aligned} \max \ & \sum_{n\in\mathcal{N}}\sum_{m\in\mathcal{M}} \varrho^n_m b_n log_2(1+\gamma^n_m) \\ \text{s.t. } & \text{a1: } b_n log_2(1+\gamma^n_n) \geq c^c_{min}, \forall n \in \mathcal{N} \\ & \text{a2: } p^n_n \leq P_{max}, \forall n \in \mathcal{N} \\ & \text{a3: } \sum_{n\in\mathcal{N}} p^n_m \leq P_{max}, \forall m \in \mathcal{M}, \end{aligned} \tag{3}$$

The constraint a1 guarantees that the capacity of the CUEs is at least $c^c_{min}$ while the constraints a2 and a3 limit the total transmission power of the CUEs and D2D pairs, respectively. The a1 is guaranteed if $\sum_{m\in\mathcal{M}} \varrho^n_m p^n_m g^n_{m,b} \leq I^n_t$, where $I^n_t$ is a maximum tolerable interference expressed as [2]:

$$I^n_t = \frac{p^n_n g^n_{n,b}}{2^{\frac{c^c_{min}}{b_n}}-1} - \sigma^2 - I^n_b, \forall n \in \mathcal{N}. \tag{4}$$

Note that if the capacity of CUE *n* is below $c^c_{min}$ even if no D2D pair occupies the channel *n*, $I^n_t$ is set to 0.

## IV. Proposed Channel and Power Allocation

The channel allocation for the D2D pairs is managed in two phases. In the initial phase, each channel is assigned to one D2D pair (denoted as a primary D2D pair). The purpose of the initial phase is to prepare a base for the novel reuse phase. In the reuse phase, multiple D2D pairs (denoted as secondary D2D pairs) can be added to each channel on top of the primary D2D pairs. Note that the D2D pair, which is in the role of the primary D2D pair at a specific channel can also be the secondary D2D pair at any other channel(s).

### A. Initial Phase

In the initial phase, the objective is to assign all available channels to the D2D pairs so that each channel is occupied by one primary D2D pair. The allocation in the initial phase is done by the Hungarian algorithm that maximizes the capacity if only one D2D pair occupies each channel [11]. To exploit the Hungarian algorithm, the potential maximal capacity of all D2D pairs at all available channels (represented by matrix $C = \{c^n_m\}$) is calculated. The potential maximal capacity ($c^n_m$) of the D2D pair *m* at the channel *n* is determined as:

$$c^n_m = b_n log_2\left(1+\frac{p^n_m g^n_{m,m}}{\sigma^2 + I^n_m + p^n_n g^n_{n,m}}\right), \tag{5}$$

To achieve the maximal capacity of the D2D pairs at each channel while guaranteeing a1, we set $p^n_m$ in (5) as:

$$\frac{I^n_t}{g^n_{m,b}} = p^n_m \leq P_{max}, \forall n \in \mathcal{N}, \forall m \in \mathcal{M}, \tag{6}$$

After the matrix $C = \{c^n_m\}$ is obtained, the Hungarian algorithm assigns each channel to a single primary D2D pair. If $N>M$, the Hungarian algorithm is run $\lceil N/M \rceil$ times, as only *M* channels are allocated during each run of the algorithm. Consequently, some D2D pairs are primary D2D pairs at several channels to fully exploit all available radio resources. On the contrary, if $N \leq M$, the Hungarian algorithm is performed only once, and some D2D pairs may not access any channel as the primary D2D pair. The pairs that get no channel in the initial phase can still access channels as the secondary D2D pairs in the reuse phase.

### B. Reuse Phase

The core part of the proposed scheme is the reuse phase. The objective of this phase is to maximize the sum D2D capacity through reusing each channel by multiple secondary D2D pairs. In general, adding new D2D pair(s) to the channel inevitably reduces the capacity of the D2D pairs already occupying the channel because of the interference originating from the newly added D2D pair(s) (see (2)). To guarantee the capacity of the D2D pairs (similarly as the capacity of the CUEs), the problem defined in (3) is extended as:

$$\begin{aligned} \max \ & \sum_{n\in\mathcal{N}}\sum_{m\in\mathcal{M}} \varrho^n_m b_n log_2(1+\gamma^n_m) \\ \text{s.t. } & \text{a1}\sim\text{a3 as defined in (3)} \\ & \text{a4: } \sum_{n\in\mathcal{N}} b_n log_2(1+\gamma^n_m) \geq c^d_{min}, \forall m \in \mathcal{M}, \end{aligned} \tag{7}$$

The constraint a4 ensures that the capacity of the D2D pairs over all channels is at least $c^d_{min}$. Thus, no additional D2D pairs can be added to the channel if the capacity of any D2D pair already using the channel is lower than $c^d_{min}$.

The channel reuse is done by the proposed low complexity Priority-Based Sequential Algorithm (PBSA) that adds secondary D2D pairs to individual channels sequentially. The order in which the secondary D2D pairs are added to the channel *n* is supposed to play an important role. The reason is that adding one secondary D2D pair can result in preventing further addition of another secondary D2D pair(s) (e.g., due to high interference generated among the secondary D2D pairs). The proposed PBSA adds the secondary D2D pairs in an order determined according to priority metric $\omega^n_{m'}$ defined as:

$$\omega^n_{m'} = p^n_{m'} g^n_{m',m'} - \sum_{m\in\mathcal{M}\setminus\{m'\}} \varrho^n_m p^n_m g^n_{m,m'}, \forall n \in \mathcal{N}, \tag{8}$$

where the first term corresponds to the signal strength received by the D2D-Rx from the D2D-Tx of the secondary D2D pair $m'$ that is supposed to be added at the channel *n* and the second term is the sum of interference from the D2D pairs already assigned to the channel *n*. Note that the priority of the secondary D2D pair is higher if $\omega^n_{m'}$ is higher. It is worth to mention that the D2D-Rx measures the sum interference from all D2D pairs using the channel. Thus, there is no need to know channel gains to all D2D pairs and the required signaling to

manage the reuse phase is the same as if no reuse would be applied at all.

In order to enumerate $\omega^n_{m'}$ according to (8), the transmission powers of the D2D pairs at each channel need to be determined. Since the constraint a1 should be guaranteed during the whole reuse phase, the following condition should hold: $\sum_{m\in\mathcal{M}} x^n_m I^n_t \leq I^n_t$, where $x^n_m I^n_t = p^n_m g^n_{m,b}$ is the interference caused by the D2D pair *m* to the CUE *n*. To find the optimal D2D power allocation (i.e., to find optimal values of $x^n_m$), we define the objective function as:

$$f(\mathbf{X^n}) = \sum_{m\in\mathcal{M}} log_2\left(1 + \frac{\varrho^n_m \frac{x^n_m I^n_t}{g^n_{m,b}} g^n_{m,m}}{I^n_s + \sum_{k\neq m} \varrho^n_k \frac{x^n_k I^n_t}{g^n_{k,b}} g^n_{k,m}}\right), \tag{9}$$

where $I^n_s = \sigma^2 + I^n_m + p^n_n g^n_{n,m}$ and $\mathbf{X^n} = \{x^n_1, x^n_2, \ldots, x^n_M\}$. Then, the optimization problem is:

$$\begin{aligned} \min_{\mathbf{X^n}} \ & -f(\mathbf{X^n}) \\ \text{s.t.} \ & 0 \leq x^n_m \leq 1, \ \forall n \in \mathcal{N}, \ \forall m \in \mathcal{M} \\ & \sum_{m\in\mathcal{M}} x^n_m \leq 1, \ \forall n \in \mathcal{N} \end{aligned} \tag{10}$$

where both constraints ensure that a1 in (3) is fulfilled. We solve (10) by a sequential quadratic programming (SQP). In general, SQP solves a quadratic programming sub-problem at each iteration. During each iteration, an estimate of the Hessian of the Lagrangian is calculated via the Broyden–Fletcher–Goldfarb–Shanno (BFGS) formula (see more details in [12]). Due to relatively high complexity of SQP, we also propose "equal" power allocation (PBSA-equal) introducing no additional complexity to the channel allocation process since the power of the D2D pairs is set so that each D2D pair causes the same interference to the CUE (i.e., $x^n_m = 1/\sum_{m\in\mathcal{M}} \varrho^n_m, \forall x^n_m \in \mathbf{X^n}$).

After acquiring the $\mathbf{X^n}$, transmission power of the D2D pair *m* occupying the channel *n* is:

$$\frac{x^n_m I^n_t}{g^n_{m,b}} = p^n_m \leq P_{max}, \forall n \in \mathcal{N}, \forall m \in \mathcal{M}, \tag{11}$$

The allocation of channels in the reuse phase is described in Algorithm 1. First, $\Omega^n = \{\omega^n_1, \omega^n_2, \ldots, \omega^n_{M-1}\}$ is determined for all *N* channels according to (8). Then, the $\Omega^n$ is sorted according to $\omega^n_{m'}$ in descending order (line 4). Subsequently, the secondary D2D pair with the highest priority at the channel *n* (i.e., the D2D pair with max($\omega^n$)) is added to the channel *n* by setting $\varrho^n_{m'} = 1$ (line 5). Then, the transmission power $p^n_m$ is updated for all D2D pairs occupying the channel according to (11) (line 6) and a new sum D2D capacity at the channel ($c^n_{m'}$) is calculated (line 7). If the sum D2D capacity is decreased by an inclusion of the secondary D2D pair $m'$ (i.e., if $c^n_{m'} < c^n_{m'-1}$) or if a4 is not fulfilled, the secondary D2D pair is removed from the channel (i.e., $\varrho^n_{m'} = 0$). Otherwise, the secondary D2D pair starts reusing the channel and $\omega^n_m$ is updated for the D2D pairs that still can be added to this channel (line 11). This whole process (lines 2–14) is repeated for all secondary D2D pairs and for all available channels.

The complexity of the channel allocation in reuse phase is up to $\mathcal{O}(N(M-1))$ as ($M-1$) secondary D2D pairs can be added to *N* channels. Note that the complexity of channel allocation process is even lower than in related works (see [2], [7]). Further, the complexity of the optimal power allocation is, in the worst case, $\mathcal{O}(M^3KN)$, where $M^3$ corresponds to the maximal complexity of quadratic programming and *K* is the number of iterations of the sequential process. The complexity of "equal" power allocation is $\mathcal{O}(1)$.

**Algorithm 1** Priority-Based Sequential Algorithm

1: determine $\Omega^n, \forall n \in \mathcal{N}$ acc. (8)
2: **for** $n$=1:$N$ **do**
3: **for** $m'$=1:($M-1$) **do**
4: sort $\Omega^n$ in descending order (D2D pairs priority)
5: $\varrho^n_{m'} = 1$ (add D2D pair $m'$ at channel $n$)
6: set $p^n_m \ \forall$ D2D pairs using channel $n$ acc. (11)
7: $c^n_{m'} = \sum_{m\in M} \varrho^n_m b_n log_2(1+\gamma^n_m)$
8: **if** $c^n_{m'} < c^n_{m'-1}$ or a4 is not satisfied **then**
9: $\varrho^n_{m'} = 0$, $c^n_{m'} = c^n_{m'-1}$
10: **else**
11: update $\omega^n_m$ for D2D pairs not yet added
12: **end if**
13: **end for**
14: **end for**

TABLE I
PARAMETERS AND SETTINGS FOR SIMULATIONS

| Parameter | Value |
|---|---|
| Simulation area | 500x500 m |
| Number of CUEs/channels ($N$) | 10 |
| Number of D2D pairs ($M$) | 2–20 |
| Channel bandwidth ($b_n$) | 2 MHz |
| Max. distance between D2D-Tx and D2D-Rx | 50 m |
| Carrier frequency | 2 GHz |
| Transmission power of CUEs ($p^n_n$) | 24 dBm [10] |
| Max. DUE's transmission power at channel $n$ ($p^n_m$) | 10 dBm [10] |
| Number of simulation drops | 200 |

## V. PERFORMANCE ANALYSIS

The proposed scheme is evaluated by simulations. The BS is located in the middle of a simulation area. For each simulation drop, the positions of CUEs, D2D-Txs, and D2D-Rxs are generated randomly with uniform distribution. The maximum distance between D2D-Tx and D2D-Rx creating one D2D pair is set to 50 m. Hence, the position of the D2D-Tx is generated first and, then, the D2D-Rx is randomly dropped within the allowed maximum radius from the D2D-Tx. Moreover, the inter-cell interference at the BS ($I^n_b$) and the D2D-Rxs ($I^n_m$) is generated randomly according to Gamma distribution [13] with a mean value of $-80$ dBm. The channel gains between individual nodes are derived according to the models defined by 3GPP. Since our objective does not target an optimization of the CUEs' transmission power, we assume fixed transmission power $p^n_n$ of the CUEs at each channel as in [10]. All major simulation parameters are summarized in Table I.

The results of the PBSA with the optimal power allocation (PBSA-opt) according to (10) and the PBSA-equal are compared with the proposed "random" algorithm, which exploits reuse, but does not consider the priority metrics (i.e., the secondary D2D pairs are added to the channels randomly). The performance of the proposed PBSA is also compared with

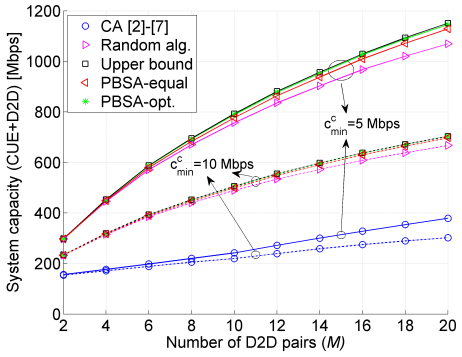


Fig. 1. System capacity depending on $M$ for $c^d_{min} = 0$.

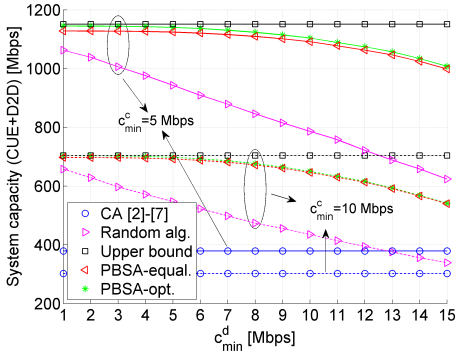


Fig. 2. System capacity depending on $c^d_{min} = 0$ for $M = 20$.

channel allocation (CA) based on [2]–[7] allowing to reuse each channel by multiple D2D pairs while only one channel can be exploited by each D2D pair. Then, we show a theoretical upper bound performance obtained by checking all possible D2D pair allocations to all channels (i.e., the optimal case) and with the D2D transmission power set to the optimal values according to (10). The complexity of the theoretical upper bound is $\mathcal{O}(N2^M)$. Note that we do not compare the proposed PBSA with the scheme in [10], since the non-cooperative game exploited in [10] does not converge if interference among the D2D pairs is high.

Fig. 1 illustrates the system capacity depending on the number of D2D pairs ($M$). Increasing $c^c_{min}$ decreases the capacity of all algorithms. The reason is that the CUEs can tolerate less amount of interference for a higher $c^c_{min}$ and, hence, $I^n_t$ is decreased (see (4)). Fig. 1 further shows that the proposed PBSA-opt provides between 1.52 and 3.26 times higher capacity (depending on $c^c_{min}$ and $M$) than the CA scheme based on [2]–[7]. These encouraging results demonstrate that the reuse of multiple channels by multiple D2D pairs results in a significant gain in capacity comparing to the CA [2]–[7], where each D2D pair can access only one channel. In addition, Fig. 1 demonstrates that the PBSA-opt reaches almost theoretical upper bound capacity (only 0.5% degradation). It is worth to mention that the performance of the PBSA-equal is at most 1.6% below that of the PBSA-opt. Thus, the equal power allocation can be applied in a real system instead of more complex optimal power allocation at the cost of only a slight decrease in the sum D2D capacity.

Fig. 1 also reveals an interesting fact: if $c^d_{min} = 0$ Mbps (no capacity is guaranteed to the D2D pairs), the order in which the secondary D2D pairs are added to the channel is not that critical. Hence, the PBSA does not outperform random adding of the D2D pairs significantly for $c^d_{min} = 0$ Mbps (up to 7.1% for 20 D2D pairs). However, Fig. 2 shows that performance gap between the random algorithm and the PBSA significantly increases with $c^d_{min}$ (up to 61.5% for $c^d_{min} = 15$ Mbps). The reason is that in the case of random adding of the D2D pairs, even the D2D pair with the capacity slightly above $c^d_{min}$ can be added to the channel at the beginning of the reuse phase. Then, other D2D pairs can be no longer allowed to reuse the same channel to guarantee $c^d_{min}$. Although the system capacity of PBSA (both -equal and -opt.) starts also decreasing for a higher $c^d_{min}$, this decrease is only marginal when compared to the random adding of the D2D pairs.

Since our main objective is to maximize the system capacity, $c^d_{min} \leq 10$ Mbps is recommended since the PBSA performance is still close to the upper bound. A specific $c^d_{min}$ should be selected according to requirements and/or priority of individual D2D pairs at each channel.

## VI. Conclusion

In this letter, we have proposed a novel low complexity resource allocation scheme maximizing sum D2D capacity. The scheme allows an efficient reuse of the channels by multiple D2D pairs while each D2D pair may access multiple channels. We show that the proposed allocation significantly outperforms the state-of-the-art approaches (increasing the sum D2D capacity at up to 3.26 times) and reaches close-to-optimum performance despite low (linear) complexity.

## References

[1] A. Asadi, Q. Wang, and V. Mancuso, "A survey on device-to-device communication in cellular networks," *IEEE Commun. Surveys Tuts.*, vol. 16, no. 4, pp. 1801–1819, 4th Quart., 2014.
[2] W. Zhao and S. Wang, "Resource sharing scheme for device-to-device communication underlaying cellular networks," *IEEE Trans. Commun.*, vol. 63, no. 12, pp. 4838–4848, Dec. 2015.
[3] D. Ma, N. Wang, and X. Mu, "Resource allocation for hybrid mode device-to-device communication networks," in *Proc. WCSP*, 2016, pp. 1–5.
[4] Y. Li, M. C. Gursoy, and S. Velipasalar, "Joint mode selection and resource allocation for D2D communications under queueing constraints," in *Proc. IEEE INFOCOM WKSHPS*, vol. 20, no. 3, 2016, pp. 490–495.
[5] R. Wang, J. Zhang, S. H. Song, and K. B. Letaief, "QoS-aware joint mode selection and channel assignment for D2D communications," in *Proc. IEEE ICC*, 2016, pp. 1–6.
[6] M. C. Lucas-Estan and J. Gozalvez, "Distributed radio resource allocation for device-to-device communications underlaying cellular networks," *J. Netw. Comput. Appl.*, vol. 99, pp. 120–130, Dec. 2017.
[7] S. M. A. Kazmi *et al.*, "Mode selection and resource allocation in device-to-device communications: A matching game approach," *IEEE Trans. Mobile Comput.*, vol. 16, no. 11, pp. 3126–3141, Nov. 2017.
[8] Y. Qian, T. Zhang, and D. He, "Resource allocation for multichannel device-to-device communications underlaying QoS-protected cellular networks," *IET Commun.*, vol. 11, no. 4, pp. 558–565, Mar. 2017.
[9] R. Alihemmati, M. Dong, B. Liang, G. Boudreau, and S. H. Seyedmehdi, "Multi-channel resource allocation toward ergodic rate maximization for underlay device-to-device communications," *IEEE Trans. Wireless Commun*, vol. 17, no. 2, pp. 1011–1025, Feb. 2018.
[10] R. Yin *et al.*, "Joint spectrum and power allocation for D2D communications underlaying cellular networks," *IEEE Trans. Veh. Technol.*, vol. 65, no. 4, pp. 2182–2195, Apr. 2016.
[11] H. W. Kuhn, "The Hungarian method for the assignment problem," *Naval Res. Logistics Quart.*, vol. 2, nos. 1–2, pp. 83–97, Mar. 1955.
[12] S. S. Rao, *Engineering Optimization: Theory and Practice*. Hoboken, NJ, USA: Wiley, 2009.
[13] I. Viering, A. Klein, M. Ivrlac, M. Castaneda, and J. A. Nossek, "On uplink intercell interference in a cellular system," in *Proc. IEEE ICC*, 2006, pp. 2095–2100.

## 4.3 Combination of VLC and RF for D2D Communication

This section introduces the combination of VLC and RF for D2D communication. Then two algorithms for RF/VLC band selection in a scenario with multiple D2D pairs are proposed. This section assumes the dedicated mode of D2D communication, however, the principles of the proposed solutions can be extended even for the shared mode.

### 4.3.1 Concept of RF-VLC D2D Communication

First, in this subsection, the principle of combining RF and VLC for D2D communication is analyzed and the possible advantages as well as challenges resulted from this combination are defined. This subsection includes the conference paper [6C].

# Combination of Visible Light and Radio Frequency Bands for Device-to-Device Communication

Pavel Mach, Zdenek Becvar, Mehyar Najla, Stanislav Zvanovec
Faculty of Electrical Engineering, Czech Technical University in Prague
Technicka 2, 166 27 Prague, Czech republic
emails: {machp2, zdenek.becvar, najlameh, xzvanove}@fel.cvut.cz

***Abstract*—Future mobile networks are supposed to serve high data rates to users. To accommodate the high data rates, a direct communication between nearby mobile terminals (MTs) can be exploited. This type of communication in mobile networks is known as Device-to-device (D2D). Furthermore, a communication in high frequency bands, such as, visible light communication (VLC), is also foreseen as an enabler for the high data rates. In a conventional D2D communication, pairs of the communicating MTs should reuse the same frequencies to maximize spectral efficiency of the system. However, this implies either interference among the D2D pairs or a need for complex resource allocation algorithms. In this paper, we introduce a new concept for D2D communication combining VLC and RF technologies in order to maximize capacity of the system. The objective of this paper is to analyze operational limits of the proposed concept and to assess potential capacity gains to give motivation for future research in this area. Thus, we also discuss several practical issues related to the proposed RF–VLC D2D concept and outline major research challenges. The performance analysis carried out in this paper shows that the RF–VLC D2D is able to improve the capacity in an indoor scenario by a factor of 4.1 and 1.5 when compared to standalone RF D2D and VLC D2D, respectively.**

***Keywords*—Device-to-device; Mode selection; Visible Light Communication; Radio frequency**

## I. Introduction

In conventional mobile networks, mobile terminals (MTs) communicate through a base station, in LTE-A denoted as an evolved node B (eNB). The concept of a direct communication among the MTs in proximity of each other, known as Device-to-Device (D2D) communication, is considered as a way to enhance the capacity of mobile networks and to increase spectral efficiency [1]. Furthermore, D2D enables to decrease packet delay and to reduce energy consumption of the MTs due to mutual proximity of the MTs [2].

In general, D2D communication can be used in either in-band or out-band fashions. In the case of in-band D2D, the MTs reuse the same frequency bands as a conventional cellular communication, e.g., licensed frequencies allocated for mobile networks. Hence, interference between D2D and the conventional cellular communication is seen as a critical problem [3]. To address this problem, many interference mitigation techniques, such as power control [4], radio resource allocation [5], scheduling [6], etc., can be applied. Nonetheless, if interference between the D2D and cellular communications cannot be sufficiently mitigated by these techniques, D2D may be forced to operate in a dedicated mode (also known as an overlay mode). In the dedicated mode, D2D exploits orthogonal resources to the cellular communication to avoid interference entirely, however, this is at the cost of decreased spectral efficiency [7].

In the case of the out-band D2D, the D2D communication takes place in unlicensed bands through WiFi-Direct or Bluetooth, as investigated, e.g., in [8]. Nevertheless, if D2D pairs in close vicinity of each other reuse the same out-band frequencies, interference among D2D pairs remains a problem and limits the benefits of D2D. To minimize interference among D2D pairs, visible light communication (VLC) can be also considered for the out-band D2D. The VLC systems operate at wavelengths of 380-750 nm (i.e., frequency bands of 400-790 THz) [9] and can result in high data rates. For example, 4.5 Gbps throughput can be achieved by the VLC systems employing carrier-less amplitude & phase modulations and a recursive least square-based adaptive equalizer as described in [10] and [11], respectively. In [12], the authors show that a combination of 16–quadrature amplitude modulation and orthogonal frequency division multiplexing (OFDM) or wavelength multiplex (RGB) allow to reach 3.4 Gbps throughput. A disadvantage of VLC can be seen in a low scalability for longer distances and its sensitivity to a volatility of the MT's orientation resulting in a sudden decrease in VLC channel quality even for small changes of the MTs' orientation (in terms of irradiance and incidence angles) [13].

A combination of communication in the conventional radio frequency (RF) and VLC bands is surveyed in [14] and further investigated, e.g., in [15],[16],[17],[18]. In all studies, the authors assume that the VLC access points are deployed at the ceiling and act as an LTE

978-1-5386-3531-5/17/$31.00 

eNB or WiFi access point. These papers do not consider D2D communication, which introduces new challenges and opportunities related to a higher sensitivity of the VLC channel on volatility of both sides of the communication chain and proximity of the MTs. To our best knowledge, the VLC for D2D is considered only in [19] and [20]. In [19], the authors propose a game theory-based mechanism choosing the optimal mode of VLC communication from three candidate modes in order to enhance channel capacity. The first mode is a direct VLC communication (VLC D2D), the second mode is a indirect VLC communication through an access point and the third mode represents a mix of the first two modes. In other words, the paper investigates behavior of a conventional D2D in VLC bands. In [20], an optical repeater-assisted VLC D2D system is presented. The VLC repeater enables VLC for longer distances and allows to enhance VLC range when the direct link between the MTs is not available. This is an analogy to D2D relaying as addressed frequently in the conventional D2D in RF bands. However, also [20] is focused purely on VLC bands and does not consider a combination of RF and VLC for D2D.

In this paper, we introduce a new concept combining in-band RF and out-band VLC for D2D communication. The new RF–VLC D2D concept takes advantage of the fact that RF and VLC do not interfere to each other and VLC signal is strongly attenuated with distance, thus, interference to other D2D pairs operating in VLC is naturally suppressed. At the same time, RF enables to preserve benefits of common D2D for larger distances at which VLC cannot operate. By allowing selection of either RF or VLC for each D2D pair, overall level of interference is significantly reduced and the system capacity is increased. To motivate further research in the area of combined RF-VLC D2D, we discuss an applicability of the new concept, analyze key practical issues, and outline future research challenges. Then, we investigate limits of the operation and gains introduced by RF-VLC D2D depending on various parameters, such as a distance between the MTs of the same D2D pairs, a distance between the D2D pairs, or irradiance/incidence angles of the MTs. As this paper is an initial work in this domain, we limit our investigation to indoor scenario where we foresee main benefits of the VLC-RF D2D. Through simulations, we show that the combination of RF and VLC for D2D allows a significant increase in the capacity of the communication system.

The paper is organized as follows. In Section II, the system model for the proposed RF-VLC D2D concept is defined. In Section III, we discuss potential use-cases for the proposed concept, contemplate key practical issues and outline future research challenges for D2D combining RF and VLC bands. Then, Section IV is dedicated to a description of the simulation scenarios and to a discussion of the simulation results. The last section concludes the paper and outlines future research directions.

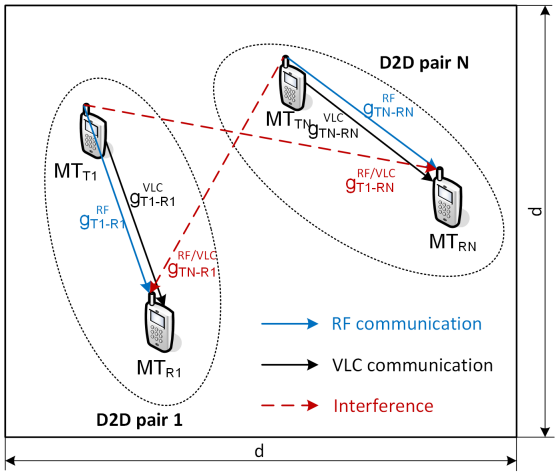


Fig. 1: System model for investigation of the proposed RF-VLC concept.

## II. System Model for RF–VLC D2D

In this section, we describe a general system model and mode selection for the proposed RF-VLC D2D concept. We assume $N$ MTs randomly distributed within a square room with a dimension $d$ (see Fig 1). As VLC is highly susceptible even to small changes in the angles between a transmitting MT ($MT_T$) and a receiving MT ($MT_R$) [21], we assume varying azimuthal orientation of both MTs. Note that the varying angles are more critical in terms of VLC channel quality than the MTs' mobility, since the mobility leads to a continuous and slow changes of the angles between the $MT_T$ and the $MT_R$. In contrast, turning the MTs leads to an immediate and a steep change of the angles. Thus, for sake of simplicity and clarity, we leave the mobility of the MTs for further research and we focus on static MTs here.

Among all $N$ active MTs, $N_p$ D2D pairs are randomly selected so that every MT is involved in just one D2D pair (i.e., $N_p = N/2$). The channel gain between the MTs within one D2D pair is denoted as $g_{T-R}^{RF}$ and $g_{T-R}^{VLC}$ for RF and VLC modes, respectively. We assume that the D2D pairs exploit dedicated uplink resources with respect to the cellular communication so there is no interference between the D2D MTs and MTs communicating with the eNBs. Contrary, all D2D pairs operate in the same RF bands and, thus, interfere with each other (see Fig. 1 where the $MT_{T1}$ causes interference to the $MT_{RN}$ and the $MT_{R1}$ is interfered by the $MT_{TN}$). Consequently, the available capacity for RF D2D is significantly influenced by the amount of interference originating from nearby D2D pairs. The $MT_T$ exploiting VLC does not introduce interference to

the $MT_R$ operating in RF as these operate at different frequencies.

The communication mode (RF or VLC) is selected with objective to maximize the capacity, that is:

$$\mathcal{M} = \begin{cases} RF: & C^{RF} \geq C^{VLC} \\ VLC: & C^{RF} < C^{VLC} \end{cases} \quad (1)$$

where capacities of RF D2D and VLC D2D are derived according to Shannon-Hartleys theorem:

$$C^{RF} = B^{RF} log_2(1 + SINR^{RF}) \quad (2)$$

$$C^{VLC} = B^{VLC} log_2(1 + SINR^{VLC}) \quad (3)$$

where $B^{RF}(B^{VLC})$ is the system bandwidth of RF (VLC) and $SINR^{RF}$ ($SINR^{VLC}$) stands for the signal to interference plus noise ratio (SINR) observed by the $MT_R$ in RF (VLC) mode. The $SINR^{RF}_{Rn}$ experienced by the $n$-th MT ($MT_{Rn}$) is expressed as:

$$SINR^{RF}_{Rn} = \frac{P^{RF}_t g^{RF}_{Tn-Rn}}{\sum_{i \neq n}(P^{RF}_t g^{RF}_{Ti-Ri}) + \sigma^2_{t,RF}} \quad (4)$$

where $P^{RF}_t$ is the RF transmitting power of the $MT_T$, $g^{RF}_{Ti-Ri}$ is the RF channel gain between the $MT_{Ti}$ and the $MT_{Ri}$ of the $i$-th D2D pair, and $\sigma^2_{t,RF}$ stands for the thermal noise in RF. The $SINR^{VLC}_{Rn}$ experienced by the $MT_{Rn}$ is defined as:

$$SINR^{VLC}_{Rn} = \frac{P^{VLC}_t g^{VLC}_{Tn-Rn} \gamma^2}{\sum_{i \neq n}(P^{VLC}_t g^{VLC}_{Ti-Ri}) + \sigma^2_{t,VLC} + \sigma^2_s} \quad (5)$$

where $P^{VLC}_t$ represents the transmitting optical power of the transmitting LED, $g^{VLC}_{Tn-Rn}$ is the VLC channel gain between the MTs of the $n$-th D2D pair, $\gamma$ is the responsivity of a photo-diode, and $\sigma^2_s$ is the shot noise.

The VLC channel gain $g^{VLC}_{Tn-Rn}$ is strongly dependent on the irradiance angle ($\phi$), incidence angle ($\psi$), and on the parameters of the optical receiver. Thus, the channel gain $g^{VLC}_{Tn-Rn}$ is expressed by the following equation:

$$g^{VLC}_{Tn-Rn} = \frac{(m+1) A cos^m(\phi) T_s g(\psi) cos(\psi)}{2\pi d^2_{TR}} \quad (6)$$

where $A$ is the physical area of a photodetector, $T_s$ stands for the gain of an optical filter, $d_{TR}$ is the distance between the $MT_T$ and $MT_R$, $g(\psi)$ is the gain of an optical concentrator, and $m$ corresponds to the order of Lambertian emission defined as follows:

$$m = \frac{-ln(2)}{ln(cos(\phi_c))} \quad (7)$$

where $\phi_c$ is the transmitter semi-angle at half power [13]. The gain of the optical concentrator ($g(\psi)$) depends on the photodetector view angle ($\psi_c$) and it is expressed as:

$$g(\psi) = \begin{cases} \frac{n^2}{sin^2(\psi_c)} & \text{if } 0 < \psi \leq \psi_c \\ 0 & otherwise \end{cases} \quad (8)$$

The thermal and shot noises for VLC are calculated as:

$$\sigma^2_{t,VLC} = (\frac{8\pi k T_k \eta A I_2 B^2}{G}) + \\ + (\frac{16\pi^2 k T_k \Gamma \eta^2 A^2 I_3 B^3}{g_m}) \quad (9)$$

$$\sigma^2_s = (2q I_{bg} I_2 B) + (2q\gamma P^{VLC}_t g^{VLC}_{Tn-Rn} B) \quad (10)$$

where $k$ is Boltzmann's constant, $T_k$ corresponds to the absolute temperature, $\eta$ is the fixed capacitance of the photodetector per unit area, $I_2$ and $I_3$ stand for the noise bandwidth factors, $B$ represents the equivalent noise bandwidth, $G$ is the open-loop voltage gain, $\Gamma$ is FET channel noise factor, $g_m$ corresponds to FET transconductance, $q$ is the charge, and $I_{bg}$ is the background current [13]. We assume the MTs are equipped with the RGB-based LED and the photodetector at the transmitter and the receiver, respectively, as assumed in [20].

## III. Use cases, practical issues and research challenges for RF-VLC D2D

In this paper, we target to demonstrate a potential efficiency of the combined RF-VLC D2D. Still, there are several research and practical issues need to be taken care of to bring the propose concept into fruition. Hence, this section discusses the applicability of the RF-VLC D2D in real network and also discusses some practical issues and research challenges of the proposed concept.

The first important aspect regarding the combination of RF and VLC for D2D is to outline its use-cases and suitable scenarios. Basically, we can expect that the combination of RF and VLC for D2D would be beneficial for future services requiring high throughput and low latencies. In general, low throughput services or calls are not seen as the most promising options for the RF-VLC D2D due to their demands on relatively low capacity and high sensitivity to sudden connection degradation. Thus, services and applications requiring rather high throughput while tolerating a throughput variation are supposed to be good target for the RF-VLC D2D. Since the VLC is beneficial especially for short distances and exhibits superior indoor performance [22], we can expect that RF-VLC D2D concept should be used primarily indoor, where the user who wants to transmit a high amount of data to another user (e.g., exchanging photos or videos) can direct their MTs towards each other to enhance capacity by VLC. To this end, we analyze requirements on angles between $MT_T$ and $MT_R$ later in this paper.

The second important aspect related to the proposed concept is a proper selection of the communication mode, i.e., a decision if it is more profitable to exploit VLC, RF, or when to use both simultaneously. A research challenge here is to exploit combination of both RF and VLC bands, while taking into account their specifics, and to develop efficient mode selection

algorithms suitable for scenarios with multiple D2D pairs coexisting with conventional cellular MTs.

In terms of control and management of the RF–VLC D2D, another important question is: Who decides which communication mode (RF or VLC) should be selected for data transmission? In general, D2D communication may be controlled in a centralized or a distributed manner. In the former case, the selection is done solely by the eNB. Consequently, the MTs should report the information regarding the channel quality to the eNB on regular basis. Since the channel quality can vary significantly (especially for VLC channel), the delay in decision at the eNB can result in an incorrect selection of the communication mode leading even in a degradation of the capacity. In the latter case, if the selection is performed directly at the MTs (i.e., in the distributed manner), the delay of the decision is significantly reduced. In general, the mode selection can be carried out by both, the $\text{MT}_T$ and the $\text{MT}_R$. Nonetheless, we suggest to make the decision at the $\text{MT}_T$ rather than at the $\text{MT}_R$ as the $\text{MT}_T$ is aware of the transmission buffer status and can perform scheduling of the RF and VLC resources accordingly. To this end, the quality of both RF and VLC channels has to be reported by the $\text{MT}_R$ to the $\text{MT}_T$ via RF. Then, the $\text{MT}_T$ can promptly react to rapid degradation of VLC channel quality and switch to RF for data transmission immediately. Therefore, there is no need for any advanced and complex mechanisms to control the proposed RF-VLC D2D concept.

Regarding resource scheduling, a single scheduler can serve both VLC and RF communications without any complication. The scheduler perceives both technologies from a perspective of scheduling metrics (capacity, delay, buffer status, etc.), which can be represented in the same way for both technologies. Inclusion of VLC on the top of RF increases flexibility in terms of radio resource scheduling because more communication resources with wide range of quality and diverse channel variation pattern and stability are available. Despite the fact that a common schedulers used in cellular networks can be applied to RF–VLC D2D, this concept opens space for a future development of new schedulers tailored for the RF–VLC D2D to maximize its performance.

Another important aspect regarding the combination of RF and VLC for D2D is to decide whether the control signaling can be transmitted also in both transmission modes (RF/VLC), like data transmission, or not. Although VLC may offer superior capacity for short distances when compared to RF, this is true only for optimal or near optimal irradiance and incidence angles (as further discuss in the next section). As a matter of fact, the VLC channel is highly susceptible to these changes and, hence, sudden decrease in channel quality may occur frequently. Consequently, the control signaling must be unconditionally transmitted via RF D2D link during the whole communication. This is supported by the fact that the amount of the signaling is incomparably lower than the amount of users data and the capacity offered by VLC cannot be fully exploited for the signaling anyway.

## IV. Performance Evaluation

This section describes the simulation scenarios, main simulation parameters and discusses results of the simulations for individual scenarios.

### A. Simulation scenario and models

We assume a scenario representing an indoor area (a room or a hall) where we foresee main benefits of the proposed concept as explained in Section III. Further, we assume the room dimension of $d$ x $d$ m. In the room, four MTs are deployed within specific distance of $MT_T$ and $MT_R$ of the same pair ($d_{TR}$) and with specific inter-pair distance $d_P$ as shown in Fig 2. We set these distances manually to understand behavior of the RF–VLC D2D over various distances in order to assess potential limits and scalability of the solution.

The orientation (azimuth) of each MT is generated in one of the following ways: Optimal, Gaussian, and Random selection. The Optimal selection means that the $MT_T$ and $MT_R$ are oriented directly towards each other (i.e., in Fig. 2, $\phi$ and $\psi$ are set to 0°). This case shows an upper bound performance as it allows reaching maximum capacity for VLC mode. In the case of Gaussian selection, the $\phi$ and $\psi$ angles are randomly generated according to the Gaussian distribution with the mean ($\mu$) set to 0° and the standard deviation ($\sigma$) set to 60°. This situation represents the case when two users are willing to exchange data and are aware of each other locations so that we assume they try to direct their MTs towards each other. Nevertheless, even if the users try to direct their MTs towards each other, they might not

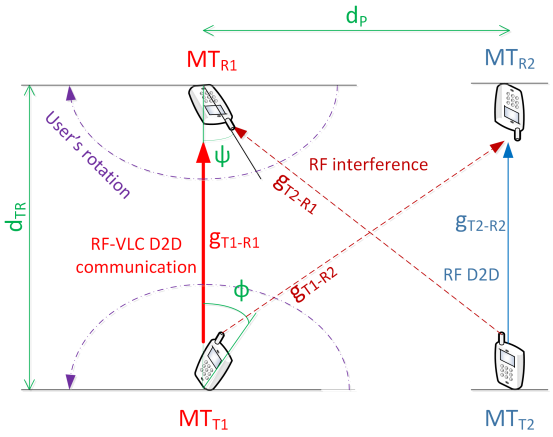


Fig. 2: Explanation of parameters and deployment scenario considered for performance assessment.

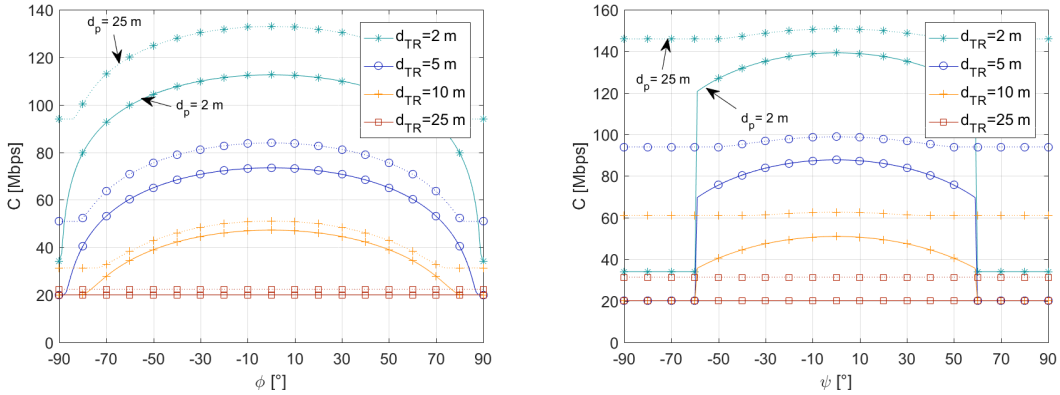


(a) (b)

Fig. 3: Performance of RF-VLC D2D for various angles $\phi$ (subplot (a)) and $\psi$ (subplot (b)) with the capacity averaged out over 180 values of the second angle (i.e., $\psi$ in subplot a) and $\phi$ in subplot b)) ranging from -90° to 90° with a step of 1°. Solid lines represent $d_p = 2$ m, dotted lines represent $d_p = 25$ m.

TABLE I: Simulation parameters.

| RF Parameters | | |
|---|---|---|
| Parameters | | Value |
| Carrier frequency | $f_c$ | 2 [MHz] |
| Bandwidth | $B^{RF}$ | 20 [MHz] |
| Transmission power of MT | $P_t^{RF}$ | 200 [mW] |
| Spec. density of thermal noise | $\sigma^2_{t,RF}$ | –174 [dBm/Hz] |
| VLC Parameters | | |
| Parameters | | Value |
| Bandwidth | $B^{VLC}$ | 10 [MHz] |
| Transmission power of MT | $P_t^{VLC}$ | 200 [mW] |
| Physical area of photodetector | $A$ | 1 $[cm]^2$ |
| Background current | $I_{bg}$ | 10 [nA] |
| Noise Bandwidth factors | $I_2$-$I_3$ | 0.562 - 0.0868 |
| Fix. capac. of photodetector | $\eta$ | $112\times10^{-8}$ [F/m] |
| FET channel noise factor | $\Gamma$ | 1.5 |
| FET transconductance | $g_m$ | 0.03 [s] |
| Responsivity of the photodiode | $\gamma$ | 0.53 [A] |
| Open-loop voltage gain | $G$ | 10 |
| Optical concentrator gain | $g(\psi)$ | 3 |
| Optical filter gain | $T_s$ | 1 |
| General Parameters | | |
| Parameters | | Value |
| Number of MTs | $N$ | 4 |
| Irradiance and incidence angle | $\phi$,$\psi$ | -90 – 90 [°] |
| Room dimension | $d$ | 30 [m] |

match the angles in a perfect way so there is a possibility of a deviation from the optimal angles. The third option, Random selection, shows one of the worst cases since $\phi$ and $\psi$ angles are selected randomly between 0° to 180°. This situation can appear when users cannot or do not want to change orientation of their MTs and keep the MT in a random direction with respect to the other MT.

The $MT_T$ transmit data to the $MT_R$ in either RF or VLC mode depending on which mode provides higher capacity at the moment as described in the system model (Section II). For the RF channel, we follow the channel modeling defined by 3GPP for indoor D2D communication as defined in [23]. The modeling of VLC channel is performed according to [13]. All simulation parameters are summarized in Table I.

### B. Simulation results and discussion

This section first analyzes an impact of $\psi$ and $\phi$ angles on the D2D capacity to understand the operational limits of RF-VLC D2D. Second, we investigate an impact of the $d_{TR}$, $d_P$, and $\phi$ on VLC usage ratio (i.e., how often VLC is used instead of RF). Third, we compare the capacity achieved by the proposed RF-VLC D2D system with RF D2D (i.e., without VLC) and VLC D2D (without RF). Note that capacity presented in all figures is understood as maximum capacity of communication channel computed according to the system models defined in Section II for both RF and VLC channels.

Fig. 3 demonstrates the impact of angles on the capacity achieved by the proposed RF-VLC D2D system for various $d_{TR}$ and $d_P$ distances . For irradiance angle ($\phi$), the change in capacity is continuous as the LED diode can operate in the whole range of 90° while for incidence angle ($\psi$), the communication is limited by the field of view (FOV) of the photodetector (set to 60° in this paper according to [24]). The $\phi$ ($\psi$) is set from -90° to 90° and depicted on $x$ axis in respective figures. For each angle on $x$ axis, the capacity is computed as an average value over corresponding $\psi$ ($\phi$) ranging from -90° to 90° with a step of 1°. This means, the capacity is defined as $C = \frac{\sum_{\psi=0}^{180} C_\psi}{180}$ in Fig. 3a and $C = \frac{\sum_{\phi=0}^{180} C_\phi}{180}$ in Fig. 3b.

In Fig. 3, we can see that the $d_{TR}$ distance plays a crucial role for the capacity. For smaller distances, i.e., if $d_{TR} < 10$ m, the capacity rises significantly with increasing $d_p$. For a larger $d_{TR}$, i.e., $d_{TR} \geq 10$ m, the impact of $d_p$ becomes less significant since the capacity provided by VLC D2D is often surpassed by the capacity offered by RF D2D capacity.

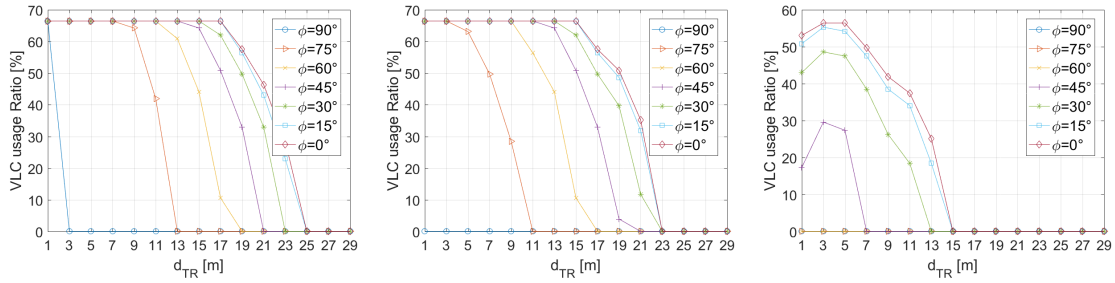


(a) $d_P = 2$ m (b) $d_P = 10$ m (c) $d_P = 25$ m

Fig. 4: The ratio of time when VLC is used for communication instead of RF according to distance between transmitter and receiver ($d_{TR}$) and distance between pairs ($d_p$).

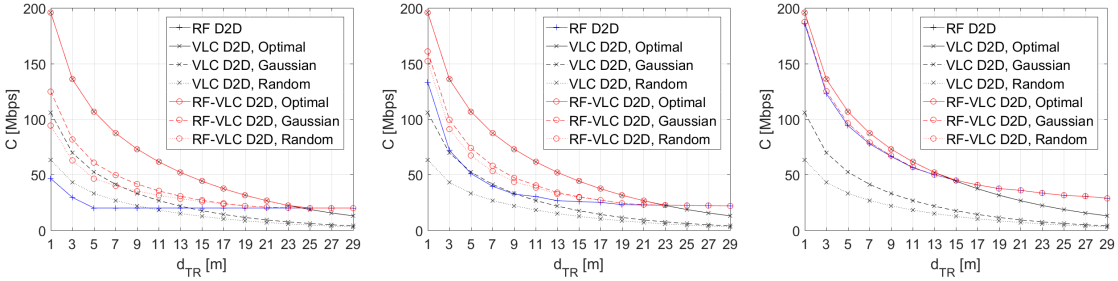


(a) $d_P = 2$ m (b) $d_P = 10$ m (c) $d_P = 25$ m

Fig. 5: System capacity for RF D2D, VLC D2D, and RF-VLC D2D over distance between transmitter and receiver ($d_{TR}$) and distance between pairs ($d_p$).

From Fig. 3, we can further see that the capacity raises as the orientation of MTs becomes close to the optimal (i.e., close to 0°). An important observation is that for $|\phi| \leq 30°$ and $|\psi| \leq 30°$, a degradation of the overall capacity is negligible (below 4% with respect to the optimal angles). Even for $|\phi| \leq 60°$ and $|\psi| \leq 60°$, the degradation of capacity is still below 10%. This observation confirms suitability of the proposed concept for practical applications as the orientation of both MTs is critical aspect in which the RF-VLC D2D concept differs from the common VLC communication assuming an access point located at the ceiling. If VLC is not available or if it provides low capacity (i.e., if $|\phi| \to 90°$ or $|\psi| > 60°$), RF band still provides good capacity for D2D communication. Fig. 3 also shows that the impact of $\phi$ and $\psi$ is getting less important with rising $d_P$ because low interference in RF gives preference to a use of RF instead of VLC. The wide range of $\phi$ and $\psi$ angles that allow reaching almost the maximum capacity indicates that RF-VLC D2D can introduce notable gains even if the MTs are not directed towards each other.

To understand better the impact of both VLC and RF on the overall capacity of RF-VLC D2D, we analyze the ratio of time when VLC is used instead of RF. Fig. 4 shows that VLC mode is exploited in about 68% if both $d_{TR}$ and $d_P$ are low. In this case, the capacity offered by VLC helps to improve the overall D2D performance and, thus, VLC is used predominantly. With increasing $d_{TR}$ and $d_P$, the orientation angle of MTs has to be closer to the optimal angle in order to keep VLC beneficial. If $d_P$ is equal or even longer than 25 m, VLC is not available and only RF mode can take place. In Fig. 4c, we can also notice that for $d_P = 25$ m and $d_{TR} = 1$ m, VLC is used less often than for $d_{TR} = 3$ or 5 m. This is due to the fact that RF can perform very well if the transmitter and the receiver of the same pair are close to each other (i.e., low $d_{TR}$) while the interfering pair is far away (i.e., $d_P$ is high). The ratio of VLC usage confirms the fact that an indoor scenario with relatively close MTs is the most suitable for the proposed RF-VLC D2D concept.

Now, we focus on comparison of the RF-VLC D2D with common RF D2D and VLC D2D systems as known today. We provide comparison for various $d_P$ in individual subplots of Fig. 5 and for three different ways of generation of $\phi$ and $\psi$ angles: Optimal, Gaussian, and Random, as described in Section IV.A. Note that the results are averaged out over $10^6$ simulation drops. Fig. 5 shows that the proposed RF-VLC D2D outperforms both competitive schemes significantly and allows to provide maximum capacity disregarding $d_{TR}$ and $d_P$. More specifically, while RF D2D suffers in terms of capacity for low $d_P$, VLC D2D provides only limited

capacity for high $d_{TR}$. In contrast, the proposed RF-VLC D2D performs well disregarding both distances. The most notable gain introduced by the novel RF-VLC D2D when compared to RF D2D is observed for low $d_{TR}$ and $d_P$, where RF-VLC D2D can provide 4.1, 2.6, and 2 times higher capacity for the Optimal, Gaussian, and Random selection of angles, respectively. Furthermore, we can see that, even at short distances, RF-VLC D2D outperforms VLC D2D by 1.2 times (Gaussian selection of angles) and 1.5 times (Random selection). Note that for the Optimal selection of angles, VLC D2D and RF-VLC D2D perform similarly for low $d_{TR}$ because VLC is used in almost 100% of time due to proximity of the $MT_T$ and $MT_R$. With increasing both $d_{TR}$ and $d_P$, the performance of the RF-VLC D2D converges to the conventional RF D2D since VLC is used only rarely. Moreover, with increasing $d_P$, the maximum $d_{TR}$ for which VLC D2D still performs the same as the proposed RF-VLC D2D is decreasing. This is due to the fact that interference in RF is decreasing as well with increasing $d_P$ and consequently RF becomes more efficient.

## V. Conclusion

In this paper, we have presented a novel D2D concept combining RF and VLC communication with the potential to increase the capacity provided by D2D. The performance analysis of the proposed RF-VLC D2D shows the ability to mitigate drawbacks in terms of limited capacity for very short and medium distances of the RF D2D and VLC D2D systems respectively. The proposed RF–VLC D2D increases the capacity by up to 4.1 and 1.5 times with respect to sole RF D2D and VLC D2D, respectively. The most notable gain in capacity is observed for low distances (up to 10 m), where VLC shows its superiority over conventional RF and, thus, the combination of both is the most beneficial.

As stated in the paper, the proposed RF-VLC opens many challenges needed to be addressed in the future. The key future research directions should cover design of new scheduling and resource allocation schemes taking advantage of flexibility and different stability of channels introduced by combining RF and VLC. Furthermore, selection of the communication mode in scenario with multiple D2D pairs and conventional cellular MTs should be developed. Also, simulations and practical tests for a wide range of scenarios and use cases need to be carried out. In this sense, a challenge is to understand better the changes of the MT's angles in a real world and consider it in all algorithms related to control and management of the RF–VLC D2D.

## Acknowledgment

This work has been supported by Grant No. GA17-17538S funded by Czech Science Foundation and by the grant of Czech Technical University in Prague No. SGS17/184/OHK3/3T/13.

## References

[1] 3GPP 36.877, "LTE device to device proximity services; User Equipment (UE) Radio Transmission and Reception," 2014.

[2] P. Mach, *et al.*, "In-band device-to-device communication in OFDMA cellular networks: A survey and challenges," *IEEE Commun. Surveys Tut.*, 17(4), 1885–1922, 2015.

[3] G. Fodor, *et al.*, "Design aspects of network assisted device-to-device communications," *IEEE Commun. Mag.*, 50(3), 2012.

[4] Y. Xu, R. Yin, T. Han, and G. Yu, "Dynamic resource allocation for device-to-device communication underlaying cellular networks," *International Journal of Communication Systems*, 27(10), 2408–2425, 2014.

[5] R. Zhang, *et al.*, "Interference-aware graph based resource sharing for device-to-device communications underlaying cellular networks," *IEEE WCNC*, 140–145, 2013.

[6] F. Wang, *et al.*, "Joint scheduling and resource allocation for device-to-device underlay communication," *IEEE WCNC 2013*, 134–139, 2013.

[7] M. Zulhasnine, C. Huang, and A. Srinivasan, "Efficient resource allocation for device-to-device communication underlaying LTE network," *IEEE WiMob*, 368–375, 2010.

[8] Z. Lin, *et al.*, "Hybrid architecture performance analysis for device-to-device communication in 5G cellular network," *Mobile Networks and Applications*, 20(6), 713–724, 2015.

[9] V. Jungnickel, *et al.*, "A european view on the next generation optical wireless communication standard," *IEEE CSCN*, 106–111, 2015.

[10] Y. Wang, *et al.*, "4.5-gb/s rgb-led based wdm visible light communication system employing cap modulation and RLS based adaptive equalization," *Optics express*, 23(10), 13626–33, 2015.

[11] X. Huang, *et al.*, "1.6 gbit/s phosphorescent white led based vlc transmission using a cascaded pre-equalization circuit and a differential outputs pin receiver," *Optics express*, 23(17), 22034–42, 2015.

[12] G. Cossu, *et al.*, "3.4 Gbit/s visible optical wireless transmission based on RGB led," *Optics express*, vol. 20, no. 26, pp. B501–B506, 2012.

[13] P. H. Pathak, *et al.*, "Visible light communication, networking, and sensing: A survey, potential and challenges," *IEEE Commun. Surveys Tut.*, 17(4), 2047–77, 2015.

[14] M. Ayyash, *et al.*, "Coexistence of WiFi and LiFi Toward 5G: Concepts, Opportunities, and Challenges," *IEEE Communications Magazine*, vol. 54, no. 2 pp. 64–74, February 2016.

[15] S. Shao, *et al.*, "An Indoor Hybrid WiFi-VLC Internet Access System," *IEEE International Conference on Mobile Ad Hoc and Sensor Systems*, 2014.

[16] L. Li, *et al.*, "A joint resources allocation approach for hybrid visible light communication and LTE system," *WiCOM*, 2015.

[17] S. Liang, H. Tian, B. Fan, and R. Bai, "A novel vertical handover algorithm in a hybrid visible light communication and LTE system," *IEEE VTC Fall 2015*, 1–5, 2015.

[18] S. Shao, *et al.*, "Design and Analysis of a Visible-Light-Communication Enhanced WiFi System," *Journal of Optical Communications and Networking*, 7(10), 960–973, 2015.

[19] Y. Liu, Z. Huang, W. Li, and Y. Ji, "Game theory-based mode cooperative selection mechanism for device-to-device visible light communication," *Optical Engineering*, 55(3), 2016.

[20] S. V. Tiwari, A. Sewaiwar, and Y.-H. Chung, "Optical repeater assisted visible light device-to-device communications," *International Journal of Electrical, Computer, Energetic, Electronic and Communication Engineering*, 10(2), 206–209, 2016.

[21] P. Pesek, *et al.*, "Mobile user connectivity in relay-assisted visible light communication," *IEEE Photonics Journal*, p. submitted, IEEE, 2017.

[22] M. B. Rahaim, T. D. C. Little, "SINR Analysis and Cell Zooming with Constant Illumination for Indoor VLC Networks," *(IWOW)*, 2013.

[23] 3GPP TR 36.843 "Study on LTE device to device proximity services," (Release 12), V12.0.1," 2014-03.

[24] A. Burton, H. Le Minh, Z. Ghassemlooy, S. Rajbhandari, and P. Haigh, "Performance analysis for 180 receiver in visible light communications," *IEEE ICCE 2012*, pp. 48–53, 2012.

### 4.3.2 Interference-based Iterative Band Selection in RF-VLC D2D Communication

This subsection deals with the problem of the RF/VLC band selection within a scenario with multiple D2D pairs. Hence, an iterative interference-based algorithm to select RF or VLC for every D2D pair is proposed. This subsection includes the journal paper [4J], which is an extension of the conference paper [5C].

IEEE Access
Multidisciplinary ⋮ Rapid Review ⋮ Open Access Journal

Received October 10, 2019, accepted November 5, 2019, date of publication November 18, 2019, date of current version December 5, 2019.

*Digital Object Identifier 10.1109/ACCESS.2019.2954049*

# Efficient Exploitation of Radio Frequency and Visible Light Communication Bands for D2D in Mobile Networks

**MEHYAR NAJLA, (Student Member, IEEE), PAVEL MACH, (Member, IEEE), ZDENEK BECVAR, (Senior Member, IEEE), PETR CHVOJKA, AND STANISLAV ZVANOVEC, (Senior Member, IEEE)**

Faculty of Electrical Engineering, Czech Technical University in Prague, 166 27 Prague, Czech Republic

Corresponding author: Mehyar Najla (najlameh@fel.cvut.cz)

This work was supported in part by the Czech Science Foundation under Grant GA17-17538S, and in part by the Czech Technical University in Prague under Grant SGS17/184/OHK3/3T/13.

**ABSTRACT** The concept of device-to-device (D2D) communication, combining common radio frequency (RF) and visible light communication (VLC), is seen as a feasible way how to cope with spectrum crunch in the RF domain and how to maximize spectral efficiency in general. In this paper, our objective is to decide when RF should be utilized or if VLC proves to be the more profitable option. The selection between RF and VLC is defined as a multi-objective optimization problem targeting primarily to minimize the outage ratio while the secondary objective is to maximize the sum capacity of D2D pairs, composed by D2D transmitters and D2D receivers. To solve this problem, we design a centralized low-complexity heuristic algorithm selecting either RF or VLC band for each D2D pair relying on the mutual interference among the pairs. For interpretation of the mutual interference among the D2D pairs, we exploit directed weighted graphs adopted from the graph theory. The simulation results show that the proposed algorithm outperforms state-of-the-art algorithms in terms of the outage ratio, sum capacity and average energy efficiency. What is more, despite a very low complexity, the proposed algorithm reaches a close-to-optimum performance provided by the exhaustive search algorithm.

**INDEX TERMS** Band selection, device-to-device, radio frequency, visible light communication.

## I. INTRODUCTION

The device-to-device (D2D) communication represents a very alluring technology due to its promise in delivering exceptionally high data rates and its potential to significantly decrease the energy consumption of contemporary mobile networks [1]. As the name suggests, the D2D communication facilitates a direct communication between any two devices in the vicinity to each other without a need to communicate through a base station, referred to in this paper as gNodeB (gNB), to be in line with 3GPP terminology for 5G mobile networks. In terms of spectrum usage, the D2D pairs (composed of D2D transmitters and D2D receivers) exploit the D2D communication in one of two basic operational communication modes: 1) the communication over a licensed spectrum dedicated for conventional cellular users (known as in-band D2D communication) or 2) the communication in an unlicensed spectrum assigned, for example, to WiFi or Bluetooth technology (also known as out-band D2D communication) [2]. Moreover, under the in-band D2D communication, the D2D user equipments (DUEs) may access the licensed radio resources in either shared or dedicated mode (more details can be found, e.g., in [2]–[5]).

In general, the D2D pairs using in-band communication suffer from high interference either from other D2D pairs or from conventional cellular users (i.e., users communicating through gNB) exploiting the same radio frequency (RF) resources. This mutual interference can partly or fully scale down the advantages offered by D2D communication and, in extreme cases, can even result in an outage situation. To avoid the outage situation, the D2D pairs should be able to use out-band frequencies, if needed. An interesting way how

The associate editor coordinating the review of this manuscript and approving it for publication was Anandakumar Haldorai.

to exploit out-band frequencies for D2D communication is presented in [6], where the DUEs within a formed cluster are allowed to use WiFi-Direct while the conventional in-band frequency is used only for the communication between the individual clusters. Even though the paper shows that the out-band D2D communication is able to enhance the network's throughput, the interference within the cluster cannot be easily mitigated since the DUEs share frequencies with conventional WiFi devices [3]. Another feasible technology for out-band D2D can be seen in visible light communication (VLC). VLC is an enticing technology as it addresses many challenges, such as bandwidth limitation, energy efficiency, electromagnetic radiation, and safety in the wireless communication systems in general [7], [8]. The VLC systems operate in higher frequency bands and have at their disposal a much wider spectrum when compared to the conventional radio systems (400-790 THz) [9], [10]. As a consequence, VLC is able to provide data rates in the order of Gbps [11], [12] while, at the same time, low power consumption is assured [13].

Hybrid VLC/RF networks have been presented in several existing papers, such as [14], [15] and [16]. Nevertheless, these papers focus on *indoor downlink exploitation of the VLC band without any D2D communication*. In contrast, VLC as an out-band D2D technology has been considered in several recent studies. While [17] and [18] *study only a standalone VLC for D2D*, a combination of RF and VLC bands for D2D communication has been initially studied in [19], where potential benefits and performance limits of the hybrid RF/VLC D2D are shown. However, the paper focuses only on a simplified scenario considering just two D2D pairs, which is not very realistic in future mobile networks with a high density of users. On top of that, the paper *does not address in any way the problem of the selection between RF and VLC bands for each D2D pair*.

Thus, in this paper, we investigate the problem of the selecting between RF or VLC for individual D2D pairs in a multi-user scenario, where the D2D pairs using the same technology (either RF or VLC) mutually interfere with each other. Note that the initial idea of this paper has been presented in our conference paper [20] in a simplified version. To this end, we extend [20] by formulating the problem in a more general way as a constrained discrete sum capacity maximization problem that might not always be solvable under the zero outage constraint. Then, we show that this problem should be transformed into a multi-objective optimization problem to guarantee the existence of a solution. In addition, this paper describes the proposed solution in more details and shows new results by evaluating the proposed algorithm in a wider scope and from several additional perspectives related to specific aspects of VLC (e.g., an impact of radiance and irradiance angles) and to the energy efficiency of the whole system, which plays a prominent role in future mobile networks. To this end, the contributions of this paper can be summarized as follows:

- We formulate the RF/VLC selection as a constrained discrete sum capacity maximization problem that might not always be solvable under the zero outage constraint. Then, we transform the problem into a solvable multi-objective optimization problem aiming to achieve a minimization of the outage as well as a maximization of the sum capacity of D2D pairs.
- We use a Lexicographic ordering to transform the multi-objective optimization problem into two single-objective optimization problems, outage minimization and sum capacity maximization, taking into account the higher priority of the outage minimization.
- We derive the optimal solution of the two problems, outage minimization and sum capacity maximization, sequentially via an exhaustive search algorithm.
- We propose an iterative two-phase heuristic centralized algorithm, which switches D2D pairs from RF to VLC aiming to minimize outage and maximize sum capacity. The switching itself occurs sequentially based on: 1) the sum of the interference generated to other D2D pairs in the vicinity and 2) the sum of the interference received from other D2D pairs.
- We show that the proposed algorithm introduces a substantial complexity reduction and reaches a close-to-optimum performance in terms of outage ratio, sum capacity and average energy efficiency compared to the optimal solution derived by the exhaustive search algorithm. In addition, we show that the proposed algorithm overcomes the state-of-the-art algorithms.

The rest of the paper is structured as follows. Section II describes the system model and formally defines the objective of the paper. Then, Section III is allocated for the presentation of the proposed heuristic algorithm including a description of the main practical assumptions and introduction of the graph theory framework for the interpretation of interference among D2D pairs. The simulation scenario and simulation results are presented in Section IV. The last section concludes the paper and further discusses future research direction.

## II. SYSTEM MODEL AND OBJECTIVES

This section describes the system model and, then, the objective of the proposed algorithm is formulated.

### A. SYSTEM MODEL DESCRIPTION

The system model assumes $N$ D2D pairs (including $N$ transmitters and $N$ receivers) deployed inside a rectangular area (as shown in Figure 1, where $N = 5$ is considered). Any transmitting DUE ($\text{DUE}_T$) is supposed to send data to a specific one receiving DUE ($\text{DUE}_R$), thus creating one D2D pair. The DUEs are assumed to be equipped with an RGB-based light-emitting diode (LED) and a photodetector for transmitting and receiving the optical signal in VLC D2D, respectively. Irradiance angle ($\phi$) and incidence angle ($\psi$) (i.e., users' directions) influencing the VLC performance [10] are either set to zero (i.e., angles are optimal), or generated according to Gaussian distribution [19].

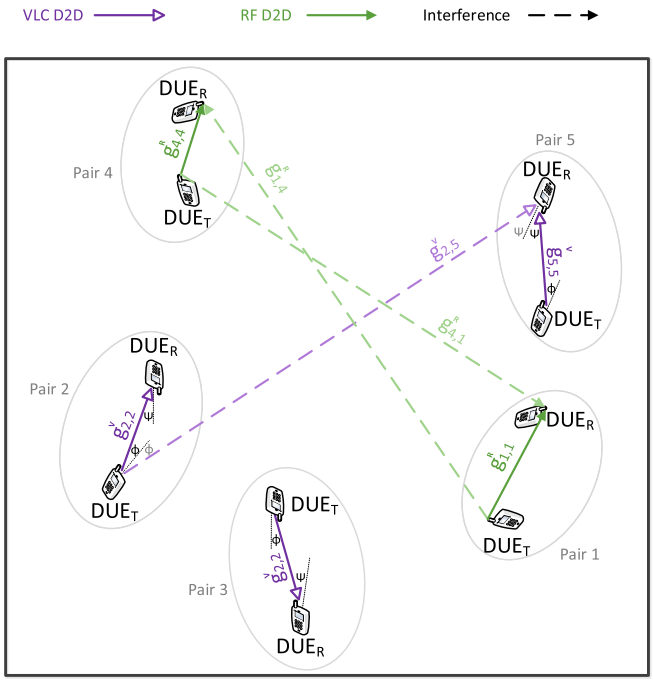


**FIGURE 1.** System model with an example of five D2D pairs operating in RF and VLC bands. Note that not all D2D pairs communicating over the VLC band interfere among each other due to the effect of the irradiance and the incidence angles.

The D2D pairs communicating over the RF band suffer from an interference caused by the active users communicating in the neighboring cells. This RF interference from neighboring cells is denoted as $I_{noise}$ and presented as a part of the RF noise in this paper. Contrary, if the D2D pair operates in the VLC mode, there is no interference from adjacent cells as VLC signal is significantly attenuated by longer distances and existing obstacles. Furthermore, to reach the high spectral efficiency we assume that the D2D pairs operating both in RF and VLC share the whole available bandwidth. In this regard, the individual capacity of each D2D pair is strongly influenced by the interference generated from other D2D pairs in the vicinity and communicating via the same band. Note that there is no interference between the group of D2D pairs exploiting RF to those utilizing VLC at the moment, as these communicate at different frequencies.

### 1) CAPACITY MODEL

The capacity of the $n$-th D2D pair in the RF-VLC D2D network is calculated according to Shannon–Hartley theorem as:

$$C_n = B\log_2(1+\gamma_n), \tag{1}$$

where $B$ is the bandwidth allocated to the D2D pair and $\gamma_n$ is the signal to interference plus noise ratio (SINR) of the $n$-th D2D pair. Since every D2D pair can communicate with only either RF or VLC at the moment, we introduce two binary variables (indicators), $\alpha_n^R$ and $\alpha_n^V$ for every $n$-th D2D pair indicating whether the pair communicates via RF or VLC bands, respectively. More specifically, for every $n$-th D2D pair we set $\alpha_n^R = 1$ and $\alpha_n^V = 0$ if the $n$-th D2D pair communicates over the RF band and vice versa $\alpha_n^R = 0$ and $\alpha_n^V = 1$ if the $n$-th D2D pair communicates over the VLC band. Notice that in the rest of the paper, the upper index "R" always represents RF band while "V" always stands for VLC. Thus, the bandwidth allocated to the $n$-th D2D pair can be expressed as:

$$B = \alpha_n^R B^R + \alpha_n^V B^V. \tag{2}$$

Moreover, the SINR of the $n$-th D2D pair is calculated as:

$$\gamma_n = \alpha_n^R \frac{p_n^R g_{n,n}^R}{\sigma^R + \sum_{m\neq n}\alpha_m^R p_m^R g_{m,n}^R} + \alpha_n^V \frac{(\mu p_n^V g_{n,n}^V)^2}{\sigma^V + \sum_{m\neq n}\alpha_m^V (\mu p_m^V g_{m,n}^V)^2}, \tag{3}$$

where $p_n$ is the transmission power of the $n$-th DUE$_T$, $p_m$ stands for the transmission power of the $m$-th DUE$_T$ causing interference to the $n$-th DUE$_R$, $g_{n,n}$ corresponds to the channel gain between the $n$-th DUE$_T$ and the $n$-th DUE$_R$, $g_{m,n}$ is the channel gain between the interfering $m$-th DUE$_T$ and the $n$-th DUE$_R$, $\sigma$ represents the noise, and $\mu$ is the responsivity of the photodetector of any DUE$_R$. Note that in this paper, line-of-sight (LOS) communication is considered for VLC D2D [10], and thus, the main VLC channel gain ($g_{n,n}^V$) and the interference VLC channel gain ($g_{m,n}^V$) are LOS channel gains and can be derived as in [21].

The noises for RF and VLC are calculated differently. Consequently, the RF noise ($\sigma^R$) is estimated as:

$$\sigma^R = B^R\sigma_o^R + I_{noise}, \tag{4}$$

where $\sigma_o^R$ stands for the RF thermal noise spectral density. However, the VLC noise $\sigma^V$ is composed of a thermal $\sigma_{thermal}$ and a shot $\sigma_{shot}$ noise [21], as follows:

$$\sigma^V = \sigma_{thermal}^2 + \sigma_{shot}^2. \tag{5}$$

Both $\sigma_{thermal}$ and $\sigma_{shot}$, are calculated based on [10].

### 2) OUTAGE

In our model, we assume that each $n$-th DUE$_R$ is able to receive data with the SINR that satisfies $\gamma_n \geq \gamma_{min}$, where $\gamma_{min}$ is the minimal SINR. If any $n$-th D2D pair has $\gamma_n < \gamma_{min}$, then, this D2D pair is assumed to be in the outage (i.e., there is no D2D communication available between the $n$-th DUE$_T$ and the $n$-th DUE$_R$). Therefore, we introduce the outage ratio $\Theta$ that represents the ratio of D2D pairs not satisfying above-mentioned condition as:

$$\Theta = \frac{N_o}{N}, \tag{6}$$

where $N_o \leq N$ is the number of D2D pairs in outage.

### 3) ENERGY EFFICIENCY

Since we also evaluate the system performance in terms of energy efficiency, the power consumption in both the RF and VLC bands needs to be calculated. The power consumption

in RF is derived according to the well established empirical model [22] that takes into account the power consumed by both the transmission and the reception of data. Specifically, the power consumed by transmission and the reception consists of base-band signal processing parts $P_t^{bb}$ and $P_r^{bb}$, radio frequency parts $P_t^{rf}$ and $P_r^{rf}$, and a consumption of communication parts circuitry $P_t^{on}$ and $P_r^{on}$. The power consumed by transmission ($P_t^R$) and the power consumed by reception ($P_r^R$) are defined as:

$$P_t^R = P_t^{bb} + P_t^{rf} + P_t^{on}, \tag{7}$$

$$P_r^R = P_r^{bb} + P_r^{rf} + P_r^{on}, \tag{8}$$

where the values and the calculations of individual parameters are explained in detail in [22].

The power consumption in VLC by transmission ($P_t^V$) is calculated according to [23] and [24] considering that the LED-based transmitter circuit is a serial-FET circuit, in which the consumed power can be derived as:

$$P_t^V = P_t^{led} + P_t^{sf} + P_t^{buck}, \tag{9}$$

where $P_t^{led}$ is the illumination power consumption in the LED, $P_t^{sf}$ stands for the power consumption in the serial-FET circuit composed of the modulation power consumption and the power consumed in the LED because of modulation, and $P_t^{buck}$ corresponds to the buck driver power consumption. All, $P_t^{led}$, $P_t^{sf}$ and $P_t^{buck}$, are calculated according to [23] and [24] considering the same electronic components in the VLC transmitter circuit. To calculate the power spent by the reception of VLC ($P_r^V$), we consider that this power consumed in the VLC receiver circuit (in the $n$-th DUE$_R$) is equal to the power consumed in the VLC transmitter circuit (in the $n$-th DUE$_T$), i.e., $P_r^V = P_t^V$.

Based on the capacity and the power consumption of the $n$-th D2D pair $C_n$ from (1), the energy efficiency of the $n$-th D2D pair is derived as:

$$EE_n = \frac{C_n}{\alpha_n^R(P_t^R + P_r^R) + \alpha_n^V(P_t^V + P_r^V)}. \tag{10}$$

### B. OBJECTIVE FORMULATION

In general, our objective is to select RF or VLC band for each D2D pair in order to maximize the sum capacity of D2D pairs keeping zero outage, formulated as:

$$\begin{aligned} \boldsymbol{\alpha^R}, \boldsymbol{\alpha^V} = argmax(&\textstyle\sum_{n=1}^{n=N} C_n) \\ \text{s.t. } (a) \quad & \alpha_n^R \in \{0,1\} \quad \forall n \in \{1,\ldots,N\}, \\ (b) \quad & \alpha_n^V \in \{0,1\} \quad \forall n \in \{1,\ldots,N\}, \\ (c) \quad & \alpha_n^R + \alpha_n^V = 1 \quad \forall n \in \{1,\ldots,N\}, \\ (d) \quad & \gamma_n \geq \gamma_{min} \quad \forall n \in \{1,\ldots,N\}), \end{aligned} \tag{11}$$

where $\boldsymbol{\alpha^R} = \{\alpha_1^R,\ldots,\alpha_N^R\}$ and $\boldsymbol{\alpha^V} = \{\alpha_1^V,\ldots,\alpha_N^V\}$ are the two sets of the binary indicators for RF and VLC bands, respectively; constraints ($a$) and ($b$) guarantee that every indicator in $\boldsymbol{\alpha^R}$ and $\boldsymbol{\alpha^V}$ is a binary variable and its value should be either zero or one as explained in Section II-A; constraint ($c$) guarantees that every $n$-th D2D pair is able to use only either RF or VLC; and constraint ($d$) keeps the SINR of all D2D pairs above the threshold $\gamma_{min}$ to maintain zero outage. Note that the problem (11) is an integer (non-linear) programming which is NP-hard.

However, the constrained discrete optimization problem (11) seeks for a solution represented by a combination of RF and VLC band selections for the D2D pairs where, first, the constraint ($d$) is satisfied and, second, the sum capacity is maximized. In other words, constraint ($d$) reflects the priority of reaching zero outage before sum capacity is maximized as it is the case in real network implementations where the network operators aim to serve as many users as possible. Nevertheless, there might be no RF/VLC combination that guarantees no outage (i.e, some $n$-th D2D pairs may always experience $\gamma_n < \gamma_{min}$), especially for a high number of D2D pairs $N$ and the corresponding high interference over both bands (RF and VLC). Thus, to guarantee the existence of a solution, we relax the problem of reaching zero outage to a problem of minimizing the outage ratio as much as possible. Hence, we transform the problem (11) into a multi-objective optimization problem written as:

$$\begin{aligned} \boldsymbol{\alpha^R}, \boldsymbol{\alpha^V} = argmax(&1/\Theta, \textstyle\sum_{n=1}^{n=N} C_n) \\ &\text{s.t. } (a)\text{–}(c) \text{ from (11)}, \end{aligned} \tag{12}$$

where the objective is both to minimize the outage and to maximize the capacity.

Generally speaking, the multi-objective optimization is concerned with optimizing multiple parameters where, in our case, we aim to minimize $\Theta$ (achieved by maximizing $1/\Theta$) and to maximize $\sum_{n=1}^{n=N} C_n$ at the same time. However, as mentioned before, minimizing outage has a higher priority in comparison to the sum capacity maximization in the real network. Thus, we consider a Lexicographic ordering of the objectives defined in (12) in a way that the outage ratio minimization is assumed to be the objective with higher priority compared to the capacity maximization, which represents the objective with lower priority. Taking this Lexicographic ordering into account, the multi-objective optimization problem in (12) can be transformed into two sequentially-solvable single-objective optimization problems: outage ratio minimization, and then, sum capacity maximization. Therefore, as a higher priority problem, the outage ratio minimization is formulated as:

$$\begin{aligned} \boldsymbol{\alpha}_{\boldsymbol{\Theta}}^{\boldsymbol{R}}, \boldsymbol{\alpha}_{\boldsymbol{\Theta}}^{\boldsymbol{V}} = argmax(&1/\Theta) \\ &\text{s.t. } (a)\text{–}(c) \text{ from (11)}, \end{aligned} \tag{13}$$

where $\boldsymbol{\alpha}_{\boldsymbol{\Theta}}^{\boldsymbol{R}}$ and $\boldsymbol{\alpha}_{\boldsymbol{\Theta}}^{\boldsymbol{V}}$ are two matrices containing the possible binary indicators for RF and VLC bands, respectively, minimizing the outage ratio. In other words, $\boldsymbol{\alpha}_{\boldsymbol{\Theta}}^{\boldsymbol{R}}$ and $\boldsymbol{\alpha}_{\boldsymbol{\Theta}}^{\boldsymbol{V}}$ represent the set of solutions (RF/VLC combinations) that reach the minimal possible outage $\Theta$ (i.e., there might be multiple RF/VLC combinations that achieve the same minimal outage $\Theta$). Then, as a lower priority problem, the sum capacity

maximization is formulated as:

$$\boldsymbol{\alpha}^{\boldsymbol{R}}, \boldsymbol{\alpha}^{\boldsymbol{V}} = argmax(\sum_{n=1}^{n=N} C_n)$$
$$\text{s.t. } (a)\text{–}(c) \text{ from } (11)$$
$$(d) \quad \Theta = \Theta^*, \tag{14}$$

where $\Theta^*$ is the minimal outage ratio achieved by solving (13) and, thus, the constraint $(d)$ in (14) guarantees that the outage achieved by solving outage minimization (13) should be kept while solving (14).

## III. PROPOSED BAND SELECTION ALGORITHM

First, we summarize the major assumptions considered in the developing of the proposed algorithm. Second, based on graph theory, we illustrate the exploitation of weighted directed graphs to interpret the interference among the D2D pairs as this interpretation is used to design the proposed band selection algorithm. Finally, we describe the proposed heuristic algorithm in detail.

### A. ASSUMPTIONS

In order to implement the proposed heuristic algorithm, several assumptions related to practical aspects and design need to be defined. These are summarized below:

- In the initial phase, before executing the proposed algorithm, all D2D pairs communicate via the RF band as it is more stable and less sensitive to the minor changes in the DUEs' orientations. For this same reason, the RF band is also assumed to serve the needed signaling and communication setup even if the data is transmitted over the VLC band.
- Within every D2D pair, the $\text{DUE}_T$ is assumed to be able to send a VLC beacon signal on a periodic basis to the $\text{DUE}_R$ even if the D2D pair communicates over the RF band. This VLC beacon is needed to evaluate the quality of the VLC channel. Note that the beacons are equivalent to the RF common reference signals used for channel estimation purposes in, e.g., LTE mobile networks (see [29]). In other words, the beacons represent reference signals transmitted at specific resources by any $\text{DUE}_T$ communicating in VLC or willing to switch its communication band from RF to VLC.
- The gNB centrally controls and manages the proposed algorithm. Thus, we assume that the estimated RF and VLC channels (via RF reference signals and VLC beacons, respectively) are reported periodically to the gNB. Then, based on the assumed full knowledge of these channels, the gNB is able to decide the D2D pair that need to switch its communication band from RF to VLC accordingly.

### B. GRAPH THEORY-BASED INTERPRETATION OF INTERFERENCE

The communication band selection (either RF or VLC) for each D2D pair is based on the interference relations among individual D2D pairs over both bands. Thus, in this section, we introduce the usage of weighted directed graphs adopted from graph theory for the interpretation of the mutual interference among the D2D pairs.

A fully connected weighted directed graph is defined as $G = (V, E)$, where the set of vertices $(V)$ stands for the D2D pairs and the set of edges $(E)$ represents the interference among them. Then, as the $G = (V, E)$ is supposed to be a weighted graph, any edge $e_{i,j}$, connecting the vertices $v_i$ with the $v_j$, is assigned with a specific weight $I_{i,j}$ corresponding to the interference from the $v_i$ to the $v_j$ (i.e., interference from $i$-th $\text{DUE}_T$ to the $j$-th $\text{DUE}_R$). Analogously, the interference from the $v_j$ to $v_i$ is interpreted as $I_{j,i}$, where the $j$-th $\text{DUE}_T$ causes interference to the $i$-th $\text{DUE}_R$.

In order to select the suitable communication band (RF or VLC) for every $i$-th D2D pair, we introduce two interference-based metrics from $G$ as follows: 1) the sum of interference caused by the $i$-th $\text{DUE}_T$ (i.e., by the $v_i$ vertex) to all other D2D pairs; and 2) the sum of interference received at the $i$-th $\text{DUE}_R$ (i.e., at the $v_i$ vertex) from all other D2D pairs. The former metric (denoted as $d^+(v_i)$) represents the out-degree of the vertex $v_i$ and it is equal to the sum of the weights of the edges that start from the vertex $v_i$:

$$d^+(v_i) = \sum_{j=1, j\neq i}^{j=N} (I_{i,j}) \tag{15}$$

The latter metric (denoted as $(d^-(v_i))$) is the in-degree of the vertex $v_i$ and it is equal to the sum of the weights of the edges that end in the vertex $v_i$:

$$d^-(v_i) = \sum_{j=1, j\neq i}^{j=N} (I_{j,i}) \tag{16}$$

Together, the sum of the in-degrees of all vertices plus the sum of out-degrees of all vertices represent the degree of the graph $G$ (denoted as $d(G)$) calculated as:

$$\begin{aligned} d(G) &= \sum_{i=1}^{i=N} d^-(v_i) + \sum_{i=1}^{i=N} d^+(v_i) \\ &= 2\sum_{i=1}^{i=N} d^-(v_i) = 2\sum_{i=1}^{i=N} d^+(v_i) \end{aligned} \tag{17}$$

It is obvious, from (17), that $\sum_{i=1}^{i=N} d^-(v_i) = \sum_{i=1}^{i=N} d^+(v_i)$. This equality between the in-degrees and out-degrees is due to the fact that every edge $e_{i,j}$ from the vertex $v_i$ to the vertex $v_j$ with a weight $I_{i,j}$ is considered as in-weight with respect to the $v_j$ as well as out-weight with respect to the $v_i$. In other words, every $I_{i,j}$ weight is a part of $d^+(v_i)$ and a part of $d^-(v_j)$ as well.

Note that when some D2D pairs communicate over the RF band while some other D2D pairs communicate over the VLC band, the D2D pairs can be represented by two separated weighted sub-graphs. The first sub-graph is a fully connected weighted sub-graph representing D2D pairs communicating over the RF band and interfering with each other. In contrast,

although the second sub-graph is a weighted directed sub-graph, it does not have to be fully connected as it represents the D2D pairs communicating over the VLC band where the interference might be absent between some D2D pairs due to various orientations of users' devices. However, there are no edges between the two sub-graphs due to the absence of interference among VLC and RF bands.

### C. DESCRIPTION OF THE PROPOSED ALGORITHM

The problem (13) can be solved by the exhaustive search algorithm as all RF/VLC combinations are checked and the set of the combinations that minimizes the outage ratio ($\Theta$) is chosen. Similarly, the exhaustive search can be applied to solve (14) by choosing the RF/VLC combination that maximizes the sum capacity of D2D pairs out of the set of combinations that minimize the outage ratio obtained from solving (13). However, the exhaustive search algorithm introduces a time complexity of $O(2^N)$. Thus, even if the number of D2D pairs is low, e.g., $N = 10$, the number of all possible combinations can be seen as too many, making the exhaustive search algorithm impractical for real networks, especially that the channel conditions are likely to change before testing all RF/VLC combinations. Thus, starting from the conventional initial state when all D2D pairs communicate over the RF band, we develop a low-complexity iterative algorithm switching the communication band of the D2D pairs sequentially from RF to VLC and converging to a final close-to-optimum performance.

**Algorithm 1** The Proposed Algorithm

1: Estimation of $\Theta$ and $\sum C_n$
2: **while** $\Theta$ is not minimized or $\sum C_n$ is not maximized **do**
3:  **if** $\Theta > 0$ **then**
4:  First phase: Outage ratio minimization
5:  **end if**
6:  Second phase: Sum capacity maximization
7: **end while**

The high level overview of the proposed algorithm is depicted in Algorithm 1. In the beginning, Algorithm 1 estimates the initial outage ($\Theta$) and the initial sum capacity ($\sum C_n$) when all D2D pairs operate in RF (see line 1). After that, two sequential phases, each solving one part of the multi-objective optimization problem, follow. More precisely, the first phase of the algorithm aims to minimize the outage ratio (line 4) unless the outage ratio is equal to zero (i.e., no outage); and the second phase maximizes the sum capacity (line 6). Both above-mentioned phases (covered by Algorithm 2 and Algorithm 3) are repeated as long as the performance may be further improved either in terms of outage ratio or sum capacity.

The first phase targeting to minimize outage ratio is handled by Algorithm 2. First, D2D pairs are sorted in a descending order according to the out-degree of the vertices, that is, according to $d^+(v_i^R)$ calculated in line with (15). In the next step, the D2D pair with the highest $d^+(v_i^R)$ is selected as the

**Algorithm 2** First Phase (Minimization of Outage Ratio)

1: Sort D2D pairs in descending order acc. to $d^+(v_i^R)$
2: **for** $i = 1, 2, \ldots N^R$ (all sorted D2D pairs in RF) **do**
3:  Check VLC channel for $i$-th pair (send beacon)
4:  Switch $i$-th D2D pair from RF to VLC
5:  Determine $\Theta^{\text{new}}$
6:  **if** $\Theta^{\text{new}} < \Theta$ **then**
7:  Keep $i$-th D2D pair in VLC
8:  $\Theta = \Theta^{\text{new}}$ (i.e., update outage)
9:  **if** $\Theta = 0$ **then**
10:  Terminate Algorithm 2
11:  **else**
12:  Break and repeat from line 1
13:  **end if**
14:  **else**
15:  Switch $i$-th D2D pair back to RF
16:  **if** $i = N^R$ (All D2D pairs in RF are tested) **then**
17:  Terminate Algorithm 2
18:  **end if**
19:  **end if**
20: **end for**

**Algorithm 3** Second Phase (Maximization of Sum Capacity)

1: Get $\Theta$ and $\sum C_n$ from Algorithm 2
2: Sort D2D pairs in descending order acc. to $d^-(v_i^R)$
3: **for** $i = 1, 2, \ldots N^R$ (all sorted D2D pairs in RF) **do**
4:  Check VLC channel for $i$-th pair (send beacon)
5:  Switch $i$-th D2D pair from RF to VLC
6:  Determine $\Theta^{\text{new}}$ and $\sum C_n^{\text{new}}$
7:  **if** $\Theta^{\text{new}} = \Theta$ and $\sum C_n^{\text{new}} > \sum C_n$ **then**
8:  Keep $i$-th D2D pair in VLC
9:  $\sum C_n = \sum C_n^{\text{new}}$ (update Capacity)
10:  Terminate Algorithm 3
11:  **else**
12:  Switch $i$-th D2D pair back to RF
13:  **if** $i = N^R$ (All D2D pairs in RF are tested) **then**
14:  Finish, $\Theta$ is minimized and $\sum C_n$ is maximized
15:  **end if**
16:  **end if**
17: **end for**

first candidate for the switching to VLC mode as this pair in particular generates the highest sum interference to other D2D pairs in RF. Of course, the D2D pair should change from RF to VLC only if the VLC channel is of a sufficient quality. Thus, the VLC channel quality is estimated by means of a beacon transmitted from the $\text{D2D}_T$ to $\text{D2D}_R$ (line 3). Then, if the D2D pair is able to use the VLC band, it is switched to the VLC (line 4) and a new outage ($\Theta^{new}$) is calculated according to (6) (see line 5). Obviously, if the outage is decreased by this process (i.e., if $\Theta^{new} < \Theta$), the D2D pair remains in VLC mode (line 7), as this is the main objective of this phase, and the outage value is updated (line 8). If the outage is not decreased by changing from VLC

to RF, however, the D2D pair goes back to RF mode (line 15). After that, the other D2D pair with the second highest $d^+(v_i^R)$ is investigated next and the whole process is repeated. This is done as long as the outage is higher than 0 (checked in line 9) or until all D2D pairs in RF have been tested (see line 16). Notice that the number of D2D pairs in RF is denoted as $N^R$ and as the switching process progress (i.e., be repeating while cycle in Algorithm 1), $N^R$ is gradually decreased since less amount of D2D pairs need to be checked.

In the second phase, represented by Algorithm 3, the aim is to improve the sum capacity of D2D pairs without increasing the outage ratio $\Theta$ achieved in the first phase. Thus, Algorithm 3 starts by adopting $\Theta$ and $\sum C_n$ reached in the first phase (line 1). Then, the D2D pairs are sorted according to in-degree $d^-(v_i^R)$ of the vertices corresponding to the D2D pairs communicating over the RF band (line 2). The first D2D pair to be checked is the one still in the RF mode and experiencing the strongest sum interference from other pairs in RF (i.e., the pair with the highest in-degree $d^-(v_i^R)$ calculated according to (16)). After that, the process is similar to the one described in Algorithm 2 during which the availability of VLC connection for this pair is tested (line 4), and then, the switching to VLC occurs if VLC is available (line 5). Nevertheless, in this second phase, the new sum capacity $\sum C_n^{new}$ is also calculated (besides the $\Theta^{new}$), as the objective of this phase is to maximize the sum capacity (line 6). The D2D pair keeps communicating over the VLC band (line 8) if $\sum C_n^{new} > \sum C_n$ while $\Theta^{new} = \Theta$ (i.e., if conditions from line 7 are satisfied). The fulfilling of both conditions also results in the termination of Algorithm 3. In the opposite case, however, the D2D pair switches back to RF (line 12), and the second pair from the sorted D2D pairs is tested (i.e., Algorithm 3 returns back to line 3). Note that if the Algorithm 3 is terminated in line 10 after a D2D pair switches to VLC, the first phase (Algorithm 2) is repeated as illustrated in Algorithm 1 in order to check the possibility of further reduction in the outage. Nonetheless, if the achieved outage is already zero, the second phase (Algorithm 3) is repeated directly without the need to go through the first phase (see Algorithm 1). After all D2D pairs in Algorithm 3 are tested (line 13) without any possibility to improve sum capacity, the whole proposed algorithm finishes (line 14) as changing any of the D2D pairs from RF to VLC cannot further decrease outage or increase sum capacity.

The graphs-based interpretation of an example with five D2D pairs switching to VLC based on the proposed algorithm is shown in Figure 2. Figure 2a presents the initial state with all D2D pairs communicating over the RF band. In such a case, the D2D pairs mutually interfere with each other leading to a possible outage. This outage is excluded by switching D2D pairs 2, 3 and 5 (represented by $v_2^V$, $v_3^V$ and $v_5^V$, respectively) to VLC as illustrated in Figure 2b.

Although the D2D pairs switched to VLC interfere among each other, this VLC interference is expected to be lower than the RF interference due to the higher signal attenuation over the VLC band in comparison to the RF band and due to the various setting of the irradiance and the incidence angles of the DUEs belonging to different D2D pairs.

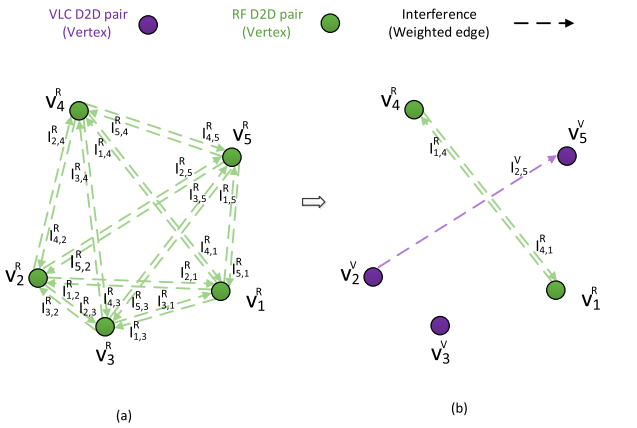


**FIGURE 2.** An example of five D2D pairs represented by two weighted directed graphs showing: (a) the initial state with all D2D pairs in RF, and (b) the final state where three D2D pairs are switched to VLC (notice that the topology of D2D pairs and the resulted RF/VLC combination are taken from Figure 1).

## IV. PERFORMANCE EVALUATION

The performance of the proposed algorithm is evaluated by means of simulations performed in MATLAB. First, this section describes in all the details the simulation scenario and the simulation parameters. Second, the competitive algorithms and the key performance metrics considered for the comparison to our proposal are introduced. Third, the extensive simulation results showing the impact of the number of D2D pairs and/or irradiance and incidence angles are presented and thoroughly discussed.

### A. SIMULATION SCENARIO AND MODELS

We assume the scenario, which is identified as the most beneficial for the whole RF-VLC D2D concept [19]. More specifically, we consider an indoor area (representing, e.g., a room or a hall) without any indoor walls. Within this area, up to ten D2D pairs are randomly dropped with a uniform distribution. We assume that the users are aware of each other and that they are willing to exchange data. Therefore, the users try to direct their DUEs approximately towards each other. This assumption is simulated using three different distributions of angles showing three possible cases. The first case is represented by optimal angles ($\phi$ and $\psi$ are set to zero), where the users direct their DUEs perfectly towards each other. The second and the third case are represented by Gaussian distribution of the irradiance and incidence angles ($\phi$ and $\psi$) of every $\text{DUE}_T$ and $\text{DUE}_R$ of the same D2D pair as in [19], with a mean of 0° and a standard deviation of 30° and 60°, respectively. The simulation consists of 3000 drops, where for each drop the positions and the angles of the all DUEs are generated independently.

For the modeling of RF channel, we follow 3GPP recommendation for indoor D2D communication as defined in [30],

**TABLE 1. Simulation parameters.**

| | | |
|---|---|---|
| RF Parameters | | |
| Carrier frequency | $f_c$ | 2 [GHz] |
| Bandwidth | $B^R$ | 20 [MHz] |
| Transmission power of any $\text{DUE}_T$ | $P^R$ | 200 [mW] |
| Interference from other cells | $I_{noise}$ | -70 [dBm] |
| Noise spectral density | $\sigma_o$ | -174 [dBm/Hz] |
| VLC Parameters | | |
| Bandwidth | $B^V$ | 10 [MHz] |
| Transmission power of any $\text{DUE}_T$ | $P^V$ | 200 [mW] |
| Responsivity of the photodetector | $\mu$ | 0.5 [A/W] |
| General Parameters | | |
| Room dimension | $d$ | 30 [m] |
| Number of D2D pairs | $N$ | 2-10 [-] |
| Minimal SINR | $\gamma_{min}$ | -10 [dB] |
| Number of simulation drops | $S_d$ | 3000 [-] |

i.e., the D2D indoor path loss model is defined as:

$$PL = 89.5 + 16log_{10}(d_{TR}) \tag{18}$$

where $d_{TR}$ is the distance between a transmitter and a receiver.

The RF interference from neighbouring cells $I_{noise}$ is set to $-70$ dBm. It is obvious that this selected value represents a high level of interference which corresponds to the high density of users expected in the future mobile networks (5G networks and beyond) [25].

The VLC channel model is in line with [30] and follows the description from Section II. However, Table 1 summarizes the parameters of RF and VLC channels in addition to the general simulation parameters. Notice that we consider the same fixed $p_n$ for any $n$-th transmitter $\text{DUE}_T$ and the exploitation of power control techniques is left for future research.

### B. COMPETITIVE ALGORITHMS AND PERFORMANCE METRICS

To the best of our knowledge, there is no algorithm selecting between RF and VLC for D2D communication. Thus, our proposed heuristic algorithm (labeled Proposed RF-VLC D2D) is compared to the following four competitive solutions:

1) *RF D2D*: The RF band is used for the D2D communication and all the D2D pairs reuse the whole bandwidth [20]. This algorithm illustrates the performance of the D2D communication in the case where only the RF band is available (without VLC D2D).
2) *VLC D2D*: The VLC band is exploited for the D2D communication according to [31]. Notice that the VLC D2D in [31] includes the possibility of relaying the VLC-based data transmission through nearby devices. Nevertheless, we do not consider any relaying in our proposed algorithm and, thus, we leave this feature out also for VLC D2D for a fair comparison. The VLC D2D demonstrates the performance of the D2D communication in the case where only the VLC band is available (without RF D2D).
3) *Random RF-VLC D2D*: This algorithm randomly selects either RF or VLC band for each D2D pair. Note that this simple algorithm is designed only for comparison purposes.
4) *Optimal RF-VLC D2D*: The optimal combination of RF and VLC bands for the D2D pairs is derived by the exhaustive search algorithm, which checks all possible combinations ($2^N$ combinations) as described in Section III-C. First, the combinations with the lowest reachable outage ratio $\Theta^*$ are chosen. Then, the algorithm selects the combination with the highest $\sum C_n$ among the previously chosen combinations with the lowest outage ratio. This algorithm is a very high complexity solution that shows the optimal performance of the RF-VLC D2D in a multi-user scenario; and it can be seen as a theoretical upper bound used to evaluate the performance quality of other algorithms.

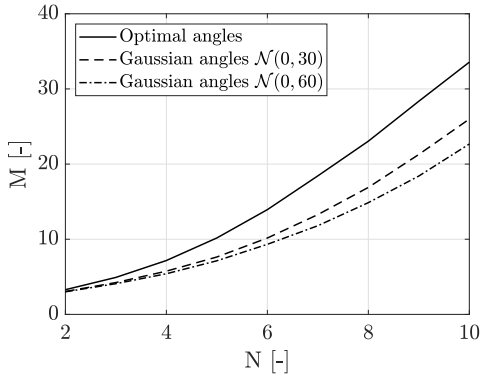


**FIGURE 3. Number of iterations *M* needed for the proposed algorithm over number of D2D pairs *N*.**

The performance of the proposed algorithm and all four competitive solutions are assessed by means of three performance metrics: 1) the outage ratio $\Theta$ (see (6)), 2) the sum capacity of D2D pairs $\sum C_n$ (denoted in figures as $C$), and 3) the average energy efficiency of D2D pairs $EE$, calculated as $EE = \frac{\sum EE_n}{N}$. Moreover, we show the complexity of the proposed algorithm presented by the number of needed iterations of the proposed algorithm (denoted as $M$) and we show the VLC usage ratio calculated as $\frac{N^V}{N}$, where $N^V$ is number of D2D pairs communicating over the VLC band.

### C. SIMULATION RESULTS AND DISCUSSION

In this sub-section, we present the results showing that the proposed algorithm is of low complexity and, at the same time, achieves a close-to-optimal performance in terms of the outage, sum capacity and average energy efficiency of D2D pairs.

Figure 3 analyzes the complexity of the proposed algorithm presented by the number of needed iterations ($M$) averaged over the simulated drops. It is obvious that the number of iterations increases with $N$ as more D2D pairs are checked and switched from RF to VLC. Figure 3 also shows that the further the irradiance and incidence angles ($\phi$ and $\psi$) are from the optimal, the less number of iterations are needed. In other words, when $\phi$ and $\psi$ are optimal (equal to zero), the proposed algorithm needs to go through the highest

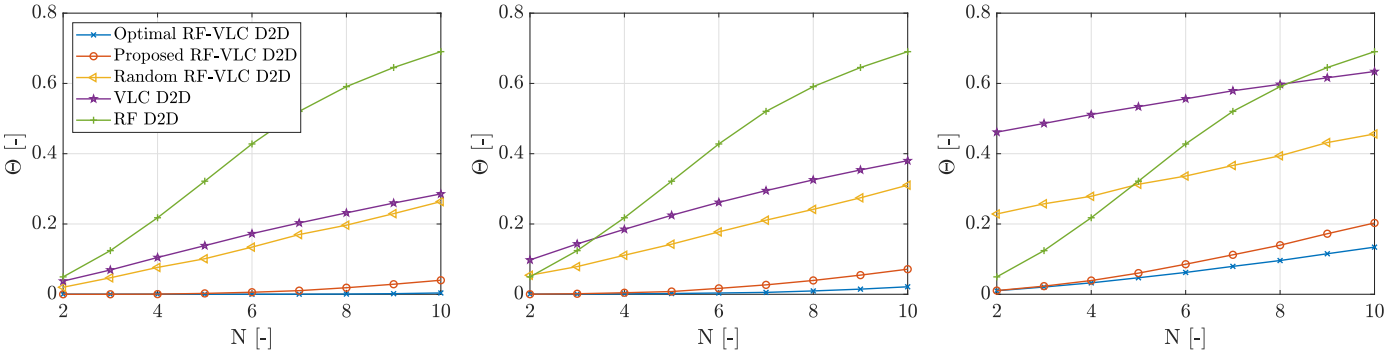


(a) $\phi = 0, \psi = 0$ (b) $\phi, \psi = \mathcal{N}(0, 30)$ (c) $\phi, \psi = \mathcal{N}(0, 60)$

**FIGURE 4.** Outage ratio Θ over the number of D2D pairs *N* for $\phi$ and $\psi$ distributed as: optimal (zero) angles (a), Gaussian distribution with the mean of 0 and the standard deviation of 30° (b) and 60° (c). Note that the common legend is shown in Figure 4a for the sake of clarity.

number of iterations in comparison to the cases when $\phi$ and $\psi$ are not optimal. This interesting behavior is, however, quite expected due to the fact that if $\phi$ and $\psi$ angles are closer to optimum there is a higher probability that a D2D pair is able to communicate over the VLC band. Thus, more D2D pairs need to be checked and switched from RF to VLC as explained in Section III-C. However, regardless of the angular distribution, we see in Figure 3 that the complexity of the proposed algorithm is much lower than the exhaustive search algorithm, e.g., for 10 D2D pairs exhaustive search checks $2^N = 2^{10} = 1024$ combinations (corresponding to 1024 iterations) while the proposed algorithm needs below 35 iterations.

Figure 4 shows the outage ratio Θ depending on number of D2D pairs and for different distributions of $\phi$ and $\psi$. For all algorithms, the Θ increases with $N$, because the interference is inevitably increasing with the density of D2D pairs as well. It can be seen in Figure 4 that the RF D2D and VLC D2D lead to the highest and the second highest outage, respectively, when angles are optimal (Figure 4a). However, when angles are not optimal, the VLC D2D shows an increasing Θ with the increasing standard deviation of the Gaussian distribution of $\phi$ and $\psi$ from 30° and 60° and, thus, VLC D2D introduces the highest outage ratio for low number of D2D pairs in Figure 4b and Figure 4c. Moreover, the increasing outage ratio of VLC D2D with angles changing from Optimal to $\mathcal{N}(0, 30)$ and then to $\mathcal{N}(0, 60)$ impacts all algorithms combining RF and VLC (i.e., Random, proposed and optimal RF-VLC D2D). The reason is that if the transmitter and the receiver of the D2D pair are in the opposite direction of each other, the D2D pair they compose cannot switch to VLC even if this pair is exposed to (or causing) high RF interference. However, Figure 4 shows that combining RF and VLC in a random RF-VLC D2D introduces unacceptable low gain in terms of outage ratio reduction. On the contrary, the proposed RF-VLC algorithm reduces the outage ratio substantially to a 0.03 and less than 0.09 for all values of $N$ when irradiance and incidence angles are optimal (Figure 4a) or relatively good (Figure 4b). Such a low outage ratio is achieved by relying on the proposed interference-based selection of the candidates for switching from RF to VLC.

In Figure 4c, where angles might be non-suitable for VLC, the outage ratio of the proposed algorithm increases up to 0.2 for 10 D2D pairs. However, we can see that when the angles are not suitable for VLC, even the optimal selection is not able to fully mitigate outage. What is more, the relatively small gap between the proposed selection and the optimal one (in the worst case the gap is roughly 0.07) can be easily justified by very low complexity of the proposed algorithm (as demonstrated in Figure 3) in contrast to the optimal exhaustive search-based solution for which the complexity increases exponentially ($2^N$) making this optimal algorithm impractical for real network implementations.

Moving to the another criteria, Figure 5 illustrates the sum capacity of D2D pairs over $N$. The sum capacity of all algorithms containing a VLC D2D (VLC D2D or RF-VLC D2D), decreases with irradiance and incidence angles changing from optimal to Gaussian distribution with a standard deviation of 30° and then 60°. Still, the bottom line is that the proposed RF-VLC D2D significantly outperforms RF D2D, VLC D2D, and random RF-VLC D2D reaching 6.1, 7.1, and 1.1 times higher sum capacity, respectively. At the same time, the proposed algorithm loses only marginally when compared to optimal RF-VLC D2D (always less than 9.5%). Figure 5 further shows that the behavior of the sum capacity over $N$ for the optimal RF-VLC D2D and the proposed RF-VLC D2D is almost similar. To be more precise, when angles are optimal (Figure 5a) or relatively good (Figure 5b), the capacity increases as long as the increasing $N$ gives more possible RF-VLC combinations that are able to manage and to limit the added interference. With further increasing of D2D pairs, however, the sum capacity starts decreasing due to the fact that further increment in $N$ leads to a high interference even if both RF and VLC bands are considered. Note that in Figure 5c, the sum capacity immediately decreases when $N$ starts to increase as adding more pairs raises the RF interference while most of the D2D pairs are not able to switch to VLC due to the unfavorable $\phi$ and $\psi$. With the continuous increase

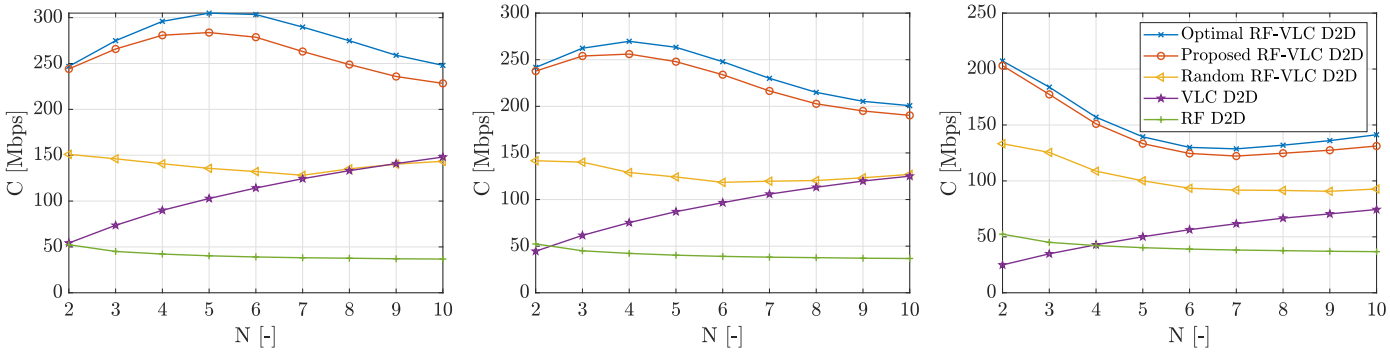


(a) $\phi = 0, \psi = 0$ (b) $\phi, \psi = \mathcal{N}(0, 30)$ (c) $\phi, \psi = \mathcal{N}(0, 60)$

**FIGURE 5.** Sum capacity *C* over number of D2D pairs *N* for $\phi$ and $\psi$ distributed as: optimal (zero) angles (a), Gaussian distribution with mean of 0 and standard deviation of 30° (b) and 60° (c). Note that the common legend is shown in Figure 5c for the sake of clarity.

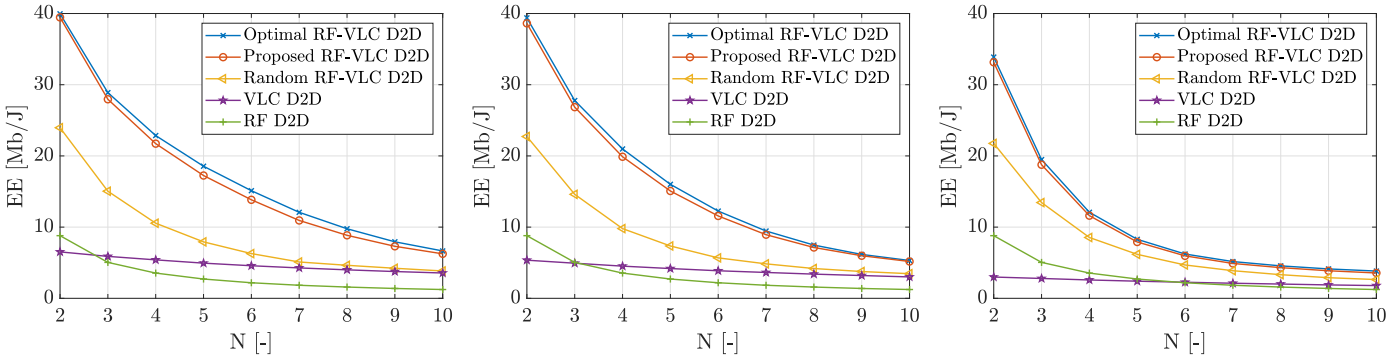


(a) $\phi = 0, \psi = 0$ (b) $\phi, \psi = \mathcal{N}(0, 30)$ (c) $\phi, \psi = \mathcal{N}(0, 60)$

**FIGURE 6.** The average energy efficiency*EE* over the number of D2D pairs *N* for $\phi$ and $\psi$ distributed as: optimal (zero) angles (a), Gaussian distribution with the mean of 0 and the standard deviation of 30° (b) and 60° (c).

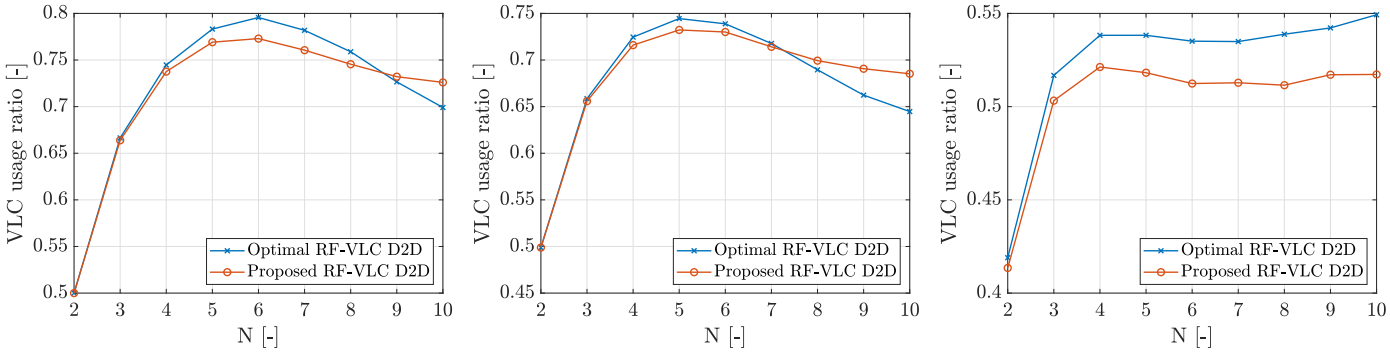


(a) $\phi = 0, \psi = 0$ (b) $\phi, \psi = \mathcal{N}(0, 30)$ (c) $\phi, \psi = \mathcal{N}(0, 60)$

**FIGURE 7.** The VLC usage ratio over the number of D2D pairs *N* for $\phi$ and $\psi$ distributed as: optimal (zero) angles (a), Gaussian distribution with the mean of 0 and the standard deviation of 30° (b) and 60° (c).

of $N$, however, the capacity starts increasing as well (i.e., if $N > 7$) since more pairs can be switched to VLC and interference among the pairs is partly mitigated.

Figure 6 provides an analysis of the average energy efficiency of D2D pairs. We can see that the average energy efficiency of D2D pairs of all algorithms decreases with $N$ due to the high corresponding increment in the consumed energy by more D2D pairs. Moreover, Figure 6 shows that the users' directions affect all algorithms containing VLC D2D, where *EE* generally decreases as $\phi$ and $\psi$ are further from the optimal ones. However, the proposed algorithm outperforms the RF D2D, VLC D2D, and random RF-VLC D2D disregarding $N$ and $\phi$ and $\psi$ distribution reaching 5.3, 10, and 1.2 times higher average energy efficiency, respectively. In addition, minor losses in *EE* are introduced by the proposed algorithm comparing to the optimal RF-VLC D2D as we see in Figure 6 (always less than 9.5%).

Finally, we show the VLC usage ratio over $N$ in Figure 7. The first obvious observation is that disregarding $N$, the VLC usage ratio decreases with $\phi$ and $\psi$ changing from optimal

to Gaussian with a standard deviation of 30° and then to Gaussian with a standard deviation of 60°. This outcome is expected since the VLC links experience lower capacity if $\phi$ and $\psi$ are further from optimal and, thus, RF is used more often. The second observation is that when $\phi$ and $\psi$ are optimal (Figure 7a) or relatively good (Figure 7b), the VLC ratio increases with $N$ as long as the increasing interference is handled by switching more pairs from RF to VLC. However, after a certain value of $N$ ($N = 6$ for optimal angles and $N = 5$ for a standard deviation of 30°), the VLC ratio starts to decrease due to the fact that the number of D2D pairs switching to VLC is not increasing any longer with $N$ due to high interference in VLC. In contrast, if $\phi$ and $\psi$ are generally far from optimal (i.e., case in 7c), the VLC usage ratio is more or less always increasing with $N$. The reason for this behavior is the fact that increasing the number of D2D pairs when UEs' angles are rarely suitable for VLC communications leads to a limited increment in VLC usage ratio and a corresponding relatively low VLC interference. Thus, VLC usage ratio keeps gradually increasing for all tested values of $N$ (even when $N > 6$).

## V. CONCLUSION

In this paper, we have proposed the centralized algorithm for the selection of either RF or VLC band for D2D communication in a multi-user scenario. The simulation results show that, compared to the exhaustive search algorithm, the proposed algorithm costs much lower complexity and, at the same time, reaches close-to-optimal performance. Moreover, the proposed algorithm outperforms all state-of-the-art algorithms in terms of capacity by up to 7.1 times and energy efficiency by up to 10 times while outage is significantly minimized.

As future work, the selection between both communication bands should be done by exploiting machine learning in order to further decrease the complexity of the selection.

## REFERENCES

[1] M. N. Tehrani, M. Uysal, and H. Yanikomeroglu, "Device-to-device communication in 5G cellular networks: Challenges, solutions, and future directions," *IEEE Commun. Mag.*, vol. 52, no. 5, pp. 86–92, May 2014.
[2] A. Asadi, Q. Wang, and V. Mancuso, "A survey on device-to-device communication in cellular networks," *IEEE Commun. Surveys Tuts.*, vol. 16, no. 4, pp. 1801–1819, 4th Quart., 2014.
[3] Y. Xu and S. Wang, "Mode selection for energy efficient content delivery in cellular networks," *IEEE Commun. Lett.*, vol. 20, no. 4, pp. 728–731, Apr. 2016.
[4] P. Mach, Z. Becvar, and M. Najla, "Combined shared and dedicated resource allocation for D2D communication," in *Proc. IEEE VTC-Spring*, Jun. 2018, pp. 1–7.
[5] R. Wang, J. Zhang, S. H. Song, and K. B. Letaief, "QoS-aware joint mode selection and channel assignment for D2D communications," in *Proc. IEEE ICC*, May 2016, pp. 1–6.
[6] Z. Lin, Z. Gao, and L. Huang, "Hybrid architecture performance analysis for device-to-device communication in 5G cellular Network," *Mobile Netw. Appl.*, vol. 20, no. 6, pp. 713–724, Dec. 2015.
[7] A. Sevincer, A. Bhattarai, M. Bilgi, M. Yuksel, and N. Pala, "LIGHTNETs: Smart LIGHTing and mobile optical wireless NETworks—A survey," *IEEE Commun. Surveys Tuts.*, vol. 15, no. 4, pp. 1620–1641, 4th Quart., 2013.
[8] F. Yang and J. Gao, "Dimming control scheme with high power and spectrum efficiency for visible light communications," *IEEE Photon. J.*, vol. 9, no. 1, Feb. 2017, Art. no. 7901612.
[9] I. Din and H. Kim, "Energy-efficient brightness control and data transmission for visible light communication," *IEEE Photon. Technol. Lett.*, vol. 26, no. 8, pp. 781–784, Apr. 15, 2014.
[10] P. H. Pathak, X. Feng, P. Hu, and P. Mohapatra, "Visible light communication, networking, and sensing: A survey, potential and challenges," *IEEE Commun. Surveys Tuts.*, vol. 17, no. 4, pp. 2047–2077, 4th Quart., 2015.
[11] Y. Wang, X. Huang, L. Tao, J. Shi, and N. Chi, "4.5-Gb/s RGB-LED based WDM visible light communication system employing CAP modulation and RLS based adaptive equalization," *Opt. Express*, vol. 23, no. 10, pp. 13626–13633, May 2015.
[12] X. Huang, Z. Wang, J. Shi, Y. Wang, and N. Chi, "1.6 Gbit/s phosphorescent white LED based VLC transmission using a cascaded pre-equalization circuit and a differential outputs PIN receiver," *Opt. Express*, vol. 23, no. 17, pp. 22034–22042, 2015.
[13] S. Rajagopal, R. D. Roberts, and S.-K. Lim, "IEEE 802.15.7 visible light communication: Modulation schemes and dimming support," *IEEE Commun. Mag.*, vol. 50, no. 3, pp. 72–82, Mar. 2012.
[14] X. Wu, M. Safari, and H. Haas, "Access point selection for hybrid Li-Fi and Wi-Fi networks," *IEEE Trans. Commun.*, vol. 65, no. 12, pp. 5375–5385, Dec. 2017.
[15] M. Kashef, M. Abdallah, and N. Al-Dhahir, "Transmit power optimization for a hybrid PLC/VLC/RF communication system," *IEEE Trans. Green Commun. Netw.*, vol. 2, no. 1, pp. 234–245, Mar. 2018.
[16] H. Tabassum and E. Hossain, "Coverage and rate analysis for co-existing RF/VLC downlink cellular networks," *IEEE Trans. Wireless Commun.*, vol. 17, no. 4, pp. 2588–2601, Apr. 2018.
[17] Y. Liu, Z. Huang, W. Li, and Y. Ji, "Game theory-based mode cooperative selection mechanism for device-to-device visible light communication," *Proc. SPIE*, vol. 55, no. 3, 2016, Art. no. 30501.
[18] S. V. Tiwari, A. Sewaiwar, and Y.-H. Chung, "Optical repeater assisted visible light device-to-device communications," *Int. J. Electr., Comput., Energetic, Electron. Commun. Eng.*, vol. 10, no. 2, pp. 206–209, 2016.
[19] P. Mach, Z. Becvar, M. Najla, and S. Zvanovec, "Combination of visible light and radio frequency bands for device-to-device communication," in *Proc. IEEE PIMRC WS*, Oct. 2017, pp. 1–7.
[20] Z. Becvar, M. Najla, and P. Mach, "Selection between radio frequency and visible light communication bands for D2D," in *Proc. IEEE VTC spring*, Jun. 2018, pp. 1–7.
[21] Z. Ghassemlooy, L. N. Alves, S. Zvanovec, and M.-A. Khalighi, *Visible Light Communications: Theory and Applications*, vol. 17, no. 4. Boca Raton, FL, USA: CRC Press, 2017.
[22] M. Lauridsen, L. Noël, T. B. Sørensen, and P. Mogensen, "An empirical LTE smartphone power model with a view to energy efficiency evolution," *Intel Technol. J.*, vol. 18, no. 1, pp. 172–193, 2014.
[23] X. Deng, K. Arulandu, Y. Wu, S. Mardanikorani, G. Zhou, and J.-P. M. G. Linnartz, "Modeling and analysis of transmitter performance in visible light communications," *IEEE Trans. Veh. Technol.*, vol. 68, no. 3, pp. 2316–2331, Mar. 2019.
[24] X. Deng and J.-P. M. G. Linnartz, "Poster: Model of extra power in the transmitter for high-speed visible light communication," in *Proc. IEEE Symp. Commun. Veh. Technol. (SCVT)*, Nov. 2016, pp. 1–5.
[25] M. I. Poulakis, A. G. Gotsis, and A. Alexiou, "Multi-cell device-to-device communications: A spectrum sharing and densification study," 2017, *arXiv:1711.03498*. [Online]. Available: https://arxiv.org/abs/1711.03498
[26] S. M. A. Kazmi, N. H. Tran, W. Saad, Z. Han, T. M. Ho, T. Z. Oo, and C. S. Hong, "Mode selection and resource allocation in device-to-device communications: A matching game approach," *IEEE Trans. Mobile Comput.*, vol. 16, no. 11, pp. 3126–3141, Nov. 2017.
[27] Y. Wang, Y. Shao, H. Shang, X. Lu, Y. Wang, J. Yu, and N. Chi, "875-Mb/s asynchronous bi-directional 64 QAM-OFDM SCM-WDM transmission over RGB-LED-based visible light communication system," in *Proc. Opt. Fiber Commun. Conf.*, 2013, Paper OTh1G-3.
[28] R. T. Marler and J. S. Arora, "Survey of multi-objective optimization methods for engineering," *Struct. Multidisciplinary Optim.*, vol. 26, no. 6, pp. 369–395, Apr. 2004.
[29] *Evolved Universal Terrestrial Radio Access (E-UTRA); Physical Channels and Modulation, Release 13*, document TS 36.211, v13.5.0, 3GPP, 2017.
[30] *Study on LTE Device to Device Proximity Services; Radio Aspects, Release 12*, document TR 36.843, v12.0.1, 3GPP, 2014.
[31] P. Pešek, S. Zvanovec, P. Chvojka, M. R. Bhatnagar, Z. Ghassemlooy, and P. Saxena, "Mobile user connectivity in relay-assisted visible light communications," *Sensors*, vol. 18, no. 4, p. 1125, 2018.

### 4.3.3 Machine Learning for Fast Band Selection in RF-VLC D2D Communication

In this subsection, another RF/VLC band selection algorithm is proposed. The algorithm proposed in this sub-subsection relies on machine learning in order to make a very fast band selection based only on limited channel knowledge. This subsection includes the journal paper [3J].

# Deep Learning for Selection between RF and VLC Bands in Device-to-Device Communication

Mehyar Najla, *Student Member, IEEE*, Pavel Mach, *Member, IEEE*, Zdenek Becvar, *Senior Member, IEEE*

***Abstract*—This letter focuses on the selection between radio frequency (RF) and visible light communications (VLC) bands for users exchanging data directly with each other via device-to-device (D2D) communication. We target to maximize the energy efficiency of D2D communication while the outage is minimized. Since the VLC channel can vary quickly due to the possible changes in irradiance and incidence angles, we aim to reach a quick band selection decision in a multi-user scenario based only on the knowledge of the received power and sum interference from all D2D transmitters at the individual D2D receivers. The proposed solution is based on a deep neural network making an initial band selection decision. Then, based on the DNN's output, a fast heuristic algorithm is proposed to further improve the band selection decision. The results show that the proposal reaches a close-to-optimal performance and outperforms the existing solutions in complexity, outage ratio, and energy efficiency.**

***Index Terms*—Device-to-device, visible light communications, band selection, deep neural networks**

## I. Introduction

Future mobile communications are expected to cope with the continuous increase in the amount of transmitted data resulting in a lack of available radio spectrum [1]. A suitable solution for an efficient use of the spectrum is device-to-device (D2D) communication allowing any pair of nearby D2D user equipment (DUE) to communicate directly and, hence, to improve the spectral efficiency and the system capacity [2]. To further enhance the system capacity, multiple D2D pairs can reuse the same radio frequency (RF) band [3]. Also, additional bands besides the RF licensed bands, such as Bluetooth or WiFi, can be exploited [4]. Another enticing option is to exploit visible light communications (VLC) operating at frequency bands of 400-790 THz. This makes VLC suitable for communicating at short distances, e.g., indoor [5].

Several studies demonstrate the benefits of the D2D communication using only VLC bands (e.g., [6]-[7]). Nevertheless, the VLC link may suffer from sudden drops in channel quality as it is highly susceptible to changes in the transmitter's ($\text{DUE}_\text{t}$) irradiance and the receiver's ($\text{DUE}_\text{r}$) incidence angles. Consequently, VLC links should not be implemented without an option to switch back to RF. An initial study on the combination of RF and VLC for D2D communication is presented in [1]. Then, in [8], an iterative two-phase heuristic algorithm is proposed to minimize the outage and to maximize the sum capacity of D2D pairs by selecting RF or VLC communication band for each pair. However, the solution in [8] relies on the assumption that channel gains among all DUEs in RF and VLC are known. Moreover, the band selection in [8] is based on an iterative algorithm, which is not suitable in dynamic scenarios, where a fast band selection is required.

To circumvent the need for the full channel knowledge, we present the band selection problem as a supervised binary classification problem targeting the selection of RF or VLC for every D2D pair. We assume only the knowledge of the received power and the received sum interference at each $\text{DUE}_r$ in RF and VLC to minimize the outage and to maximize the average energy efficiency of the D2D communication. We solve this band selection problem via deep neural network (DNN). We choose DNNs as they make no prior assumptions on the data sets and give an instantaneous probabilistic output in a negligible time. Moreover, a trained DNN can be stored with low memory requirements while it still enables to extract a complex model/relation connecting its inputs and outputs as required by the nature of our problem.

To minimize the potential gap between the performance of the DNN exploiting limited channel knowledge among D2D pairs and the optimal case when full information is available, we design a low-complexity heuristic algorithm built upon the DNN's output to further improve the accuracy of the band selection. The algorithm relies on the probabilities of each D2D pair to communicate via RF (and VLC) obtained by the DNN, and copes with the inherent uncertainties in the DNN's decisions. Despite the proposed solution is of a very low complexity and requires only a limited knowledge of channels, the simulations demonstrate its close-to-optimal performance.

## II. System Model and Problem Formulation

We assume $N$ D2D pairs uniformly deployed in a square area. The RF (VLC) channel with a bandwidth $B_R$ ($B_V$) is exploited by all D2D pairs communicating in RF (VLC). The D2D pairs using VLC are affected by the $\text{DUE}_\text{t}$ irradiance and $\text{DUE}_\text{r}$ incidence angles, which are generated randomly. Since any $n$-th D2D pair can communicate in either the RF or VLC band, we define a band indicator $z^n$. If the $n$-th D2D pair communicates over the RF band, $z^n$ is set to 1, while if the $n$-th pair uses VLC, $z^n$ is set to 0. Based on this, the energy efficiency of the $n$-th D2D pair is expressed as:

$$EE^n = \frac{C^n}{z^n(P_R^{t,n} + P_R^{r,n}) + (1 - z^n)(P_V^{t,n} P_V^{r,n})} \quad (1)$$

where $P_R^{t,n}$ and $P_V^{t,n}$ are the powers consumed by the $n$-th $\text{DUE}_\text{t}$ during the transmission in RF and VLC, respectively; $P_R^{r,n}$ and $P_V^{r,n}$ are the powers consumed by the $n$-th $\text{DUE}_\text{r}$

This work has been supported by the grant no. GA17-17538S funded by Czech Science Foundation and the grant no. SGS17/184/OHK3/3T/13 funded by CTU in Prague. The authors are with the Department of Telecommunication Engineering, Faculty of Electrical Engineering, Czech Technical University in Prague, Prague, 166 27 Czech Republic (emails: najlameh@fel.cvut.cz; machp2@fel.cvut.cz; zdenek.becvar@fel.cvut.cz).

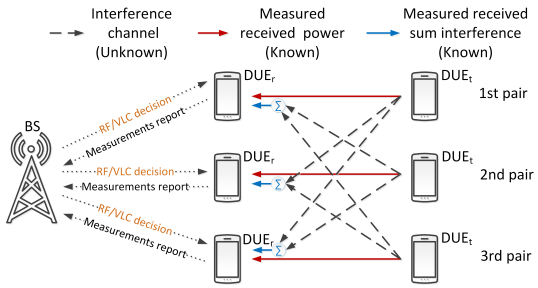


Fig. 1: System model.

during the data reception in RF and VLC, respectively (the consumed powers in RF and VLC are modeled in line with [9] and [8], respectively); and $C^n$ denotes the capacity of the $n$-th D2D pair defined as:

$$C^n = Blog_2(1+\gamma^n) \tag{2}$$

where $B$ is the communication channel bandwidth and $\gamma^n$ is the signal to interference plus noise ratio (SINR). Considering the band indicator $z^n$, the bandwidth $B$ in (2) is:

$$B = z^n B_R + (1-z^n)B_V \tag{3}$$

Similarly, $\gamma^n$ is calculated as:

$$\begin{aligned}\gamma^n = z^n \frac{p_R^n g_R^{n,n}}{N_R + \sum_{m\neq n} z^m p_R^m g_R^{m,n}} \\ +(1-z^n)\frac{p_V^n g_V^{n,n}}{N_V + \sum_{m\neq n}(1-z^m) p_V^m g_V^{m,n}}\end{aligned} \tag{4}$$

where $p^n$ is the transmission power of the $n$-th D2D pair, $g^{n,n}$ is the channel gain between the DUE$_t$ and the DUE$_r$ of the $n$-th D2D pair, $p^m$ is the transmission power of the $m$-th D2D pair that is inducing interference to the $n$-th D2D pair, $g^{m,n}$ is the channel gain between the DUE$_t$ of the $m$-th pair and the DUE$_r$ of the $n$-th pair, and $N_R$ and $N_V$ are the noises in RF and VLC, respectively. Note that, in VLC, the channel gains and the noise are functions of the users' directions (i.e., irradiance and incidence angles) and other parameters related to the LED and the photodetector in line with [10].

We consider that every $n$-th D2D pair requires an SINR satisfying $\gamma^n \geq \gamma^{th}$, where $\gamma^{th}$ is the minimal SINR ensuring a reliable communication between the DUE$_t$ and the DUE$_r$. Thus, if $\gamma^n < \gamma^{th}$, the $n$-th D2D pair is considered to be in outage and the outage ratio is, then, calculated as:

$$\phi = N_o/N \tag{5}$$

where $N_o$ represents the number of D2D pairs in outage.

We further assume that all D2D pairs transmit a VLC reference signal at the same time to measure the VLC communication quality [8] (similarly to the RF band, where the reference signals are used to measure the communication quality [11]). Moreover, the DUE$_r$ of every $n$-th D2D pair measures the received power from its corresponding transmitter (i.e., $p_R^n g_R^{n,n}$ and $p_V^n g_V^{n,n}$) and the sum interference induced by all other transmitters (i.e., $\sum_{m\neq n} p_R^m g_R^{m,n}$ and $\sum_{m\neq n} p_V^m g_V^{m,n}$) based on existing reference signals in RF and VLC. The reference signals are conventionally exploited in mobile networks and our solution requires no additional signaling to obtain the required information. Also, the assumption on the knowledge of the received powers and sum interferences is in line with 3GPP recommendations related to the reported RSRP/RSRQ in the conventional networks [12]. The measured received power and the sum interference are reported to and processed in a centralized unit (e.g., a nearby base station).

This letter aims to solve the multi-objective optimization problem of minimizing the outage ratio (i.e., $\phi$) and maximizing the average energy efficiency (i.e., $EE = \sum_{n=1}^{n=N} EE^n/N$) by selecting either RF or VLC band for each D2D pair. The problem is formulated as:

$$\begin{aligned}\mathbf{Z}^* = \underset{\mathbf{Z}}{\text{argmax}}(-\phi, \textstyle\sum_{n=1}^{n=N} \frac{EE^n}{N}) \\ \text{s.t. } z^n \in \{0,1\} \forall n \in \{1,...,N\} \; (a)\end{aligned} \tag{6}$$

The optimization problem in (6) is discrete with multiple non-linear objective functions and, thus, this problem is hard to solve. The problem can be solved sequentially by an exhaustive search if the outage minimization is selected as the objective with a higher priority than the energy efficiency maximization. First, a set of solutions achieving the minimal possible $\phi$ is determined. Second, the solution maximizing $EE$ is selected out of the solutions obtained in the first phase. However, the exhaustive search is not feasible for practical implementation due to its very high complexity equal to $\mathcal{O}(2^N)$. Therefore, in the next section, we propose a novel DNN-based approach to select RF or VLC for each D2D pair.

## III. Proposed Band Selection Scheme

DNNs have proven their efficiency in solving various mobile networks-related problems, such as, binary power control [13], channel prediction [14], or antenna selection [15], just to name a few. This efficiency is justified by the ability of the DNNs to obtain an output (and make a decision) instantly in a single step. The decision whether RF or VLC should be used by individual D2D pairs, as targeted in this letter, depends on the individual channel gains among all DUEs. However, to alleviate the problem of the high signaling required to obtain the individual channel gains among all DUEs (as assumed, e.g., in [8]), we consider that only the received powers and the received sum interferences in RF and VLC are known. With such information, it is not possible to determine individually the level of interference caused by one D2D pair to another D2D pair. Therefore, there is no possibility to extract analytically the relation of the received power and the received sum interferences to the correct band selection (RF or VLC) for every D2D pair. Hence, we rely on DNNs due to their ability to extract complex models connecting the limited available information (in our case received powers and sum interferences) with the targeted output (selection of RF or VLC). Moreover, a trained DNN selects the band instantaneously in one step. Thus, this section describes the proposed DNN-based framework for band selection. Then, a low-complexity heuristic algorithm is designed to cope with the potential uncertainties in the DNN-based band selection in order to obtain a close-to-optimal performance.

### A. DNN-based framework for communication band selection

The band selection (RF/VLC) for every D2D pair from the $N$ pairs can be seen as $N$ identical binary classification problems. Thus, we design a DNN with $4 \times N$ input vector (denoted as $\mathbf{X_1}$) containing the received powers measured by every $\text{DUE}_r$ from its related $\text{DUE}_\text{t}$ and the sum interference imposed on every $\text{DUE}_\text{r}$. Both these values are reported for VLC and RF, and the $\text{DUE}_\text{r}$ reports its four measurements within one message. Then, based on $\mathbf{X_1}$, the DNN returns the proper band selection for the $n$-th D2D pair. Due to the nature of the defined RF/VLC band selection problem based on the received powers and sum interferences, the DNN is required to have a fully-connected architecture without neither features' extraction nor feed-back connections. Hence, the DNN is composed of an input layer (i.e., $l_0$), represented by $\mathbf{X_1}$, $L$ sequential hidden layers (i.e., $\{l_1, l_2, ..., l_L\}$), and an output layer (i.e., $l_{L+1}$), see Fig. 2. The elements of $\mathbf{X_1}$ are fed to $l_1$ and, then, the output vector of each layer is the input vector of the following layer. Every hidden layer $l_j$ (where $j \in \{1, \ldots, L\}$) is composed of $K_j$ neurons and the output layer $l_{L+1}$ is composed of a single neuron for binary classification. Every layer $l_j$, except the input layer, inserts each input element $i$ from its input vector $\mathbf{X_j}$ to every neuron $u$ in this layer with a corresponding weight $w^j_{i,u}$. Every neuron in the layer $l_j$: i) performs the dot product between the input vector $\mathbf{X_j}$ and the corresponding weights, ii) adds the corresponding bias $b^j_u$, and iii) inserts the resulting value to a sigmoid activation function. Hence, the output of the layer $l_j$ (i.e., any hidden layer or the output layer $l_{L+1}$) is:

$$\mathbf{Y^n_j} = sigmoid(\mathbf{W^j}.\mathbf{X_j} + \mathbf{b^j}) \tag{7}$$

where $sigmoid(.)$ is the sigmoid function $sigmoid(A) = \frac{1}{1+exp(-A)}$ which returns output values between zero and one, $\mathbf{W^j}$ contains all weights of the links between the inputs of $l_j$ (i.e., $\mathbf{X_j}$) and all $\mathbf{K_j}$ neurons in $l_j$, and $\mathbf{b^j}$ includes the biases of all $\mathbf{K_j}$ neurons in $l_j$. The output of any hidden layer $\mathbf{Y^n_j} = \mathbf{X_{j+1}}$ for $j \in \{1, \ldots, L\}$ is of a length $K_j$. Similarly, as the output layer $l_{L+1}$ contains one neuron (i.e., $K_{L+1} = 1$), the output of $l_{L+1}$ (i.e., $Y^n_{L+1}$) is a single value that represents the probability that the $n$-th D2D pair should select the RF band. Hence, the DNN's output represents the band selection as:

$$z^n_{DNN} = \begin{cases} 1 & \text{if } Y^n_{L+1} > 0.5 \\ 0 & \text{otherwise} \end{cases} \tag{8}$$

To train the DNN, a set of "training samples" is collected.

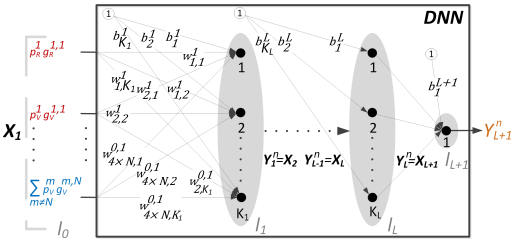


Fig. 2: Proposed DNN to select RF or VLC for a D2D pair.

Each training sample contains the measured received powers and sum interferences from every $\text{DUE}_\text{r}$ in both RF and VLC (i.e., $\mathbf{X_1}$), accompanied with a targeted output, which is the optimal selection of RF or VLC for the $n$-th D2D pair derived by the exhaustive search ($z^{n*}$). The collected samples are fed to the DNN with random weights and biases. Then, the difference between the predicted and targeted band selection is evaluated via binary cross-entropy loss function defined as:

$$\delta = -[\![z^{n*} == 1]\!] log\left(Y^n_{L+1}\right) - [\![z^{n*} == 0]\!] log\left(1 - Y^n_{L+1}\right) \tag{9}$$

Using scaled-conjugate gradient back-propagation [16], the weights and the biases in the DNN are continuously and iteratively updated to minimize the average loss function over the training samples. The training of the DNN continues until the maximal number of iterations is reached or the prediction accuracy improvement becomes negligible.

Note that collecting the training samples and training the proposed DNN is executed offline, e.g., by simulations. Then, in the real mobile network, the previously trained DNN is used to instantly determine the most suitable band (RF or VLC) for every D2D pair simultaneously. In order to select RF or VLC for all D2D pairs, the elements of the DNN's input vector $\mathbf{X_1}$ are resorted for each pair in line with the way the DNN is trained. For instance, let us say that the DNN is trained to predict the band selection for the first D2D pair (the pair for which the received powers and the sum interferences in RF and VLC are put at the beginning of $\mathbf{X_1}$). Then, to predict the band selection for the second D2D pair, we put the received powers and the sum interference powers (in RF and VLC) measured at the $\text{DUE}_\text{r}$ of the second pair at the beginning of $\mathbf{X_1}$. Hence, the same DNN is copied $N$ times and the inputs are inserted to each of the $N$ DNNs in a different order to extract the band selection of all $N$ D2D pairs simultaneously and in parallel within a single step (i.e., not sequentially).

### B. Proposed heuristic algorithm for DNN's output adjustment

The received sum interferences in the DNN's inputs do not always explicitly express the mutual relations among the D2D pairs. Thus, potential uncertainties in the DNN's decision can appear and a gap can exist between the reachable statistical prediction accuracy when only the received powers and sum interferences are known and the accuracy if all channel gains would be perfectly known. This gap in the prediction accuracy can impact negatively on the communication quality due to the fact that our problem is a binary decision problem and any misclassification (incorrect decision at the DNN's output) can lead to an increase in the interference. Thus, we propose a very low-complexity heuristic approach that deals with the impact of the DNN uncertainties and minimizes the gap in the prediction accuracy of the DNN. The proposed heuristic algorithm builds on the probabilities of RF and VLC resulting from the DNN and corrects the potential misclassifications in order to improve the performance of the band selection and to reach a communication quality that is closer to the optimum. The DNN's output $Y^n_{L+1}$ represents the probability of the $n$-th pair using RF. Thus, the closer the output is to 0.5, the higher the uncertainty about the band selection is.

**Algorithm 1** The proposed band selection scheme

1: **for all** $n \in \{1, ..., N\}$ (processed in parallel) **do**
2: derive $Y^n_{L+1}$ via DNN
3: determine $z^n_{DNN}$ based on (8)
4: set $z^n_{I-DNN} = z^n_{DNN}$ (Initial band selection)
5: **if** $Y^n_{L+1} \in [0.5-\alpha, 0.5+\alpha]$ **then** $S_{uc} = S_{uc} \cup \{n\}$
6: determine initial $\phi$ and $EE$
7: sort all pairs in $S_{uc}$ in ascending order acc. to $|Y^n_{L+1} - 0.5|$
8: **for** $n \in S_{uc}$ (sequentially acc. to the sorting in line 7) **do**
9: $z^n_{I-DNN} = 1 - z^n_{I-DNN}$ (switch band of $n$-th pair)
10: determine new $\phi$ and $EE$
11: **if** new $\phi <$ old $\phi$ **then**
12: keep $z^n_{I-DNN}$ (keep new band)
13: **else**
14: **if** new $EE >$ old $EE$ & new $\phi =$ old $\phi$ **then**
15: keep $z^n_{I-DNN}$ (keep new band)
16: **else**
17: $z^n_{I-DNN} = 1 - z^n_{I-DNN}$ (retrieve initial band)

This uncertainty motivates us to improve the decisions for less confident situation(s). Thus, we introduce a parameter $\alpha \in \langle 0, 0.5\rangle$ considering that the DNN is uncertain about the band selection if $Y^n_{L+1} \in [0.5-\alpha, 0.5+\alpha]$. Hence, the improved DNN's decision $z^n_{I-DNN}$ is expressed as:

$$z^n_{I-DNN} \begin{cases} z^n_{DNN} & \text{if } Y^n_{L+1} < 0.5-\alpha \text{ or } Y^n_{L+1} > 0.5+\alpha \\ z^n_x & \text{if } 0.5-\alpha \le Y^n_{L+1} \le 0.5+\alpha \end{cases} \tag{10}$$

where $z^n_x$ indicates the uncertainty in the band decision if the DNN's output for the $n$-th D2D pair is within an *uncertainty domain* $[0.5-\alpha, 0.5+\alpha]$ and the DNN's decision is revised. Based on this, we introduce a set $S_{uc}$ that includes all D2D pairs from the uncertainty domain ($S_{uc}$ includes $|S_{uc}| = N_{uc}$ pairs). The proposed heuristic algorithm (see Algorithm 1) starts after the DNN performs its decision (based on (8)) for all D2D pairs (lines 1, 2, and 3 in Algorithm 1). Then, the D2D pairs from $S_{uc}$ are sorted according to $|Y^n_{L+1} - 0.5|$ in an ascending order (line 7). Following this ascending order, the D2D pair for which the DNN's decision is closest to 0.5 switches its communication band to VLC if this pair is assigned to use the RF band according to the DNN's decision and vice versa (line 9). If the outage ratio is decreased by the switching or if a higher average energy efficiency is reached without increasing the outage, the D2D pair remains in the new band (lines 12 and 15). Otherwise, the D2D pair switches back to its initial assigned band in line with the DNN's decision (line 17). This process is done sequentially for all other sorted D2D pairs in the uncertainty domain. After checking all pairs in the uncertainty domain, the algorithm is terminated. Considering $N_{uc}$ D2D pairs in the uncertainty domain, the proposed algorithm checks the band switching $N_{uc}$ times, where $N_{uc} \le N$ depends on $\alpha$.

## IV. Performance Analysis

For simulations, we assume a 30×30 m indoor area with two to nine D2D pairs deployed uniformly. As in [8], we assume that every two users are willing to communicate with each other. Hence, within every pair, the angles of the transmitter and the receiver with respect to each other are generated with a zero-mean Gaussian distribution with a standard deviation of 30°. In RF and VLC, we set the transmission power to 100 mW and the channel bandwidth to 20 MHz. The VLC bandwidth is set as in [17],[18] taking into account that LED-based VLC commonly utilize commercial LEDs which have a modest bandwidth [19]. The channel models and noise are based on [20] for RF and [10] for VLC.

For the training, the DNN's architecture is set by trial and error approach and the used structure is composed of four hidden layers with 18, 15, 12, and 6 neurons, respectively. To this end, many DNN's architectures have been tested and we have chosen the most suitable one in terms of the achievable prediction accuracy as well as the training complexity. The total number of collected samples for training is $2\times10^6$. Some samples are omitted and not included in the training in order to keep an equal number of samples that correspond to each of the possible outputs (RF or VLC) to avoid the class imbalance problem [21]. The results are averaged out over 20,000 drops, each with new users' positions and angles.

Fig. 3a shows the prediction accuracy achieved by the proposed DNN both without (denoted as DNN) and with the proposed heuristic algorithm (denoted as I-DNN) for different values of $\alpha$. The two cases of $\alpha = 0.5$ and $\alpha = 0$ represent the two extremes when either all or none of the D2D pairs are checked by the proposed heuristic algorithm. Thus, the latter case is equivalent to the DNN without the heuristic algorithm. Fig. 3a demonstrates that the prediction accuracy increases with $\alpha$ and the heuristic algorithm is able to add an additional 10% accuracy on top of the accuracy reached by the proposed DNN when $\alpha$=0.5. Fig. 3b illustrates that the higher accuracy achieved by increasing $\alpha$ is at the cost of a higher complexity (i.e., more D2D pairs need to be checked as more of them are in the uncertainty domain). Still, even if $\alpha$=0.5, the average number of band switching is significantly reduced (by up to 78%) comparing to the iterative algorithm in [8]. To analyze the outage and the energy efficiency, we compare the proposed solution with: 1) the optimal RF/VLC combination derived by the exhaustive search (denoted as Optimum), 2) a random band selection (Random), 3) RF only, where all pairs use RF, 4) VLC only, where all pairs use VLC, and 5) the iterative algorithm from [8], which reaches a close-to-optimal performance but requires the knowledge of all channel gains

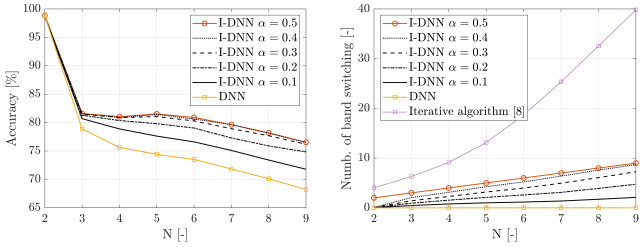


(a) Prediction accuracy (b) Numb. of band switching

Fig. 3: Statistical results for DNN efficiency evaluation vs $N$

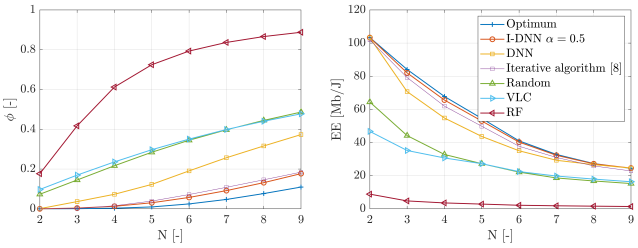


(a) Outage ratio (b) Energy efficiency

Fig. 4: Evaluation of communication quality vs $N$

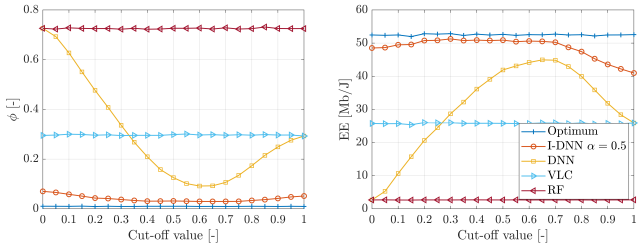


(a) Outage ratio (b) Energy efficiency

Fig. 5: Evaluation of communication quality vs cut-off value

between all DUEs and results in a higher complexity (see Fig. 3b).

As shown in Fig. 4a, the outage ratio increases with the number of D2D pairs for all algorithms due to the increasing interference. Disregarding whether the proposed heuristic algorithm is employed or not, the proposal outperforms all competitive algorithms. Fig. 4a further demonstrates that the I-DNN improves the DNN and reaches a close-to-optimal performance. The outage of the I-DNN is higher compared to the Optimum by only up to 6%, and lower than RF only, VLC only, and Random by up to 71%, 41%, and 40%, respectively.

The average energy efficiency (Fig. 4b) decreases with the increasing number of D2D pairs due to the increasing interference in both bands. Fig. 4b shows that the I-DNN increases the energy efficiency by up to 18, 2.2, and 2 times compared to RF only, VLC only, and Random, respectively. The I-DNN also outperforms the DNN by up to 22% and reaches almost optimal performance for all numbers of pairs.

We study also the effect of the DNN's cut-off value, i.e., the threshold value that represents the edge between the selection of RF or VLC based on the DNN's output $Y^n_{L+1}$. Note that the cut-off value is set to 0.5 in (8) and in the previous figures. Fig. 5 presents the outage ratio (Fig. 5a) and the average energy efficiency (Fig. 5b) versus the cut-off value. Fig. 5 shows that increasing the cut-off value improves the performance of DNN as the VLC usage ratio is higher than RF usage ratio. Thus, a higher cut-off value increases the accuracy of VLC selection more significantly than the inaccuracy of RF selection. Hence, the total prediction accuracy increases. Fig. 5 also demonstrates that with a cut-off value of 0.7, the DNN reaches the highest performance, but the I-DNN still reduces the outage by 70% (from 0.1 to 0.03) and achieves 12% gain in the energy efficiency comparing to the DNN. However, the I-DNN achieves the same outage and energy efficiency for all cut-off values between 0.4 and 0.7.

## V. Conclusions

This letter has presented a DNN-based framework to select RF or VLC for D2D pairs to maximize the energy efficiency while minimizing the outage. A DNN is designed to give an initial band selection decision. Then, a low-complexity heuristic algorithm that copes with the possible uncertainties in the DNN's band selection decisions is proposed. The proposed solution is of a very low complexity and reaches a close-to-optimal performance and overcomes the existing works in terms of outage and energy efficiency.

The future research direction should aim at a distributed solution, where the bands are selected by the users based only on their local information without sharing any information centrally.

## References


[1] T. Cogalan, H. Haas, "Why would 5G need optical wireless communications?," *IEEE PIMRC WS*, 2017.

[2] M. N. Tehrani, et al., "Device-to-Device Communication in 5G Cellular Networks: Challenges, Solutions, and Future Directions," *IEEE Commun. Mag.*, 52(5), pp. 86–92, 2014.

[3] P. Mach, et al., "Resource Allocation for D2D communication with Multiple D2D pairs reusing Multiple Channels," *IEEE Wireless Commun. Lett.*, 2019.

[4] Z. Lin, et al., "Hybrid architecture performance analysis for device-to-device communication in 5G cellular network," *Mobile Networks and Applications*, vol. 20, no. 6, pp. 713–724, 2015.

[5] A. Jovicic, et al., "Visible light communication: opportunities, challenges and the path to market," *IEEE Commun. Mag.*, 51(12), pp. 26–32, 2013

[6] Y. Liu, et al., "Game Theory-based Mode Cooperative Selection Mechanism for Device-to-Device Visible Light Communication," *Optical Engineering*, 55(3), pp. 30501–30501, 2016.

[7] S. V. Tiwari, et al., "Optical Repeater Assisted Visible Light Device-to-Device Communications," *WASET*, 10(2), pp. 206–209, 2016.

[8] M. Najla, et al., "Efficient Exploitation of Radio Frequency and Visible Light Communication Bands for D2D in Mobile Networks," *IEEE Access*, 2019.

[9] M. Lauridsen, et al., "An empirical lte smartphone power modele with a view to energy efficiency evolution," *Intel Technol. J.*, 18(1), 2014.

[10] X. Deng, et al., "Modelling and Analysis of Transmitter Performance in Visible Light Communications," *IEEE Transactions on Vehicular Technology*, 68(3), pp. 2316–2331, 2019.

[11] 3GPP TS 36.211, "Evolved Universal Terrestrial Radio Access (E-UTRA); Physical channels and modulation," v13.5.0, Release 13, 2017.

[12] 3GPP TS 36.214, "Evolved Universal Terrestrial Radio Access (E-UTRA); Physical layer; Measurements," v12.2.0, Release 12, 2015.

[13] P. de Kerret, at al., "Team deep neural networks for interference channels," *IEEE ICC Workshops*, pp. 1-6, 2018.

[14] H. Ye, et al.,"Power of deep learning for channel estimation and signal detection in OFDM systems," *IEEE Wireless Commmunication Letters*, 7(1), pp. 114–117, 2018.

[15] M. S. Ibrahim, et al.,"Learning-based antenna selection for multicastings," *IEEE 19th International Workshop on Signal Processing Advances in Wireless Communications (SPAWC)*, pp. 1–5, 2018.

[16] M. F. Moller et al., " A scaled conjugate gradient algorithm for fast supervised learning," *Neural Networks*, 6(4), pp. 525-533, 1993.

[17] S. Idris, at al., "Visible Light Communication: A potential 5G and beyond Communication Technology," *15th International Conference on Electronics, Computer and Computation (ICECCO)*, pp. 1-6, 2019.

[18] S. Feng, at al., "Hybrid positioning aided amorphous-cell assisted user-centric visible light downlink techniques," *IEEE ACCESS*, 2016.

[19] R. X. Ferreira, at al., "High bandwidth GaN-based micro-LEDs for multi-Gb/s visible light communications," *IEEE Photonics Technology Letters*, 28(19), pp. 2023-2026, 2016.

[20] 3GPP TR 36.843, "Study on LTE device to device proximity services; Radio aspects," v12.0.1, Release 12, 2014.

[21] J. M. Johnson, at al., "Survey on deep learning with class imbalance," *Journal of Big Data*, 6(1), pp. 27, 2019.

## 4.4 Prediction of channel for radio resource management in D2D

This section deals with the CSI knowledge problem and proposes prediction schemes based on machine learning in order to reduce the signaling overhead in the network. Note that the ideas presented in this section (and covered in the corresponding attached papers) are also included in the filled US patent [1P].

### 4.4.1 D2D Channels Prediction

All of the previous algorithms and solutions require the knowledge of D2D channels (CSI knowledge). This problem is a critical problem in D2D communication as the number of D2D channels that need to be estimated to achieve a full CSI knowledge is X(X-1) for X users. We solve this problem by using neural networks to predict the D2D channel gains from the cellular channel gains, which refer to the channels between the users and the surrounding BSs. This idea is motivated by the fact that there exist a hidden non-explicit relation between the D2D and cellular channel gains due to the dependency of both on the network's topology, buildings, and environment in a specific area. Therefore, this subsection introduces the use of machine learning (more specifically, deep neural networks) to extract this hidden relation between the cellular and the D2D channel gains. This approach is valid for real mobile networks implementation as the cellular gains between the users and the surrounding BSs are measured/estimated periodically in the network for handover and communication-related purposes. This subsection includes the journal paper [2J].

# Predicting Device-to-Device Channels from Cellular Channel Measurements: A Learning Approach

Mehyar Najla, *Student Member, IEEE,* Zdenek Becvar, *Senior Member, IEEE,* Pavel Mach, *Member, IEEE,* and David Gesbert, *Fellow Member, IEEE,*

***Abstract*—Device-to-device (D2D) communication, which enables a direct connection between users while bypassing the cellular channels to base stations (BSs), is a promising way to offload the traffic from conventional cellular networks. In D2D communication, optimizing the resource allocation requires the knowledge of D2D channel gains. However, such knowledge is hard to obtain at reasonable signaling costs. In this paper, we show this problem can be circumvented by tapping into the information provided by the estimated cellular channels between the users and surrounding BSs as these channels are estimated anyway for a normal operation of the network. While the cellular and D2D channel gains exhibit independent fast fading behavior, we show that average gains of the cellular and D2D channels share a non-explicit relation, which is rooted into the network topology, terrain, and buildings setup. We propose a deep learning approach to predict the D2D channel gains from seemingly independent cellular channels. Our results show a high degree of convergence between the true and predicted D2D channel gains. Moreover, we demonstrate the robustness of the proposed scheme against environment changes and inaccuracies during the offline training. The predicted gains allow to reach a near-optimal capacity in many radio resource management algorithms.**

***Keywords*—Device-to-device, Channel prediction, Deep neural networks, Supervised machine learning**

## I. Introduction

In device-to-device (D2D) communication, data is transmitted over a direct link between a pair of nearby user equipment (UEs) instead of being relayed via a base station (BS) [1],[2]. Conventionally, the D2D pairs can exploit two communication modes: shared and dedicated [3]. In the shared mode, the D2D pairs reuse the same radio resources as cellular users (CUEs) that send data through the BS [4]. On the contrary, the D2D pairs in the dedicated mode are allocated with resources that are orthogonal to the resources of CUEs [5].

An efficient exploitation of the D2D network often entails challenging radio resource management (RRM) problems, such as, selection between shared and dedicated modes [5]-[9], interference management to/from CUEs [10]-[13], channels and power allocation [14]-[21], to name a few. Conventional algorithms addressing the above RRM problems in D2D networks assume a prior estimation of the D2D channel gains (i.e., channel gains among all UEs involved in D2D). In some cases, the full knowledge can be relaxed to a partial knowledge, where only a subset of the distributed D2D channel gains is required (e.g., in [19]). Nevertheless, even the partial knowledge of the D2D channel gains implies a substantial cost in terms of an additional signaling overhead on top of the one generated in classical cellular communications. In fact, the cellular channel gains (i.e., channel gains between the UEs and the BSs) are typically estimated by default as these are needed for handover as well as user attachment, authorization, and classical cellular communication purposes. More precisely, even the users that wish to engage in D2D communications must be recognized by the network and thereby their cellular channel gains must be estimated initially. Thus, these cellular channels are periodically reported to the BSs, and can be leveraged at no additional signaling overhead. An interesting question then arises as to whether the by-default cellular channel gains carry information that is relevant to D2D communication and could help "for free" to solve the D2D resource management problems.

The idea set forth in this paper is that, while the cellular channel gains should exhibit fading coefficients that are known to be independent of those measured on the direct channels among the UEs, there actually exists common information between these data at the statistical level. In order to build up the reader's intuition, consider the following toy example. Imagine a green-field (free space) propagation scenario, in which the location of all UEs is made available to the network (even for those devices not interested in communicating with the network), then both the cellular and the D2D channel gains would be easily predictable from the UEs' locations and the use of a deterministic free-space channel model with line of sight (LOS) among all entities. Therefor, in a LOS environment, both D2D and cellular channel gains directly relate to each other via the user location knowledge. In practice, however, the UEs' locations may not be known due to privacy issues or may not be simply available. More importantly, in non-line of sight (NLOS) scenarios (such as suburban or urban areas), the D2D channels and the cellular channels may be obstructed in completely independent manners making the channel prediction from the UEs' locations seemingly impossible. For instance, two devices might experience a strong LOS D2D channel while a building may block the cellular channel between one of these devices (or more) and a given BS, thus making the D2D and cellular channel gains seemingly quite a bit less related than in the pure LOS scenario.

In this paper, we show that, in contrast to initial belief, a hidden and non-explicit relation between the cellular and

M. Najla, Z. Becvar and P. Mach are with the Faculty of Electrical Engineering, Czech Technical University in Prague, Czech republic e-mails: {najlameh, zdenek.becvar, machp2}@fel.cvut.cz

D. Gesbert is with the Communication Systems Department, EURECOM, Sophia Antipolis, France e-mail: david.gesbert@eurecom.fr

the D2D channels still exists in the NLOS case, and can be made even stronger by leveraging cellular measurements from additional surrounding BSs. The hidden relation is a result of the dependency of the D2D and cellular channels gains not only on the network topology, but also on the relative locations of the users and the obstacles. Thus, this relation is complex and its derivation is, by its nature, a typical complex model extraction problem, where machine learning is a suitable and efficient solution. Therefore, we exploit a deep neural network (DNN) to extract the complex model for the prediction of the D2D channel gains from the cellular channel gains.

Another interesting by-product of our prediction scheme lies in seeing that the set of cellular gains often constitute an order-of-magnitude smaller dimensional object than the D2D channels that we are trying to predict (i.e., there are just X cellular gains for one cell with X users in it, in contrast to X(X-1) direct and interference D2D gains). Hence, the proposed approach not only offers to capitalize on easier-to-get information (cellular channel estimation) rather than on the harder-to-get D2D channel gains for the optimization of D2D communications, but it also promises substantial savings in signaling for the channel estimation.

In the literature, existing channel prediction works related to this paper typically focus on predicting the channel quality between a single UE and an antenna at the BS at a specific frequency based on either: i) knowing the channel between this UE and the BS antenna at another frequency [22]-[31], or ii) knowing the channel between this BS antenna and another UE that is close to the original UE [32], or iii) knowing the channel between this UE and another close-by antenna at the same BS [33]. However, the problem presented in this paper, which is predicting D2D channel gains based on the cellular channel gains, is of a different nature from the above-mentioned prediction problems solved in the literature because a strong commonality of space can't be relied upon. Note that this paper builds on and extends our previous work presented in [34], where we introduced the idea of the DNN-based prediction of the transmission powers for D2D communication. Instead, in this paper, we generalize the problem to predicting directly the D2D channel gains. This allows for a more powerful framework, which yields applications to various radio resource management (RRM) related optimization problems in D2D networks.

The main contributions of this paper are summarized as follows:

- We present a novel framework for the D2D channel gains prediction based on the cellular channel gains in order to solve various problems related to radio resource management in D2D communication without incurring the pilot overhead that is usually expected in D2D communication.
- We design a DNN to build up a regression model connecting the cellular channel gains (as DNN inputs) to the D2D channel gains (as DNN outputs). The DNN is trained offline via simulations of the targeted area. Thus, the training samples (cellular and D2D channel gains) are collected based on the simulations and, then, used to train the DNN. Our results show a high convergence between the true and the predicted D2D channel gains, even in typical urban NLOS scenarios.
- We demonstrate the efficiency of the proposed framework by applying the predicted D2D gains to existing channel allocation and power control algorithms presented [20] and [21], respectively.
- We analyze the signaling overhead in terms of the number of channel gains needed to implement the radio resource management algorithms from [20] and [21] with and without the proposed DNN-based D2D channel gains prediction scheme to show the benefits of the proposed concept.
- We demonstrate the robustness of the proposed scheme against the environment changes and possible inaccuracies in the simulations of the targeted area during the offline training.

The rest of the paper is organized as follows. In Section II, we present the system model and formulate the problem of D2D channel gains prediction. Then, Section III describes the proposed DNN-based scheme for the prediction of D2D channel gains. Performance evaluation and simulation results are illustrated in Section IV. Finally, Section V concludes the paper.

## II. System model and problem formulation

In this section, we present our system model, and then, we formulate the problem of the D2D channel gains prediction.

### A. System model

In our model, we consider $L$ base stations (BSs) deployed randomly in a square area together with $U$ UEs as shown in Fig. 1. The UEs are divided into $M$ CUEs and $2N$ D2D user equipments (DUEs) composing $N$ D2D pairs, hence, $U = 2N + M$. Each D2D pair consists of a transmitter, $\text{DUE}_\text{T}$, and a receiver, $\text{DUE}_\text{R}$.

The capacity of the $n$-th D2D pair at the $k$-th communication channel is defined as:

$$C_n^k = B_k log_2 \left( 1 + \frac{p_n^k \, g_{n,n}}{B_k \sigma_o + \sum_{\substack{q=1 \\ q \neq n}}^{q=N} p_q^k g_{q,n} + \sum_{m=1}^{m=M} p_m^k g_{m,n}} \right) \quad (1)$$

where, for the $k$-th channel, $B_k$ is the channel bandwidth, $p_n^k$ is the transmission power of the $\text{DUE}_\text{T}$ of the $n$-th D2D pair, $p_m^k$ is the transmission power of the $m$-th CUE, and $p_q^k$ is the transmission power of the $\text{DUE}_\text{T}$ of the $q$-th D2D pair causing interference to the $n$-th D2D pair (i.e., $q \in \{1, \ldots, N\}/\{n\}$). Further, $g_{n,n}$ represents the channel gain between the $\text{DUE}_\text{T}$ and the $\text{DUE}_\text{R}$ of the $n$-th D2D pair, $\sigma_o$ is the noise density, $g_{m,n}$ is the interference channel gain between the $m$-th CUE and the $\text{DUE}_\text{R}$ of the $n$-th D2D pair, and $g_{q,n}$ is the interference channel gain between the $\text{DUE}_\text{T}$ of the $q$-th D2D pair and the $\text{DUE}_\text{R}$ of the $n$-th D2D pair. Note that, without loss of generality, (1) assumes that the noise is an Additive White Gaussian Noise similarly as in [35]-[36] and the interference is treated as Gaussian noise. In this paper, the term "channel gain" refers to the magnitude of the channel gain (as in, e.g., [37]-[38]), as the magnitude is commonly exploited for, e.g.,

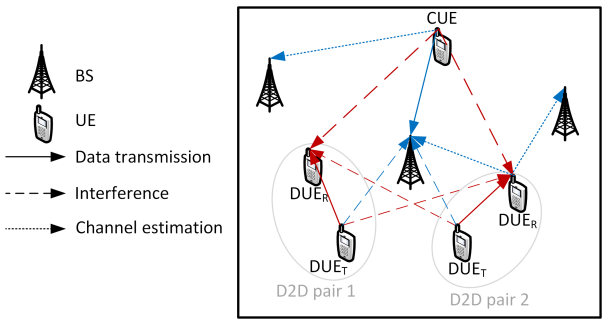


Fig. 1: System model: An example with four DUEs, one CUE and three BSs. Note that red and blue colors are used for D2D and cellular channels, respectively, and only part of the signaling (channel estimation) is shown for sake of clarity.

channel allocation, power control, or to determine the system capacity.

This paper assumes a complete absence of channel gains knowledge among the UEs. Thus, the channel between $\text{DUE}_\text{T}$ and $\text{DUE}_\text{R}$ of the same D2D pair, interference channels among DUEs of different D2D pairs, and interference channels among the CUEs and the DUEs (i.e., $g_{n,n}$, $g_{q,n}$, and $g_{m,n}$ in (1)) are unknown.

The DUEs and the CUEs need to estimate uplink/downlink channels to manage efficiently resource allocation and for handover purposes. Thus, although the D2D channel gains are not known by the network, still, the information on the channel quality between each UE (CUE or DUE) and its neighboring BSs are sent periodically to the serving BS in order to update the network information [39]. The corresponding estimated channel gain between any $i$-th (or $j$-th) UE and the $l$-th BS is denoted as $G_{i,l}$ (or $G_{j,l}$). These cellular channel gains ($G_{i,l}$ and $G_{j,l}$) are assumed to be represented by uplink channel gains estimated (measured) by the BS using the common way from the existing reference signals [40]. Nevertheless, it is worth to mention that even downlink channel gains can also be used to estimate quality of cellular channels as the downlink gains can be estimated (measured) by the UEs and fed back to the BS.

### B. Problem formulation

We aim to predict the real (true) channel gain $g_{i,j}$ between any $i$-th and $j$-th UEs, that can be, then, exploited for any existing RRM algorithms. Our goal is to minimize the prediction error and we formulate the problem as:

$$\min_{g^*_{i,j}} (g_{i,j} - g^*_{i,j})^2 \tag{2}$$

where $g^*_{i,j}$ is the predicted channel gain between the $i$-th and the $j$-th UEs. To predict the channel gain between any two UEs, we exploit only the available information about each UE, i.e., cellular channel gains. In the next section, we propose a novel DNN-based scheme for the prediction of $g_{i,j}$ relying on the knowledge of the cellular channel gains of the $i$-th and the $j$-th UEs.

## III. Prediction scheme

This section describes the proposed scheme for predicting the D2D channel gains. First, we illustrate the principle of the D2D channel gains prediction. Then, we describe the architecture of the proposed DNN and clarify the training process. Moreover, we discuss the signaling overhead reduction reached by the proposed prediction scheme and its implementation aspects.

### A. Principle of DNN-based prediction of D2D channel gains exploiting cellular channel gains

In general, it is clear that in a green-field (free space) propagation scenario, in which the location of all UEs is made available to the network, both the cellular and the D2D channel gains are easily predictable from the UEs' locations. In the free space area with LOS, the cellular channel from the UE to at least three BSs corresponds to a single specific location of the UE. Consequently, the D2D channel gain value between two UEs can be easily predicted in such (unrealistic) scenario. However, in practice, the UEs' locations may not be known due to privacy issues or may not be simply available. Moreover, in NLOS (urban or suburban) scenarios, the D2D channels and the cellular channels may be obstructed in completely independent manner and the D2D channel prediction from the UEs' locations seems to be impossible. For instance, two devices might experience a strong LOS D2D channel while a building(s) obstructs the cellular channel between one of these devices (or more) and the given BS (see Fig. 2). In such a case, the D2D channel gain between the two UEs might be hard to predict based on the cellular channel gains. However, in contrast to this initial belief, a strong relation between the cellular and the D2D channels is still expected by accounting for additional surrounding BS. The reason behind this is that increasing the number of known cellular channel gains from each UE leads to a higher confidence related to the UE's location and provides information about the position (and shape) of obstructing elements of the terrain. This information can then, in principle, be mapped into a cartography of D2D gains.

To put the above-mentioned intuition into more rigorous terms, given a specific area with certain topology, terrain and buildings' setup, there exists a mapping $\mathbf{F}$ connecting the cellular channel gains of the existing UEs (denoted as $\mathbf{G^C}$) and the D2D channel gains among these UEs (denoted as $\mathbf{g}$) so that:

$$\mathbf{g} = \mathbf{F}(\mathbf{G^C}) \tag{3}$$

It is obvious that solving the problem (2) can be achieved by approximating the function $\mathbf{F}$ from (3). Nevertheless, this approximation is hard to be done taking into account the changeable size of $\mathbf{G^C}$ and $\mathbf{g}$ when the number of UEs changes. In other words, a different function $\mathbf{F}$ needs to be approximated for every possible number of UEs making the solution unrealistic. Therefore, taking into account the problem defined in (2), we circumvent this problem by approximating the mapping $\mathbf{F}$ between $\mathbf{G^C_{i,j}}$ and $g_{i,j}$ where $\mathbf{G^C_{i,j}} = \{G_{i,1}, \dots G_{i,L}, G_{j,1}, \dots G_{j,L}\}$ includes the gains of the

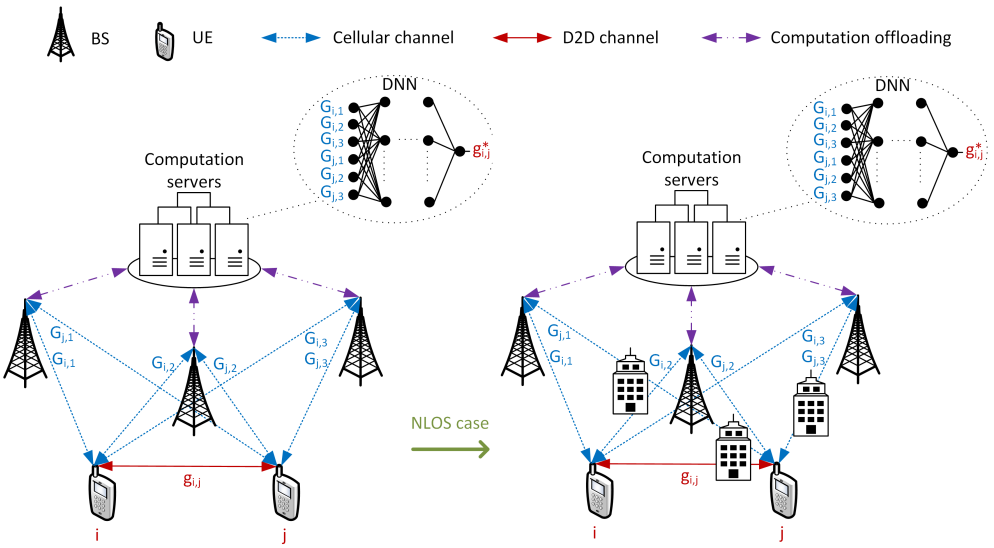


Fig. 2: Illustration of D2D channels prediction based on cellular channels for LOS (left part of figure) and NLOS (right part) scenarios.

cellular channels from $L$ BSs to any $i$-th and $j$-th UEs. In such a way, regardless of the number of the existing UEs, the D2D channel between any two UEs can be predicted by knowing the gains of the cellular channels from these two UEs and the surrounding BSs. hence, the problem (2) is written as:

$$\min_{F}(g_{i,j} - F(\mathbf{G^C_{i,j}}))^2 \tag{4}$$

The optimization problem (4) aims, by approximating $F$, to minimize the difference between the true (real) and the predicted gains of the D2D channel between any $i$-th UE and $j$-th UE; based on the knowledge of the cellular channel gains of these two UEs.

Deep neural networks are typical up-to-date tools for functions approximation and regression models creation. Thus, in this paper, we exploit the DNN to predict $g_{i,j}$ based on $\mathbf{G^C_{i,j}}$.

Note that, for any UE (DUE or CUE), the cellular channel gains between this particular UE and the surrounding BSs are periodically reported to the BSs for purposes related to the conventional communication and/or handover. In addition, in the future mobile networks, the network computations are supposed to be offloaded to powerful computation servers reducing network's energy consumption. Thus, even the proposed DNN can be deployed on these computation servers. The servers collect the estimated cellular channel gains (purple dash-dotted lines in Fig.2) and perform the prediction of $g_{i,j}$. Note that the computation servers can be located at any unit or entity in the network, such as a base station or in the core network. For example, an edge computing server can be exploited. With respect to the conventional architectures of mobile networks (e.g., 4G), the edge computing brings the computing power to the edge of the network where the potential radio resource management algorithms can be run. However, the specific deployment is up to the service provider or the network operator and the prediction should be located as close as possible to the place, where the radio resource management is performed to avoid any additional delay in the radio resource management.

### B. The architecture of the proposed DNN

The problem of predicting the D2D channel gain between the $i$-th and the $j$-th UEs based on the cellular channel gains from both the $i$-th and $j$-th UEs to the $L$ BSs is a regression problem, which can be solved by the deep neural network designed to build the regression model. Fig. 3 shows the proposed fully-connected DNN for regression. The proposed DNN is composed of an input layer ($X_0$), $H$ hidden layers ($X_1, ..., X_H$) and an output layer ($X_{H+1}$). The input layer contains the cellular channel gains between the $i$-th UE and the $L$ BSs and between the $j$-th UE and the $L$ BSs (i.e., $\mathbf{G^C_{i,j}}$) aligned as an input vector in the input layer as illustrated in Fig. 3. Thus, the output of the input layer $\mathbf{out_0}$ is the cellular channel

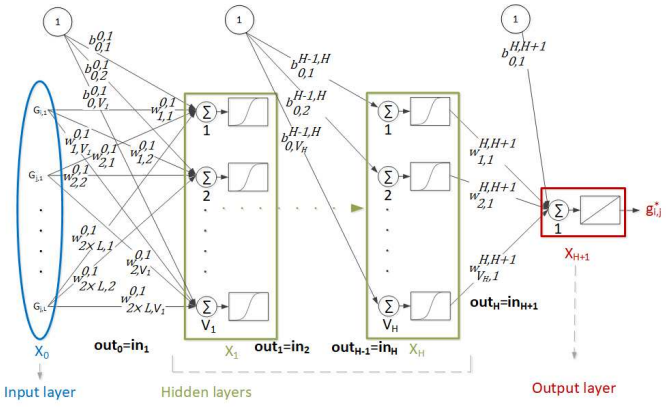


Fig. 3: The proposed DNN to build up a regression model connecting input variables (cellular channel gains from two UEs ($i$ and $j$) to $L$ BSs) and a single output variable (the D2D channel gain between the $i$-th and the $j$-th UE).

gains vector $\mathbf{G^C_{i,j}} = \{G_{i,1}, \dots G_{i,L}, G_{j,1}, \dots G_{j,L}\}$ of length $2\times L$. Then, the DNN contains $H$ hidden layers whereas every hidden layer $X_h$ is composed of $V_h$ neurons. Every hidden layer $X_h$ has an input vector $\mathbf{in_h}$ equivalent to the output of the previous layer $\mathbf{out_{h-1}}$ (i.e., $\mathbf{in_h} = \mathbf{out_{h-1}}, \forall h \in \{1, \dots, H\}$). Each input element z in $\mathbf{in_h}$ is fed to every neuron $v$ in the hidden layer $X_h$ with a weight $w^{h-1,h}_{z,v}$. Consequently, every neuron $v$ performs dot product between the input elements in $\mathbf{in_h}$ and the corresponding weights. The result of the dot product is added to a corresponding bias $b^{h-1,h}_{0,v}$ and processed by the commonly used sigmoid function giving the output of the neuron. Hence, the hidden layer $X_h$ with $V_h$ neurons and input vector $\mathbf{in_h}$ gives an output vector $\mathbf{out_h}$ of the length $V_h$ and this output vector $\mathbf{out_h}$ is, thus, written as:

$$\mathbf{out_h} = Sig(\mathbf{W^{h-1,h}in_h} + \mathbf{b^{h-1,h}}) = Sig(\mathbf{W^{h-1,h}out_{h-1}} + \mathbf{b^{h-1,h}}) \tag{5}$$

where $Sig$ is the sigmoid function $Sig(\mathbf{Z}) = \frac{1}{1+exp(-\mathbf{Z})}$ , $\mathbf{W^{h-1,h}}$ is the matrix of weights of the links between every input element of $X_h$ (i.e., equivalent to the output of $X_{h-1}$) and every neuron in $X_h$ and $\mathbf{b^{h-1,h}}$ is the vector of biases attached to the neurons.

The output of the last hidden layer $\mathbf{out_H}$ is followed by the output layer. The output layer in the DNN for regression of a single variable is composed of one neuron. The single neuron of the output layer performs the dot product between $\mathbf{out_H}$ and the corresponding weights $\mathbf{W^{H,H+1}}$ (i.e., the vector of weights dedicated to the links between the outputs of the last hidden layer $X_H$ and the single neuron in the output layer $X_{H+1}$). Then, the output layer neuron also sums its attached bias scalar $b^{H,H+1}$ and implements a linear activation function giving an output as:

$$g^*_{i,j} = Lin(\mathbf{W^{H,H+1}out_H} + b^{H,H+1}) \tag{6}$$

where $Lin$ is the linear activation function $Lin(Z) = Z$ and the output $g^*_{i,j}$ of the proposed DNN is the predicted D2D channel gain between the $i$-th and the $j$-th UEs.

### C. Offline learning and exploitation of the proposed DNN

We propose an offline supervised learning-based solution to predict the D2D channel gain between any two UEs from their cellular channel gains. Actually, the significant benefit of the offline training is that the measurements for the training phase are not needed. Instead, the offline training can be performed by simulations before the channel prediction is adopted for the real world. This offline training process starts with the simulation of the targeted area (e.g., a cell). Within the area, the positions of the UEs, e.g., $i$ and $j$, are uniformly generated. The cellular channels between the $i$-th UE and $L$ BSs as well as between the $j$-th UE and $L$ BSs ($\mathbf{G^C_{i,j}}$) are calculated together with the D2D channels between the $i$-th and $j$-th UEs $g_{i,j}$ based on the statistical models of the channel gains. The calculated cellular gains (presenting features) and the D2D gain (presenting the target) compose together a single learning sample. Then, the process is repeated by generating the new positions of the UEs and calculating the channels to constitute new samples. After the samples are collected, the training process is done offline following the typical way used to train any supervised learning-based neural network. In detail, the learning samples are split into a training set and a test set. The samples from the training set are used to train the proposed DNN while the samples in the test set are used to test the accuracy of the trained DNN on a set of samples that is not used for training to prevent overfitting [42]. During the training process, a loss function is defined to evaluate the regression model prediction accuracy. The loss function in the DNN that builds the regression model predicting a single variable is, typically, a measurement showing how far is the predicted value of the variable from the true value of this variable ($g^*_{i,j}$ and $g_{i,j}$ in our case). Therefore, taking the optimization problem (4) into account, we consider a mean square error loss function that can be written as:

$$\iota = \frac{1}{S}\sum_{s=1}^{s=S}(g^s_{i,j} - g^{s*}_{i,j})^2 \tag{7}$$

where $S$ is the number of the training samples, $g^s_{i,j}$ is the target (true D2D channel gain) of the $s$-th training sample, and $g^{s*}_{i,j}$ is the predicted D2D channel gain based on the cellular channel gains of the $s$-th training sample.

To minimize the mean square error loss function, the weights and biases of the proposed DNN are updated using Levenberg-Marquardt Backpropagation algorithm, which is an optimization method designed to solve non-linear least squares problems [43]. Thus, Levenberg-Marquardt algorithm can be applied with backpropagation for the neural networks training when the loss function is a sum of squares [44].

The learning steps are done offline based on the samples collected from the simulations of the area with randomly deployed UEs, but without any connection to these specific UEs. The training is focused on obtaining a "mapping" from the cellular channel gains of any two UEs to the channel gain between these two UEs. Thus, the DNN can learn the general relation between the cellular channels and the D2D channels in the targeted area and the built model is not dedicated to any specific UEs.

After the offline learning is done, the trained DNN is uploaded to the unit where the radio resource management takes place and this DNN is ready to be used in the real mobile network to predict the D2D channel gains between any pair of UEs in the real area. Thus, for multiple UEs, the trained (and tested) DNN is utilized to predict all needed channel gains among every pair of UEs independently and in parallel. To be more specific, based on the cellular channel gains of the UEs, we utilize the trained DNN to obtain all D2D channel gains, such as the channel gains between every two DUEs of the same D2D pair, interference channel gains between every couple of DUEs from different D2D pairs and interference channels between the CUEs and the DUEs. These can be, then, exploited to solve any RRM problem using the existing algorithms.

### D. Analysis of reduction in signaling overhead

In this subsection, we discuss the signaling overhead in terms of the number of channel gains that need to be estimated (measured) in the network.

In the existing network, the cellular channel gains between the UEs and the neighboring BSs are commonly estimated (i.e., for conventional communication and handover purposes). The number of the commonly estimated cellular gains is $L(2N + M)$. Note that even the DUEs might need to change from the D2D communication to the conventional communication in the case of a sudden D2D communication quality drop and, therefore, the cellular channels of DUEs are also periodically estimated and reported.

In the literature, for conventional RRM algorithms related to the D2D communication (e.g., power control algorithm from [21]), additional $2N(2N - 1)$ direct and interference D2D channels need to be estimated between the $2N$ DUEs. Moreover, for the D2D in shared mode, interference channels between the CUEs and the DUEs have to be estimated and reported as well. The number of those interference channels between the $M$ CUEs and the $2N$ DUES that should be estimated is $2NM$. Thus, the number of estimated channel gains in the common network with the D2D communication is:

$$\Sigma = L(2N + M) + 2N(2N - 1) + 2NM \tag{8}$$

In this paper, we predict the D2D channel gains from the common estimated cellular gains. In other words, in the network with D2D communication utilizing the proposed prediction scheme, the number of channel gains need to be estimated (measured) is limited to the estimation of $L(2N+M)$ channel gains, which are used to predict the remaining needed D2D channel gains. Thus, by subtracting $L(2N + M)$ from (8), we can calculate the reduction in the number of estimated channel gains. This reduction, in the shared mode, is equal to:

$$\Delta\Sigma = \Sigma - L(2N + M) = 2N(2N - 1) + 2NM \tag{9}$$

In the dedicated mode, the CUEs do not affect the D2D communication as the channels allocated to the CUEs are orthogonal to those allocated to the D2D pairs. In such case, the reduction in the number of estimated channel gains achieved by the proposed prediction scheme is determined by setting $M$ to zero in (8) and (9), respectively.

### *E. Implementation and design aspects*

In this subsection, we discuss key implementation and design aspects of the proposed DNN-based prediction of D2D channels.

The first aspect is the number of samples to be collected for the training. The proposed DNN is trained offline. Thus, collecting even a high number of samples (if needed) is feasible, as the samples can be collected by the simulation of targeted area before using the trained DNN in the real world as explained in Section III-C.

Another aspect related to the practical implementation of the prediction scheme is the computational complexity of DNN. In general, the computational complexity of the DNN depends on the number of multiplications done by every neuron in every layer between the inputs of this layer and the corresponding weights. In detail, considering that: 1) the DNN contains $H$ hidden layers with $X_H$ neurons in each layer, 2) the number of DNN inputs is $2L$ (cellular gains between two UEs and $L$ BSs), and 3) the number of DNN outputs is one (the D2D gain between two UEs), then, the number of the multiplications performed for the D2D channel prediction is:

$$\rho = 2LX_1 + \sum_{h=1}^{h=H-1} X_h X_{h+1} + X_H \tag{10}$$

This computational complexity affects the latency with which the channels are predicted in the network. Considering a reasonable number of hidden layers and neurons per each layer (i.e., our DNN includes five hidden layers with 20, 18, 15, 12 and 8 neurons); the number of the performed multiplications (i.e., $\rho = 1034$ multiplications in our DNN when $L = 3$ BSs), consumes a negligible computing time. Hence, we can claim that the latency introduced by the DNN is negligible and the overall delay is (at most) the same as the latency of any other existing centralized approach, within which the D2D channel gains need to be estimated via reference signals, and then reported to the same unit where the DNN is running. Note that with a high number of users, the high signaling in the conventional centralized approaches leads to the need of a high number of reference signals transmitted/received. The high number of the reference signals requires to reserve a lot of resources and can lead to an additional delay due to the channel measurement scheduling. In our case, however, such delay is avoided and the overall delay is reduced to simple multiplications executed by the DNN.

The last practical question is how the proposed prediction scheme copes with RRM algorithms in dynamic environments or scenarios (e.g., moving users, users becoming active/inactive, etc). In such scenarios, disregarding whether our prediction scheme is exploited or not, the RRM algorithm (e.g., channel allocation, power control, etc.) should be performed periodically. Thus, also the proposed prediction scheme is expected to be repeated periodically to update the predicted D2D channel gains. The predicted D2D channels at each time instant are just inserted as the inputs to the RRM algorithms and every DUE is told to change its communication parameters (e.g., the channels the DUE is occupying, the DUE's transmission power at every channel, etc).

## IV. Performance evaluation

In this section, we describe the simulation scenarios and parameters, and then, we discuss simulation results from three different perspectives as follows. First, we analyze the accuracy of the prediction scheme statistically showing how close the predicted D2D channel gains are to the true gains of the D2D channels. Second, we illustrate the performance of the proposed prediction scheme on selected examples of existing algorithms for D2D RRM in the mobile network, and we show how this prediction scheme affects the D2D communication quality and network's signaling overhead. The proposed prediction scheme aims to reduce the signaling overhead needed for D2D communication without significant losses in the communication quality. Last, we evaluate the robustness of the proposed scheme against the environment changes and the potential inaccuracies in the simulations during the training phase.

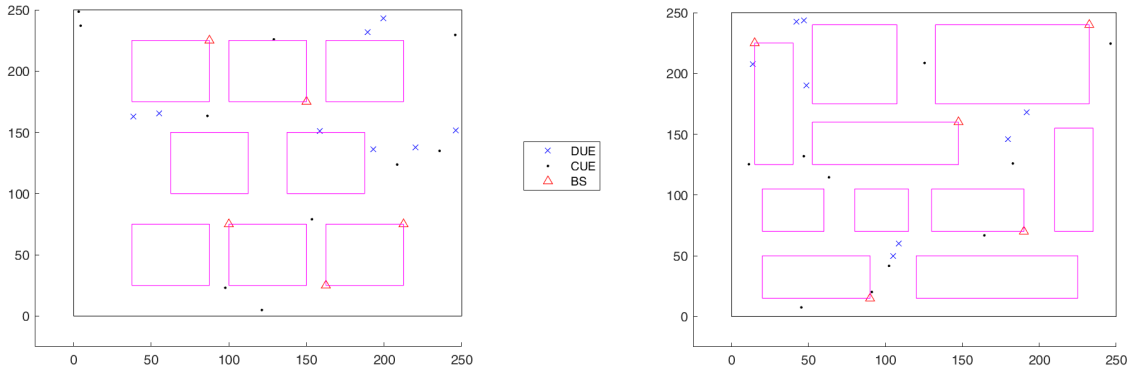


(a) Urban1 (b) Urban2

Fig. 4: Example of simulation deployment with $N = 4$, $M = 10$ and $L = 5$ and several buildings (fixed obstacles) represented by the pink rectangles. Note that the Rural area is of the same size as Urban1/Urban2 without any buildings or obstacles.

### A. Simulation scenarios and performance metrics

We consider up to 20 DUEs (composing up to 10 D2D pairs) and 10 CUEs deployed uniformly within an area of $250 \times 250$ m$^2$ covered by up to 5 BSs. Although the DUEs are uniformly distributed, the maximum distance between the DUE$_\text{T}$ and the DUE$_\text{R}$ of the same D2D pair is upper-bounded by a maximal distance of $d_{max} = 50$ m as in [45]-[46] to guarantee the availability of D2D communication. For any D2D transmitter, the maximal and the minimal transmission powers are set to $p_{max} = 24$ dBm and $p_{min} = 1$ dBm, respectively, like in [34].

We consider three different scenarios according to the signal propagation between the UEs and the BSs and among all UEs. The first scenario assumes an open rural area denoted as Rural with a full availability of line-of-sight (LOS) for all channels (D2D channels and cellular channels). The other two scenarios, illustrated in Fig. 4a and Fig. 4b, correspond to two different urban areas (such as scenario C2 in [47]) with fixed obstacles (FOs) representing e.g., buildings, and we denote these two urban areas as Urban1 and Urban2. In Urban1 and Urban2, the buildings lead to a certain probability of non-line-of-sight (NLOS) for both the D2D and cellular channels. Note that two different urban areas are simulated to validate our prediction approach for different buildings topologies without any changes in the DNN architecture.

In all areas, Rural, Urban1 and Urban2, the LOS path loss is generated in line with 3GPP recommendations [48]. In the urban areas, we assume that the communication channel intercepted by a single or more building walls is exposed to an additional loss of 10 dB per wall as in [34]. Note that Fig. 4 presents a 2D projection of the simulated urban areas, nevertheless, in our simulations, the building heights are distributed uniformly between 20 and 30 m to randomly affect NLOS and LOS probabilities. Simulation parameters are summarized in Table I.

For the learning process, we collect 1 000 000 samples. Note that obtaining such a number of samples is feasible, as the training process is done offline by the simulations. Still, we also study the impact of the number of learning samples on the prediction accuracy in the next subsection. The samples are then divided into samples used for DNN training (70% of samples are used as the training set) and 30% of samples are for the testing (i.e., the test set).

The proposed DNN exploits five hidden layers composed of 20, 18, 15, 12, and 8 neurons, respectively. The number of hidden layers and the number of neurons in each layer are set by trial and error approach. These specific numbers of hidden layers and neurons are tested for the case when the number of the DNN inputs is $2 - 10$ (i.e., the cellular channels between two UEs and $1 - 5$ BSs); and for three areas (Rural, Urban1, and Urban2). Thus, as the number of DNN's outputs is always fixed to one (a single D2D channel gain is being predicted), this number of hidden layers and neurons is expected to be suitable for learning the relation between the cellular gains and the D2D channel gains in different areas.

TABLE I: Simulation parameters.

| Parameter | | Value |
|---|---|---|
| Carrier frequency | $f_c$ | 2 GHz |
| Bandwidth | $B$ | 20 MHz |
| Number of D2D pairs | $N$ | $2 - 10$ |
| Number of CUEs (shared mode only) | $M$ | 10 |
| Number of channels (shared mode only) | $K$ | 10 |
| Bandwidth per any $k$-th channel (shared mode only) | $B_k$ | 2 MHz |
| Maximal distance between DUE$_\text{T}$ and DUE$_\text{R}$ of the same pair | $d_{max}$ | 50 m |
| Number of BSs | $L$ | $1 - 5$ |
| Maximal transmission power | $p_{max}$ | 24 dBm [34] |
| Minimal transmission power | $p_{min}$ | 1 dBm [34] |
| Noise power spectral density | $\sigma_o$ | $-174$ dBm/Hz |

In this paper, we evaluate the proposed prediction scheme from following perspectives:

*i*) Statistical evaluation of the prediction accuracy before implementing the prediction scheme in the mobile network. For the statistical evaluation, we consider the well-known Pearson correlation coefficient as a performance metric to show the accuracy of the predicted D2D channel gains with respect to the true channel gains. The Pearson correlation coefficient values range between zero and one where the value of one represents a complete matching between the predicted and the true values of the D2D channel gains.

*ii*) Performance of the D2D communication with the proposed prediction. The performance is represented by the sum capacity of the D2D pairs: $C = \sum_{n=1}^{n=N} \sum_{k=1}^{k=K} C_n^k$ and by the signaling overhead corresponding to the number of channel gains to be estimated/reported in the network.

*iii*) Robustness of the proposed scheme to identify the impact of potential inaccuracies between the simulations of the targeted area for training and the actual real-world area and the resistance to the changes in the real-world environment.

The three above-mentioned evaluation perspectives are presented in the next subsections.

### B. Statistical analysis of the prediction scheme

In this subsection, we analyze the results related to $g_{i,j}$ prediction statistically. In other words, as the training is done offline before its usage in the mobile network, we aim to study the prediction accuracy from the statistical point of view showing how close we expect the predicted gain of a D2D channel to be compared to the true gain of this channel. We show the statistical results of predicting a single D2D channel gain by testing the trained DNN on the test set.

Fig. 5 shows Pearson correlation coefficient between true and predicted D2D channel gains over different number of BSs. As expected, the Pearson correlation coefficient increases with the number of BSs in all areas. In detail, for the Rural area, a single BS is not enough to extract a well-performing relation between the cellular and the D2D gains (i.e., the Pearson correlation coefficient is around 0.64 for the Rural area when one BS is available). Then, when two or more BSs exist, the Pearson correlation coefficient in the Rural area reaches almost a perfect value (i.e., 0.999). For the urban areas, the Pearson correlation coefficient values are, in general, similar and the difference between Urban1 and Urban2 decreases for a higher number of the BSs. For only one BS, the correlation coefficients for both urban areas vary by about 0.09 due to the effect of the BSs location and the fixed obstacles' (i.e., buildings) locations. Then, already for two BSs, the difference is only below 0.03, and for three BSs, the Pearson correlation coefficients are almost the same for both areas (the difference is less than 0.01). We see, in Fig. 5, that for three or more BSs the correlation coefficient almost saturates for both urban areas reaching, approximately, their maximal values. Note that the Pearson correlation coefficient achieved by the urban areas (i.e., around 0.95) is lower compared to the Rural area (i.e., 0.999) because the cellular channel gains are less random in the Rural area where the buildings are absent and only LOS channels are present.

Fig. 6 shows the regression plot for Rural (Fig. 6a), Urban1 (Fig. 6b), and Urban2 (Fig. 6c) with $L = 3$ BSs and considering 1 000 testing samples from the test set. In general, we see that the values of the path loss in the urban areas are spread in a wider domain compared to the Rural area. This is because of the presence of the FOs and, thus, also NLOS links as explained in Section IV-A. Note that the path loss values in the Urban2 area are spread a little bit more (up to 220 dB) comparing to the Urban1 area (up to 200 dB) as the former one contains more FOs than the latter one. We can also see, in Fig. 6a, that the predicted path loss (i.e., $10log_{10}(1/g^*_{i,j})$) matches almost perfectly the true path loss (i.e., $10log_{10}(1/g_{i,j})$) for the Rural area. However, some deviation of the predicted path losses from the true values can be seen in Fig. 6b and Fig. 6c in both urban areas. This deviation is a result of the existence of the FOs producing some randomness and uncertainty in the values of the estimated channel gains. Nevertheless, the predicted and the true path losses are, still, highly correlated and Pearson correlation coefficient equals 0.94 and 0.934 for the Urban1 and Urban2 areas, respectively. Actually, the reached Pearson correlation coefficient in the Urban2 area is almost the same as that for Urban1 area(the difference is about 0.006).

Note that results presented in Fig. 5 and Fig. 6 are based on learning with 1 000 000 samples. Consequently, to illustrate the influence of the number of samples on the learning accuracy, Fig. 7 shows Pearson correlation coefficient over number of samples for the Rural and both of the urban areas. In all areas, the correlation coefficient increases with the number of samples rapidly at the beginning for lower numbers of the samples. Then, the correlation coefficient increment with the number of learning samples becomes negligible and the Pearson correlation coefficient saturates to (almost) a fixed maximal value. We further see that, in the Rural area, 10 000 samples are sufficient to reach almost a perfect matching between the predicted and the true D2D channel gains. For both urban areas, more samples should be collected due to

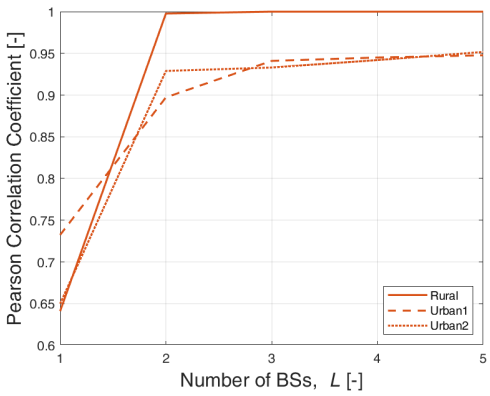


Fig. 5: Pearson correlation coefficient between the true and the predicted D2D channel gains versus number of BSs $L$.

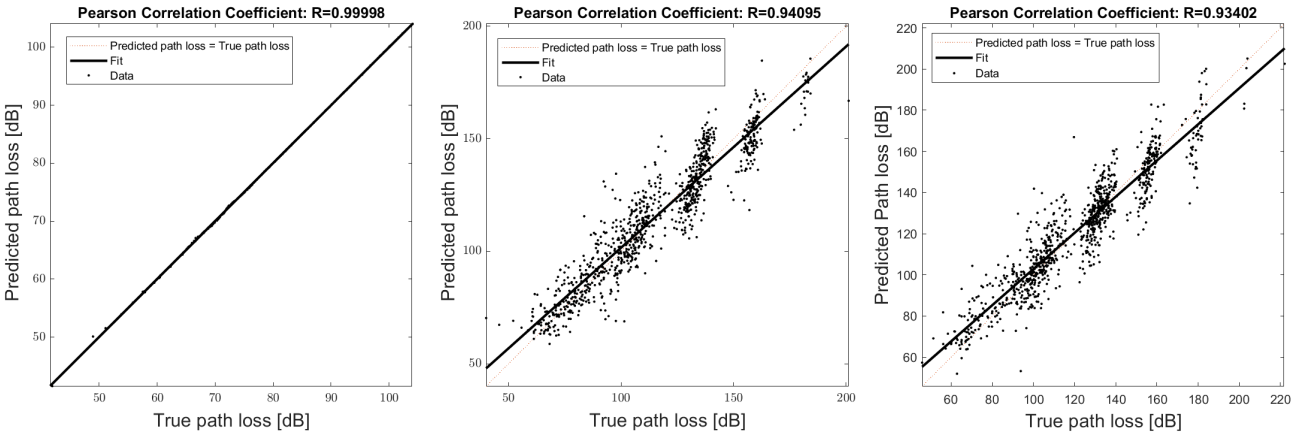


(a) Rural (b) Urban1 (c) Urban2

Fig. 6: Regression plot for $L = 3$ BSs.

the higher difficulty of constructing the regression model that connects the cellular channel gains to the D2D channel gains if the FOs are present and randomize the path loss. In detail, Fig. 7 illustrates that the values of the Pearson correlation coefficient in the Urban2 area are higher compared to the Urban1 area for low number of samples. This is explained by the fact that the outdoor space is smaller in the Urban2 and, thus, fewer learning samples (compared to the Urban1) can give a clearer idea about the general relation between the cellular and the D2D gains. Thus, the Pearson correlation coefficient is closer to the saturation value in the Urban2 area with respect to the Urban1 area for low number of samples. However, with the increasing number of samples, the DNN used for the Urban1 starts to learn the topology of the area and the Pearson correlation coefficient increases and saturates to a final value that is slightly higher than the one reached in the Urban2 area. The reason is that the higher number of FOs in the Urban2 makes it harder for the DNN to memorize the corresponding network topology and to extract the relation between the cellular and the D2D gains. Notice that, for both urban areas, even 10 000 samples are enough to reach correlation coefficients above 0.88.

In Fig. 8, we show the effect of the possible noise and inaccuracy in the estimation (measurement) of the conventional cellular channels by the BSs. To this end, we define $SNR_G$ as zero-mean Gaussian noise (i.e., the error) added to the modeled cellular channel gain estimation. Hence, $SNR_G$ represents the cellular channel gain estimation accuracy and it is expressed as the ratio between the true cellular channel gain (UE to BS) and the noise representing an error in estimation of the UE to BS channel. Thus, we add the noise of $\mathcal{N}(0, e)$ (where $SNR_G = 10log_{10}(\frac{G_{i,l}}{e})$ dB) to the estimated cellular channel gain $G_{i,l}$. Fig. 8 shows that, with the increasing accuracy of the estimated cellular channels, the correlation coefficient between the true and predicted D2D channel gains increases gradually until the saturation is reached when $SNR_G$ is equal to 25 $dB$, 20 $dB$, and 17.5 $dB$ for the Rural, Urban1, and Urban2 areas, respectively. This is, however, an interesting

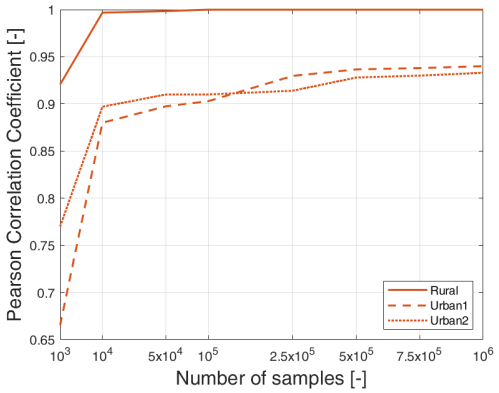


Fig. 7: Pearson correlation coefficient between the true and the predicted D2D channel gains versus number of learning samples for $L = 3$ BSs.

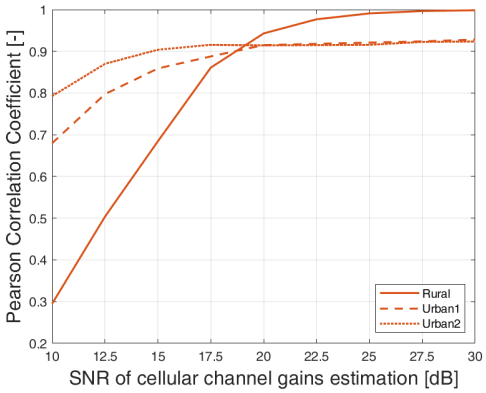


Fig. 8: Pearson correlation coefficient between the true and the predicted D2D channel gains versus the cellular channel estimation accuracy represented via estimation SNR ($L = 3$BSs).

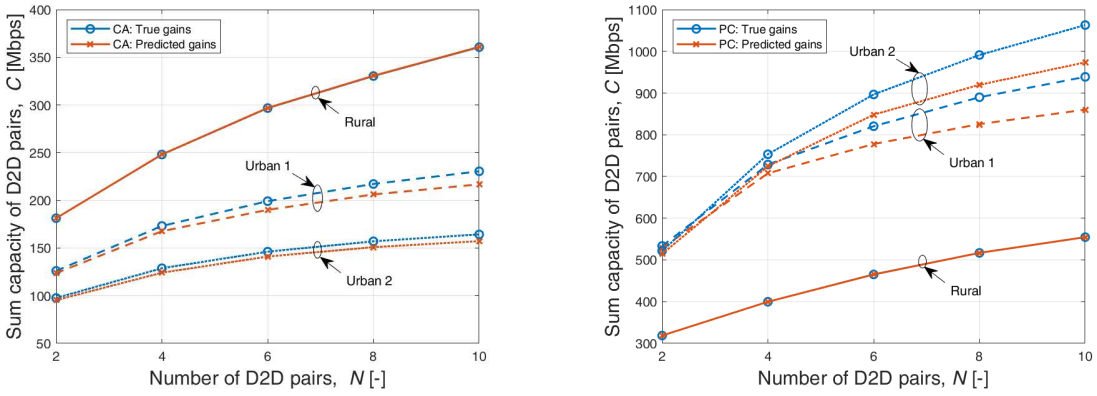


(a) Channel allocation

(b) Power control

Fig. 9: Sum capacity of D2D pairs versus number of D2D pairs when channel allocation scheme from [20] for D2D shared mode (a), and binary power control algorithm from [21] for D2D dedicated mode (b), are implemented on the true and the predicted D2D channel gains ($L$ = 3 BS and $M$ = 10 CUEs)

behaviour where a higher probability of LOS leads to a higher sensitivity of the prediction scheme to the channel estimation noise. Consequently, the trained model for the D2D channel prediction in the Rural area is more sensitive to the channel estimation noise than the trained model for the Urban1 area. Similarly, the trained model for the D2D channel prediction in the Urban1 area is more sensitive to the channel estimation noise than the trained model for the Urban2 area. The reason is that, in the Urban2 area, more space is occupied by the FOs (i.e., buildings) compared to the Urban1 area, while the Rural area contains no FOs (i.e., the LOS probability in the Rural area is higher than in the Urban1 area, and the LOS probability of the Urban1 area is higher than in the Urban2 area).

### *C. Performance of D2D communication aided by the prediction scheme*

In this subsection, we show the impact of exploiting the proposed D2D channel prediction scheme based on machine learning for the D2D communication in the mobile network. For this purpose, we adopt two up-to-date RRM algorithms, one for the channel allocation in the D2D shared mode [20] and one greedy algorithm for a binary power control in the D2D dedicated mode [21]. For both algorithms, we compare the performance (i.e., sum capacity of D2D pairs and the number of channels need to be estimated) in the case when these algorithms are supported by our proposed D2D channel prediction scheme with the case when these algorithms are implemented without the machine learning-based prediction approach according to the respective original papers [20] and [21]. The purpose of this comparison is to show that the performance of the existing RRM schemes reached with the proposed prediction scheme is not impaired while a substantial reduction in signaling overhead is achieved. Note that, in the legend of this subsection's figures, CA and PC are used to denote channel allocation scheme from [20] in the shared mode and binary power control from [21] in the dedicated mode.

Fig. 9a shows the sum capacity of D2D pairs over the number of D2D pairs communicating in the shared mode and with the channel allocation scheme from [20] implemented on the true and the predicted D2D channel gains. Fig. 9a illustrates that, by comparing the sum capacity reached when the true D2D gains are known and when the predicted D2D channel gains are used, the capacity loss induced by the prediction scheme reaches 0%, 4%, and 6% for the Rural, Urban1, and Urban2, respectively. This behavior is expected as the Rural area contains no FOs and our prediction scheme reaches a higher Pearson correlation coefficient in this Rural area comparing to the Urban1 and Urban2 areas. Moreover, the Urban1 area contains less FOs and our prediction scheme reaches a slightly higher Pearson correlation coefficient in the Urban1 than in the Urban2, thus a lower gap in the sum capacity between the true and the predicted gains is achieved in the Urban1 area.

Note that, In Fig. 9a, the changes of the sum capacity of D2D pairs over different numbers of D2D pairs, in all areas, follows the behavior described in [20].

The performance of the greedy algorithm for binary power control in D2D dedicated mode from [21] is shown in Fig. 9b, where the D2D pairs are considered to reuse the whole bandwidth. Then, the greedy algorithm is implemented to make a binary transmission power decision for each D2D pair with true and predicted D2D channel gains. In the Rural area, a perfect matching between the binary power control implemented on true and on predicted gains is achieved due to the very high accuracy in the prediction of the D2D channel gains. In the urban areas, only a small loss in the sum capacity, ranging from 1% (for two pairs) to 9% (for ten pairs) in both the Urban1 and the Urban2 areas, is introduced by implementing the binary power control on the predicted D2D channel gains comparing to the binary power control based on the true gains. However, such a loss can be expected by the fact that making a binary decision about the transmission power of each D2D pair is critical and highly sensitive to the accuracy of the predicted D2D channel gains. Nevertheless, ten

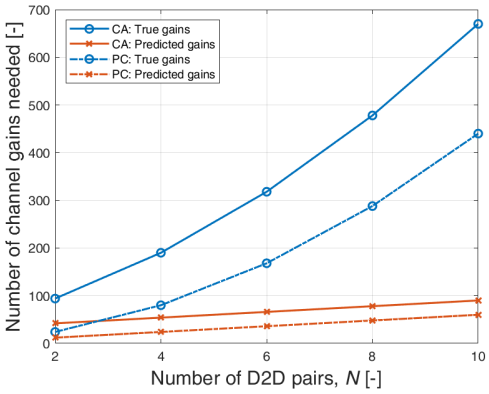


Fig. 10: Signaling overhead in terms of number of channels need to be estimated by the network versus number of D2D pairs; when channel allocation scheme from [20] or binary power control from [21] is implemented on true and predicted D2D channel gains ($L$ = 3 BS and $M$ = 10 CUEs).

D2D pairs in proximity reusing a single channel is an extreme case that is not expected to occur often in the real network. In contrast, a reasonable case is when, approximately, four or six D2D pairs reuse a single channel. For instance, with four D2D pairs, the binary power control implemented on the predicted D2D channel gains loses only 2.9% and 3.9% in the Urban1 and Urban2 areas, respectively, comparing to the binary power control with full knowledge of the true D2D channel gains. Such small difference between the Urban1 and the Urban2 areas is understandable as the Urban1 area contains less FOs, and our prediction scheme reaches a slightly higher Pearson correlation coefficient in the Urban1 area than in the Urban2 area.

Note that, In Fig. 9b, the changes of the sum capacity of D2D pairs over different numbers of D2D pairs, in all areas, follow the behavior described in [21].

In Fig. 10, we show the signaling overhead in terms of the number of channels estimated by the network if the channel allocation scheme from [20] and the greedy algorithm for binary power control from [21] are implemented on true and predicted D2D channel gains. As shown in Fig. 10, for both the channel allocation scheme from [20] and the power control algorithm from [21], the number of estimated channel gains with the proposed prediction scheme is significantly lower than when all the channel gains would need to be estimated. More specifically, we need to estimate/report up to approximately seven times less channel gains if the proposed DNN-based prediction is used for the channel allocation scheme from [20] or the power control algorithm from [21] comparing to the case when the knowledge of all gains would be required.

### *D. Robustness of the proposed scheme*

In this subsection, we analyze the robustness of the proposed scheme when the offline simulation-based trained DNN is used to predict the D2D channel gains in the real-world environment that differs from the simulated area used for training or if the real-world environment changes.

First, we study the impact of moving obstacles', MOs, presence in the real-world urban area(s) on the proposed prediction scheme as the presence and the movement of these MOs is not captured during the offline training by means of simulations. In this respect, up to 30 MOs representing, e.g., vehicles or position-changing obstacles, are uniformly distributed outdoor in both urban areas (see Fig. 11). The dimensions of each MO and its attenuation are also uniformly generated such that the length of the MO is between 2 and 6 m, the width varies from 0.5 to 2 m, the height is from 1.5 to 3 m, and the attenuation varies between 1 and 5 dB. Note that all above-mentioned values are regenerated randomly in every simulation drop.

In Fig. 12, we analyze the effect of the MOs on the channel allocation algorithm from [20] and the binary power control algorithm from [21] while four D2D pairs are considered. As expected, the difference between the sum capacity when the D2D true channel gains are known and the case when the prediction scheme is exploited, increases with the number of MOs in the area. This is due to the signal attenuation differences induced by the MOs' presence in the environment with respect to the training one simulated without those MOs. Particularly, for the channel allocation and with 30 MOs in the area, the additional capacity losses are 2.4% (5.7% – 3.3%) and 0.6% (3.8% – 3.2%) for the Urban1 and Urban2 areas, respectively (see Fig. 12a). In the case of power control (Fig. 12b), the additional capacity losses for 30 MOs in the area are 2% (5% – 3%) and 0.4% (4.4% – 4%) for the Urban1 and Urban2 areas, respectively. Such low losses are acceptable considering the fact that no specific D2D channel measurements are required and, still, the D2D communication can be enabled due to our proposed channel prediction.

Fig. 12 also shows that the prediction scheme is more sensitive to the MOs' existence in the Urban1 area compared to the Urban2 area. In fact, this is in line with Fig. 8, which shows that the higher ratio of LOS communication in the area (i.e., the lower number of obstacles) leads to a higher sensitivity to the noise in the channel gains estimation. Note that the attenuation added by the MOs can be considered as noise because its unpredictable. Hence, the MOs presence affects the Urban1 area more than the Urban2 area, as the Urban1 contains a larger area where LOS communication is possible due to the smaller space occupied by the buildings.

Second, we test the case when the trained DNN is utilized in the urban areas with changed volumes of the buildings (i.e., the fixed obstacles, FOs), see Fig. 13. In our evaluation, the volume of every FO can either increase (the probability of this is set to 0.5) or decrease (the probability of this is also set to 0.5). Then, the percentage of the changes in the volume of every FO is randomly generated so that the average change in the FOs' volume is fixed and corresponds to the targeted value of the change in order to present the results in the figures (i.e., the $x$ axis in Fig. 14 represents the average change in the volumes of the FOs). We consider that the average percentage of FO's change is up to 25% and, without loss of generality, the change in the volume of any FO is divided equally over its three dimensions (i.e., length, width, and height). For instance, if the FO's volume decreases by 25%, every dimension of

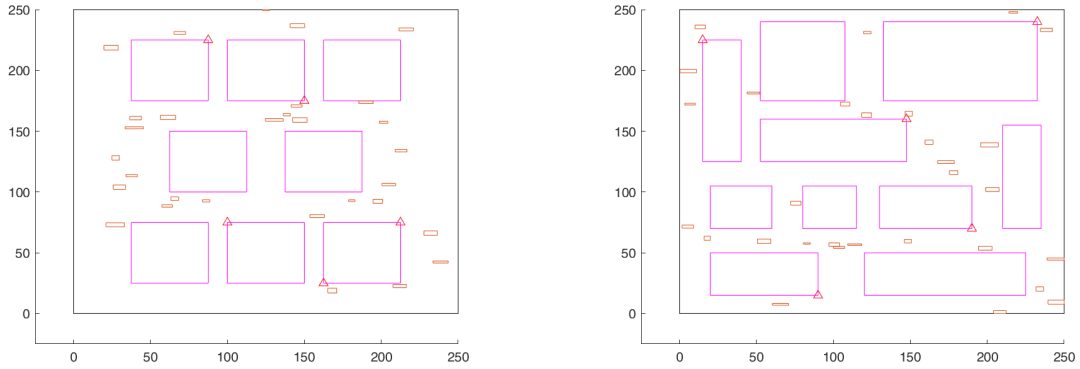

(a) Urban1 (b) Urban2

Fig. 11: Example of simulation deployment with 30 vehicles (moving obstacles) represented by the orange elements, in addition to the buildings (fixed obstacles) represented by the pink rectangles. Note that the red triangles represent the BSs.

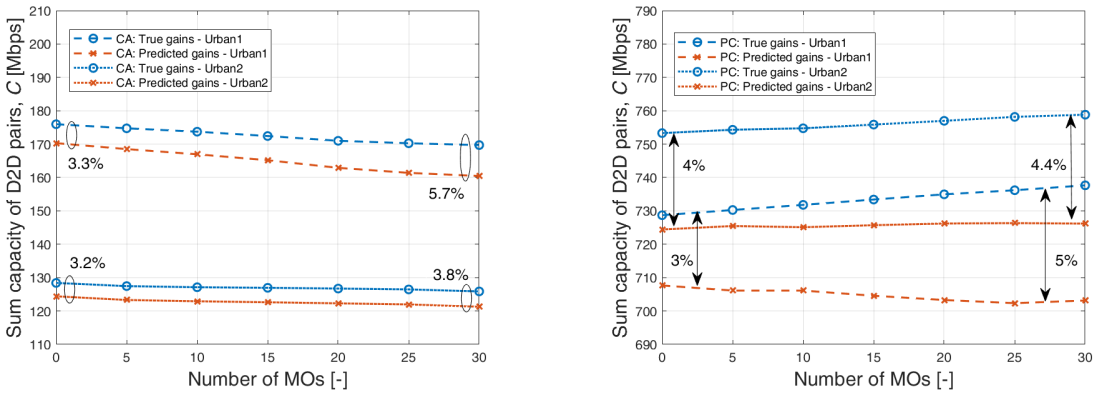


(a) Channel allocation (b) Power control

Fig. 12: Effect of the vehicles (moving obstacles) for four D2D pairs, $N = 4$.

this FO is decreased by approximately 9%. Fig. 13 shows an example of the real Urban1 and Urban2 areas after the changes in the volumes of FOs' with respect to the simulated volumes of the FOs that are used for training.

In Fig. 14, we show the effect of the changes in the volumes of the FOs on the channel allocation algorithm from [20] and the binary power control algorithm from [21] in both urban areas and with four D2D pairs. Similar to the MOs case, the sum capacity reached when the proposed prediction scheme is exploited modestly decreases comparing to the case when the D2D true channel gains are known. This decrease is slightly more notable for larger changes in the volumes of the FOs as expected. However, the capacity decrease induced by the FOs' volume changes is only up to 2.1% (5.5% − 3.4%) and 1.4% (5%−3.6%) in the case of channel allocation (Fig. 14a) for the Urban1 and Urban2 areas, respectively. Similarly, the power control (Fig. 14b) is affected only negligibly by up to only 1.8% (5%−3.2%) and 1.1% (4.9%−3.8%) for the Urban1 and Urban2 areas, respectively. Comparing the sensitivity of the Urban1 and Urban2 areas to the changes in the volume of FOs, we see that the Urban1 area is slightly more sensitive to the changes in the FOs' volumes. This is, however, expected due to the higher influence of the channel estimation noise on the Urban1 area, which is a result of the higher LOS probability compared to the Urban2 area as explained for the MOs.

These encouraging results, confirm the robustness of the proposed prediction scheme against the changes in the real-world environment and the potential inaccuracies in the training phase.

## V. Conclusion

In this paper, we have proposed a novel D2D channel gains prediction scheme based on the cellular channel gains between the UEs and multiple BSs. The proposed prediction scheme takes the advantage of the network topology-related correlation between the cellular and D2D channel gains. Supervised learning-based approach exploiting deep neural networks has been implemented to extract the mapping between the cellular channel gains of any couple of the UEs (i.e., gains of channels between these two UEs and multiple BSs) and the gain of the D2D channel between these two UEs. The proposed prediction scheme achieves a high Pearson correlation coefficient between the true and the predicted D2D channel gains.

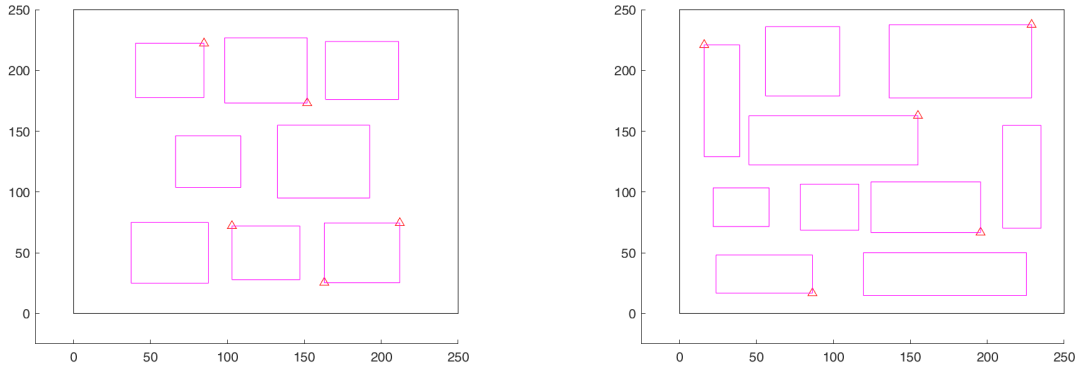

(a) Urban1 (b) Urban2

Fig. 13: Example of simulation deployment with a 25% average change in the volumes of the buildings (fixed obstacles) represented by the pink rectangles, compared to their volumes in Fig. 4. Note that the red triangles represent the BSs.

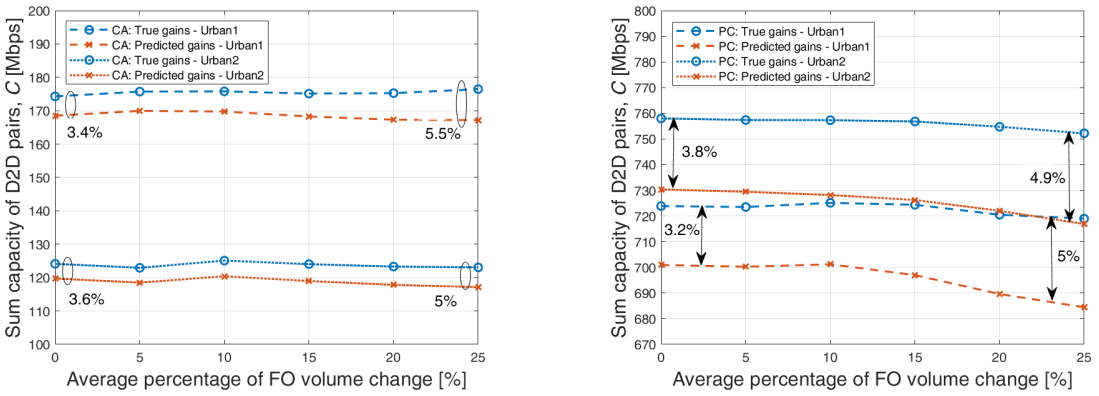


(a) Channel allocation (b) Power control

Fig. 14: Effect of the changes in the volumes of the buildings (fixed obstacles) for four D2D pairs, $N = 4$.

In addition, we show that the proposed prediction scheme significantly reduces the networks' signaling (represented by channel state information) overhead if applied to realistic radio resource management algorithms. This saving of the channel information is at the cost of only a negligible performance losses in terms of communication capacity comparing to the conventional implementation of these algorithms with knowledge of all channels. We have also demonstrated that the proposal is robust and resilient to the possible changes in the environment induced by various moving obstacles or potential changes in the fixed obstacles (e.g., the buildings) that exist in the area.

The future work should focus on improving the prediction scheme performance (prediction accuracy) for scenarios with buildings and obstacles existence. Moreover the future work should include studying the proposed prediction scheme performance for more RRM algorithms and in different possible scenarios and cellular cell types.

## Acknowledgment

This work was supported by project No. LTT18007 funded by Ministry of Education, Youth and Sports, Czech Republic. The work of David Gesbert was partially supported by HUAWEI-EURECOM Chair on Advanced Mobile Systems towards 6G.

## References

[1] M. N. Tehrani, et al., "Device-to-Device Communication in 5G Cellular Networks: Challenges, Solutions, and Future Directions," *IEEE Communications Magazine*, 52(5), pp. 86–92, 2014.

[2] P. Mach, et al., "In-band Device-to-Device Communication in OFDMA Cellular Networks: A Survey and Challenges," *IEEE Communications Surveys & Tutorials*, vol. 17, no. 4, pp. 1885–1922, 2015.

[3] P. Mach, Z. Becvar, and M. Najla, "Combined Shared and Dedicated Resource Allocation for D2D communication," accepted to *IEEE VTC-Spring*, 2018.

[4] F.H. Khan, Y.J. Choi, and S. Bahk, "Opportunistic Mode Selection and RB Assignment for D2D Underlay Operation in LTE Networks," *IEEE 79th Vehicular Technology Conference (VTC Spring)*, pp. 1–5, 2014.

[5] Y. Huang, et al., "Mode Selection, Resource Allocation, and Power Control for D2D-Enabled Two-Tier Cellular Network," *IEEE Transactions on Communications*, 64(8), pp. 3534–3547, 2016.

[6] J. Kim, S. Kim, J. Bang, and D. Hong, "Adaptive Mode Selection in D2D Communications Considering the Bursty Traffic Model," *IEEE Communications Letters*, 20(4), 712-715, 2016.

[7] D. Ma, N. Wang, and X. Mu, "Resource Allocation for Hybrid Mode Device-to-Device Communication Networks," *IEEE WCSP*, 2016.

[8] Y. Li, M.C. Gursoy, and S. Velipasalar, "Joint Mode Selection and Resource Allocation for D2D Communications under Queueing Constraints," *IEEE Infocom Workshop*, 2016.

[9] F. Jiang, et al., "Mode Selection and Resource Allocation for Device-to-Device Communications in 5G Cellular Networks," *China Communications*, 13(6), 32-47, 2016

[10] S. Shamaei, et al., "Interference Management in D2D-Enabled Heterogeneous Cellular Networks Using Matching Theory," *IEEE Transactions on Mobile Computing*, 18(9), pp. 2091–2102, 2018.

[11] S.M.A. Kazmi, et al., "Mode selection and Resource Allocation in Device-to-Device Communications: A Matching Game Approach," *IEEE Transactions on Mobile Computing*, 16(11), pp. 3126–3141, 2017.

[12] T. Huynh, at al., "Joint Downlink and Uplink Interference Management for Device-to-Device Communication Underlaying Cellular Networks," *IEEE Access*, 4, pp. 4420–4430, 2016.

[13] Y. Gu, et al., "Matching and Cheating in Device-to-Device Communications Underlying Cellular Networks," *IEEE Journal on Selected Sreas in Communications*, 33(10), pp. 2156–2166, 2015.

[14] R. Wang, et al. "Qos-Aware Joint Mode Selection and Channel Assignment for D2D Communications," *IEEE International Conference on Communications (ICC)*, pp. 1–6, 2016.

[15] R. AliHemmati, et al., "Power Allocation for Underlay Device-to-Device Communication over Multiple Channels," *IEEE Transactions on Signal and Information Processing over Networks*, 4(3), pp. 467–480, 2018.

[16] R. AliHemmati, et al., "Multi-Channel Resource Allocation Toward Ergodic Rate Maximization for Underlay Device-to-Device Communications," *IEEE Transactions on Wireless Communications*, 17(2), pp. 1011–1025, 2018.

[17] Y. Qian, T. Zhang, and D. He, "Resource Allocation for Multichannel Device-to-Device Communications Underlaying QoS-Protected Cellular Networks," *IET Communications*, 11(4), pp. 558–565, 2017.

[18] R. Yin, et al., "Joint Spectrum and Power Allocation for D2D Communications Underlaying Cellular Networks," *IEEE Transactions on Vehicular Technology*, 65(4), pp. 2182–2195, 2016.

[19] W. Lee, et al., "Deep power control: Transmit power control scheme based on convolutional neural network," *IEEE Communications Letters*, 22(6), pp. 1276–1279, 2018.

[20] P. Mach, Z. Becvar, and M. Najla, "Resource Allocation for D2D Communication with Multiple D2D Pairs Reusing Multiple Channels," *IEEE Wireless Communications Letters*, 8(4), pp. 1008-1011, 2019.

[21] A. Gjendemsjo, et al.,"Binary Power Control for Sum Rate Maximization Over Multiple Interfering Links," *IEEE Trans. on Wireless Commun.*, 7(8), pp. 3164-3173, 2008.

[22] K. Hugl, et al., "Downlink Beamforming Avoiding DOA Estimation for Cellular Mobile Communications," *IEEE International Conference on Acoustics, Speech, and Signal Processing*, 6, pp. VI–3313, 1998

[23] T. Aste, et al., "Downlink Beamforming for Frequency Division Duplex Systems," *IEEE Global Communications Conference (GLOBECOM)*, 4, pp. 2097–2101, 1999.

[24] Y.C. Liang, et al., "Downlink Channel Covariance Matrix (DCCM) Estimation and Its Applications in Wireless DS-CDMA Systems," *IEEE Journal on Selected Sreas in Communications*, 19(2), pp. 222–232, 2001.

[25] K. Hugl, et al., "Spatial Reciprocity of Uplink and Downlink Radio Channels in FDD Systems," *Proc. COST*, 273(2), p. 066, 2002.

[26] B.K. Chalise, et al., "Robust Uplink to Downlink Spatial Covariance Matrix Transformation for Downlink Beamforming," *IEEE International Conference on Communications*, 5, pp. 3010–3014, 2004.

[27] M. Jordan, et al., "Conversion of the Spatio-Temporal Correlation from Uplink to Downlink in FDD Systems," *IEEE Wireless Communications and Networking Conference*, pp. 1–6, 2009.

[28] M. Arnold, et al., "Enabling FDD Massive MIMO through Deep Learning-based Channel Prediction," *arXiv preprint arXiv:1901.03664.*, pp. 1–6, 2019.

[29] N. González-Prelcic, et al., "Millimeter-Wave Communication With Out-of-Band Information," *IEEE Communications Magazine*, 55(12), pp. 1038-1052, 2017.

[30] A. Ali, et al., "Millimeter Wave Beam-Selection Using Out-of-Band Spatial Information," *IEEE Transactions on Wireless Communications*, 17(2), pp. 140-146, 2017.

[31] A. Ali, et al., "Estimating Millimeter Wave Channels Using Out-of-Band Measurements," *Information Theory and Applications Workshop*, pp. 1-6, 2016.

[32] R. Deng, et al., "A Two-Step Learning and Interpolation Method for Location-based Channel Database Construction," *IEEE Global Communications Conference (GLOBECOM)*, pp. 1-6, 2018.

[33] P. Dong, et al., "Machine Learning Prediction Based CSI Acquisition for FDD Massive MIMO Downlink," *IEEE Global Communications Conference (GLOBECOM)*, pp. 1-6, 2018.

[34] M. Najla, et al., "Machine Learning for Power Control in D2D Communication based on Cellular Channel Gains," in *IEEE Global Communications Conference Workshop on Machine Learning for Wireless Communications*, pp. 1-6, 2019.

[35] X. Li, et al., "Resource allocation for underlay D2D communication with proportional fairness," *IEEE Transactions on Vehicular Technology*, 67(7), pp. 6244-6258, 2018.

[36] S. Lin, et al., "Sum-rate optimization for Device-to-Device communications over Rayleigh fading channel," *IEEE VTC Spring*, pp. 1-6, 2017.

[37] Z. Chu, et al., "Low-Latency Driven Energy Efficiency for D2D Communications," *IEEE ICC*, pp. 1-6, 2019.

[38] R. AliHemmati, et al., "Multi-Channel Resource Allocation Toward Ergodic Rate Maximization for Underlay Device-to-Device Communications," *IEEE Transactions on Wireless Communications*, 17(2), pp. 1011-1025, 2017.

[39] D. Astely, et al., "LTE: The Evolution of Mobile Broadband," *IEEE Communications Magazine*, 47(4), pp. 44–51, 2009.

[40] 3GPP TS 36.211, "Evolved Universal Terrestrial Radio Access (E-UTRA); Physical channels and modulation," v13.5.0, Release 13, 2017.

[41] P. Mach, et al., "Mobile Edge Computing: A Survey on Architecture and Computation Offloading," *IEEE Communications Surveys & Tutorials*, 19(3), pp. 1628–1656, 2017.

[42] D.M. Hawkins, "The Problem of Overfitting," *Journal of chemical information and computer sciences*, 44(1), pp. 1–12, 2004.

[43] D. Marquardt, "An Algorithm for Least-Squares Estimation of Nonlinear Parameters," *SIAM Journal on Applied Mathematics*, 11(2), pp. 431–441, 1963.

[44] M.T. Hagan, "Training Feed-Forward Networks With The Marquardt Algorithm," *IEEE Transactions on Neural Networks*, 5(6), pp. 989–993, 1994.

[45] L. Melki et al., "Interference Management Scheme for Network-Assisted Multi-Hop D2D Communications," *IEEE PIMRC*, pp. 1–5, 2016.

[46] T. D. Hoang et al., "Energy-Efficient Resource Allocation for D2D Communications in Cellular Networks," *IEEE Transactions on Vehicular Technology*, 65(9), pp. 6972–6986, 2016.

[47] YD. Bultitude et al., "T. IST-4-027756 WINNER II D1. 1.2 V1. 2 WINNER II Channel Models," Tech. Rep., Tech. Rep. 2007.

[48] 3GPP TR 36.843, "Study on LTE Device to Device Proximity Services; Radio Aspects," v12.0.1, Release 12, 2014.

### 4.4.2 Prediction of D2D Transmission Power Setting

As a continuation of the previous subsection, this subsection shows that the cellular channel gains can be used to predict the D2D resource allocation decisions immediately (without predicting the D2D channels as a middle step). In this subsection, we use the cellular channels to set the transmission power that should be used by every D2D pair. This subsection includes the conference paper [3C].

# Machine Learning for Power Control in D2D Communication based on Cellular Channel Gains

Mehyar Najla †, David Gesbert *, Zdenek Becvar †, and Pavel Mach †
† Dpt. of Telecommunication Engineering, FEE, Czech Technical University in Prague, Prague, Czech republic
* Communicarion Systems Department, EURECOM, Sophia Antipolis, France
emails: † {najlameh, zdenek.becvar, machp2}@fel.cvut.cz, * david.gesbert@eurecom.fr

***Abstract*—We consider a mobile network with users seeking to engage in a device-to-device (D2D) communication. Two D2D users (DUEs), a transmitter and a receiver, compose one D2D pair. We assume that the D2D pairs reuse a single communication channel to increase the spectral efficiency. Thus, a power control is needed to manage interference among the D2D pairs and to maximize capacity. We address the problem of D2D power control in the case when only standard cellular channel gains between the DUEs and base stations (BSs) are known while channel gains among DUEs are not available at all. We exploit supervised machine learning to determine transmission powers for individual D2D pairs. We show that the cellular channel gains can, in fact, be exploited to predict the transmission power setting for D2D pairs and, still, close-to-optimum sum capacity of the D2D pairs is reached. Moreover, even if our proposed power control requires no knowledge of the channel gains among DUEs and, thus, introduces no additional signalling, the sum capacity can be increased by $16\%$ to $41.9\%$ with respect to no power control, as demonstrated via simulations.**

***Index Terms*—Device-to-device; Power control; Deep neural networks; Supervised machine learning**

## I. Introduction

Device-to-Device (D2D) communication is one of the promising technologies to provide higher data rates and spectral efficiency in future mobile networks [1]. In D2D communication, data is transmitted directly between two user equipment (UEs) in proximity of each other to offload the legacy cellular links relayed via a base station (BS) [2]. Each pair of D2D UEs (denoted as DUEs) is composed of a transmitter ($\text{DUE}_\text{T}$) and a receiver ($\text{DUE}_\text{R}$).

Various important problems arise when considering the use of D2D communication, including the question of resource allocation across both D2D pairs and legacy cellular links to maximize D2D capacity or to minimize negative impact to the cellular links [3]-[4]. Pursuing the goal to increase the spectral efficiency of the system, multiple D2D pairs can reuse the same channel [3]-[4]. However, mutual interference among the D2D pairs accessing the same channel occurs inevitably. The mutual interference can be, fortunately, efficiently suppressed by a power control [3].

The power control as a resource allocation problem to maximize spectral efficiency of D2D (or ad-hoc) networks has been considered extensively [5]-[14]. In general, sum capacity-oriented power control over D2D pairs is a non-convex optimization problem. Thus, various iterative methods with different levels of complexity are presented in the literature such as, binary power control [5], weighted minimum mean square error [6], or water-filling algorithm [7], to name a few. However, iterative methods can pose latency issues. As an alternative, researchers have focused recently on exploiting deep neural networks (DNN) for instantaneous power control in D2D communication [8]. The DNN highly reduces power control complexity via either supervised [9]-[10] or unsupervised [11]-[14] learning, which is based on offline training (i.e., the DNN is firstly trained offline and then exploited for power control). Crucially, power control techniques utilizing the DNN with unsupervised learning are able to outperform the existing iterative methods in terms of sum capacity. However, the unsupervised learning needs a DNN loss function that connects the input and the output of the DNN, e.g., the sum capacity as a function of channel gains among DUEs and DUEs transmission powers.

A significant drawback of all above-mentioned, both conventional and DNN-based approaches is that they typically consider full (centralized) knowledge of all the D2D channel gains (i.e., channel gains among all DUEs). In machine learning methods, the D2D channel gains are placed as an input for the neural network in order to set the transmission powers. In some cases, the full knowledge can be relaxed to limit the channel state information (CSI) requirement to a subset of distributed D2D channel gain values. Still, even partial knowledge of the D2D channel gains implies a substantial cost in terms of additional channel estimation and signaling compared with the signaling involved in classical cellular communications. In contrast, the channel gains over the cellular links (i.e., linking DUEs to BSs) are typically de-facto estimated by a default design of the network. An interesting question then arises as to whether the cellular channel gains (i.e., channel gains between DUEs and BSs) carry information that somehow relates to the D2D channel gains themselves and could be exploited as a low-cost replacement of the D2D channel gains for the D2D power control prediction. The intuition behind this idea is that, while cellular channel gains exhibit fading coefficients that are independent of those measured among the DUEs, and also constitute a far smaller dimensional object (only $M$ cellular gains for one cell with $M$ users, in contrast with $M(M-1)$ direct and interference D2D gains), there is actually much common information between

978-1-7281-0960-2/19/$31.00 ©2019 IEEE

these data at the statistical level. In fact, it is clear that both statistical cellular gains and statistical D2D gains could be predicted from DUEs' location information if this information would be assumed available (which is not the case here). Hence, the existence of common information between the cellular and D2D gains suggests the use of a machine learning approach so as to implicitly extract the D2D channel gains and exploit it for the power control.

This is the core idea of this paper, where we propose a novel DNN learning-based power control scheme for the D2D communication that needs absolutely no additional knowledge of the D2D channel gains. Hence, no signaling overhead is generated at all, since the channel quality to all BSs in the user vicinity is reported during a common network operation notwithstanding [15]. First, our proposed DNN aims to find a relation between the cellular and D2D channel gains. This relation is, then, exploited for the transmission power setting of the D2D pairs to maximize the sum capacity. It is worth to mention that there is no known function that captures the relation between the cellular channel gains and the sum capacity of D2D pairs. Thus, it is difficult to propose a proper loss function for an unsupervised learning-based DNN. Due to this fact, we follow a supervised learning approach, where the targeted DUEs transmission powers maximizing the sum capacity are derived first. Subsequently, the DNN is trained to build a mapping between cellular channel gains and the targeted transmission powers with an aim to reach targeted power setting. The whole training process is done offline and the trained DNN is used for immediate power control decision in the real network without any training needed during the communication.

The rest of the paper is organized as follows. First, in Section II, system model is described and optimization problem is formulated. Then, Section III presents the principle of power control based on cellular channel gains, illustrates the architecture of the proposed DNN for power control, and gives detailed description regarding training process. In Section IV, simulated scenarios are described and results are discussed. Finally, Section V concludes the paper.

## II. System model and problem formulation

In this section, the system model is described and the optimization problem is formulated.

### A. System model

We consider a model with $L$ BSs and $M$ DUEs forming $N$ D2D pairs (i.e., $N = M/2$ assuming $M$ is even number) deployed within a square area. The distance between the transmitter $\text{DUE}_\text{T}$ and the receiver $\text{DUE}_\text{R}$ composing the D2D pair is limited by a maximum distance $d_{max}$ to guarantee feasibility of the D2D communication similarly as in [16],[17]. The D2D pairs are assumed to share the same channel. As the channel is occupied by multiple D2D pairs, the pairs interfere mutually with each other. Thus, the capacity of the $n$-th D2D pair is defined as:

$$C_n = B\ log_2\left(1 + \frac{p_n g_{n,n}}{\sigma_o B + \sum_{\substack{j=1 \\ j\neq n}}^{j=N} p_j g_{j,n}}\right) \quad (1)$$

where $B$ is the channel bandwidth, $p_n$ is the transmission power of the $n$-th $\text{DUE}_\text{T}$, $g_{n,n}$ is the channel gain between the $n$-th $\text{DUE}_\text{T}$ and the $n$-th $\text{DUE}_\text{R}$ of the $n$-th D2D pair, $\sigma_o$ is the noise power spectral density on the carrier frequency, $p_j$ is the transmission power of the $j$-th $\text{DUE}_\text{T}$, and $g_{j,n}$ is the channel gain between the $j$-th $\text{DUE}_\text{T}$ and the $n$-th $\text{DUE}_\text{R}$. Note that contrary to state-of-the-art works (e.g., [9]-[14]), a channel between any $\text{DUE}_\text{T}$ and $\text{DUE}_\text{R}$ ($g_{n,n}$ and $g_{j,n}$) is supposed to be unknown due to the difficulty of D2D channel gains estimation and its high cost in terms of signaling overhead.

Since the DUEs continuously monitor channels to the serving BS (for estimation, decoding, etc.) and to the neighboring BSs (for handover, interference management, etc.), the information on channel quality between each DUE and the surrounding BSs is assumed to be measured and reported periodically to the serving BS [15]. The corresponding estimated channel gain between the $m$-th DUE and the $l$-th BS is denoted as $G_{m,l}$.

### B. Problem formulation

The objective of this paper is to set the transmission power $p_n$ for each $n$-th D2D pair in such a way that the sum capacity of D2D pairs is maximized. In [5], it has been proven that a binary power control, in which every D2D pair transmits at either maximal or minimal transmission power level, reaches close-to-optimal performance. Therefore, we also adopt the binary power control so that $p_n \in \{p_{min}, p_{max}\}$, where $p_{min}$ and $p_{max}$ are the minimal and maximal transmission powers, respectively. Consequently, the problem of setting the transmission power of the D2D pairs to maximize the sum capacity of D2D pairs is written as:

$$\mathbf{P} = \text{argmax} \sum_{n=1}^{n=N} C_n \quad (2)$$

$$\text{s.t. } p_n \in \{p_{min}, p_{max}\}, \forall n \in \{1, 2, ...N\} \quad (a)$$

where $\mathbf{P} = \{p_1, \ldots, p_N\}$ is the vector containing the transmission powers of all D2D pairs maximizing the sum capacity of D2D pairs and constraint (a) guarantees that the transmission power of each D2D pair is set either to $p_{min}$ or $p_{max}$.

The optimization problem in (2) aims to maximize the sum capacity of D2D pairs. However, from (1), we see that $C_n$ depends on D2D channel gains. Unlike existing schemes, where the authors assume full or at least partial knowledge of the D2D channel gains, we focus on the case when these gains are not known at all. Thus, in the next section we propose a power control scheme based solely on the common knowledge of the cellular channel gains while no knowledge of the D2D channels among the DUEs is required whatsoever.

## III. Power control for D2D pairs based on cellular channel gains

The optimization problem in (2) relies on the fact that a mathematical relation exists between the D2D channel gains and the cellular channel gains. However, the relation between D2D channel gains and cellular channel gains is not known for mobile networks and cannot be even analytically derived from any known parameters of the mobile network. Thus, we propose to use a Deep Neural Networks (DNN) to learn this relation on its own and to set transmission power of the D2D pairs accordingly. More to the point, the DNN can be seen as a 'black box', which is able to set transmission power of the D2D pairs based simply on the knowledge of cellular channel gains from the DUEs to the BSs. The proposed DNN architecture and the learning process itself are thoroughly described in the following subsections.

### A. Architecture of DNN for power control

Considering the binary power control, the optimization problem in (2) is to set the transmission power of each D2D pair either to $p_n = p_{min}$ or to $p_n = p_{max}$. Thus, setting the transmission power for $N$ D2D pairs can be presented as $N$ identical binary classification problems. Hence, we propose a fully-connected DNN to build up the mapping between the cellular channel gains and the proper binary transmission power setting for any $n$-th D2D pair maximizing the sum capacity of D2D pairs.

Fig. 1 shows the proposed fully-connected DNN for binary classification. The proposed DNN is composed of an input layer ($X_0$), $H$ hidden layers ($X_1$,...,$X_H$), and an output layer ($X_{H+1}$). The DNN input layer contains an input vector, and thus, the cellular channel gains from the DUEs to the BSs are aligned as an input vector in the input layer of the proposed DNN (see Fig. 1). The output of the input layer $\mathbf{out_0}$ is a vector of the cellular channel gains between the DUEs and the BSs $\mathbf{out_0} = \{G_{1,1}, G_{1,2}, \ldots, G_{M,L}\}$ with a length of $M \times L$. Every hidden layer $X_h$ has an input vector $\mathbf{in_h}$ equivalent to the output of the previous layer $\mathbf{out_{h-1}}$ (i.e., $\mathbf{in_h} = \mathbf{out_{h-1}}$, $\forall h \in \{1, \ldots, H\}$). Each hidden layer $X_h$ is composed of $V_h$ neurons. In this respect, each $i$-th input element in $\mathbf{in_h}$ is fed to every neuron $v$ in the hidden layer $X_h$ with a weight $w_{i,v}^{h-1,h}$. Consequently, every neuron $v$ performs dot product between the input elements in $\mathbf{in_h}$ and the corresponding weights. The result of the dot product is added to a corresponding bias $b_{0,v}^{h-1,h}$ and processed by commonly used sigmoid activation function, giving the output of the neuron. Hence, the hidden layer $X_h$ (with $V_h$ neurons) and its input vector $\mathbf{in_h}$ serve to determine the hidden layer output vector $\mathbf{out_h}$ of the length $V_h$ as:

$$\begin{aligned} \mathbf{out_h} &= Sig(\mathbf{W^{h-1,h}in_h} + \mathbf{b^{h-1,h}}) \\ &= Sig(\mathbf{W^{h-1,h}out_{h-1}} + \mathbf{b^{h-1,h}}) \end{aligned} \tag{3}$$

where $Sig$ is the sigmoid function $Sig(Z) = \frac{1}{1+exp(-Z)}$, $\mathbf{W^{h-1,h}}$ is the matrix of weights of the links between every input element of $X_h$ (i.e., equivalent to the output of $X_{h-1}$) and every neuron in $X_h$, and $\mathbf{b^{h-1,h}}$ is the vector of biases attached to the neurons in the layer $X_h$.

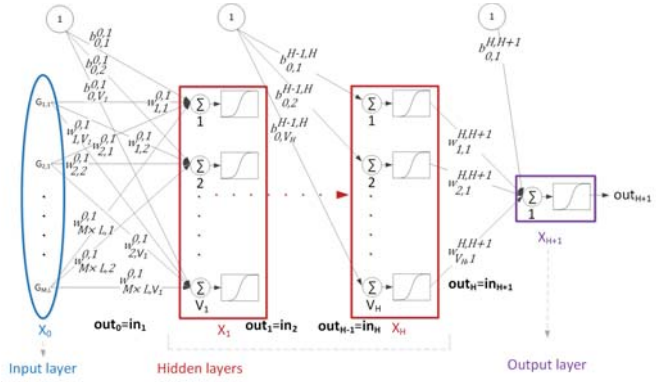


Fig. 1: Proposed architecture of DNN for binary classification corresponding to the transmission power of a single D2D pair.

The output of the last hidden layer $\mathbf{out_H}$ is followed by the output layer. The output layer in a DNN for binary classification is composed of one neuron. The single neuron of the output layer performs the dot product between $\mathbf{out_H}$ and the corresponding weights $\mathbf{W^{H,H+1}}$ (i.e., the vector of weights related to the links between the outputs of the last hidden layer $X_H$ and the single neuron in the output layer $X_{H+1}$). Then, the output layer neuron also sums its attached bias scalar $b^{H,H+1}$ and implements the sigmoid function defining the output of the DNN as:

$$out_{H+1} = Sig(\mathbf{W^{H,H+1}out_h} + b^{H,H+1}) \tag{4}$$

Note that the sigmoid function value is between 0 and 1, and thus, the output of our DNN is $out_{H+1} \in [0, 1]$ which presents the probability of $p_n = p_{max}$. Hence, the transmission power of the $n$-th D2D pair is set as:

$$p_n = \begin{cases} p_{max} & \text{if } out_{H+1} > 0.5 \\ p_{min} & \text{otherwise} \end{cases} \tag{5}$$

### B. Offline learning and exploitation of the proposed DNN

There is no direct analytical function connecting the cellular channel gains and the sum capacity of D2D pairs in order to set the transmission power of the D2D pairs. Therefore, we propose an offline supervised learning-based solution in which the optimal binary transmission powers are derived by an exhaustive search to maximize the sum capacity of D2D pairs. Then, the transmission power of the $n$-th D2D pair is fed to the proposed DNN as a targeted class attached to the set of the cellular channel gains as features. The features (i.e., cellular channel gains) and the targeted class (i.e., the transmission power of the $n$-th D2D pair) compose together a single learning sample. The learning samples are collected and, then, split into a training set and a test set. While the former is used to train the DNN the latter is run over the

trained DNN to show the accuracy on a set of cellular channel gains samples that are not used for training.

During training process of the proposed DNN, a loss function is defined to evaluate the misclassifications between the targeted transmission powers and the predicted transmission powers (from (5)) after every training iteration. Our DNN considers binary cross-entropy loss function written as:

$$\begin{aligned}\iota = &-[\![p_T == p_{max}]\!] log\left(out_{H+1}\right) \\ &- [\![p_T == p_{min}]\!] log\left(1 - out_{H+1}\right)\end{aligned} \tag{6}$$

where $p_T$ is the targeted transmission power for the corresponding sample.

The binary cross-entropy loss function is averaged out over all training samples at the end of each iteration. Then, the weights and biases of the proposed DNN are updated using scaled-conjugate gradient backpropagation [18].

It is worth to mention that the whole learning phase (i.e., including collecting samples, training, and testing the proposed DNN) is done offline, i.e., before its application to the real network (or before its testing by means of simulations). Therefore, the cellular channel gains derived from the simulations can be used for the offline training and testing of the DNN, and then, the trained DNN is exploited directly in the real network. The proposed DNN is able to predict the transmission power of a single D2D pair in order to maximize the sum capacity of D2D pairs. Thus, for $N$ D2D pairs, the trained and tested DNN is utilized to predict the transmission power for each D2D pair independently maximizing the sum capacity of D2D pairs.

## IV. Performance evaluation

In this section we describe simulation scenarios and parameters. Then, simulation results are discussed including offline learning results and performance analysis related to D2D communication with the proposed power control scheme.

### A. Simulation scenarios

We consider six DUEs composing three D2D pairs (like in [10]) deployed uniformly within an area of $250 \times 250$ m$^2$. Although the DUEs are uniformly distributed, the maximum distance between the DUE$_\text{T}$ and the DUE$_\text{R}$ of the same D2D pair is upper-bounded by a maximal distance of $d_{max} = 50$ m as in [16],[17]. Nevertheless, we also show the effect of different values of $d_{max}$ on the performance of our proposal. Without loss of generality, we set the bandwidth of the channel reused by the D2D pairs to 1 Hz [10] as the capacity scales with the bandwidth (see (1)). Moreover, for any D2D transmitter, the maximal transmission power $p_{max}$ is considered to be 24 dBm like in [3]; while the minimal transmission power $p_{min}$ is set to 1 dBm to guarantee existence of data transmission.

We consider two different scenarios according to the signal propagation between the DUEs and the BSs and among all DUEs. The first scenario assumes an open rural area with full availability of line-of-sight (LOS) for all channels (D2D channels and channels to BSs). The second scenario, shown in Fig. 2, presents an urban area (such as scenario C2 in [19]) with building blocks forming a regular Manhattan-like grid (see the pink rectangular building blocks in Fig. 2). The BSs are deployed on the roof tops serving outdoor DUEs at the street level. In the second scenario, the buildings lead to a non-line-of-sight (NLOS) D2D and cellular channels. In both rural and urban areas, the LOS path loss is generated in line with 3GPP recommendations [20]. However, in the urban scenario, we assume that the communication channel intercepted by a single or more building walls is exposed to an additional loss [21]. We set the value of the signal attenuation induced by a single wall to 10 $dB$. Note that Fig. 2 presents a 2D projection of the simulated urban area, while in our simulations, building heights range uniformly from 20 to 30 m and, thus, affect NLOS and LOS probabilities.

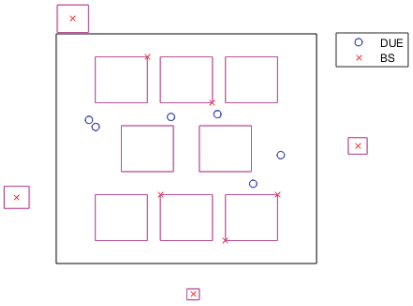


Fig. 2: Example of simulation deployment with buildings (pink rectangles) for urban area. Note that no buildings are present in rural area.

For the training of DNN, 500 000 samples are collected and 70% of these samples are used for training (i.e., the training set), while the remaining 30% are left for testing (i.e., the test set). The proposed DNN exploits six hidden layers composed of 24, 20, 18, 15, 12, and 8 neurons, respectively. Note that the number of hidden layers and number of neurons in each layer are set by trial and error approach.

For the evaluation of D2D communication with the proposed power control scheme, the sum capacity of D2D pairs (i.e., $C = \sum_{n=1}^{n=N} C_n$ ) is averaged out over 1 000 drops. Simulation parameters are summarized in Table I.

TABLE I: Simulation parameters.

| Parameter | | Value |
|---|---|---|
| Carrier frequency | $f_c$ | 2 $GHz$ |
| Bandwidth | $B$ | 1 $Hz$ [10] |
| Noise power spectral density | $\sigma_o$ | $-174$ $dBm/Hz$ |
| Number of D2D pairs | $N$ | 3 [10] |
| Number of BSs | $L$ | $3-9$ |
| Maximal transmission power | $p_{max}$ | 24 $dBm$[3] |
| Minimal transmission power | $p_{min}$ | 1 $dBm$ |

### B. Simulation results

In this subsection, we present first the offline learning results, i.e., the accuracy of the learning process. Then, we show the impact of the proposed power control scheme on the performance of D2D communication.

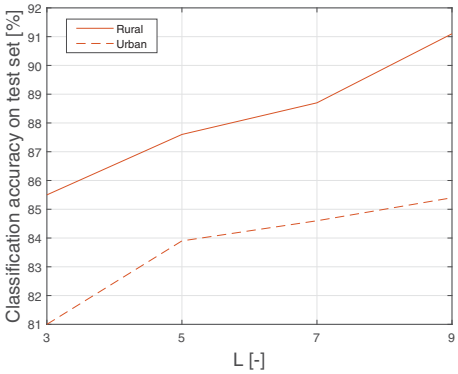


Fig. 3: Classification accuracy on the test set over number of BSs $L$ for $d_{max} = 50m$.

| Rural | | | Urban | | |
|---|---|---|---|---|---|
| $p_{min}$ | $p_{max}$ | $p_T$ \ $p_n$ | $p_{min}$ | $p_{max}$ | $p_T$ \ $p_n$ |
| 46.7% | 5.4% | $p_{min}$ | 44.4% | 8.8% | $p_{min}$ |
| 3.6% | 44.3% | $p_{max}$ | 5.8% | 41.0% | $p_{max}$ |
| Acc. on $p_{min}$ 92.9% | Acc. on $p_{max}$ 89.2% | **Total accuracy 91.1%** | Acc. on $p_{min}$ 88.4% | Acc. on $p_{max}$ 82.4% | **Total accuracy 85.4%** |

TABLE II: Confusion matrices for rural and urban areas for 9 BSs and $d_{max} = 50m$, showing learning accuracy.

*1) Learning results:* The proposed DNN is trained via samples of cellular channel gains from the training set and their corresponding targeted transmission powers. Then, the trained DNN is tested on the test set to show the classification accuracy on the set of samples with cellular channel gains that are not used for the training to prevent overfitting.

Fig. 3 shows the total accuracy of the transmission power prediction on the test set for the rural and urban areas over different numbers of BSs $L$. As expected, the prediction accuracy increases with the number of BSs. This accuracy improvement with more BSs is a result of knowing more information about each DUE (i.e., knowing cellular channel gains to more BSs). Furthermore, we can see that the prediction accuracy on the test set for the rural area is higher than for the urban area. This can be explained by the fact that the cellular channel gains to the BSs are less random in the rural area with LOS comparing to the urban area where the probability of NLOS is high. Therefore, in the rural area, our proposed DNN is able to build a better-performing mapping between the cellular channel gains of the DUEs and the proper transmission power.

Table. II shows the confusion matrices for rural and urban areas with $L = 9$ BSs. Considering that $p_T$ is the targeted transmission power and $p_n$ is the transmission power predicted by the proposed DNN, there are four possible outcomes of prediction result as the binary power control is applied. Each confusion matrix in Table. II shows the probability of each of the four possible cases. For rural area, the accuracy of the correct prediction on $p_{min}$ and $p_{max}$ is 92.9% and 89.2%, respectively. For urban area, the accuracy of correct prediction is 88.4% and 82.4% for $p_{min}$ and $p_{max}$, respectively. We can also see that the total accuracy on both $p_{min}$ and $p_{max}$ is 91.1% and 85.4% for the rural and urban areas, respectively.

It is worth to remember that the proposed DNN predicts the transmission power of a single D2D pair as explained in Section III-A, and based on this predicted transmission power, the shown accuracy is calculated. However, in the next subsection, the trained DNN is exploited to predict the transmission power of multiple D2D pairs (three D2D pairs in this paper), each independently, aiming to maximize the sum capacity of D2D pairs as clarified in Section III-B. Note that as the DNN is trained to predict $p_n$ of the $n$-th D2D pair, every D2D pair is considered to be the $n$-th D2D pair to predict its transmission power, and the cellular channel gains at the input of the DNN are sorted accordingly.

*2) Evaluation of the proposed power control scheme:* In this subsection, we analyze the performance of D2D communication when the proposed DNN predicts the transmission power of each D2D pair. Up to our best knowledge, there is no work in the literature exploiting the cellular channel gains of the DUEs for D2D power control. Thus, the proposed power control scheme (denoted as proposal) is compared with two other existing schemes. The first one is the optimal binary power control derived by the exhaustive search. The optimal binary power control (denoted as Target) corresponds to the targeted transmission powers, which are used as the proposed DNN benchmark and which the DNN tries to reach (see Section III-B). The second scheme assumes that each D2D pair transmits with the full power without power control (denoted as No-PC). The perfect estimation of the cellular channel gains is considered for the rural area. In the urban area, an error in the estimation of the cellular channel gains might occur in the real network. Thus, for any channel gain between the $m$-th DUE and the $l$-th BS $G_{m,l}$, we add an estimation error $e_{m,l}$ as a percentage of the real channel gain in the urban area. The error percentage for cellular channel gain estimation is generated via the Gaussian distribution with a mean of 0% and a standard deviation of 5%.

Fig. 4 shows the sum capacity of D2D pairs over the number of BSs $L$ for the rural and urban areas. Comparing to the No-PC, our proposed DNN-based solution achieves a gain ranging from 18.7% to 21.4% and from 16% to 18.7% for the rural and urban areas, respectively. Moreover, we observe that the sum capacity of D2D pairs of the proposal reaches close-to-optimal sum capacity (i.e., close to Target) even for a low number of BSs. The small loss of our proposal with respect to the Target further decreases with the availability of the cellular channel information to more BSs. To be more specific, increasing the number of BSs from 3 to 9 decreases the loss comparing to the Target from 3.5% to 1.6% and from 5.4% to 3.2% for rural and urban areas, respectively.

In Fig. 5, the effect of different values of $d_{max}$ on the sum capacity of D2D pairs is illustrated for $L = 9$ BSs. The sum capacity of D2D pairs for all schemes decreases with increasing $d_{max}$ due to the corresponding increment in the attenuation of signal between $\text{DUE}_\text{T}$ and $\text{DUE}_\text{R}$. Fig. 5 shows that when compared to No-PC, our proposal introduces

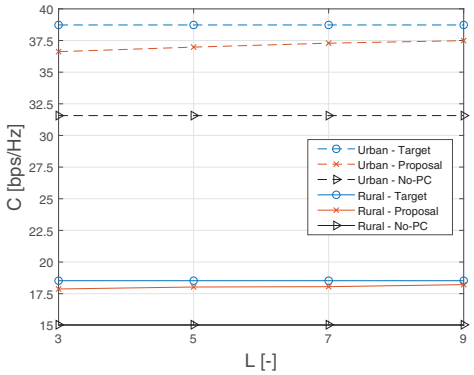


Fig. 4: Sum capacity over number of BSs $L$ for $d_{max} = 50m$.

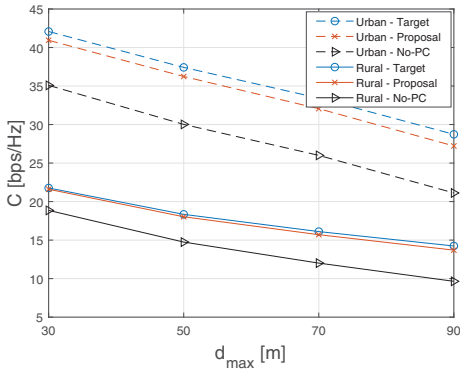


Fig. 5: Sum capacity over $d_{max}$ for $L = 9$.

a gain up to $41.9\%$ and $28.8\%$ for rural and urban areas, respectively. In addition, comparing to the Target, the loss in the performance of the proposal ranges from $2.7\%$ to $5.2\%$ for the urban area. Nevertheless, for the rural area, our proposal loses only between $0.7\%$ and $3.7\%$, depending on $d_{max}$, in terms of the sum capacity.

It is worth to remind that with respect to existing schemes that rely on the knowledge of the D2D channel gains, our proposed scheme requires no additional signaling to set the transmission power of the D2D pairs except the signaling that is anyway available for classical communication via BS.

## V. Conclusion

In this paper, we have proposed a new power control scheme for D2D communication requiring absolutely no knowledge of the D2D channel gains. The proposed scheme relies on a deep neural network that exploits solely the cellular channel gains between DUEs and neighboring BSs to set the transmission power of each D2D pair. The key benefit of the proposed scheme, comparing to existing works, is that there is no additional signaling overhead to the network. Only the cellular channel gains, reported anyway periodically for multiple purposes related to conventional communication and handover, are needed to be known. The proposed scheme reaches close-to-optimal sum capacity of D2D pairs and outperforms the case with no power control by 16% to 41.9%.

The future work should focus on generalization of the proposed solution towards prediction of the D2D channel gains that can be, then, exploited for any radio resource management problem (e.g., power control, channel allocation, D2D relay selection, etc.).

## Acknowledgment

This work has been supported by grant No. GA17-17538S funded by Czech Science Foundation and by the grant of Czech Technical University in Prague No. SGS17/184/OHK3/3T/13. The work of David Gesbert was partially supported by HUAWEI-EURECOM Chair on Advanced Mobile Systems towards 6G.

## References

[1] M. N. Tehrani, at al., "Device-to-Device Communication in 5G Cellular Networks: Challenges, Solutions, and Future Directions," *IEEE Communications Magazine*, 52(5), pp. 86–92, 2014.

[2] P. Mach, at al., "In-band device-to-device communication in OFDMA cellular networks: A survey and challenges," *IEEE Communications Surveys & Tutorials*, vol. 17, no. 4, pp. 1885–1922, 2015.

[3] R. Yin, at al., "Joint spectrum and power allocation for D2D communications underlaying cellular networks," *IEEE Transactions on Vehicular Technology*, 65(4), pp. 2182–2195, 2016.

[4] P. Mach, at al.,"Resource Allocation for D2D communication with Multiple D2D pairs reusing Multiple Channels," *IEEE Wireless Communications Letters*, 2019.

[5] A. Gjendemsjo, at al.,"Binary power control for sum rate maximization over multiple interfering links," *IEEE Trans. on Wireless Commun.*, vol. 7, no. 8, pp. 3164-3173, 2008.

[6] Q. Shi, at al., "An iteratively weighted MMSE approach to distributed sum-utility maximization for a MIMO interfering broadcast channel ," *IEEE Trans. Signal Process.*, vol. 59, no. 9, pp. 4331-4340, 2011.

[7] W. Yu, at al., "Distributed multiuser power control for digital subscriber lines," *IEEE J. Sel. Areas Commun.*, vol. 20, no. 5, pp. 1105-1115, 2019.

[8] D. Gunduz, at al., "Machine Learning in the Air," *IEEE J. Sel. Areas Commun.*, arXiv preprint, arXiv:1904.12385, 2019.

[9] H. Sun, at al., "Learning to optimize: Training deep neural networks for wireless resource management," *IEEE 18th International Workshop on Signal Process. Advances in Wireless Commun. (SPAWC)*, pp. 1-6, 2017.

[10] P. de Kerret, at al., "Team deep neural networks for interference channels," *IEEE ICC Workshops)*, pp. 1-6, 2018.

[11] W. Lee, at al., "Deep power control: Transmit power control scheme based on convolutional neural network," *IEEE Communications Letters*, 22(6), pp. 1276-1279, 2018.

[12] M. Kim, at al., "Learning to Cooperate in Decentralized Wireless Networks," *52nd Asilomar Conference on Signals, Systems, and Computers*, pp. 281-285, 2018.

[13] W. Lee, at al., "Transmit Power Control Using Deep Neural Network for Underlay Device-to-Device Communication," *IEEE Communications Letters*, 8(1), pp. 141-144, 2018.

[14] F. Liang, at al., "Towards optimal power control via ensembling deep neural networks", arXiv preprint arXiv:1807.10025, 2018.

[15] D. Astely, at al., "LTE: the evolution of mobile broadband," *IEEE Communications Magazine*, 47(4), pp. 44–51, 2009.

[16] L. Melki at al., "Interference management scheme for network-assisted multi-hop D2D communications," *IEEE PIMRC*, pp. 1–5, 2016.

[17] T. D. Hoang at al., "Energy-efficient resource allocation for D2D communications in cellular networks," *IEEE Transactions on Vehicular Technology*, 65(9), pp. 6972–6986, 2016.

[18] M. F. Moller at al., " A scaled conjugate gradient algorithm for fast supervised learning," *Neural Networks*, 6(4), pp. 525-533, 1993.

[19] YD. Bultitude at al., "T. IST-4-027756 WINNER II D1. 1.2 V1. 2 WINNER II Channel Models," Tech. Rep., Tech. Rep. 2007.

[20] 3GPP TR 36.843, "Study on LTE device to device proximity services; Radio aspects," v12.0.1, Release 12, 2014.

[21] J. D. Hobby at al., "Deployment options for femtocells and their impact on existing macrocellular networks," *Bell Labs Technical Journal*, 13(4), pp. 145-160, 2009.

### 4.4.3 Prediction of UEs' Association in Networks with FlyBSs

In the mobile networks, two devices communicating directly with each other do not have to be mobile terminals. The principle of the D2D channel prediction can be also applied to mobile networks with FlyBSs, which relays data between the static base stations (SBSs) and the users. This subsection shows that the cellular gains between the users and the SBSs can be used to predict the users' association (e.g., to which FlyBS every user should be associated) without any knowledge related to the D2D channel quality between the users and the FlyBSs. This solution enables the deployment of light-weighted FlyBSs acting as transparent relays [83] with reduced energy consumption. This subsection includes the conference paper [1C].

# Integrating UAVs as Transparent Relays into Mobile Networks: A Deep Learning Approach

Mehyar Najla †, Zdenek Becvar †, Pavel Mach †, and David Gesbert *
† Dpt. of Telecommunication Engineering, FEE, Czech Technical University in Prague, Prague, Czech republic
* Communication Systems Department, EURECOM, Sophia Antipolis, France
emails: † {najlameh, zdenek.becvar, machp2}@fel.cvut.cz, * gesbert@eurecom.fr

***Abstract*—Since flying base stations (FlyBSs) are energy constrained, it is convenient for them to act as transparent relays with minimal communication control and management functionalities. The challenge when using the transparent relays is the inability to measure the relaying channel quality between the relay and user equipment (UE). This channel quality information is required for communication-related functions, such as the UE association, however, this information is not available to the network. In this letter, we show that it is possible to determine the UEs' association based only on the information commonly available to the network, i.e., the quality of the cellular channels between conventional static base stations (SBSs) and the UEs. Our proposed association scheme is implemented through deep neural networks, which capitalize on the mutual relation between the unknown relaying channel from any UE to the FlyBS and the known cellular channels from this UE to multiple surrounding SBSs. We demonstrate that our proposed framework yields a sum capacity that is close to the capacity reached by solving the association via exhaustive search.**

***Index Terms*—Unmanned Aerial Vehicles, transparent relays, users' association, deep neural networks**

## I. Introduction

Unmanned Aerial Vehicles (UAVs) are expected to be integrated in future mobile networks as flying base stations (FlyBSs) complementing conventional static base stations (SBS) in some areas of the network, at the time when the high density of users and the dynamicity of the network are difficult to adapt to with a purely fixed infrastructure [1]. In such scenarios, the FlyBS relays the communication between the conventional SBS and the user equipment (UE).

The relays can be classified into non-transparent and transparent [2]. The non-transparent relays are distinguished by their high complexity as these are supposed to perform all the communication-related functions, such as data processing, radio resource management, or signaling, in a similar way as the conventional SBSs [3]. In contrast, the transparent relays represent a simplified and a lightweight version of the relays, for which the majority of the communication functions are managed centrally by the conventional SBS [4]. Consequently, the transparent relays are significantly cheaper and less energy demanding in comparison to the non-transparent relays as that transparent type requires less complex hardware [2]. Since the energy consumption of the FlyBSs is directly proportional to their operational time, the transparent relays are seen as suitable and convenient candidates for the FlyBSs.

To this end, the main obstacle facing the deployment of the FlyBSs acting as transparent relays arises from the fact that the transparent relays are not able to obtain the information about the quality of the channels between the UEs and the FlyBSs due to their simple nature. The reason is that the transparent relays do not transmit their own reference signals, which are required to determine the channel quality (see, e.g., [4], [5]). To solve this problem, the statistical channel gains between the UEs and the FlyBSs can be derived based on the existing path loss models. Nevertheless, these statistical channel gains rely on the knowledge of UEs' locations [6]-[8] or, at least, on the knowledge of the spatial distribution of UEs [9]-[10]. However, the information about the UEs' locations might not be available to the network due to the privacy preferences or the specific location of the user (e.g., the UE is at a place where no localization system is available). In such case, it is hard to decide whether to associate the UEs to a specific FlyBS or directly to the SBS.

In this paper, we focus on the case where the FlyBSs represent transparent relays, and we target the problem of the inability of the transparent FlyBSs to measure the channel gains between the UEs and the FlyBSs for the UEs' association. We also consider a practical scenario where an arbitrary part of the UEs makes their locations available to the network while another part of the UEs do not disclose their locations. To this end, we propose a deep neural network (DNN) that is able to predict the association of the UEs not disclosing their locations neither to the SBS nor to one of the FlyBSs. The objective is to maximize the sum capacity of these UEs. The UEs' association is predicted by the DNN based only on the knowledge of information commonly available to the network: 1) the quality of cellular channels between the UEs and the surrounding SBSs (note that the qualities of cellular channels are reported periodically in common networks [11], e.g., for handover purposes), 2) the FlyBSs' positions, which are known for the FlyBSs' navigation purposes, and 3) the number of the UEs already attached to each base station

This work has been supported by Grant No. P102-18-27023S funded by Czech Science Foundation and by the project of Czech Technical University in Prague no. SGS20/169/OHK3/3T/13.

(BS) as this number affects the resource allocation at the BSs (this information is known a priori for general radio resource management purposes). The DNN is trained offline and, then, exploited to associate the UEs. The DNN ability to make the association decision instantaneously is a significant asset of the proposed scheme from the practical implementation point of view in the real mobile network.

The rest of the paper is organized as follows. In Section II, the system model is presented and the targeted optimization problem is formulated. Then, in Section III, the proposed DNN-based scheme for UEs' association is described in detail. Section IV presents the simulation scenarios and discusses the results. Finally, Section V concludes the paper.

## II. System Model and Problem Formulation

We consider a set $\mathcal{N}$ containing $|\mathcal{N}|$ uniformly deployed UEs with their locations known to the network. In addition, there exist another set $\mathcal{M}$ of $|\mathcal{M}|$ uniformly deployed UEs for which the locations are not known. All UEs are deployed within a single cell and belong to a set $\mathcal{U}$ of $|\mathcal{U}|$ UEs where $\mathcal{U} = \mathcal{N} \cup \mathcal{M}$, $\mathcal{N} \cap \mathcal{M} = \emptyset$, and $|\mathcal{U}| = |\mathcal{N}| + |\mathcal{M}|$. The UEs are served by $|\mathcal{L}|$ BSs included in a set $\mathcal{L}$, encompassing one SBS and $|\mathcal{L}|-1$ FlyBSs acting as the transparent relays (note that, in this paper, the BS denotes arbitrary type of base station including SBS as well as FlyBS). Without loss of generality, we assume that all UEs communicate in the downlink direction. As in [12], the 2D positions (i.e., with fixed altitude) of the FlyBSs are determined with respect to the known locations of the UEs from $\mathcal{N}$ via K-means. Note that, while the association of the UEs from $\mathcal{N}$ is done based on their known locations (as in [12]), the association of the UEs with unknown locations from $\mathcal{M}$ is the targeted problem in this paper. Although we focus specifically on a single cell, there is also a set $\mathcal{K}$ of $|\mathcal{K}|$ SBSs in the vicinity. The qualities of the channels between every UE and all the $|\mathcal{K}|$ neighboring SBSs are measured and reported periodically as in conventional mobile networks, e.g., for mobility management and handover purposes.

Without loss of generality, we assume that the deployed $|\mathcal{K}|+1$ SBSs use orthogonal bandwidths (i.e., every SBS exploits its own dedicated bandwidth). In contrast, all FlyBSs reuse the same bandwidth $B$ of their serving SBS to ensure a high spectral efficiency (see Fig. 1). The serving SBS divides the whole bandwidth $B$ equally among all served UEs. The UE communicates either directly with the SBS (via direct channel from the SBS to the UE) or via the FlyBS (occupying the backhaul channel from the SBS to the FlyBS and the channel from the FlyBS to the UE). Note that the bandwidth allocation to individual UEs for the communication from the FlyBS to the UE is determined by the SBS as the FlyBSs represent transparent relays with limited functionalities. Further, every FlyBS is able to receive and transmit data at the same time. Since the same bandwidth is reused by all BSs, communication of each FlyBS with the SBS over backhaul is exposed to an interference induced by other FlyBSs. Similarly, each UE

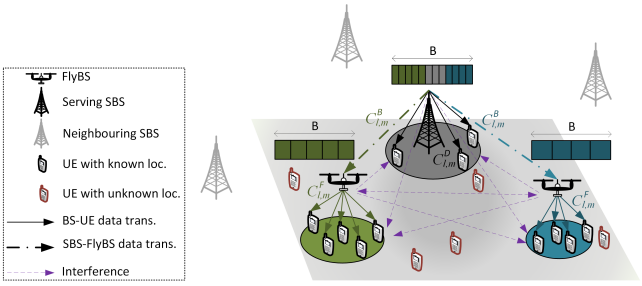


Fig. 1: System model.

experiences an interference from all BSs (either SBS or FlyBS) except the serving one.

If the $m$-th UE from $\mathcal{M}$ is served directly by the SBS, its capacity $C^D_{l,m}$ is defined as:

$$C^D_{l,m} = \frac{B}{|\mathcal{U}|} log_2\left(1 + \frac{\frac{p_1}{|\mathcal{U}|} g_{1,m}}{\frac{B}{|\mathcal{U}|}\sigma + \sum\limits_{l=2}^{l=|\mathcal{L}|} \frac{p_l}{|\mathcal{U}|} g_{l,m}}\right) \tag{1}$$

where $p_l$ is the transmission power of the $l$-th BS over the whole allocated bandwidth, $g_{l,m}$ is the channel gain between the $l$-th BS and the $m$-th UE, and $\sigma$ is the noise spectral density. Note that $l = 1$ refers to the serving SBS and, thus, $p_1$ and $g_{1,m}$ are the transmission power of the serving SBS and the channel gain between this SBS and the $m$-th UE. Moreover, in (1), we see that all FlyBSs cause interference to the $m$-th UE if this UE is associated directly to the serving SBS.

If the $m$-th UE is attached to the SBS through an intermediate FlyBS, the backhaul capacity $C^B_{l,m}$ (between the SBS and the relaying FlyBS) is calculated as:

$$C^B_{l,m} = \frac{B}{|\mathcal{U}|} log_2\left(1 + \frac{\frac{p_1}{|\mathcal{U}|} g_{1,l}}{\frac{B}{|\mathcal{U}|}\sigma + \sum\limits_{\substack{i=2 \\ i\neq l}}^{i=|\mathcal{L}|} \frac{p_l}{|\mathcal{U}|} g_{i,l}}\right) \tag{2}$$

where $g_{1,l}$ is the channel gain between the serving SBS and the $l$-th FlyBS to which the $m$-th UE is attached, and $g_{i,l}$ is the interference channel gain between the $i$-th FlyBS inducing the interference and the $l$-th FlyBS through which the $m$-th UE is served. Similarly, the capacity $C^F_{l,m}$ of the channel between the $l$-th FlyBS and the $m$-th UE is derived as:

$$C^F_{l,m} = \frac{B}{n_l} log_2\left(1 + \frac{\frac{p_l}{n_l} g_{l,m}}{\frac{B}{n_l}\sigma + \sum\limits_{\substack{i=1 \\ i\neq l}}^{i=|\mathcal{L}|} \frac{p_l}{n_l} g_{i,m}}\right) \tag{3}$$

where $n_l$ is the number of all UEs from $\mathcal{U}$ associated to the $l$-th FlyBS (i.e., $n_l \leq |\mathcal{U}|$), $g_{l,m}$ is the channel gain between the $l$-th FlyBS and the $m$-th UE attached to it, and $g_{i,m}$ is the interference caused by the $i$-th BS to the $m$-th UE.

Then, the capacity of the $m$-th UE associated to the $l$-th

FlyBS is derived as:

$$C_{l,m} = \begin{cases} C^D_{l,m} & \text{if } l = 1 \\ min(C^B_{l,m}, C^F_{l,m}) & \text{if } l > 1 \end{cases} \quad (4)$$

In order to define whether the $m$-th UE is associated to the SBS or to one of the FlyBSs, we introduce the association matrix $\boldsymbol{\alpha}$ expressed as:

$$\boldsymbol{\alpha} = \begin{bmatrix} \alpha^1_1 & \dots & \alpha^{|\mathcal{L}|}_1 \\ \vdots & \ddots & \vdots \\ \alpha^1_{|\mathcal{M}|} & \dots & \alpha^L_{|\mathcal{M}|} \end{bmatrix} \quad (5)$$

where $\alpha^l_m = 1$ indicates that the $m$-th UE is associated to the $l$-th BS, otherwise $\alpha^l_m$ is set to 0. Taking this into consideration, $n_l$ in (3) is calculated as:

$$n_l = N_l + \sum_{m=1}^{m=|\mathcal{M}|} \alpha^l_m \quad (6)$$

where $N_l$ is the number of the UEs from $\mathcal{N}$ that are attached to the $l$-th FlyBS and $\sum_{m=1}^{m=|\mathcal{M}|} \alpha^l_m$ represents the number of UEs from $\mathcal{M}$ that become attached to the $l$-th FlyBS.

Based on (1)-(6), the mathematical formulation of the problem of maximizing the sum capacity of the UEs with unknown locations (i.e., the $|\mathcal{M}|$ UEs from $\mathcal{M}$), is written as:

$$\boldsymbol{\alpha}^* = \underset{\boldsymbol{\alpha}}{\text{argmax}} \left(\sum_{m=1}^{m=|\mathcal{M}|} \sum_{l=1}^{l=|\mathcal{L}|} \alpha^l_m C^l_m\right) \quad (7)$$
$$\text{s.t. } \sum_{l=1}^{l=|\mathcal{L}|} \alpha^l_m = 1 \;\; \forall\, m \in \mathcal{M} \;\; (a)$$

where $\boldsymbol{\alpha}^*$ represents the targeted $\boldsymbol{\alpha}$ that maximizes the sum capacity of the $|\mathcal{M}|$ UEs, and the constraint (a) guarantees that each UE is associated to only one BS at a time.

The solution of the problem presented in (7) is not only affected by the quality of the channels between the $|\mathcal{M}|$ UEs and the $|\mathcal{L}|$ BSs, but it is also influenced by the bandwidth allocation for each UE at individual BSs as the bandwidth allocation changes with the association. In addition, the bandwidth splitting is also affected by the number of UEs attached to each BS. Moreover, $C^l_m$ is a function of $n_l$, which is a function of $\boldsymbol{\alpha}$ as shown in (6). Thus, the problem in (7) is an integer non-linear programming problem that is known to be NP-hard. Such problem can be generally solved by an exhaustive search. Nevertheless, the absence of the information on the locations of the $|\mathcal{M}|$ UEs as well as the FlyBSs' inability to measure the channel quality between themselves and the $|\mathcal{M}|$ UEs *make the problem unsolvable* in real networks *even with the exhaustive search*. Thus, in the next section, we rely only on the commonly known and periodically measured (and reported) cellular channel gains between the $|\mathcal{M}|$ UEs and the serving SBS together with $K$ surrounding SBSs to design the DNN that is able to make an instantaneous decision on the association of the $|\mathcal{M}|$ UEs whose locations are not known.

## III. Proposed association of UEs in networks with transparent relays

In this section, we, first, explain the principle of the proposed UEs' association scheme based on the cellular channels. Then, the proposed DNN architecture, training and exploitation in real mobile networks are explained.

### A. Principle of cellular channels-based UEs' association

Generally, when the FlyBSs act as the transparent relays, the relaying channels between the UEs and those FlyBSs cannot be estimated as explained in Section I. Hence, to associate the UEs from $\mathcal{M}$, an exploitation of the statistical channel gains derived based on existing channel models is the only known solution. Still, the statistical channel gain between any UE and the FlyBS with the existing channel models can be determined only if the locations of both the UE and the FlyBS are known. However, the locations of the UEs from $M$ are not available and the problem should be circumvented by an exploitation of another available information about these UEs. In fact, the cellular channels between any UE and the surrounding SBSs are commonly known as these cellular channels are measured and reported periodically for, e.g., mobility management and handover purposes. In an open field, a single UE can be distinguished by the cellular channels from this UE to the surrounding (neighboring) SBSs. Therefore, for the UEs with unknown locations from $\mathcal{M}$, the cellular channels between these UEs and multiple surrounding SBSs are seen as a proper substitution of the missing information on the channels to the FlyBSs taking into account that the positions of these FlyBSs are known.

Based on this principle, the problem presented in (7), can be solved knowing: i) the cellular channels between the UEs and multiple neighboring SBSs (reported periodically), ii) the FlyBSs' positions (known for the FlyBSs' navigation), and iii) the number of UEs from $\mathcal{N}$ attached to every BS, i.e., every $N_l$ $\forall l \in \mathcal{L}$ from (6) (this information affects the bandwidth splitting at the BSs and it is known by network operator as the resource allocation for all FlyBSs is done by the serving SBS). Nevertheless, the mapping between this available information (UEs' cellular gains, FlyBSs' locations, the number of the UEs attached to every BS) and the optimal association of the UEs from $\mathcal{M}$ is not known and cannot be analytically derived. Hence, we train the DNN to build the mapping between the pre-mentioned available information and the optimal association of the $|\mathcal{M}|$ UEs with unknown locations. This trained DNN is stored at the serving SBS, which decides and controls the association of all $|\mathcal{M}|$ UEs to the SBS or to one of the FlyBSs.

### B. Architecture of proposed DNN

The association of every UE from $\mathcal{M}$ to one of the $|\mathcal{L}|$ BSs can be seen as $|\mathcal{M}|$ identical classification problems. Thus, we train one DNN for multi-class classification in order to predict the association of any $m$-th UE from $\mathcal{M}$ to either the serving SBS or to one of the FlyBSs. Then, the trained DNN is exploited to predict the association of every UE at the

same time in parallel (details are explained later in Section III-C). The architecture of the DNN includes one input layer, $H$ hidden layers, and finally a SOFTMAX layer serving as the output layer (see Fig. 2).

The input vector $\mathbf{I_1}$, which represents the input layer, is composed of three parts $\mathbf{I_1^1}$, $\mathbf{I_1^2}$ and $\mathbf{I_1^3}$. The first part provides the DNN with the information regarding the cellular channel gains of all $|\mathcal{M}|$ UEs to every SBS in proximity to these UEs. Thus, the length of the first part $\mathbf{I_1^1}$ of the DNN's input is equal to the number of the reported/known UEs' cellular gains, i.e.:

$$|\mathbf{I_1^1}| = (|\mathcal{K}|+1)|\mathcal{M}| \tag{8}$$

The second part $\mathbf{I_1^2}$ of the input expresses the locations of individual FlyBSs under the SBS coverage, thus, the length of this second part is:

$$|\mathbf{I_1^2}| = 3(|\mathcal{L}|-1) \tag{9}$$

where the number "3" represents three coordinates of each FlyBS in 3D space. The third part $\mathbf{I_1^3}$, constituting the DNN input, corresponds to the number of the UEs from $\mathcal{N}$ already attached to each BS. Hence, the length of this third part is:

$$|\mathbf{I_1^3}| = |\mathcal{L}| \tag{10}$$

As a result, the input vector of DNN is of a length:

$$|\mathbf{I_1}| = |\mathbf{I_1^1}|+|\mathbf{I_1^2}|+|\mathbf{I_1^3}| = (|\mathcal{K}|+1)|\mathcal{M}|+3(|\mathcal{L}|-1)+|\mathcal{L}| \tag{11}$$

The DNN input $\mathbf{I_1}$ is followed by $H$ sequential hidden layers. Consequently, $\mathbf{I_1}$ is the input of the first hidden layer $h_1$. Then, the input of any other hidden layer is, at the same time, the output of the previous hidden layer. Every hidden layer $h_j$ is composed of $X_j$ neurons, where each input element from the inputs of $h_j$ is fed to each of these $X_j$ neurons with a corresponding weight. In every neuron in the layer $h_j$, the dot product between the inputs of $h_j$ and the corresponding weights is performed. Then, the neuron adds its bias to the result of the dot product and implements the sigmoid activation function resulting in the neuron's output (i.e., a single value). Thus, the output of any hidden layer $h_j$ with $X_j$ neurons is a vector of a length $X_j$, and this output is calculated as:

$$\mathbf{O_j} = sig(\mathbf{W_j}.\mathbf{I_j} + \mathbf{b_j}) \tag{12}$$

where sig(.) is the sigmoid function such that $sig(\boldsymbol{\gamma}) = \frac{1}{1+exp(-\boldsymbol{\gamma})}$, $\mathbf{I_j}$ is the vector that contains the inputs of the hidden layer $h_j$, $\mathbf{W_j}$ is the matrix containing the weights of the links connecting every input in $\mathbf{I_j}$ and every neuron in $h_j$, and $\mathbf{b_j}$ represents the vector that includes the biases of the $X_j$ neurons in $h_j$.

The output vector of the last hidden layer (i.e., the vector $\mathbf{O_H}$ from (12) with $j = H$ representing the last hidden layer) is the input of the SOFTMAX output layer. The SOFTMAX layer is composed of $|\mathcal{L}|$ neurons as the number of classes in our problem is also $|\mathcal{L}|$ (i.e., the number of available options for the association of the $m$-th UE). Every neuron $l$ in the SOFTMAX layer implements the dot product between $\mathbf{O_H}$ and

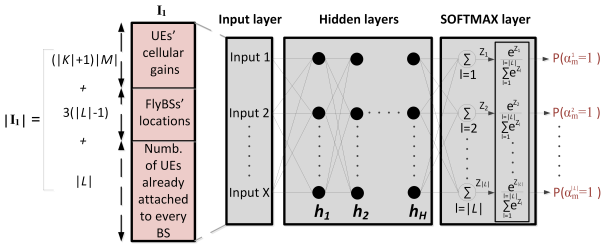


Fig. 2: Proposed DNN to predict the association of a single UE from $\mathcal{M}$.

the corresponding weights and adds the corresponding bias, resulting in the value $Z_l$. Hence, considering all the $|\mathcal{L}|$ neurons in the SOFTMAX layer, we get the vector $\mathbf{Z}$ of a length $|\mathcal{L}|$, such that $\mathbf{Z} = \{Z_1, Z_2, ..., Z_{|\mathcal{L}|}\}$. Finally, the elements in $\mathbf{Z}$ are inserted to the SOFTMAX function giving, for every element $Z_l$ with $l \in \mathcal{L}$, a final single output $P(\alpha_m^l)$. Note that $P(\alpha_m^l)$ represents the probability of the $m$-th UE being associated to the $l$-th BS (the probability that $\alpha_m^l = 1$). This probability is calculated as:

$$P(\alpha_m^l) = \frac{exp(Z_l)}{\sum_{l=1}^{l=|\mathcal{L}|} exp(Z_l)} \tag{13}$$

From (13), we see that $\sum_{l=1}^{l=|\mathcal{L}|} P(\alpha_m^l) = 1$. Hence, the final chosen association for the $m$-th UE is:

$$\alpha_m^l = \begin{cases} 1 & \text{if } P(\alpha_m^l) > P(\alpha_m^q) \ \forall \ q \in \mathcal{L}/\{l\} \\ 0 & \text{otherwise} \end{cases} \tag{14}$$

### *C. Training and exploitation of proposed DNN for UEs' association*

The proposed DNN utilizes supervised learning approach trying to reach a specific target. In our case, the target is derived by the exhaustive search when all possible association combinations for $|\mathcal{M}|$ UEs (i.e., $|\mathcal{L}|^{|\mathcal{M}|}$ combinations) are checked and the one yielding the highest sum capacity is selected as the optimal association combination. Then, for any $m$-th UE from the $|\mathcal{M}|$ UEs (e.g., the first UE in $\mathcal{M}$), the index of the chosen BS (i.e., $l^*$ where $l^* \in \mathcal{L}$) is considered as the target that the DNN aims to predict. To that end, the learning process starts with collecting a set of training samples, e.g., by simulating the targeted area and scenario. Each sample represents a single simulation drop and includes the set of available information (i.e., the information feed to the input of the DNN described in Section III-B) as features and the corresponding target. Then, the features of each sample are inserted to the DNN with randomly set weights and biases giving, at its output, the association of the $m$-th UE. Next, the comparison between the DNN output and the targeted output for each sample is performed via cross-entropy loss function

written as:

$$\delta = -\sum_{l=1}^{l=|\mathcal{L}|} [\![l^* == l]\!] log\left(P(\alpha_m^l)\right) \quad (15)$$

The cross-entropy loss function averaged over the training samples is minimized by subsequent updating of the weights and the biases of the DNN via the scaled-conjugate gradient back-propagation [13]. Then, a new training iteration is performed with the updated weights and biases. The training process is terminated if the number of iterations exceeds the maximal number of iterations or if the prediction accuracy increment from one iteration to another becomes very small.

Key benefit of the proposed solution is that the training process is performed offline and there is no training needed online in the real mobile network. Then, in the real mobile network, the same already trained DNN is exploited to instantly determine the optimal association of every UE from the $|\mathcal{M}|$ UEs simultaneously. For example, consider that the DNN is trained to predict the optimal association for the first UE from $\mathcal{M}$ (the UE for which the cellular gains are put at the beginning of $\mathbf{I_1}$). In such case, to predict the optimal association for the second UE, we put the cellular gains of this second UE at the beginning of $\mathbf{I_1}$.

## IV. Performance Analysis

The simulations are done in MATLAB considering a $500 \times 500$ m area within which $|\mathcal{N}|= 10$ UEs with known locations and up to $|\mathcal{M}|= 5$ UEs with unknown locations are uniformly deployed. The area contains also one serving SBS deployed in the middle of the area and two FlyBSs acting as transparent relays (as shown in Fig. 1). In addition to the serving SBS, we assume $|\mathcal{K}|= 2, 3$, or 4 additional SBSs in the neighboring areas with fixed uniformly generated locations. We consider that the $|\mathcal{N}|$ UEs with known locations are already associated to the serving SBS either directly or through one of the two available FlyBSs, while the $|\mathcal{M}|$ UEs with unknown locations are, then, associated based on the proposed scheme illustrated in Section III. The height and the transmission power (over all channels) $p_l$ of each BS are set to 30 m and 27 dBm, respectively. The total bandwidth $B$ reused by every BS is set to 20 MHz. The gains of the channels between the FlyBSs and the UEs, between the SBS and the UEs, and between the SBS and the FlyBSs are generated in line with path loss models from [14] with 2 GHz carrier frequency.

Note that the DNN is trained for each value of $|\mathcal{M}|$ separately, and with a total number of collected samples equal to $3 \times 10^5$. Note that the number of samples is set by trial and error approach and the learning accuracy increment is negligible for larger numbers of samples.

Fig. 3 shows the DNN prediction accuracy (the percentage of the DNN's outputs that match the optimal targeted association) versus different numbers of UEs in $\mathcal{M}$ and for different numbers of available neighboring SBSs (i.e., $|\mathcal{K}|$). As expected, with the increasing number of SBSs the prediction accuracy is increasing as the DNN is able to better learn the scenario layout. Thus, if four SBSs are in vicinity (in addition to the serving one), the accuracy varies between 92.5% (for $|\mathcal{M}|= 1$) and 96.7% (for $|\mathcal{M}|= 5$). Still, even for a lower number of SBSs (i.e., $|\mathcal{K}|= 2$ or $|\mathcal{K}|= 3$), the prediction accuracy is always higher than 90%. Fig. 3 further demonstrates that the prediction accuracy decreases with the increasing $|\mathcal{M}|$ due to the growing complexity of the association problem (more UEs need to be associated with different channels and bandwidth splitting options).

Fig. 4 illustrates the sum capacity of the $|\mathcal{M}|$ UEs if $|\mathcal{K}|= 2$. To the best of our knowledge, there is no existing work that solves the UEs' association for the case when both the UEs' locations as well as the relaying channels between the FlyBSs (acting as the transparent relays) and the UEs are absent. Thus, the proposed DNN is compared to the following association schemes: 1) Optimal association derived by the exhaustive search (in the figure denoted as $Optimum$), 2) Random association where each UE is associated with equal probability to the serving SBS or one of the FlyBSs (denoted as $Random$), 3) all UEs are associated to one of the FlyBS (denoted as $Only\ FlyBS$), and 4) all UEs are associated to the serving SBS (denoted as $Only\ SBS$). Note that $Optimum$ is not derivable

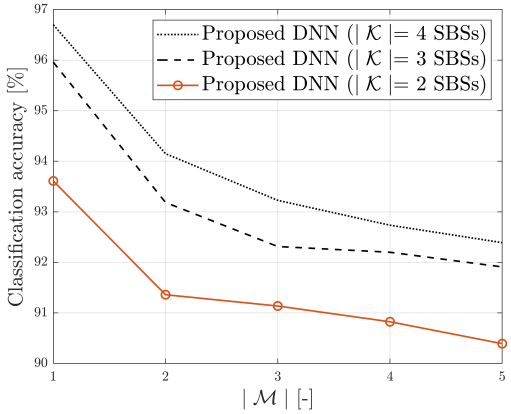


Fig. 3: Classification accuracy vs $|\mathcal{M}|$.

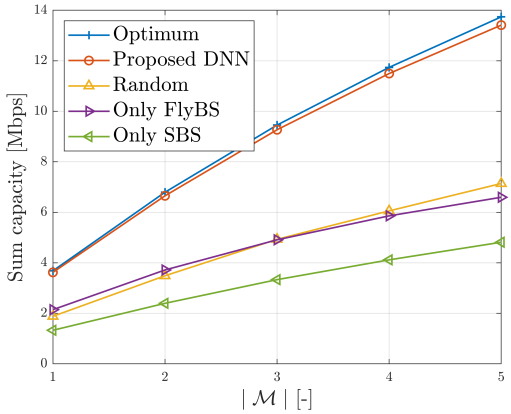


Fig. 4: Sum capacity of the $|\mathcal{M}|$ UEs for $|\mathcal{K}|$=2.

in real networks with the FlyBSs acting as transparent relays and the locations of the $|\mathcal{M}|$ UEs being unknown. In this paper, we depict $Optimum$ only for benchmarking purposes.

Fig. 4 demonstrates that the proposed scheme, with only three SBSs ($|\mathcal{K}|= 2$ neighboring SBSs plus the serving SBS), reaches a close-to-optimal sum capacity with a loss with respect to the optimum always below 2.4%. Moreover, the sum capacity reached by the proposed scheme with respect to the capacity of the other three association schemes is increased by up to 91%, 103%, and 280% when compared to $Random$, $Only\ FlyBS$ and $Only\ SBS$, respectively.

## V. Conclusions

In this paper, we have proposed a novel DNN-based framework to determine the association of the UEs with unknown locations either to the serving SBS or to one of the FlyBSs acting as the transparent relays. The transparent relay mode for the FlyBSs is selected as the transparent relays are lighter, less expensive, and consume less energy comparing to the non-transparent ones. This makes the transparent relays suitable for FlyBSs. To this end, we exploit the knowledge of cellular channels between the UEs and the surrounding SBS to overcome the problem of the transparent relays' inability to measure the quality of the channels between themselves and the UEs as well as the absence of the UEs' location information. By knowing the UEs' periodically reported cellular channels, our proposed DNN determines the UEs' association maximizing their sum capacity. The results confirm the close-to-optimal performance of our proposal.

## References


[1] Y. Zeng, et al., "Wireless communications with unmanned aerial vehicles: Opportunities and challenges," *IEEE Communications Magazine*, 54(5), pp. 36–42, 2016.

[2] Huawei, " Understanding on Type 1 and Type 2 Relay," *3GPP TSG RAN WG1 Meeting #57bis*, Los Angeles, USA, June 29- July3, 2009 (R1 092370).

[3] C. Hoymann, et al., "Relaying operation in GPP LTE: challenges and solutions," *IEEE Communications Magazine*, 50(2), pp. 156–162, 2012.

[4] Motorola, "Discussion of Type II (Transparent) Relays for LTE," *3GPP TSG RAN WG1 Meeting #57*, San Francisco, USA, May 4-8, 2009 (R1 091941).

[5] Huawei, "Issues of Type 2 Relay," *3GPP TSG RAN WG1 Meeting #57bis*, Los Angeles, USA, June 29- July3, 2009 (R1 092372).

[6] J. Chen, et al., "'Optimal positioning of flying relays for wireless networks: A LOS map approach," *IEEE international conference on communications (ICC)*, pp. 1–6, 2017.

[7] M. Alzenad, et al., "3-D placement of an unmanned aerial vehicle base station for maximum coverage of users with different QoS requirements," *IEEE Wireless Communication Letters*, 7(1), pp. 38–41, 2016.

[8] J. Plachy, et al., "Joint positioning of Flying Base stations and Association of Users: Evolutionary-based approach," *IEEE Access*, 7, pp. 11454–11463, 2019.

[9] M. Mozaffari, et al., "Optimal transport theory for cell association in UAV-enabled cellular networks," *IEEE Communications Letters*, 21(9), pp. 2053–2056, 2017.

[10] M. Mozaffari, et al., "Wireless communication using unmanned aerial vehicles (UAVs): Optimal transport theory for hover time optimization," *IEEE Transactions on Wireless Communications*, 16(12), pp. 8052–8066, 2017.

[11] D. Astely, at al., "LTE: the evolution of mobile broadband," *IEEE Communications Magazine*, 47(4), pp. 44–51, 2009.

[12] B. Galkin, at al., "Deployment of UAV-mounted access points according to spatial user locations in two-tier cellular networks," *Wireless Days (WD)*, pp. 1–6, 2016.

[13] M. F. Moller at al., " A scaled conjugate gradient algorithm for fast supervised learning," *Neural Networks*, 6(4), pp. 525-533, 1993.

[14] YD. Bultitude at al., "T. IST-4-027756 WINNER II D1. 1.2 V1. 2 WINNER II Channel Models," Tech. Rep., Tech. Rep. 2007.

# Chapter 5

# Conclusion and Future Research Directions

This dissertation thesis has addressed the optimization of three aspects related to the D2D communication. First, the resource allocation in D2D communication have been optimized. In detail, a combined shared/dedicated (CSD) resource allocation scheme for the D2D communication has been proposed. The proposed CSD scheme allows the D2D pairs to utilize resources in both shared and dedicated regions simultaneously. In addition, the same resources can be exploited by several D2D pairs in order to enhance the spectral efficiency of the system and to increase the sum capacity of D2D pairs. In this regard, a graph theory-based framework has been proposed for an efficient resource allocation. Within this framework, the BS creates a graph showing neighborhood relations among the CUEs and the D2D pairs and among the individual D2D pairs. After the decomposition of the graphs into sub-graphs and the determination of the maximal cliques, the BS is able to allocate the resources maximizing the D2D pairs' sum capacity. The results show that the D2D capacity is significantly improved (typically by roughly 2 times) when compared to the scheme selecting only the shared or the dedicated region. This proposed combined shared/dedicated resource allocation scheme satisfies Objective 1 from the list of the objectives of this dissertation thesis.

The resource allocation and the channel reuse have been further optimized in each D2D communication mode separately in the thesis. In the dedicated mode, a new resource allocation scheme allowing multiple pairs to reuse multiple channels for the D2D communication has been designed in order to maximize the sum capacity of D2D pairs while maintaining the minimal individual capacity required by every D2D pair. The proposed resource allocation scheme encompasses an initial bandwidth allocation, channel reuse, and power allocation over the reused channels. The channel reuse is presented as a coalition structure generation problem, where the D2D pairs composing one coalition reuse the channels originally dedicated to each other. The coalition structure generation problem has been optimally solved via dynamic programming. As the dynamic programming is of a high complexity, we have also developed a low-complexity sequential bargaining algorithm solving the reuse problem while

reaching close-to-optimal sum capacity of the D2D pairs. The performance analysis shows that the sum capacity of D2D pairs is significantly increased (up to 300 % gain) by the proposed resource allocation scheme compared to the existing algorithms. In addition, although the interference is imposed among the D2D pairs reusing the same channel, the minimal required capacity for each D2D pair is still guaranteed after the channel reuse. In the D2D shared mode, this dissertation thesis has proposed a novel low complexity resource allocation scheme that allows an efficient reuse of the channels by multiple D2D pairs while each D2D pair can access multiple channels. Such solution maximizes the sum capacity of D2D pairs keeping the percentage of the reduction in the capacity of the cellular users below a pre-defined relative threshold. The results has shown that the proposed allocation significantly outperforms the state-of-the-art approaches and reaches a close-to-optimum performance despite a low (linear) complexity. These two proposed resource allocation schemes for dedicated and shared modes respectively satisfy Objective 2 from the list of the objectives of this dissertation thesis.

Second, this dissertation thesis has introduced the novel concept combining RF and VLC communication to increase the communication capacity provided by the D2D communication. The performance analysis of the proposed RF-VLC D2D has shown the ability to mitigate the drawbacks in terms of limited capacity for very short distances (few meters) in the RF D2D and medium distances (few tens of meters) in VLC D2D systems. The proposed RF-VLC D2D improves the achievable capacity with respect to sole RF D2D and VLC D2D. The most notable gain in the capacity is observed for low distances, where VLC shows its superiority over the conventional RF and, thus, the combination of both is the most beneficial. However, the analysis indicates that the key challenge in RF-VLC D2D is an efficient selection of the communication band for individual D2D pairs in a scenario with multiple D2D pairs. To this end, two RF/VLC band selection algorithms have been proposed. The first algorithm is a centralized low-complexity heuristic algorithm selecting either RF or VLC band for each D2D pair relying on the mutual interference among the pairs. For interpretation of the mutual interference among the D2D pairs, the algorithm exploits directed weighted graphs. The simulation results demonstrate that the proposed algorithm outperforms state-of-the-art algorithms in terms of the communication capacity by up to 7.1 times and in terms of the energy efficiency by up to 10 times while the outage is significantly suppressed. Moreover, despite its very low complexity, the proposed algorithm reaches a close-to-optimum performance obtained by the exhaustive search. Then, for the scenarios with a limited channel knowledge information and for the cases when a very fast band selection is required, a second band selection scheme that relies only on the knowledge of the received power and sum interference from all D2D transmitters at the individual D2D receivers has been proposed. This second proposed solution is based on a deep neural network making an initial band selection. Then, based on the neural network's output, a fast heuristic algorithm has been designed to further improve the band selection. The results show that the proposal reaches a close-to-optimal performance and outperforms the existing

solutions as well as the former proposed algorithm in terms of the complexity, outage ratio, and energy efficiency. The study related to the concept and the benefits of RF-VLC D2D as well as the two proposed RF/VLC band selection algorithms fulfill Objective 3 from the list of the objectives of this dissertation thesis.

Finally, a novel D2D channel gains prediction based on the cellular channel gains between the UEs and multiple neighboring BSs has been proposed. The proposed prediction takes the advantage of the network topology-related correlation between the cellular and D2D channel gains. A supervised learning, exploiting deep neural networks, extracts the mapping between the cellular channel gains of any couple of the UEs (i.e., gains of channels between these two UEs and multiple BSs) and the gain of the D2D channel between these two UEs. The proposed prediction achieves a very high Pearson correlation coefficient (above 94%) between the true and the predicted D2D channel gains. The simulations results have shown that the proposed prediction scheme significantly reduces the amount of signaling (represented by channel state information) for a determination of the channel quality if applied to realistic radio resource management algorithms. This saving of the channel information is at the cost of only negligible performance losses in terms of the communication capacity comparing to the conventional implementation of these algorithms with full knowledge of all channels. The simulations results, further, demonstrate that the proposed prediction scheme is robust and resilient to the possible changes in the environment induced by various moving obstacles or potential changes in the fixed obstacles (e.g., the buildings) that exist in the area. In addition, this dissertation thesis has confirmed that the cellular gains between the UEs and the surrounding BSs can be also used to predict communication-related decisions directly, with minimal capacity losses compared to optimum, and without the need to predict the D2D channels as an intermediate step. This finding has been confirmed for D2D binary power control as well as UEs' association problem in the mobile networks with flying base stations acting as transparent relays. The proposed novel D2D channel gains prediction framework as well as the proposed immediate prediction of radio resource management decisions fulfill Objective 4 from the list of the objectives of this dissertation thesis.

## 5.1 Summary of Contributions

The research contributions of the work within the dissertation thesis are summarized as follows:

- A novel concept of combining shared and dedicated D2D modes has been introduced. In detail, a resource allocation scheme for D2D communication allowing shared as well as dedicated resources to be allocated, simultaneously, to every D2D pair has been proposed. This combination between the shared and the dedicated modes notably improves the sum capacity of D2D pairs compared to the classical case when a D2D pair can access a single mode only. This is presented in the conference paper

[4C].

- A game-theoretic resource allocation scheme for D2D dedicated mode has been proposed, enabling the reuse of multiple channels by multiple D2D pairs. The proposed scheme maximizes the sum capacity of D2D pairs while still guaranteeing the minimal individual capacity required by every D2D pair. The proposed scheme overcomes the existing approaches from the literature and increases the reachable communication capacity significantly. This is, partially, presented in the conference paper [2C] and fully detailed in the journal paper [1J].

- A heuristic low-complexity algorithm for the resource allocation in D2D shared mode, allowing the reuse of multiple channels by multiple D2D pairs has been proposed. The designed solution maximizes the sum capacity of D2D pairs under a constraint related to the maximal allowed reduction in the capacity of the CUEs. The proposed algorithm outperforms the existing approaches and improves the achievable communication capacity dramatically. This is presented in the journal paper [5J].

- A new combination between VLC out-band D2D with the in-band RF D2D (denoted as RF-VLC D2D) has been introduced. The benefits and the challenges facing the proposed RF-VLC D2D have been studied. This was, however, the first study on combining RF and VLC for D2D and the performed analysis pave the way to understand and properly deploy RF-VLC D2D in future mobile networks. This is included in the conference paper [6C].

- For RF-VLC D2D, an iterative interference-based algorithm to select RF or VLC for every D2D pair in a scenario with multiple D2D pairs has been proposed. The proposed algorithm significantly increases the sum capacity of D2D pairs compared to the case when only RF or only VlC is used. This is included, partially, in the conference paper [5C] and fully detailed in the journal paper [4J].

- A second machine learning-based algorithm for a quick band selection in RF-VLC D2D communication has been presented. This solution requires only limited information related to the quality of the D2D channels compared to the former band selection algorithm. Hence, this approach facilitates the RF/VLC band selection in more realistic scenarios with limited channel information and, still, overcomes the existing schemes. This is presented in the journal paper [3J].

- A D2D channel prediction framework has been proposed. The framework relies on the knowledge of the cellular channel gains between the UEs and the surrounding BSs. Deep neural networks (DNNs) are exploited to perform the D2D channel prediction. This prediction scheme highly reduces the number of reference signals saving more resources for data transmission. Moreover, the idea of predicting the D2D channel gains from the

cellular channel gains might be a game-changer in D2D communication enabling its practical implementation even with massive number of D2D pairs in future mobile networks. This is presented in the journal paper [2J] and included in the filled US patent [1P].

- The prediction of power control decisions for D2D communication immediately from the cellular channel gains of the UEs (without the need to predict the D2D channels as an intermediate step) has been presented. This is included in the conference paper [3C] and included in the filled US patent [1P]. Moreover, the dependency on the cellular gains to make immediate radio resource management decisions has been also exploited for networks with flying BSs (FlyBSs). In detail, considering that the communication between the UEs and the FlyBSs as a type of D2D communication, the prediction of UEs' association based on the cellular gains of the UEs (without the need to know the D2D channel quality between the UEs and the FlyBSs) has been proposed. This is presented in the conference paper [1C] and included in the filled US patent [1P]. Both, power control and users' association are implemented to confirm that the cellular channel gains of the users can be used for immediate D2D-related radio resource management decisions. This approach highly reduces signaling overhead and, further, facilitates the practical implementation of radio resource management in future mobile networks compared to other approaches in the literature.

## 5.2 Future Work

The main direction for further research is related to the practical implementation and testing of the proposed approaches in a testbed. Based on this, real training data can be collected and used to practically test the D2D channel gains prediction scheme proposed in this dissertation thesis. This goes in parallel with further practical exploitation of all machine learning-based prediction schemes presented in this dissertation thesis. In detail, distributed and federated learning should be tested and investigated. Moreover, in the real mobile network, the possible future research directions include studying the possibility of collecting real measurements to train neural networks in order to make the decisions related to D2D communication as shown in this dissertation thesis. To this end, another aspect for further research is related to answering the open question about whether it is possible to merge artificial simulation-based training data with real measurements to build larger and more realistic data sets for achieving a higher performance in terms of D2D communication quality in the real mobile network.

# References


[1] M. N. Tehrani, et al., "Device-to-Device Communication in 5G Cellular Networks: Challenges, Solutions, and Future Directions," *IEEE Communications Magazine*, 52(5), pp. 86–92, 2014.

[2] A. Asadi, Q. Wang, and V. Mancuso, "A Survey on Device-to-Device Communication in Cellular Networks," *IEEE Comunnications Surveys & Tutorials*, 16(4), pp. 1801-1819, 2014.

[3] P. Mach and Z. Becvar, "In-Band Device-to-Device Communication in OFDMA Cellular Networks: A Survey and Challenges," *IEEE Comunnications Surveys & Tutorials*, 17(4), pp. 1885-1922, 2015.

[4] L. Wei, R.Q. Hu, Y. Qian, and G. Wu, "Enable device-to-device communications underlaying cellular networks: challenges and research aspects," *IEEE Comunnications Magazine*, 52(6), pp. 90-96, 2014.

[5] J. Dai, et al., "Analytical Modeling of Resource Allocation in D2D Overlaying Multihop Multichannel Uplink Cellular Networks," *IEEE Transactions on Vehicular Technology*, 66(8), pp. 6633–6644, 2017.

[6] P.H. Pathak, X. Feng, P. Hu, and P. Mohapatra, "Visible light communication, networking, and sensing: A survey, potential and challenges," *IEEE Comunnications Surveys & Tutorials*, 17(4), pp. 2047–2077, 2015.

[7] S.A. asnayaka, and H. Haas, "Hybrid RF and VLC systems: Improving user data rate performance of VLC systems," *IEEE Vehicular Technology Conference (VTC Spring)*, pp. 1–5, 2015.

[8] 3GPP TS 36.211, "Evolved Universal Terrestrial Radio Access (E-UTRA); Physical channels and modulation," v13.5.0, Release 13, 2017.

[9] Z. Zhou, M. Dong, K. Ota, J. Wu, and T. Sato, "Energy efficiency and spectral efficiency tradeoff in device-to-device (D2D) communications," *IEEE Wireless Communications Letters*, 3(5), pp.485–488, 2014.

[10] R. Ma, N. Xia, H.H. Chen, C.Y. Chiu, and C.S. Yang, "Mode selection, radio resource allocation, and power coordination in D2D communications," *IEEE Wireless Communications*, 24(3), pp. 112–121, 2017.

[11] S. Wen, X. Zhu, X. Zhang, and D. Yang, "QoS-aware mode selection and resource allocation scheme for device-to-device (D2D) communication in cellular networks," *IEEE International Conference on Communications Workshops (ICC)*, pp. 101–105, 2013.

[12] H. ElSawy, E. Hossain, and M.S. Alouini, "Analytical modeling of mode selection and power control for underlay D2D communication in cellular networks," *IEEE Transactions on Communications*, 62(11), pp 4147–4161, 2014.

[13] X. Li, R. Shankaran, M.A. Orgun, G. Fang, and Y. Xu, "Resource allocation for underlay D2D communication with proportional fairness," *IEEE Transactions on Vehicular Technology*, 67(7), pp. 6244–6258, 2018.

[14] X. Liu, and C. Huang, "Machine Learning for QoS-Aware Fairness of a D2D Network." *IEEE Vehicular Technology Conference (VTC2020-Spring)*, pp. 1–5, 2020

[15] D.M. Soleymani, M.R. Gholami, J. Mueckenheim, and A. Mitschele-Thiel, "Dedicated Sub-Granting Radio Resource in Overlay D2D Communication." *IEEE 30th Annual International Symposium on Personal, Indoor and Mobile Radio Communications (PIMRC),* pp. 1–7, 2019.

[16] W. Sun, E.G. Ström, F. Brännström, Y. Sui, and K.C. Sou "D2D-based V2V communications with latency and reliability constraints"' *IEEE Globecom Workshops (GC Wkshps)*, pp. 1414–1419, 2014

[17] R. Wang, J. Zhang, S.H. Song, and K. B. Letaief, "QoS-Aware Joint Mode Selection and Channel Assignment for D2D Communications," *IEEE International Conference on Communications (ICC)*, 2016.

[18] M. Klugel and W. Kellerer, "Leveraging The D2D-Gain: Resource Efficiency Based Mode Selection for Device-to-Device Communication," *IEEE Global Communications Conference (GLOBECOM)*, 2016.

[19] Y. Liu, "Optimal Mode Selection in D2D-Enabled Multibase Station Systems," *IEEE Communication Letters*, 20(3), 470-473, 2016.

[20] M. Azam, et al., "Joint Admission Control, Mode Selection, and Power Allocation in D2D Communication Systems," *IEEE Transactions on Vehicular Technology*, 65(9), 7322-7333, 2016.

[21] E. Naghipour and M. Rasti, "A Distributed Joint Power Control and Mode Selection Scheme for D2D Communication Underlaying LTE-A Networks," *IEEE Wireless Communications and Networking Conference (WCNC)*, 2016.

[22] H.J. Chou and R. Y. Chang, "Joint Mode Selection and Interference Management in Device-to-Device Communications Underlaid MIMO Cellular Networks," *IEEE Transactions on Wireless Communications*, 16(2), 1120-1134, 2017.

[23] F. Jiang, "Mode Selection and Resource Allocation for Device-to-Device Communications in 5G Cellular Networks," *China Communications*, 13(6), 32-47, 2016.

[24] D. Ma, N. Wang, and X. Mu, "Resource Allocation for Hybrid Mode Device-to-Device Communication Networks," *International Conference on Wireless Communications & Signal Processing (WCSP)*, 2016.

[25] Y. Huang, et al., "Mode Selection, Resource Allocation, and Power Control for D2D-Enabled Two-Tier Cellular Network," *IEEE Transactions on Communications*, 64(8), 3534-3547, 2016.

[26] Y. Li, M. C. Gursoy, and S. Velipasalar, "Joint Mode Selection and Resource Allocation for D2D Communications under Queueing Constraints," *IEEE Infocom Workshop*, 2016.

[27] J. Kim, S. Kim, J. Bang, and D. Hong, "Adaptive Mode Selection in D2D Communications Considering the Bursty Traffic Model," *IEEE Communications Letters*, 20(4), 712-715, 2016.

[28] D., Feng, L. Lu, Y. Yuan-Wu, G.Y. Li, S. Li, and G. Feng, "Device-to-device communications in cellular networks," *IEEE Communications Magazine*, 52(4), pp. 49–55, 2014.

[29] G.A. Safdar, M. Ur-Rehman, M. Muhammad, M.A. Imran, and R. Tafazolli, "Interference mitigation in D2D communication underlaying LTE-A network," *IEEE Access*, 4, pp. 7967–7987, 2016.

[30] Z., Yang, N. Huang, H. Xu, Y. Pan, Y. Li, and M. Chen, "Downlink resource allocation and power control for device-to-device communication underlaying cellular networks," *IEEE Communications Letters*, 20(7), pp. 1449–1452, 2016.

[31] C.H. Yu, et al., "Resource Sharing Optimization for Device-to-Device Communication Underlaying Cellular Networks," *IEEE Transactions on Wireless Communications*, 10(8), pp. 2752–2763, 2011.

[32] Y. Qian, T. Zhang, and D. He, "Resource allocation for multichannel device-to-device communications underlaying QoS-protected cellular networks," *IET Communications*, 11(4), 558-565, 2017.

[33] R. AliHemmati, et .al., "Multi-Channel Resource Allocation Toward Ergodic Rate Maximization for Underlay Device-to-Device Communications," *IEEE Transactions on Wireless Communications*, 17(2), 1011-1025, 2018.

[34] R. AliHemmati, et al., "Power Allocation for Underlay Device-to-Device Communication over Multiple Channels," *IEEE Transactions on Signal and Information Processing over Networks*, 4(3), pp. 467–480, 2017.

[35] Y. Xiao, et al., "A Bayesian overlapping coalition formation game for device-to-device spectrum sharing in cellular networks," *IEEE Transactions on Wireless Communications*, 14(7), pp. 4034–4051, 2015.

[36] M. Hasan, et al., "Distributed Resource Allocation for Relay-Aided Device-to-Device Communication Under Channel Uncertainties: A Stable Matching Approach," *IEEE Transactions on Communications*, 63(10), pp. 3882–3897, 2015.

[37] Y. Zhang, et al., "Incentive compatible overlay D2D system: A group-based framework without CQI feedback," *IEEE Transactions on Mobile Computing*, 17(9), pp. 2069–2086, 2018.

[38] W. Zhao and S. Wang, "Resource Sharing Scheme for Device-to-Device Communication Underlaying Cellular Networks," *IEEE Transactions on Communications*, 63(12), 4838-4848, Dec. 2015.

[39] M.C. Lucas-Estan and J. Gozalvez, "Distributed radio resource allocation for device-to-device communications underlaying cellular networks," *Journal of Network and Computer Applications*, 120-130, 2017.

[40] S. M. A. Kazmi, et al., "Mode Selection and Resource Allocation in Device-to-Device Communications: A Matching Game Approach," *IEEE Transactions on Mobile Computing*, 16(11), 3126-3141, Nov 2017.

[41] A. Asheralieva, et al., "Bayesian Reinforcement Learning-Based Coalition Formation for Distributed Resource Sharing by Device-to-Device Users in Heterogeneous Cellular Networks," *IEEE Transactions on Wireless Communications*, 16(8), pp. 5016–5032, 2017.

[42] S. Maghsudi, et al., "Channel Selection for Network-Assisted D2D Communication via No-Regret Bandit Learning With Calibrated Forecasting," *IEEE Transactions on Wireless Communications*, 14(3), pp. 1309–1322, 2015.

[43] Y. Li, et al., "Coalitional Games for Resource Allocation in the Device-to-Device Uplink Underlaying Cellular Networks," *IEEE Transactions on Wireless Communications*, 13(7), pp. 3965–3977, 2014.

[44] A. Asheralieva, et al., "An Asymmetric Evolutionary Bayesian Coalition Formation Game for Distributed Resource Sharing in a Multi-Cell Device-to-Device Enabled Cellular Network," *IEEE Transactions on Wireless Communications*, 17(6), pp. 3752–3767, 2018.

[45] T. Liu, et al., "Resource Allocation for Device-to-Device Communications as an Underlay Using Nash Bargaining Game Theory," *International Conference on Information and Communication Technology Convergence (ICTC)*, pp. 366–371, 2015.

[46] D. H. Lee, et al.,"Resource allocation scheme for device-to-device communication for maximizing spatial reuse," *IEEE Wireless Communications and Networking Conference (WCNC)*, pp. 112–117, 2013.

[47] W. Zhibo, et al.," Clustering and power control for reliability improvement in Device-to-Device networks," *IEEE Globecom Workshops (GC Wkshps)*, pp. 573–578, 2013.

[48] Z. Y. Yang, et al.," Efficient resource allocation algorithm for overlay D2D communication," *Computer Networks*, 124, pp. 61–71, 2017.

[49] A. Abrardo, et al.," Distributed power allocation for D2D communications underlaying/overlaying OFDMA cellular networks," *IEEE Transactions on Wireless Communications*, 16(3), pp. 1466–1479, 2016.

[50] R. Yin, et al., "Joint Spectrum and Power Allocation for D2D Communications Underlaying Cellular Networks," *IEEE Transactions on Vehicular Technology*, 65(4), 2182-2195, 2016.

[51] I. Din and H. Kim, "Energy-efficient Brightness Control and Data Transmission for Visible Light Communication," *IEEE Photonics Technology Letters*, 26(8), pp. 781–784, 2014.

[52] Y. Wang, et al., "4.5-Gb/s RGB-led Based WDM Visible Light Communication System Employing Cap Modulation and RLS Based Adaptive Equalization," *Optics express*, 23(10), pp. 13626–13633, 2015.

[53] X. Huang, et al., "1.6 Gbit/s Phosphorescent White LED Based VLC Transmission Using a Cascaded Pre-equalization Circuit and a Differential Outputs PIN Receiver," *Optics express*, 23(17), pp. 22034–42, 2015.

[54] G. Cossu, A. Khalid, P. Choudhury, R. Corsini, and E. Ciaramella, "3.4 Gbit/s visible optical wireless transmission based on RGB led," *Optics express*, vol. 20, no. 26, pp. B501–B506, 2012.

[55] A. Jovicic, J. Li, and T. Richardson, "Visible light communication: opportunities, challenges and the path to market," *IEEE Communications Magazine*, 51(12), pp. 26-32, 2013.

[56] X. Wu, D. Basnayaka, M. Safari, and H. Haas, "Two-stage access point selection for hybrid VLC and RF networks," *IEEE 27th Annual International Symposium on Personal, Indoor, and Mobile Radio Communications (PIMRC)*, pp. 1–6, 2016.

[57] X. Wu, et al., "Access point selection for hybrid li-fi and wi-fi networks," *IEEE Transactions on Communications*, 65(12), pp. 5375–5385, 2017.

[58] M. Kashef, et al., "Transmit Power Optimization for a Hybrid PLC/VLC/RF Communication System," *IEEE Transactions on Green Communications and Networking*, 2(1), pp. 234–245, 2018.

[59] H. Tabassum, et al., "Coverage and Rate Analysis for Co-Existing RF/VLC Downlink Cellular Networks," *IEEE Transactions on Wireless Communications*, 17(4), pp. 2588–2601, 2018.

[60] L. Li, H. Tian, and B. Fan, "A joint resources allocation approach for hybrid visible light communication and LTE system," *International Conference on Wireless Communications, Networking and Mobile Computing (WiCOM 2015)*, 2015.

[61] S. Liang, H. Tian, B. Fan, and R. Bai, "A novel vertical handover algorithm in a hybrid visible light communication and LTE system," *IEEE Vehicular Technology Conference (IEEE VTC-Fall 2015)*, pp. 1–5, 2015.

[62] Y. Liu, Z. Huang, W. Li, and Y. Ji, "Game theory-based mode cooperative selection mechanism for device-to-device visible light communication," *Optical Engineering*, vol. 55, no. 3, pp. 30501–30501, 2016.

[63] S. V. Tiwari, A. Sewaiwar, and Y.-H. Chung, "Optical repeater assisted visible light device-to-device communications," *World Academy of Science, Engineering and Technology, International Journal of Electrical, Computer, Energetic, Electronic and Communication Engineering*, vol. 10, no. 2, pp. 206–209, 2016.

[64] H. Nishiyama, M. Ito, and N. Kato, "Relay-by-smartphone: realizing multihop device-to-device communications," *IEEE Communications Magazine*, 52(4), pp. 56–65. 2014.

[65] J. Chen, Z. Wang, and R. Jiang, "Downlink Interference Management in Cell-Free VLC Network," *IEEE Transactions on Vehicular Technology*, 68(9), pp. 9007–9017, 2019.

[66] P. H. Pathak, X. Feng, P. Hu, and P. Mohapatra, "Visible Light Communication, Networking, and Sensing: A Survey, Potential and Challenges," *Communicayion Surveys & Tutorials.*, 17(4), pp. 2047–2077, 2015.

[67] Y.L. Lee, T.C. Chuah, J. Loo, and A. Vinel, "Recent advances in radio resource management for heterogeneous LTE/LTE-A networks," *IEEE Communications Surveys & Tutorials*, 16(4), pp. 2142–2180, 2014.

[68] H.Y. Nam, Y. Akimoto, Y. Kim, M.I. Lee, K. Bhattad, and A. Ekpenyongl, "Evolution of reference signals for LTE-advanced systems," *IEEE Communications Magazine*, 50(2), pp. 132–138, 2012

[69] K. Hugl, et al., "Downlink Beamforming Avoiding DOA Estimation for Cellular Mobile Communications," *IEEE International Conference on Acoustics, Speech, and Signal Processing*, 6, pp. VI–3313, 1998

[70] T. Aste, et al., "Downlink Beamforming for Frequency Division Duplex Systems," *IEEE Global Communications Conference (GLOBECOM)*, 4, pp. 2097–2101, 1999.

[71] Y.C. Liang, et al., "Downlink Channel Covariance Matrix (DCCM) Estimation and Its Applications in Wireless DS-CDMA Systems," *IEEE Journal on Selected Sreas in Communications*, 19(2), pp. 222–232, 2001.

[72] K. Hugl, et al., "Spatial Reciprocity of Uplink and Downlink Radio Channels in FDD Systems," *Proc. COST*, 273(2), p. 066, 2002.

[73] B.K. Chalise, et al., "Robust Uplink to Downlink Spatial Covariance Matrix Transformation for Downlink Beamforming," *IEEE International Conference on Communications*, 5, pp. 3010–3014, 2004.

[74] M. Jordan, et al., "Conversion of the Spatio-Temporal Correlation from Uplink to Downlink in FDD Systems," *IEEE Wireless Communications and Networking Conference*, pp. 1–6, 2009.

[75] M. Arnold, et al., "Enabling FDD Massive MIMO through Deep Learning-based Channel Prediction," *arXiv preprint arXiv:1901.03664.*, pp. 1–6, 2019.

[76] N. González-Prelcic, et al., "Millimeter-Wave Communication With Out-of-Band Information," *IEEE Communications Magazine*, 55(12), pp. 1038-1052, 2017.

[77] A. Ali, et al., "Millimeter Wave Beam-Selection Using Out-of-Band Spatial Information," *IEEE Transactions on Wireless Communications*, 17(2), pp. 140-146, 2017.

[78] A. Ali, et al., "Estimating Millimeter Wave Channels Using Out-of-Band Measurements," *Information Theory and Applications Workshop*, pp. 1-6, 2016.

[79] R. Deng, et al., "A Two-Step Learning and Interpolation Method for Location-based Channel Database Construction," *IEEE Global Communications Conference (GLOBECOM)*, pp. 1-6, 2018.

[80] P. Dong, et al., "Machine Learning Prediction Based CSI Acquisition for FDD Massive MIMO Downlink," *IEEE Global Communications Conference (GLOBECOM)*, pp. 1-6, 2018.

[81] W. Lee, et al., "Transmit Power Control Using Deep Neural Network for Underlay Device-to-Device Communication," *IEEE Wireless Communications Letters*, 8(1), pp. 141–144, 2019.

[82] W. Lee, et al., "Deep power control: Transmit power control scheme based on convolutional neural network," *IEEE Communications Letters*, 22(6), pp. 1276–1279, 2018.

[83] Motorola, "Discussion of Type II (Transparent) Relays for LTE," *3GPP TSG RAN WG1 Meeting #57*, San Francisco, USA, May 4-8, 2009 (R1 091941).

# List of Research Projects

**Project no. LTT 20004** funded by The Ministry of Education, Youth and Sports.
**Project title**: "Cooperation with the International Research Centre in Area of Digital Communication Systems".
**Project period**: 2020-2024.

**Project no. SGS20/169/OHK3/3T/132** funded by Czech Tech. Uni. in Prague.
**Project period**: 2020-2022.

**Project no. P102/18/27023S** funded by Czech Science Foundation.
**Project title**: "Communication in Self-optimizing Mobile Networks with Drones".
**Project period**: 2018-2020.

**Project no. LTT18007** funded by The Ministry of Education, Youth and Sports.
**Project title**: "Cooperation with the International Research Centre in Area of Communication Systems".
**Project period**: 2017-2019.

**Project no. P102/17/17538S** funded by Czech Science Foundation.
**Project title**: "Combined Radio Frequency and Visible Light Bands for Device-to-Device communication".
**Project period**: 2017-2019.

**Project no. SGS17/184/OHK3/3T/13** funded by Czech Tech. Uni. in Prague.
**Project period**: 2017-2019.

# List of Publications

All authors of every listed publication have contributed equally to the content of the corresponding publication unless it is mentioned otherwise. The papers are sorted based on date starting from the most recent ones.

## Publications Related to the Topic of the Dissertation Thesis

### Patents

[1P] M. Najla, Z. Becvar, P. Mach, and D. Gesbert, "SYSTEM AND METHOD FOR DEVICE-TO-DEVICE COMMUNICATION," *US Patent* filled in July 2020.

### Journal papers (with impact factor)

[1J] M. Najla, Z. Becvar, and P. Mach , "Reuse of Multiple Channels by Multiple D2D Pairs in Dedicated Mode: Game Theoretic Approach," second minor revisions in *IEEE Transactions on Wireless Communications* submitted in July 2020.

[2J] M. Najla, Z. Becvar, P. Mach, and D. Gesbert, "Predicting Device-to-Device Channels from Cellular Channel Measurements: A Learning Approach," accepted in *IEEE Transactions on Wireless Communications*, 2020.

[3J] M. Najla, P. Mach, and Z. Becvar, "Deep Learning for Selection between RF and VLC Bands in Device-to-Device Communication," accepted in *IEEE Wireless Communications Letters*, 2020.

[4J] M. Najla, P. Mach, Z. Becvar, P. Chvojka, S. Zvanovec, "Efficient Exploitation of Radio Frequency and Visible Light Communication Bands for D2D in Mobile Networks," *IEEE Access*, vol. 7, pp. 168922-168933, 2019. The contribution of Mehyar Najla in this paper is 30 %.

[5J] P. Mach, Z. Becvar, M. Najla, "Resource Allocation for D2D Communication with Multiple D2D Pairs Reusing Multiple Channels", *IEEE Wireless Communications Letters*, vol. 8, no. 4, pp. 1008–1011, 2019.

### Conference papers

[1C] M. Najla, Z. Becvar, P. Mach, and D. Gesbert, "Integrating UAVs as Transparent Relays into Mobile Networks: A Deep Learning Approach," *IEEE International Symposium on Personal, Indoor and Mobile Radio Communications (IEEE PIMRC 2020)*, 2020.

[2C] M. Najla, Z. Becvar, and P. Mach , "Sequential Bargaining Game for Reuse of Radio Resources in D2D Communication in Dedicated Mode," *IEEE Vehicular Technology Conference (IEEE VTC-Spring 2020)*, pp. 1–6, 2020.

[3C] M. Najla, D. Gesbert, Z. Becvar, P. Mach, "Machine Learning for Power Control in D2D Communication based on Cellular Channel Gains," *IEEE Global Communications Conference (IEEE Globecom 2019) workshop on Machine Learning for Wireless Communications*, pp. 1-6, 2019.

[4C] P. Mach, Z. Becvar, and M. Najla, "Combined Shared and Dedicated Resource Allocation for D2D Communication," *IEEE Vehicular Technology Conference (IEEE VTC-Spring 2018)*, pp. 1–7, 2018.

[5C] Z. Becvar, M. Najla, P. Mach, "Selection between Radio Frequency and Visible Light Communication Bands for D2D," *IEEE Vehicular Technology Conference (IEEE VTC-Spring 2018) recent results*, pp. 1-7, 2018.

[6C] P. Mach, Z. Becvar, M. Najla, S. Zvanovec, "Combination of Visible Light and Radio Frequency Bands for Device-to-Device Communication," *IEEE International Symposium on Personal, Indoor and Mobile Radio Communications (IEEE PIMRC 2017), workshop on Coexisting Radio and Optical Wireless Deplymnets*, pp. 1-7, 2017.

## Publications Non-Related to the Topic of the Dissertation Thesis

[7C] P. Mach, Z. Becvar, and M. Najla, "Joint Association, Transmission Power Allocation and Positioning of Flying Base Stations Considering Limited Backhaul," *IEEE Vehicular Technology Conference (IEEE VTC-fall 2020)*, 2020.

# Citations

This Chapter includes publications which have cited the author's work according to Google Scholar excluding the self-citations.

[1*] O.A. Amodu, M. Othman, N.K. Noordin, and I. Ahmad, "A primer on design aspects, recent advances, and challenges in cellular device-to-device communication," *Ad Hoc Networks*, 94, p. 01938, 2019.
This paper cites the journal paper [5J].

[2*] C. Kai, Y. Wu, X. Hu, and W. Huang, "Joint Subcarrier and Power Allocation in D2D Communications Underlaying Cellular Networks," *IEEE Wireless Communications and Networking Conference (WCNC)*, pp. 1–6, 2020.
This paper cites the journal paper [5J].

[3*] R. Gour, and A. Tyagi, "Cluster oriented resource allocation and power optimization for D2D network in cellular communications," *IET Networks*, 2020.
This paper cites the journal paper [5J].

[4*] H. Abuella, M. Elamassie, M. Uysal, Z. Xu, E. Serpedin, k.a. Qaraqe, and S. Ekin, "Hybrid RF/VLC Systems: A Comprehensive Survey on Network Topologies, Performance Analyses, Applications, and Future Directions," *arXiv preprint arXiv:2007.02466*, 2020.
This paper cites the two conference papers [5C] and [4C].

[5*] H. Zhang, W. Ding, F. Yang, J. Song, and Z. Han, "Resource Allocation in Heterogeneous Network With Visible Light Communication and D2D: A Hierarchical Game Approach," *IEEE Transactions on Communications*, 67(11), pp. 7616–7628, 2019.
This paper cites the conference paper [6C].

[6*] D.N. Anwar, and A. Srivastava, "Energy saver VLC using off-the-shelf devices: an experimental study," *IEEE International Conference on Advanced Networks and Telecommunications Systems (ANTS)*, 2018.
This paper cites the conference paper [6C].

[7*] H. Liu, Z. Lin, Y. Chen, and P. Xin, "Elite User Clustering-Based Indoor Heterogeneous VLC Interference Management and Sub-Channel Allocation Strategy," *IEEE Access*, 8, pp. 43582–43591, 2020.
This paper cites the conference paper [5C].

[8*] I. Singh, and N.P. Singh, "Analysis of success probability for device-to-device communication underlaid cellular networks operating over generalized $k$ - $\mu$ fading," *Optik*, 178, pp. 731–739, 2019.
This paper cites the conference paper [4C].